

Molecular role of the Ste50 adaptor protein in
regulating mating-pheromone signaling specificity
in *Saccharomyces cerevisiae*

By
Nusrat Sharmeen

Division of Experimental Medicine
Department of Medicine
McGill University
Montreal, Canada

A dissertation submitted to McGill University in partial fulfillment of the
requirements of the degree of Doctor of Philosophy (PhD)

July 2019

© Nusrat Sharmeen, 2019

Abstract

Living cells are continuously receiving stimuli from their external environments to bring out biological responses required for growth, maintenance and safety. Cells realize this through a network of signaling pathways that are dedicated to produce precise biological responses. Because pathways often share components, a fundamental question in the field of signal transduction is how the myriads of inputs are sensed, integrated and transduced accurately so that each elicits a specific and proper biological response.

In the yeast *Saccharomyces cerevisiae*, three major mitogen activated protein kinase (MAPK) pathways, which control the mating process in response to pheromone, the glycerol production in response to hyperosmotic stress and the filamentous growth in response to nutrient deprivation, share a common Ste11MAP3K and an adaptor protein Ste50, which has an N-terminal SAM (sterile alpha motif) domain and a C-terminal RA (Ras-association) domain. Ste11 and Ste50 interact through their respective SAM domains. The role of C-terminal Ste50-RA domain in conferring signaling specificity in the hyperosmolar glycerol and filamentous growth pathways has been established, however, the mechanism through which the Ste50-RA domain connects the mating pathway remains unknown.

In this dissertation, I have demonstrated that RA domain of Ste50 adaptor protein uses genetically separable surfaces to differentially connect to distinct MAPK signaling pathways. Using random mutagenesis, I built and screened Ste50-RA domain mutant libraries and identified mutants with interesting phenotypes. The mutants were grouped into three classes displaying defects specific to the mating pathway, or to the HOG pathway, or to both signaling pathways. The RA domain residues involved in these different mutant classes, when mapped onto the solution structure of the folded RA domain, showed distinct structural localizations and clustering according to their phenotypic traits. Analyses with structural meta-prediction tools indicate that all these residues showed a high propensity to engage in protein-protein interactions. I further performed microscopic studies with GFP fusions of the different Ste50 alleles in cells under pheromone stimulation, and

showed that wild type Ste50 accumulates at the polarization front of the shmoo structure, while the specifically pheromone response defective mutants are unable to form shmoos and fail to accumulate Ste50 at the polarized shmoo tip, indicating a loss of association of the *ste50* mutants with the shmoo polarization complex. These results suggest that Ste50-RA domain uses differential interactions to connect different MAPK pathways to exert early layer control of signaling specificity.

Subsequently, in detailed microscopic studies, I showed the dynamic cellular localization of the wild type Ste50 protein, as well as the location of the specifically-pheromone-signaling-defective Ste50 mutant protein. The mutant showed a strong defect in its dynamic cellular localization, suggesting a link between this localization and proper function of Ste50 in mating pheromone signaling.

Finally, I performed a suppressor study to find genetic suppressor of the specifically-pheromone-response-defective mutants. I expected that overexpressing some regulator(s) of Ste50 might identify suppressors that can compensate for the functional defects of these mutants. The genetic screen identified *RIE1* as a Ste50 mutant dependent suppressor of the pheromone signaling pathway. Deleting *RIE1* caused defective pheromone signaling, aberrant shmoo morphology and defective cell cycle arrest. These results suggest that *RIE1* is a new component of the mating-pheromone response pathway.

Key words: Ste50, Adaptor protein, MAPK signaling, Signaling specificity, Pheromone response pathway, Protein localization, Suppressors.

Résumé

Les cellules vivantes reçoivent en permanence des stimuli de leur environnement externe pour induire les réponses biologiques nécessaires à la croissance, à la maintenance et à la sécurité. Les cellules le réalisent grâce à un réseau de voies de signalisation dédiées à l'élaboration de réponses biologiques précises. Parce que les voies partagent souvent des composants, une question fondamentale dans le domaine de la transduction du signal est de savoir comment la myriade d'entrées est détectée, intégrée et traduite avec précision de manière à ce que chacune suscite une réponse biologique spécifique et correcte.

Dans la levure *Saccharomyces cerevisiae*, trois voies majeures de la protéine kinase activée par les mitogènes (MAPK), qui contrôlent le processus de reproduction en réponse à la phéromone, à la production de glycérol en réponse au stress hyperosmotique et à la croissance filamenteuse en réponse à la privation de nutriments, partagent un Ste11MAP3K commun une protéine adaptatrice Ste50 qui comporte un domaine SAM (sterile alpha motif) dans la portion N-terminale et un domaine RA (Ras association) au C-terminus. Ste11 interagit avec Ste50 par l'intermédiaire de leurs domaines de motif alpha stérile (SAM) respectifs. Le rôle du domaine C-terminal Ste50-RA dans la définition de la spécificité de signalisation dans les voies de croissance hyperosmolaire du glycérol et des filaments de croissance a été établi. Cependant, le mécanisme par lequel le domaine Ste50-RA se connecte à la voie d'accouplement reste inconnu.

Dans cette thèse, j'ai démontré que le domaine RA de la protéine adaptatrice Ste50 utilise des surfaces génétiquement séparables pour connecter différemment des voies de signalisation MAPK distinctes. En utilisant la mutagenèse aléatoire, j'ai construit et criblé des bibliothèques de mutants du domaine Ste50-RA et identifié des mutants présentant des phénotypes intéressants. Les mutants ont été regroupés en trois classes présentant des défauts spécifiques soit dans la voie d'accouplement, la voie HOG, soit dans les deux voies de signalisation. Les résidus du domaine RA impliqués dans ces différentes classes de mutants, une fois localisés sur la structure de solution du domaine RA plié, ont montré des localisations structurelles distinctes et une classification en fonction de leurs traits

phénotypiques. Des analyses avec des outils de méta-prédiction structurale indiquent que tous ces résidus ont une forte propension à s'engager dans des interactions protéine-protéine. J'ai ensuite effectué des études microscopiques avec des fusions de GFP des différents allèles Ste50 sous stimulation par phéromone et montré que le type sauvage Ste50 s'accumule au niveau de la polarisation de la structure shmoo, tandis que les mutants défectueux à réponse de phéromone sont incapables de former shmoo et ne peuvent pas accumuler Ste50 la pointe de shmoo polarisée, indiquant une perte d'association des mutants ste50 avec le complexe de polarisation de shmoo. Ces résultats suggèrent que le domaine Ste50-RA utilise des interactions différentielles pour connecter différentes voies MAPK afin d'exercer un contrôle précoce de la spécificité de signalisation.

Par la suite, dans un contexte connexe avec des études microscopiques de détail, j'ai montré les localisations cellulaires dynamiques de Ste50, ainsi que le mutant Ste50 présentant une signalisation spécifique de la phéromone. Spécifiquement, le mutant défectueux à réponse de phéromone a montré de forts défauts dans la localisation dynamique des protéines cellulaires, suggérant un lien entre la régulation de la localisation cellulaire et le bon fonctionnement de Ste50 dans la signalisation de la phéromone d'accouplement.

Enfin, j'ai effectué une étude sur les supprimeurs afin de trouver un suppresseur génétique des mutants défectueux à réponse de phéromone. Je m'attendais à ce que la surexpression de certains régulateurs de Ste50 puisse identifier des supprimeurs capables de compenser les défauts fonctionnels de ces mutants. Le crible suppresseur génétique a identifié *RIE1* en tant que régulateur dépendant de Ste50 de la voie de signalisation par la phéromone. La suppression de *RIE1* conduit à une signalisation de phéromone défectueuse, à une morphologie de shmoo aberrante et à un arrêt du cycle cellulaire défectueux. Ces résultats suggèrent que *RIE1* pourrait être un nouveau composant de la voie de réponse de phéromone d'accouplement.

Mots clés: Ste50, Protéine adaptatrice, Signalisation MAPK, Spécificité de signalisation, Voie de réponse aux phéromones, Localisation de protéines, Supprimeurs.

Acknowledgements

I started my PhD with a notion to make this world a better place. No matter how small the contribution is at the end; it has the potential to make this world better in its own little way. I want to thank every one who has made this special journey possible!

First, I want to thank my family for their unconditional support throughout this very intense process: most importantly my husband, for his patience and sacrifice (doing household chores and tolerating lack of social life while I am on the computer). He has no knowledge of yeast research, but knew that I am devoted to find some fundamental truth. I am thankful to my son Yasir, whose genius help was invaluable in learning software manipulations for graphics, and my daughter Meghan for her encouragements.

I am grateful to my thesis committee, Dr. Bernard Turcotte, Dr. Michael Sacher, my comprehensive committee, Dr. Catherine Bachewich, Dr. Christopher Brett, Dr. Ursula Stochaj for mentoring me with advice and suggestions for my thesis work. Thanks to my academic advisor Dr. Andrew Moulard for his considerate guidance.

I am expressing my sincere gratitude to the GPD of Experimental Medicine, Dr. Anne-Marie Lauzon for monitoring my progress and nominating me for CSHRF student research competition. To all the staff: Dominique Besso, Marylin Linhares, Katrine Couvrette and Sandra Morrison, thank you for your administrative support throughout my PhD.

Stimulating discussions with Dr. Stephen Michnick and Dr. Pascal Chartrand of University of Montreal, Dr. Alisa Piekny and Dr. Aashiq Kachroo of Concordia University were extremely insightful and an eye opener, made me think outside the box, putting the philosophy back into the doctor of philosophy.

I am grateful to my collaborators Dr. Traian Sulea at the NRC, Dr. Marlene Oeffinger at the IRCM for opening their doors with invaluable help to complete my thesis. I am also grateful

to Dr. Brian Slaughter, Dr. Serge Pelet and Dr. Yasushi Tamura for sharing their plasmids to carry out the thesis work.

I am indebted to Dr. Chris Law for educating me in different aspects of microscopy and image analysis. His sincerity, encouragement, participation and patience were invaluable for all microscopic aspect of this thesis, as well as editing the thesis. Thanks also to my colleague Samatha Sarapani for her spontaneous help in translating the abstract to French.

I am also thankful to my colleagues for their cooperation, companionship and support through out my journey. Special thanks to Dr. Hannah Regan for teaching me sequence analysis, Dr. Jaideep Mallick for stimulating discussions plus support with lab work and Ifthiha Mohideen for providing *E. coli* competent cells.

I want to thank the whole scientific community, during my PhD research, many times I have reached out to the scientific community around the world with questions and concerns. I was pleasantly surprised how genuinely they communicated and gave me directions to achieve my goals.

This research would not have been possible without the financial support of NSERC, McGill University and the Whiteway lab; I want to thank them for believing in this research.

Most importantly, I want to thank my supervisor, Dr. Cunle Wu and co-supervisor Dr. Malcolm Whiteway, who were my mentors in teaching basic bench research to global perspective of the science behind my project. I appreciate how they have given me the framework and opportunity to pursue independent thinking and develop my own ideas. Their incentive, critical perspectives and scientific opinion will be something I will carry with me for the rest of my life.

Dedication

To my loving father

who had kindled the joy of learning in me.

See, in these silences where things
give over and seem on the verge of betraying
their final secret,
sometimes we feel we're about
to uncover an error in Nature,
the still point of the world, the link that won't hold,
the thread to untangle that will finally lead
to the heart of a truth.

The eye scans its surroundings,
the mind inquires aligns divides
in the perfume that gets diffused
at the day's most languid.

It's in these silences you see
in every fleeting human
shadow some disturbed Divinity.

Eugenio Montale, OSSI de SEPPIA 1920-1927

CUTTLEFISH BONES / Movements

Translated by Jonathan Galassi

Preface and original contributions

This thesis is prepared to complete the PhD in Experimental Medicine at McGill University. The thesis adheres all the requirements by the Graduate and Postdoctoral Studies at McGill University. This is a manuscript-based thesis, there are three manuscripts, published or organized to be published with their abstract, introduction, results, discussion and references. An introduction on the different topics researched is presented in chapter I. Chapter II is a manuscript with original work that has been published in *Molecular Biology of the Cell*. I am the first author of this publication. I wrote the original manuscript and carried out all the research except the structural bioinformatics, which was performed by Dr. Traian Sulea at the National Research Council of Canada. Details of the author contributions are presented at the beginning of each manuscript. This work generated some original contributions regarding signaling specificity. I showed in this work how multiple signaling pathways that share common components retain their signaling specificity. In this manuscript I demonstrated that the RA domain of the Ste50 adaptor protein has critical residues specifically directing signaling through the mating and HOG MAPK signaling pathways in yeast *Saccharomyces cerevisiae*. These residues form distinct patches with residues specifically required for one pathway clustered together on the three-dimensional structure of the RA domain that could be potential protein-protein interaction sites. I showed that the critical residues responsible for specific pheromone signaling are required for Ste50p association and localization during shmoo formation. Thus, this study shows that the RA domain of Ste50p uses different structural modes for associating with potential partner proteins conferring MAPK signaling specificity.

With a continued effort to understand the tip localization dynamics and other localization functions of the adaptor protein Ste50 that may be linked to the pheromone signaling specificity, in chapter III, I performed detailed microscopic studies. This work also generated some novel findings. Here, I have designed and performed all the experimental work except for setting up and running the microscope for time-lapse imaging, which was performed by Dr. Chris Law. He also wrote the macros for image analysis. I performed all

the image analysis and wrote the original manuscript. Details of the author contributions are presented at the beginning of the manuscript. Here, I first described how Ste50 polarity patch formation correlates with the polarized shmoo growth and pheromone stimulus. I described that Ste50 has no involvement in the vegetative bud polarization, while enhanced bud-neck localization prior to cytokinesis requires Ste50-RA domain pheromone specific residues, which may prime the polarization of shmoo formation that is required for the pheromone signaling. I also found that Ste50 localizes to the nucleus in a cell cycle dependent manner and this localization is impaired in cells with a specifically pheromone response defective mutant of Ste50, indicating that nuclear translocation of the protein may be involved in pheromone signaling function.

In chapter II and chapter III, I proposed that the Ste50-RA domain is required to regulate the pheromone signaling pathway in yeast, and I generated RA domain mutants that are specifically defective in pheromone signaling. This gave me the opportunity to take advantage of the mutants' distinct phenotype and isolate high-copy genetic suppressors of the mating signaling defect. I designed and performed all the experiments including the genetic screens. I wrote the original manuscript. Details of all the author contributions are presented at the beginning of the manuscript. My genetic screens isolated *RIE1* as a suppressor gene. Further gene deletion studies established that *RIE1* is a new component of the mating-pheromone- signaling pathway.

There is an overall discussion of all the contributions in chapter V of this dissertation and a conclusion. Complying with the requirements by the McGill thesis preparation rules for a manuscript based thesis, each manuscript has its own references and there is a bibliography at the end that includes the references for chapter I (Introduction) and chapter V (Discussion) in this dissertation.

Table of Contents

Abstract	ii
Résumé	iv
Acknowledgements	vi
Dedication	viii
Preface and original contributions	x
List of Tables	xv
List of Figures	xvi
Abbreviations	xix
Chapter I: Introduction	1
1.1 Overview of cell signaling	1
1.1.1 Signal recognition and transduction	2
1.1.2 Signaling pathways	5
1.1.3 Mitogen activated protein kinase pathways	5
1.2 Yeast as a model organism	7
1.3 Yeast MAPK signaling pathways	9
1.3.1 Cell wall integrity pathway	10
1.3.2 Spore wall assembly pathway	11
1.3.3 Filamentous growth pathway	11
1.3.4 High-osmolarity glycerol pathway	12
1.3.5 Pheromone response pathway	14
1.4 Mating-pheromone response pathway	15
1.4.1 The mating type cells	15
1.4.2 Receptor stimulation and activation of the G-protein	17
1.4.3 Intracellular signal processing downstream of G β γ	18
1.4.4 Scaffold protein of MAPK signaling	20
1.4.5 Activation of Fus3 and its substrate activation	21
1.4.6 Transcriptional activation	21
1.4.7 Cell cycle arrest	22

1.4.8 Polarization	22
1.5 Adaptor proteins.....	23
1.5.1 Ste50 adaptor protein.....	24
1.5.1.1 SAM domain	25
1.5.1.2 RA domain	26
1.6 Specificity of signaling.....	27
1.6.1 Mechanisms of signaling specificity.....	27
1.6.2 RA domain in MAPK signaling specificity.....	31
1.7 Protein localization dynamics	32
1.7.1 Protein transport	34
1.7.1.1 Nuclear transport.....	34
1.8 Genetic suppression of mutants	35
1.9 Objectives	36
Chapter II: Adaptor protein Ste50 directly modulates yeast MAPK signaling specificity through differential connections of its RA domain.....	39
2.1 Preface.....	40
2.2 Abstract.....	41
2.3 Introduction.....	42
2.4 Results	45
2.5 Discussion.....	62
2.6 Materials and Methods.....	66
2.7 References.....	71
2.8 Supplementary Materials.....	77
Chapter III: Proper pheromone signaling requires spatiotemporally dynamic cellular localization of the adaptor protein Ste50.....	87
3.1 Preface.....	88
3.2 Abstract	89
3.3 Introduction.....	90
3.4 Results	92
3.5 Discussion.....	106
3.6 Materials and Methods.....	112
3.7 References.....	115

3.8 Supplementary Materials.....	122
Chapter IV: Multicopy suppressor analysis with Ste50 mutants identified <i>RIE1</i> as a component of the mating signalling process in <i>Saccharomyces cerevisiae</i>.....	132
4.1 Preface.....	133
4.2 Abstract.....	134
4.3 Introduction.....	135
4.4 Results.....	137
4.5 Discussion.....	146
4.6 Materials and Methods.....	148
4.7 References.....	152
Chapter V: Discussion and future studies.....	155
Bibliography.....	166

List of Tables

Chapter II

TABLE 1: Ste50-RA domain desired mutants from library screens	49
TABLE 2: Mutational dissections of multiple mutations to find causal mutation(s)	50
TABLE S1: Ste50-RA domain point mutants with no selectable phenotypes	82
TABLE S2: Stability analysis of Ste50-RA domain mutants	83
TABLE S3: Site-directed mutagenesis of Ste50-RA domain	84
TABLE S4: List of plasmids used in this study	85
TABLE S5: List of oligonucleotides used in this study	86

Chapter IV

TABLE 1. Suppression growth characterization	139
TABLE 2. Yeast genomic library clones that suppressed pheromone signaling defect of the STE50 mutant	140
TABLE 3. Strains used in this study	149

List of Figures

Chapter I

FIGURE 1: Schematics of general cellular signaling.....	4
FIGURE 2: MAPK signaling pathways.....	6
FIGURE 3: <i>Saccharomyces cerevisiae</i> or budding yeast.....	7
FIGURE 4: <i>S. cerevisiae</i> MAPK pathways.....	9
FIGURE 5: <i>S. cerevisiae</i> hyperosmolar glycerol pathway.....	13
FIGURE 6: The mating locus of <i>S. cerevisiae</i>	15
FIGURE 7: <i>S. cerevisiae</i> response to pheromone.....	16
FIGURE 8: <i>S. cerevisiae</i> mating-pheromone response pathway.....	19
FIGURE 9: NMR solution structure of Ste50-RA domain.....	26
FIGURE 10: Kinetic insulation.....	29
FIGURE 11: Kinase-substrate specificity.....	30

Chapter II

FIGURE 1: MAPK pathways with shared components in <i>Saccharomyces cerevisiae</i>	43
FIGURE 2: Ste50-RA domain mutant library construction and screening.....	47
FIGURE 3: Ste50p amino acid sequence showing point mutations.....	48
FIGURE 4: Transcriptional activation of Ste50-RA domain mutants.....	51
FIGURE 5: Structural clustering of Ste50-RA domain residues according to their functional phenotypes.....	54
FIGURE 6: Growth characterization of Ste50-RA domain mutants specifically defective in pheromone response.....	56
FIGURE 7: Residues 283 and 294 are critically required for shmoo formation.....	58

FIGURE 8: Ste50-GFP localization profile.....	60
FIGURE S1: Dissection of multiple mutations to find the causal mutation(s)	78
FIGURE S2: Location of the functional interfaces of Ste50-RA domain mapped in this study relative to the canonical interaction mode of RA domain with small GTPases.....	78
FIGURE S3: Growth assay of Ste50-RA domain mutant weak alleles specifically defective in pheromone response	79
FIGURE S4: Growth assay of <i>ste50</i> mutants defective specifically in HOG pathway or in both HOG and pheromone response pathway signaling	80
FIGURE S5: GFP tagged proteins retain their respective phenotypic cell cycle arrest.....	81

Chapter III

FIGURE 1: Characterization of shmoo tip localization of Ste50.....	93
FIGURE 2: Ste50 polarity patch on the cell cortex is an early indicator of shmoo formation	96
FIGURE 3: Ste50 localizes to the shmoo tip until shmoo maturation.	97
FIGURE 4: Bud-neck localization of Ste50-GFP	101
FIGURE 5: Ste50 localizes to the nucleus	102
FIGURE 6: Ste50 localizes in the nucleus in cell cycle dependent manner	105
FIGURE 7: Nuclear localization of Ste50 alleles.....	107
FIGURE S1: Transcriptional activation of Ste50-RA domain mutant R296G.....	122
FIGURE S2: Potential NLS of Ste50.....	123
MACRO S3: Nuclear localization of Ste50-GFP intensity measurement	123
MACRO S4: Shmoo localization of Ste50-GFP intensity measurement	128

Chapter IV

FIGURE 1: Yeast genomic library clone 12 is a genetic suppressor of the Ste50-RA domain mutant G.....	138
FIGURE 2: <i>MGA1</i> and <i>RIE1</i> chromosomal locations	142
FIGURE 3: Multicopy <i>RIE1</i> can suppress pheromone signaling defect of Ste50 mutant R296G.....	143
FIGURE 4: Phenotypes of the <i>RIE1</i> suppressor deletion strain	144
FIGURE 5: Characterization of $\Delta r i e 1$ yeast strain	145

Abbreviations

WT	Wild type
SAM	Sterile alpha motif
RA	Ras association
HOG	High osmolarity glycerol
IVR	<i>In vivo</i> recombination
PPI	Protein/Protein interaction
GTPase	Guanosine triphosphatase
Opy2	Overproduction-induced pheromone-resistant protein 2
Cdc42	Cell division control protein 42
PAK	p21 activated kinase
PI3K	Phosphoinositide 3-kinase
RalGDS	Ral guanine nucleotide dissociation stimulator
SD	Synthetic defined
Mg	Magnesium
RASSF	Ras-association domain family
NMR	Nuclear magnetic resonance
bp	Base pair
Ca ²⁺	Calcium ion
CFU-C	Colony forming unit - culture
DAPI	4,6-diamidino-2-phenylindole, dihydrochloride
EDTA	Ethylenediamine tetra-acetate
GFP	Green fluorescent protein
KO	Knock out
MAPK	Mitogen activated protein kinase
MAP2K	Mitogen activated protein kinase kinase
MAP3K	Mitogen activated protein kinase kinase kinase
GPCR	G-protein coupled receptor
PKA	Protein kinase A

CDK	Cyclin dependent kinase
GEF	Guanine nucleotide exchange factor
GAP	GTPase-activating protein
GTP	Guanosine triphosphate
GDP	Guanosine diphosphate
ATP	Adenosine triphosphate
AMP	Adenosine monophosphate
cAMP	Cyclic adenosine monophosphate
K	Kinase
P	Phosphatase
ORF	Open reading frame
DNA	Deoxy ribonucleic acid
RNA	Ribonucleic acid
<i>E. coli</i>	<i>Escherichia coli</i>
<i>S. cerevisiae</i>	<i>Saccharomyces cerevisiae</i>
LB medium	Luria-Bertani medium
YPD	Yeast extract Peptone Dextrose
SD	Synthetic defined
SC	Synthetic complete
DIC	Differential interference contrast
FITC	Fluorescein Isothiocyanate
MA	Massachusetts
CYCLoPs	Collection of yeast cells and localization patterns
Grb2	Growth factor receptor-bound protein 2
MgCl ₂	Magnesium chloride
MnCl ₂	Manganese chloride
IDT	Integrated DNA Technologies
DTT	Dithiothreitol
ECL	Enhanced Chemoluminescence
°C	Degree Celcius

Kb	Kilo bases
KDa	Kilo Dalton
pH	Potential of Hydrogen
TBS	Tris-buffered saline
PBS	Phosphate-buffered saline
Tris	Tris(hydroxymethyl)aminomethane
TBST	Tris-buffered saline tween
SDS	Sodium dodecyl sulfate
Rpm	Rounds per minute
PCR	Polymerase chain reaction
OD	Optical density
PAGE	Polyacrylamide gel electrophoresis
ml	milliliter
μl	microliter
mg	milligram
μg	microgram
mM	milli molar
nM	nano molar
μM	micro molar
NE	Nebraska
SOS	Son of Sevenless
MYD88	Innate Immune Signal Transduction Adaptor
ERK	Extracellular signal regulated kinase
JNK	c-Jun N-terminal kinase
RTK	Receptor tyrosine kinase
Ptp	Protein tyrosine phosphatase
Gpa1	Guanine nucleotide binding protein alpha-1
Bem1	Bud emergence
PH	Pleckstrin homology
Dig	Down-regulator of invasive growth

PRE	Pheromone response element
SH2	src homology 2
SGA	Synthetic genetic array
CRK	v-crk sarcoma virus CT10 oncogene homolog adaptor protein
EGF	Epidermal growth factor
KSR	Kinase suppressor of Ras
PTB	Polypyrimidine tract binding protein
<i>GAL1</i>	Galactokinase
<i>ADH1</i>	Alcohol dehydrogenase

Chapter I: Introduction

1.1 Overview of cell signaling

In nature, the survival of organisms depends on processing cellular information from their surroundings to provide them with cues, which are transmitted to generate biochemical or gene expression changes eliciting cellular responses; this is cellular signaling. It is an ancient evolutionary process that is found in all living organisms on earth, be it prokaryotes, such as bacteria, or unicellular eukaryotes, such as yeasts, molds and protozoans, or complex multicellular organisms, such as humans. For simple unicellular organisms the information is mostly from the external environment, while for multicellular organisms different types of cells within the organism communicate with each other, as well as responding to extracellular changes.

Mostly cells receive signals that are chemical in nature; for example, simple unicellular organisms sense nutrients in their environment and orient themselves toward the food (Weibull, 1960; Adler, 1966). Cells also send out signals, for example, unicellular eukaryotes such as baker's yeast transmit pheromones to the opposite mating partners to trigger conjugation (Osumi *et al.*, 1974). It is now known that bacteria use quorum sensing by secreting microbial hormones, which are required to bring out metabolic changes and gauge population density (Swift *et al.*, 1996; Pestova *et al.*, 1996; Kleerebezem *et al.*, 1997). Plants are also constantly monitoring the environmental changes of light, dark and temperature that control their growth, fruiting and flowering (Chen *et al.*, 2004; Leivar *et al.*, 2008). In complex multicellular organisms, there are many intracellular chemicals that change cellular behaviors, such as neurotransmitters, hormones, growth factors, and cytokines, which are released in direct vicinity or can travel long distance to bring out their responses (Alberts *et al.*, 2002).

Since proper signaling is vital to carry out biological processes, each cellular signal should be specifically directed to bring out the desired result. But in light of the complexity of the

systems, often cells receive multiple signals, which must be sorted out carefully for specific responses or integrated into a coordinated outcome. This is crucial since the failure to integrate signals properly can have fatal consequences, for example, unicellular eukaryotes such as yeast with genetic alterations in genes responsible for sensing osmotic stress can undergo a lethal hyperosmolar shock (Saito & Posas, 2012). In higher animals or humans, deregulation of signaling causes many diseases that have been uncovered. Diseases such as diabetes, cancer, Alzheimer's, Parkinson's are caused by defective communications due to disrupted normal cellular signaling (De Felice & Ferreira, 2014; Mashima & Tsuruo, 2005; Liu *et al.*, 2014; Timmons *et al.*, 2009). Therefore, organisms must precisely maintain cellular signaling to insure proper growth, differentiation and homeostasis.

1.1.1 Signal recognition and transduction

Signals can be mechanical, chemical, temperature, light or osmolarity. Cells convert mechanical signals, such as touch, balance, and hearing into electrochemical or chemical signals (Gillespie & Walker, 2001). Osmolar signals are sensed by the cell as force on the membrane that can be transduced by the cell, such as hyperosmolar stress signaling in yeast (Mager & Siderius, 2002). In the case of chemical signals, there are many different molecules, such as proteins, ions, gases and lipids (Albert *et al.*, 2002); they exert their effects either within a cell or among different cells at long distances. Light is sensed by the activation of the light sensitive cells in the eye, the photoreceptor cells rods and cone participate in the process of vision (Frumkes *et al.*, 1973).

In many instances extracellular signal recognition is done through cell surface receptors (Cuatrecasas, 1974). The recognition of a signal by a receptor molecule causes a chemical or physical change in the receptor, which is transmitted to the downstream effector molecules to cause a cellular response. For example, epidermal growth factor receptors are activated by binding with the epidermal growth factor ligand and activate the cytoplasmic domain of the tyrosine kinase receptor causing autophosphorylation of a number of tyrosine residues (Carpenter, 1983). Furthermore, it is now known that the quorum sensing in bacteria is either through binding of the hormone to cell surface receptors or through the hormone entering the cell via membrane-associated transporters initiating the signal transduction process (Fairweather, 2004). In the plant, *Arabidopsis*, one of the signal

transduction is through membrane bound receptor-like kinases (serine-threonine-kinase) (Wang, 2012). Higher organisms, such as humans have complex signaling pathways connected to numerous cell surface receptors, which are proteins that bind specific molecules known collectively as ligands. Receptor-ligand binding triggers transduction of the signal to the cytoplasmic side of the plasma membrane; examples of this process include G-protein coupled receptors, receptor tyrosine kinases and integrins. Many receptors are solely intracellular, such as nuclear receptors and cytosolic receptors, which bind intracellularly presented ligands (Mainwaring, 1976; Oppenheimer *et al.*, 1976).

In a majority of the cases receptor activation involves binding with the ligand causing conformational changes, which then trigger the transmission of the stimulus to the interior of the cell. Inside the cell the stimulus usually activates a cascade of intercommunicating proteins, generally these are target enzymes and their activities are often modulated through phosphorylation. The chain of events usually ends with a DNA binding protein whose binding with DNA causes activation/repression of gene expression [Figure 1].

Signal transduction can also recruit adaptors, which are proteins that provide various binding structural modules to act as a platform for binding other signaling molecules to create a coordinated activation complex. These short-lived complexes transduce membrane activation signals to the downstream signaling components. Examples include human growth factor receptor bound protein (Grb2) (Lowenstein *et al.*, 1992), SHC transforming protein 1 (SHC1) (Pelicci *et al.*, 1992), and Myeloid differentiation primary response 88 (MYD88) (Lord *et al.*, 1990; Arancibia *et al.*, 2007; Warner & Núñez 2013).

Cells may also have intercellular signaling that constitutes different forms of short-range and long-range communications. These include extracellular second messengers, gap-junctions, cell-to-cell interaction through surface proteins, electrical signaling.

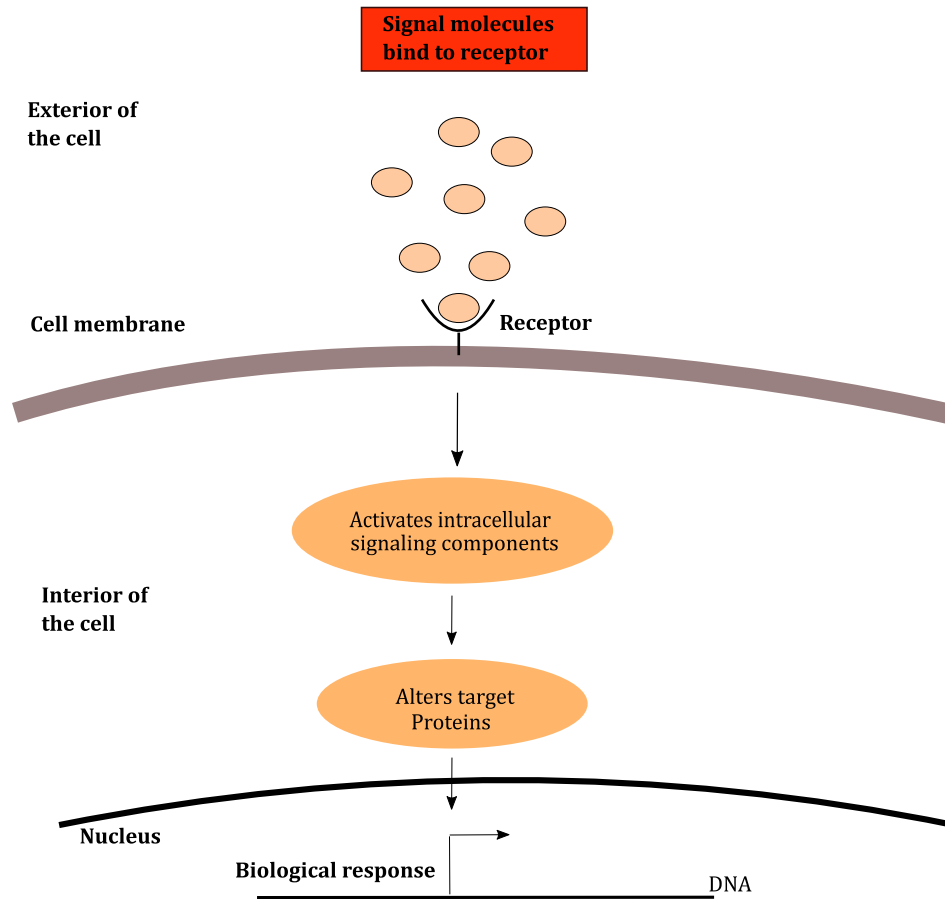


FIGURE 1: Schematics of general cellular signaling. Usually at the membrane, stimuli are sensed by specific receptors that activate intracellular signaling components generating signal specific responses.

Cells need to terminate signaling, which may take milliseconds to hours. Ligand withdrawal from the receptor is the simplest way to terminate signaling (Bohm *et al.*, 1997). Other mechanisms include feedback inhibition by a synthesized protein (Renner & Schmitz 2009), protein conformational changes (Borhan *et al.*, 2000) and autoinhibition by feedback regulation (Kleene, 2008). Thus for ligand-receptor based signaling, proteins involved in the signal transduction are the receptors and the cytosolic or nuclear components that relay the message and thus constitute a specific signaling pathway.

1.1.2 Signaling pathways

Unicellular organisms mainly communicate with the external environment to adapt to changes, but multicellular organisms need to respond to the environmental stimulus, as well as coordinate activities with other cells. In multicellular organisms, different cells are organized into specialized tissues that need information sharing for their development, morphology, localization and differentiated functions. This enormous demand requires a complex network of communications between cells through signaling pathways. Therefore, in higher organisms, the pathways have evolved to maintain the coordinated functions of distinct tissues and organs, as well as changes to the outside environment through cell growth, differentiation, development, motility, metabolic functions, adaptation, sensory information processing and change in morphology. Over 300 signaling pathways have been identified in human to carry out these cellular functions (Valdespino-Gómez *et al.*, 2015).

1.1.3 Mitogen activated protein kinase pathways

Mitogen activated protein kinase (MAPK) pathways are among the most well studied intracellular signaling pathways because they control vital processes, such as proliferation, differentiation and apoptosis. Historically, around 1987 a series of investigations by Sturgill and Ray systematically showed that by exposure of 3T3-L1 adipocytes cell extracts to insulin, activated a protein kinase that phosphorylated microtubule-associated protein-2 (MAP-2) (Sturgill & Ray, 1986). This kinase was later purified and characterized to be a serine/threonine protein kinase that is phosphorylated on its specific serine/threonine and tyrosine residues concomitant to its activation. Dephosphorylation of this kinase by tyrosine or serine/threonine protein phosphatases resulted in deactivation of the kinase. Interestingly, profuse phosphorylation of proteins at their serine/threonine residues was found in cells that expressed constitutively active tyrosine kinase, which exceeded tyrosine phosphorylation by 100-1000 fold (Cooper & Hunter, 1981). Many features of this kinase were interesting and drew intense attention, a kinase that phosphorylates downstream effectors and a possible substrate of tyrosine kinase itself (Ray & Sturgill, 1988).

We now know that this kinase is part of a highly conserved protein kinase cascade found

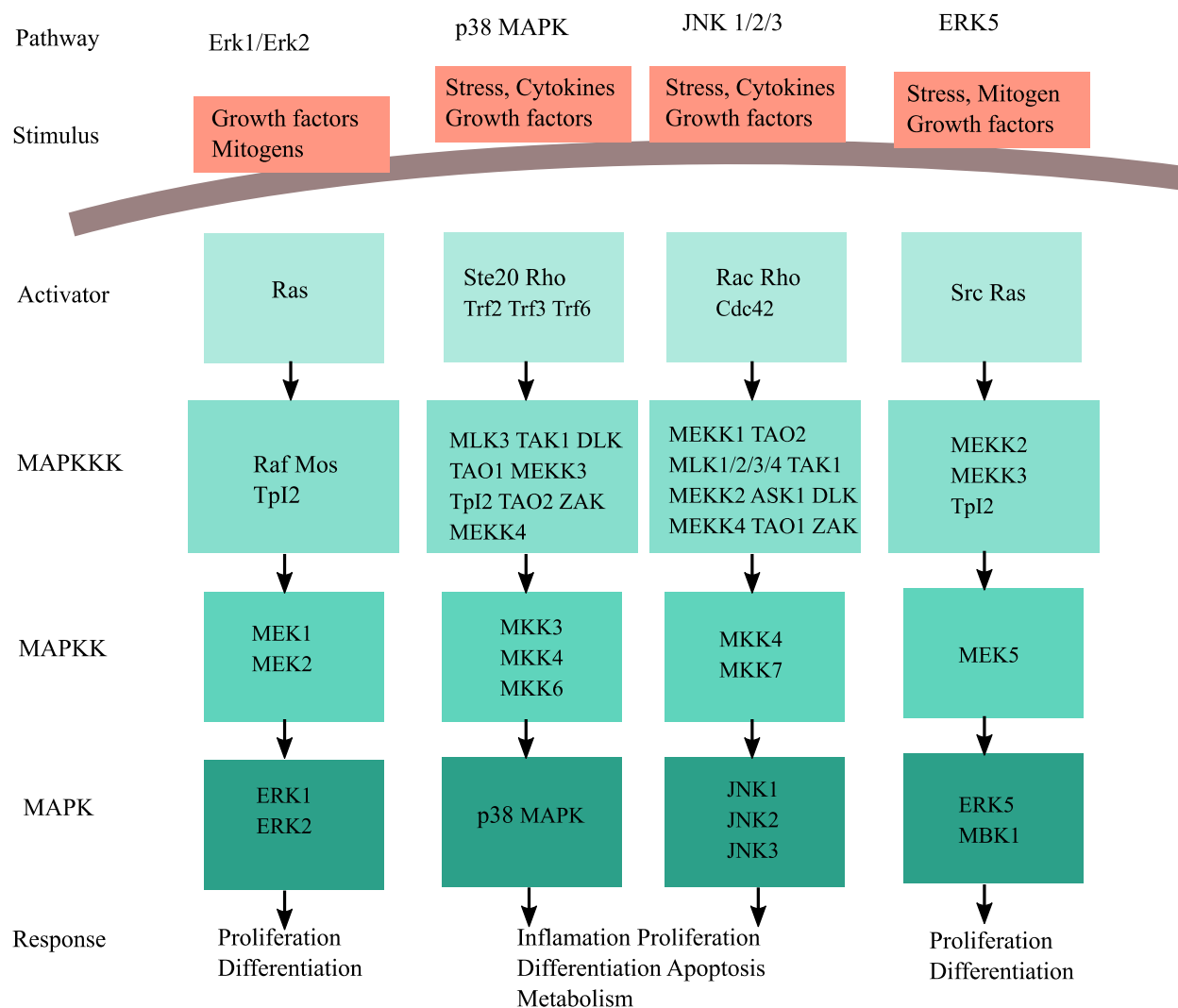


FIGURE 2: MAPK signaling pathways. The major MAPK pathways in mammalian cells are: ERK1/2; p38 MAPK; c-JUN N-terminal kinase 1, 2, and 3; ERK5

from yeasts to humans. In humans, six different MAPK pathways have been identified, these involve ERK1/2, ERK3/4, ERK5, ERK7/8, Jun N-terminal kinase (JNK1, JNK2, JNK3), and the p38 isoforms $\alpha/\beta/\gamma$, (ERK6)/ δ (Zlobin *et al.*, 2019). Four major MAPK pathways are shown in Figure 2. All of these pathways have the conserved core MAPK module: MAP3K, MAP2K and MAPK. One of the most important tyrosine kinase pathways is the Ras-Raf MAPK pathway, which is responsible for cellular proliferation and differentiation and is activated by the growth factors, such as EGF, platelet derived growth factor, Met growth factor (Carpenter, 1983; Ullrich & Schlessinger, 1990). For example, binding with the epidermal growth factor ligand activates the cytoplasmic domain of the tyrosine kinase receptor causing autophosphorylation of a number of tyrosine residues. GRB2 is a SH3 and

SH2 domain containing protein and its SH2 domain binds with the phosphorylated residues of the tyrosine kinase. The proline rich residues of the SH3 domain of GRB2 bind SOS (GEF of Ras) and activate it to bind Ras. Binding of Ras with its GEF (SOS) causes nucleotide exchange (GTP to GDP) on Ras that activates it to bind Raf. This triggers downstream activation and signaling by MEK, and MAPK (Carpenter, 1983; Ullrich & Schlessinger, 1990). Other MAPK pathways control many other functions such as inflammation, motility, invasiveness, angiogenesis, apoptosis and metabolism.

This is an over-simplified picture of the MAPK pathways; details of these pathways are highly complex. There are many effector molecules and often these molecules are shared. These types of signaling require a receptor or sensors on the cell membrane, intracellular enzymes, adaptors and scaffolds, and second messengers.

1.2 Yeast as a model organism

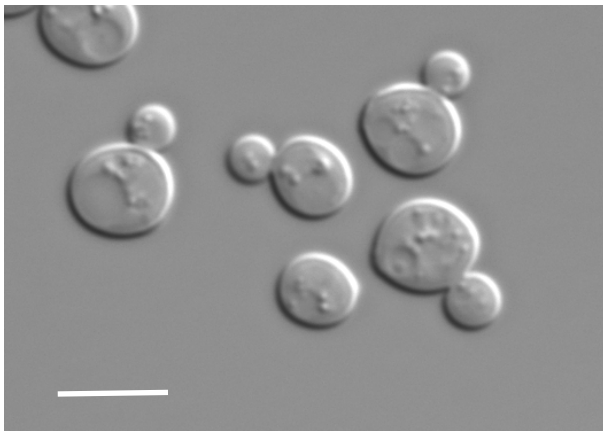


FIGURE 3: *Saccharomyces cerevisiae* or budding yeast. Bar 5 μ m.

Saccharomyces cerevisiae, or budding yeast, is a fungus that was being used by humans for more than 5000 years in fermentations without actually knowing of its existence. Later, with the invention of microscope, it was identified as a living organism. Budding yeast [Figure 3] is a unicellular eukaryote organized in a similar way to higher eukaryotes - the DNA being packed in chromosome inside a membrane bound nucleus. The yeast genome was the first

eukaryotic genome to be completely sequenced and surprisingly, although the lineage of yeast and humans separated billions of years ago, (Douzery *et al.*, 2004) still about 30% of yeast genes have been found to be similar to genes in humans, and among these 20% have been associated with human diseases. There are thousands of human orthologous genes (O'Brien *et al.*, 2005) in yeast and it is believed that orthologous genes from distant organisms many still have similar functions. An example includes the human Ras gene that

was found to be functional in yeast (Kataoka *et al.*, 1985; Michael *et al.*, 2007). However, in yeast Ras activates adenylate cyclase (Tamanoi, 2011). Interestingly, recently many yeast genes have been swapped with their human orthologs and the human genes were found to be functional in yeast in a pathway specific way (Kachroo *et al.*, 2015).

Because of the organizational and functional similarities between yeast and other organisms, many insights in cellular biology have come from studying yeast (Botstein *et al.*, 1997, 2011). *S. cerevisiae* is very easy to grow and culture in the laboratory, it is inexpensive to work with and its genome is very easy to manipulate, therefore studying yeast can quickly provide us with clues as to how many of the fundamental pathways in human cellular biology may work. In signaling studies, yeast is used extensively since it can sense many environmental stimuli and produce specific biological responses, providing an excellent system to understand stimulus-response behavior. Yeast MAPK pathways also consist a module of MAP3K-MAPK2K-MAPK, which is highly conserved in higher organisms including humans. Many proteins belonging to this module have counterparts in human, such as heterotrimeric G-proteins, p38, CDK (cycline dependent kinase) (Han *et al.*, 1994); since some MAPK pathways share common components, yeast is the ideal system to investigate molecular signaling specificity of these pathways.

A very convenient and useful feature of yeast is that it can exist either as a haploid or diploid organism; haploids are very easy to work with in case of gene deletion and phenotypic observations. Diploids are useful for making genetic crosses. Moreover, homologous recombination is extremely efficient in yeast, which can be used effectively for most of the non-essential gene deletions. Haploids can also be very useful for studying essential genes whose expression is under regulated control. These features have made many signaling studies possible, leading to advances in our understanding of signal transduction, cross talk, regulation and specificity. There already exists for yeast a comprehensive genetic database, resources and methods that can be applied conveniently to investigate fundamental questions such as how a protein from a gene of interest forms complexes, how it is regulated, what are the biochemical processes involved and how these relate to cell metabolism. One can also study a mutant; its phenotypic changes and how it disrupts a pathway, which when applied to humans may provide us with a link to the

molecular basis of a disease. All of the above makes yeast a strong candidate as a model organism for cellular signaling study.

1.3 Yeast MAPK signaling pathways

S. cerevisiae has five MAPK signaling pathways with conserved eukaryotic MAP3K-MAP2K-MAPK modules consisting of intracellular protein kinases. These three-component module signal relay systems are regulated by sequential phosphorylation on certain relatively conserved amino acid residues located in so-called “activation loops”. The sequential activation of such signaling modules involves a MAP3K activating a MAP2K, which in turn activates a MAPK [Figure 4] (Gustin *et al.*, 1998; Chen & Thorner, 2007). An activated MAPK undergoes conformational changes that facilitate phosphorylation of various

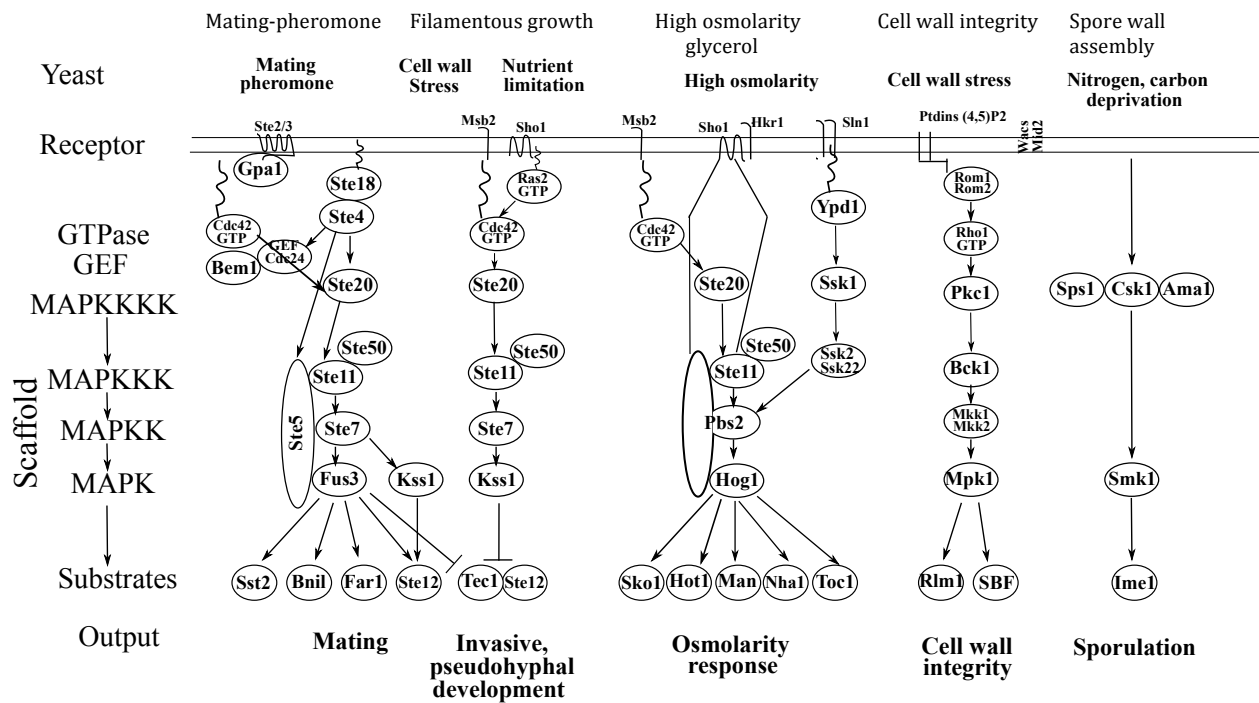


FIGURE 4: *S. cerevisiae* MAPK pathways. The mating pathway responds to pheromone, the nutrient deprivation pathway responds to lack of nutrients, the hyperosmolar glycerol pathway responds to osmolar changes, differences in cell wall stress is managed by cell wall integrity pathway and lack of nitrogen and carbon is sensed by spore-forming

sporulation pathway directed at forming spores. Adapted from Qi and Elion, 2005 (Reproduced/adapted with permission); Chen and Thorner, 2007; Piekarska *et al.*, 2010.

proteins including transcription factors, phosphatases, mammalian (Masuda *et al.*, 2003) translational regulators (Shively *et al.*, 2015) and ultimately causes a variety of responses including transcriptional activation of pathway-specific genes, changes in cell morphology and altered metabolism required for cell homeostasis, growth, survival, differentiation and mating. Although the MAPK module is conserved, both the upstream and downstream elements of these pathways differ considerably. For example, the upstream components can connect to the pathway-specific MAPK module through a two-component system, a heterotrimeric G-protein or a small monomeric G-protein. How the specific MAP3K gets activated depends on the respective MAPK pathway, and will be described later in the chapter for each distinct MAPK pathway.

There are five different MAPK pathways in *Saccharomyces cerevisiae*; the mating-pheromone response, the high osmolarity growth, the filamentous-invasion, the cell integrity and the spore wall assembly pathways. An important concept that has emerged from these MAPK pathways is that besides the basic modules, there are scaffolds and adaptor proteins that have major roles in either tethering the components together or linking them to other regulatory proteins for pathway function (Hunter and Plowman, 1997; Gustin *et al.*, 1998). Different MAPK pathways will be briefly described in this section.

1.3.1 Cell wall integrity pathway

The yeast cell wall is under continuous changes throughout its lifetime during growth, shmoo formation, osmotic stress, budding and sporulation (Levin, 2011). It also has to adjust to environmental changes of pH, available nutrients, temperature and mating pheromone (Aguilar-Uscanga & Francois, 2003; Schiavone *et al.*, 2014); under these stressful conditions, the integrity of the cell wall structure is challenged. The cell wall integrity (CWI) signaling pathway detects cell cycle and environmental changes, which are perceived through the cell surface sensors, Wsc1-3, Mid2 and Mtl1 that are coupled to the Rho1 G-protein. Rho1 is the master regulator for signals both due to cell surface changes

and the cell cycle. Activation of Rho1 by nucleotide exchange triggers a cascade of phosphorylation to the downstream components of this MAPK pathway [Figure 4] and activates MAPK Slt2/Mpk1. The effectors downstream of this MAPK regulate synthesis of cell wall materials for the delivery to the sites of cell wall remodeling.

1.3.2 Spore wall assembly pathway

Under deprivation of both nitrogen and fermentable carbon sources, diploid yeast cells exit mitotic cell division, and undergo a meiotic program known as sporulation (Neiman, 2011) that results in haploid spores. This allows survival in unfavorable conditions and re-entry into usual vegetative growth when nutrients are restored. Smk1 is the MAPK responsible for the development of spore wall assembly (Krisak *et al.*, 1994; Huang *et al.*, 2005) [Figure 4]. When cells are deprived of nutrition, Cln/Cdk activity is decreased causing the expression of IME1 and the transport of this protein in to the nucleus. This results in the activation of sporulation related genes, such as IME2 (Zaman *et al.*, 2008).

1.3.3 Filamentous growth pathway

Yeast cells respond to nutrient deficient conditions by differentiating and transforming into a filamentous form, a change thought to be a nutritional scavenging response found in many fungal species to facilitate their spreading out the surface area in search of nutrients (Gimeno *et al.*, 1992; Pan X, 2000; Cullen & Sprague, 2012, Ryan *et al.*, 2012). This differentiation behavior is characterized by dramatic changes in cell shape, polarity (Gimeno *et al.*, 1992; Roberts & Fink, 1994; Pruyne & Bretscher, 2000; Cullen & Sprague, 2002; Bi & Park, 2012), cell adhesion characteristics (Lambrechts *et al.*, 1996; Lo & Dranginis, 1998) and is controlled by coordinated action of a number of signaling pathways, one of which is a Kss1 MAPK signaling pathway [Figure 4]. This MAPK pathway regulates the filamentous growth by sensing nutritional changes in the environment through the signaling mucin Msb2 sensor (Cullen *et al.*, 2004) in the plasma membrane that is activated in glucose limited conditions. When nitrogen is limited, yeast cells undergo pseudohyphal growth where they form multicellular chains or filaments of elongated cells (Gimeo *et al.*, 1992; Cullen & Sprague, 2000).

1.3.4 High-osmolarity glycerol pathway

Extreme environmental osmolar change can threaten the survival of the organism. Yeast cells overcome this by adaptive responses that include readjustment by changes in the synthesis, uptake and retention of glycerol to balance osmotic stress (Albertyn *et al.*, 1994; Blomberg & Adler, 1989; Brewster *et al.*, 1993; Ferreira *et al.*, 2005; Lee *et al.*, 2013), the transcription of regulatory genes and the halting of the cell cycle to gain time for adjustment to the new situation. The environmental stress signals are regulated by the Hog1 MAPK, which is connected to the upstream elements by two functionally redundant branches of this MAPK pathway [Figure 5]. These upstream branches are the Sln1 and the Sho1 circuits whose mechanistic osmosensing functions are different (O'Rourke *et al.*, 2004). Between the two pathways, the Sln1 branch is more responsive to hyperosmolar stress and can restore complete osmotic balance even in the absence of the Sho1 branch. Such a necessity required the Sln1 branch to be highly conserved among all fungi, while not all fungi seem to use the Sho1 branch for HOG MAPK regulation (Furukawa *et al.*, 2005).

The Sln1 branch starts with the membrane localized osmosensor Sln1 (Posas *et al.*, 1996) that senses change in membrane turgor pressure (Reiser, 2003). This branch works with a two-component system forming a phospho-relay system with Sln1, Ypd1 and Ssk1 (Posas, 1996). Sln1 is functional under normal condition and autophosphorylates a histidine residue. The phosphate is then transferred to the receiver domain in Sln1, which transfers it to Ypd1 and then to Ssk1. Phosphorylated Ssk1 is inactive and blocks the downstream signal flow (Posas & Saito, 1998a). During hyperosmotic shock, Ssk1 becomes dephosphorylated and gets activated, and then binds to the regulatory domain of Ssk2 and Ssk22 MAP3Ks and activates them by triggering their autophosphorylation. From here on, a cascade of phosphorylation events happen whereby activated Ssk2/Ssk22 phosphorylates the Pbs2 MAP2K, which in turn phosphorylates the HOG1 MAPK (Maeda *et al.*, 1994, 1995).

The Sho1 osmoregulatory branch begins with membrane mucin-like osmosensors Msb2, Hkr1 (Tatebayashi *et al.*, 2007; de Nadal *et al.*, 2007). The MAPK module in this branch consists of Ste11 MAP3K, Pbs2 MAP2K and Hog1 MAPK. Sho1 is a transmembrane protein

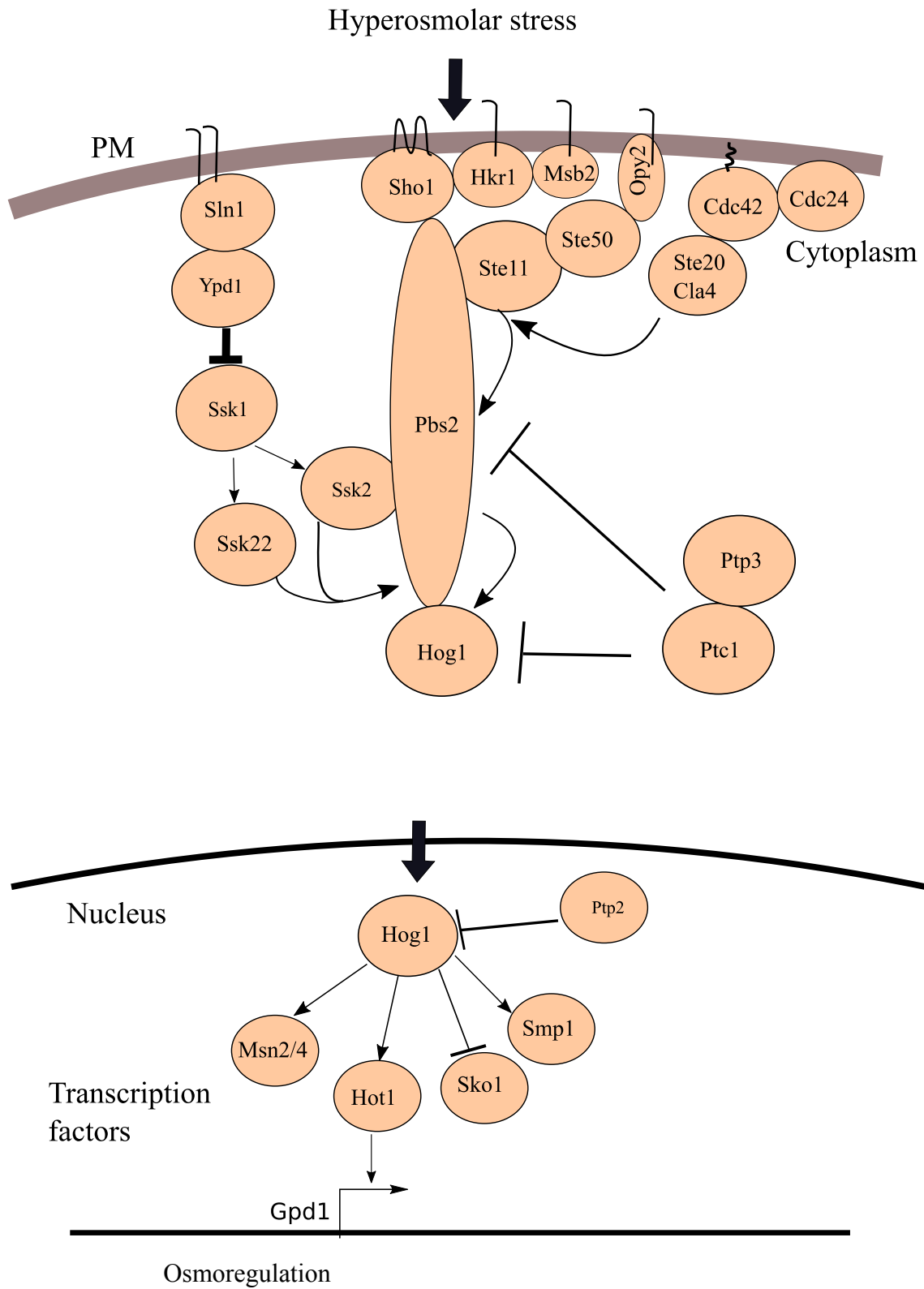


FIGURE 5: *S. cerevisiae* hyperosmolar glycerol pathway.

that acts as a scaffold protein in tethering components of this pathway for signaling and found active in places of cellular polar growth (Reiser *et al.*, 2000; Tatebayeshi *et al.*, 2015). Although how the upstream elements function is not completely understood, a recent study describes communications among Sho1, Msb2, Hkr1 and Opy2 are required for activation of downstream pathway components (Takayama *et al.*, 2019). The MAP2K component Pbs2 probably acts as a scaffold tethering Ste11 MAP3K to the membrane during hyperosmolar condition, positioning Ste11 near the Ste20 and Cla4 kinases for phosphorylation (van Drogen *et al.*, 2000; Raitt *et al.*, 2000). A transmembrane protein Opy2 that interacts with Ste50 adaptor protein also brings Ste11 near the membrane. Activated Ste11 then phosphorylates Pbs2, which in turn phosphorylates and activates Hog1 MAPK (Hohmann, 2002; 2009; de Nadal *et al.*, 2002), which translocates to the nucleus (Ferrigno *et al.*, 1998) and activates responsive promoter elements for regulatory gene transcription (Alepez *et al.*, 2001; Harsen *et al.*, 2008; Mas *et al.*, 2009;).

The level of phosphorylated Hog1 is regulated by phospho-tyrosine cytoplasmic phosphatase Ptp3 and nuclear phosphatase Ptp2 (Mattison *et al.*, 2000; Jacoby *et al.*, 1997) where Ptp3 binds Hog1 in the cytoplasm and Ptp2 sequesters it in the nucleus thus regulating Hog1 localization.

Interestingly, beside nuclear targets Hog1 kinase also has cytoplasmic targets (Bilsland-Marchesan *et al.*, 2000; Proft & Struhl, 2004; Thorsen *et al.*, 2006) that are involved in the production of glycerol and osmo-adaptation. Hog1 mediated transcriptional induction is not required for cell survival under hyperosmotic stress (Westfall *et al.*, 2008), this was shown by preventing Hog1 nuclear entry (*nmd5Δ* cells), or by tethering it to the plasma membrane as the sole source of this MAPK.

1.3.5 Pheromone response pathway

The fifth MAPK pathway is the mating-pheromone response pathway, which is the focus of this thesis and will be discussed in detail in the following section.

1.4 Mating-pheromone response pathway

S. cerevisiae responds to mating pheromone in the presence of opposite mating partner through a signal transduction pathway that ultimately results in conjugation and mating. The mating pheromone response pathway has been exploited exhaustively to study molecular signal transduction due to its simplicity and knowledge about its pathway components that were being identified systematically, starting with the historical discovery of a series of yeast mutants by Hartwell and MacKay that caused sterility in yeast, hence they are called “*STE*” (Hartwell, 1980; MacKay, 1993). Discovery of these mutants created an explosion of studies, and tremendous progress has been made since then to uncover the spatial arrangements of the different components of the pheromone response pathway, their connections with each other, protein-protein interactions, signal flow and how the response is mediated through gene transcription, all of which are generally well understood now. The following sections will describe how this important MAPK signaling pathway works.

1.4.1 The mating type cells

Unicellular yeast can stably exist in three cell types, either as two types of haploids or in the diploid form. The two different haploid cells are *MATa* and *MAT α* , originating from the same *MAT* mating locus, which is under the control of the *HO* gene that encodes a DNA endonuclease. The genetic information present at the *HML* and *HMR* is used to repair the

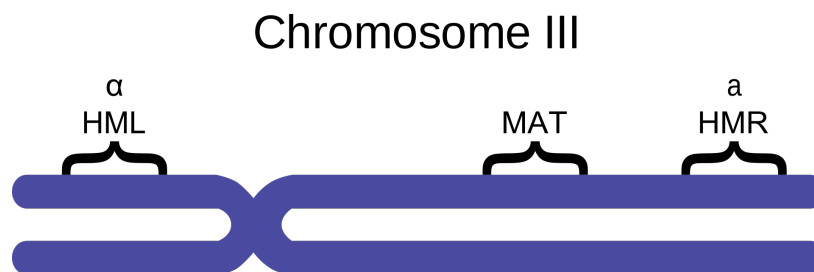


FIGURE 6: The mating locus of *S. cerevisiae*.
https://en.wikipedia.org/wiki/Mating_of_yeast

HO-induced DNA damage (Haber, 2012) [Figure 6] to create either the *MATa* or *MAT α* gene with the characteristics of these two haploid cell types. Yeast cells can either reproduce vegetatively by budding, or the two different haploid forms (*MATa* and *MAT α*) can mate

and fuse forming a $MATa/MAT\alpha$ diploid that can undergo meiosis and generate haploid progeny. For mating to take place, the haploid cells secrete a cell-specific pheromone for the opposite mating partner, which is received as a stimulus through the membrane

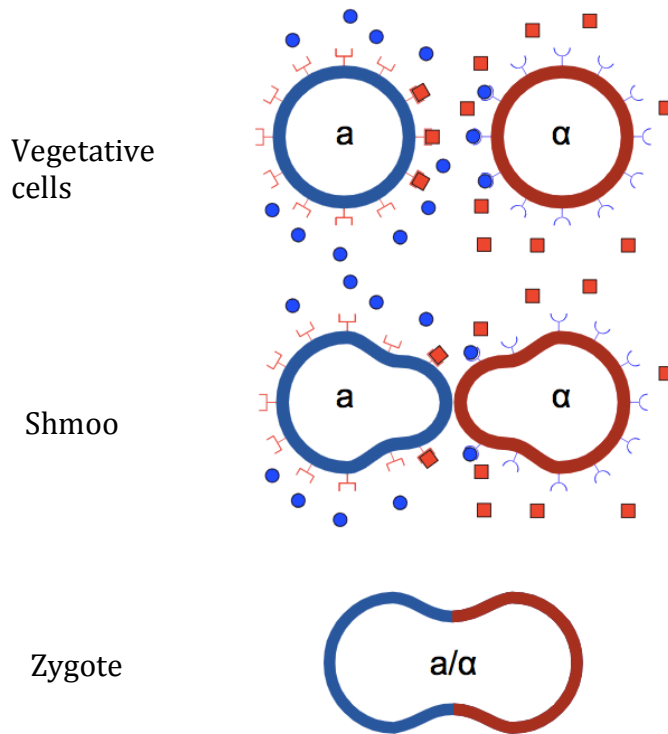


FIGURE 7: *S. cerevisiae* response to pheromone.
https://en.wikipedia.org/wiki/Mating_of_yeast

bound receptors. $MATa$ cells secrete a peptide pheromone called a-factor and $MAT\alpha$ cells secrete α -factor. α -factor is a 13-residue peptide with a sequence WHWLQLKPGQPMY, while a-Factor is a 12-residue farnesylated peptide with a sequence YIIKGVFWD PAC. $MATa$ cells receive and respond to α -factor by arresting at the G1 phase and then structurally polarizing towards the source of α -factor by a process called shmoo formation [Figure 7]. In a similar fashion, $MAT\alpha$ cells also receive and respond to a-factor, arrest their cell cycle and polarize towards the source of a-factor. The landmarks of pheromone response are cell cycle arrest, mating specific gene expression, morphological changes to form shmoo, fusion of shmoo from opposite mating cell types and ultimately nuclear fusion. The fused cell is called a zygote and is a diploid (Osumi *et al.*, 1974; Byers & Goetsch, 1975; Cross *et al.*, 1988; Fields 1990; Jackson & Hartwell, 1990a; Jackson & Hartwell, 1990b; Erdman & Snyder 2001).

1.4.2 Receptor stimulation and activation of the G-protein

Receptor stimulation in yeast is a prototypical ligand-receptor interaction; *MATa* and *MAT α* cells have receptors in their plasma membranes to specifically bind the ligands α -factor and a-factor, respectively. Both of these receptors have a seven-transmembrane helix architecture. The receptor on *MATa* cells, Ste2, is activated by binding to α -factor secreted by the *MAT α* cells. Conversely, the receptor on *MAT α* cells is Ste3, which binds to a-factor secreted from *MATa* cells. Ste2 and Ste3 were the first G-protein coupled receptors (GPCR) that were identified and cloned (Nakayama *et al.*, 1985). Both *MATa* and *MAT α* cells have the ability to sense the pheromone concentration gradient, thus allowing them to differentiate into shmoo structures in the direction of the highest pheromone producing prospecting mating partner present in the vicinity (Jackson & Harwell, 1990a). Although these receptors are grouped as GPCRs, they hardly have any sequence similarity to the mammalian GPCRs (Nakayama *et al.*, 1985; Versele *et al.*, 2001), while functionally they activate a heterotrimeric G-protein very similar to mammalian heterotrimeric G-proteins. Interestingly, mammalian GPCRs can replace the yeast GPCRs and mechanistically activate the mating pathway (Price *et al.*, 1995; Brown *et al.*, 2000).

Mating signaling is initiated when pheromone binds to a receptor (Ste2/Ste3) coupled to a prototypical heterotrimeric G-protein composed of a α subunit (Dietzel & Kurjan 1987; Nakafuku *et al.*, 1988; Nakayama *et al.*, 1988; Nomoto *et al.*, 1990) and a $\beta\gamma$ dimer (Ste4/Ste18) (Whiteway *et al.*, 1989). Both Ste2 and Ste3 are coupled to the same trimeric G-protein (Nomoto *et al.*, 1990; Horn *et al.*, 1998, Ford *et al.*, 1998) and utilize the same downstream effector molecules. Pheromone binding to the receptor (e.g. Ste2) causes receptor conformational changes and modifies it to act as a guanine-nucleotide exchange factor (GEF) on the G-protein α subunit (Gpa1) replacing a GDP for GTP. The resulting conformational changes on Gpa1 leads to the dissociation of the α subunit from the $\beta\gamma$ subunits (Ste4/Ste18) (Whiteway *et al.*, 1988; Kang *et al.*, 1990; Nomoto *et al.*, 1990; Conklin & Bourne 1993; Klein *et al.*, 2000) [Figure 8]. Dissociated G $\beta\gamma$ activates target proteins and initiates pheromone signaling. Roles of Gpa1 have been found by Metodiev *et al.* 2002 and show how Gpa1 modulates the mating pathway; Gpa1 directly interacts with MAP kinase Fus3, which positively regulates polarization and mating by membrane

localization of Fus3, whereas disruption of this interaction negatively regulates mating and promotes adaptation. Further study showed that G α subunit in its dissociated state acts as a negative regulator of pheromone response by inhibiting the pheromone induced localization of Fus3 in the nucleus (Blackwell *et al.*, 2003). Sst2, a GTPase-activating protein (GAP) augments the hydrolysis of GTP to GDP on G α causing G α to associate with G $\beta\gamma$ to form the G $\alpha\beta\gamma$ trimeric protein and prevent further signal transduction to the downstream effectors and cellular response for mating (Dohlman & Thorner, 1997, 2001; Lan *et al.*, 2000). Thus *S. cerevisiae* has a self-regulatory mechanism to control pheromone induced response; $\beta\gamma$ subunits activate the pathway and in contrast, G α subunit uses a negative regulatory mechanism to shut off pheromone signal downstream of the receptor.

1.4.3 Intracellular signal processing downstream of G $\beta\gamma$

G $\beta\gamma$ is tightly anchored to the plasma membrane through the γ subunit and recruits members of the effector molecules [Figure 7]. G $\beta\gamma$ promotes pheromone response signaling through activating three different effectors: the Far1-Cdc24 complex, Ste20 and Ste5, to regulate signaling for cell polarization, as well as for cell cycle arrest. In the polarization branch, G $\beta\gamma$ recruits Far1 bound to Cdc24, which is a GEF for the Rho-like small GTPase Cdc42 (Nern & Arkowitz, 1999). The Far1-Cdc24 complex undergoes dramatic nucleocytoplasmic shuttling; G $\beta\gamma$ binds the complex in the cytoplasm and bringing them to the plasma membrane where both Far1 and Cdc24 can be further anchored and stabilized by their pleckstrin homology domains (PH). When attached to the plasma membrane, Cdc24 activates its effector Cdc42, which is also bound to the membrane by geranylgeranylation (Klein *et al.*, 2000), by exchanging its GDP for GTP. Cdc24 also binds Bem1 (scaffold protein for complex that include Cdc24) (Ogura *et al.*, 2009) for establishing morphogenesis and cell polarity.

Activated Cdc42 activates a PAK-like protein kinase Ste20 that accumulates in the plasma membrane due to its binding with G $\beta\gamma$ through its specific G $\beta\gamma$ -binding domain (GBB) present at its C-terminus (Leberer *et al.*, 2000; Takahashi & Pryciak, 2007). Bem1 binds to the specific docking motif on Ste20, thus bringing the activated Cdc42 in juxtaposition to activate Ste20 (Winters & Pryciak, 2005b). Cdc42 induces auto-phosphorylation in the

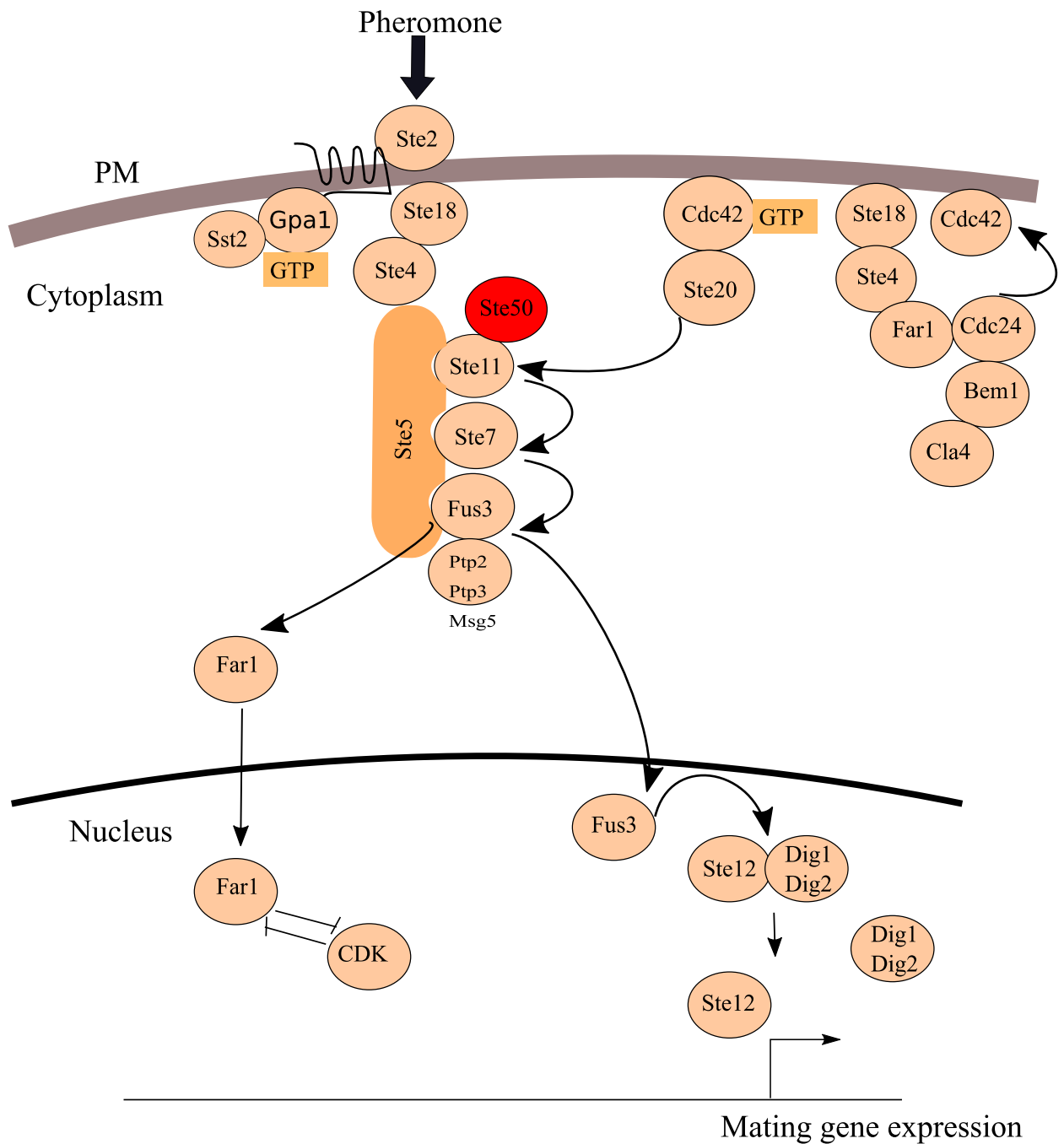


FIGURE 8: *S. cerevisiae* mating-pheromone response pathway.

activation loop of Ste20 thereby activates the first kinase in the mating signaling pathway. Ste20 is a MAP4K and activates the Ste11 MAP3K (Wu *et al.*, 1995; van Drogen *et al.*, 2000; Dan *et al.*, 2001).

Ste11 is restricted to the plasma membrane by two different means. First, Ste11 is connected to an adaptor protein Ste50 by interaction between their respective N-terminal

sterile alpha motifs (SAM) (Bhattacharjya *et al.*, 2004; Kwan *et al.*, 2006) and the C-terminal Ras association (RA) domain, which binds to Cdc42-GTP (Truckses *et al.*, 2006) that is plasma membrane bound. Secondly, the Ste11 interacts with the scaffold protein Ste5 that serves as a platform (Yerko *et al.*, 2013) and gathers the MAPK effectors Ste7 MAP2K and Fus3 MAPK to place them close together for facilitating their activation and thus signal transduction (Elion, 2001). Ste5 is complexed with these components and shuttles between nucleus/cytoplasm (Mahanty *et al.*, 1999). G β y captures the cytoplasmic Ste5 by its RING-H2 domain (Whiteway *et al.*, 1995; Inouye *et al.*, 1997) to tether it near the plasma membrane (Pryciak & Huntress, 1998), in a manner similar to Far1-Cdc24 complex. Membrane localization of Ste5 is further reinforced by an N-terminal phosphoinositide-binding (Winters & Pryciak, 2005a) and by a PH domain (Garrenton *et al.*, 2006). Bem1 was also shown to bind the SH3 recognition motif in Ste5 (Leeuw *et al.*, 1995) and thus pulls all of these components in close proximity at the membrane. Membrane recruitment of Ste5 initiates the cascade of phosphorylation events that ultimately lead to the phosphorylation and activation of a MAPK Fus3.

1.4.4 Scaffold protein of MAPK signaling

The MAPK cascade involves an evolutionarily conserved MAPK module consisting of MAP3K Ste11, MAP2K Ste7, MAPK Fus3. The scaffold protein Ste5 serves as a platform for the assembly of these proteins whether or not cells are exposed to pheromone (Choi *et al.*, 1994; Elion, 1995). By tethering the cascade components, Ste5 presumably provides insulation and prevents cross talk between pathways that share components (Schwartz & Madhani, 2004; Flatauer *et al.*, 2005). Ste5 binds Ste11, Ste7, Fus3 (Choi *et al.*, 1994; Marcus *et al.*, 1994; Printen & Sprague, 1994; Elion, 1995) and also binds the G-protein beta subunit (Whiteway *et al.*, 1995) and a polarity protein Bem1 (Leeuw *et al.*, 1995). Membrane recruitment of Ste5 delivers all the necessary effector molecules of this cascade to be in juxtaposition (Pryciak & Huntress, 1998; Feng *et al.*, 1998; Qi & Elion, 2005) and the signal transmission begins when Ste20 phosphorylates the N-terminal regulatory domain of Ste11 (Van Drogen *et al.*, 2000) brought in close proximity by Ste5. Activated Ste11 then phosphorylates conserved residues in the activation loop of Ste7 (Cairns *et al.*, 1992), which in turn phosphorylates and activates Fus3 MAPK and Kss1 MAPK (Gartner *et al.*, 1992; Errede *et al.*, 1993).

The view of Ste5 as a passive organizational platform is changing since many studies have shown it to be actively involved in signal regulation. One of the regulations involves allosterically assisting Ste7 MAP2K to selectively activate Fus3; activated Fus3 in turn phosphorylates Ste5 and negatively regulates the transcriptional output (Bhattacharyya *et al.*, 2006). Ste5 also discriminates between Fus3 and Kss1 MAP kinases; Ste5 is absolutely required for Fus3 activation, but not so much required for Kss1 activation (Choi *et al.*, 1994; Andersson *et al.*, 2004; Good *et al.*, 2009). The phosphatase Msg5 is also recruited by Ste5 to specifically inactivate Fus3 and not Kss1 (Andersson *et al.*, 2004).

1.4.5 Activation of Fus3 and its substrate activation

Fus3 gets activated by phosphorylation on its tyrosine and threonine residues located in the activation loop by Ste7 (Gartner *et al.*, 1992, Errede *et al.*, 1993), detaches from Ste5 and activates a number of substrates (Elion *et al.*, 1993). Fus3 has many protein substrates in diverse locations: the cytoplasm; the nucleus; the plasma membrane. Each substrate is focused toward a distinct cellular function; proteins that cause morphological changes are required for mating structure formation (shmoo); cell cycle arrest proteins allow the yeast to prepare for mating; cell membrane fusion proteins allow the shmoos to fuse.

1.4.6 Transcriptional activation

Activated Fus3 translocates to the nucleus and phosphorylates the Dig1/Rst1 and Dig2/Rst2 proteins. Unphosphorylated Dig1 and Dig2 bind and repress transcription factor Ste12 (Cook *et al.*, 1996; Tedford *et al.*, 1997). Dig1 and Dig2 bind different DNA region of Ste12 and repress Ste12 (Olson *et al.*, 2000). Phosphorylation of Dig1 and Dig2 relieves its repression of Ste12 and allow Ste12 to get phosphorylated and activated by Fus3 (Cook *et al.*, 1996; Tedford *et al.*, 1997). Activated Ste12 then binds to a consensus DNA motif, either as a homo-/ or heterooligomer with the Mcm1p protein, that are present in the pheromone responsive element (PRE) (Harrison & DeLisi, 2002) of gene promoters and activates transcription of many genes (about 200) related to polarization, cell fusion and mating (Roberts *et al.*, 2000).

1.4.7 Cell cycle arrest

The first cellular-level response to extracellular pheromone in budding yeast is to undergo cell cycle arrest, which halts multiplication processes in order to allow for mating preparation. Activated Fus3 is the mediator for this physiological change; it imparts G1 cell cycle arrest by phosphorylating the cell cycle inhibitor Far1 that inhibits Cdc28, a G1 cyclin bound form of CDK1, (Elion *et al.*, 1993; Peter & Herskowitz, 1994) and brings both *MAT α* and *MAT α* cells to the same stage of cell cycle. The mechanism of this cell cycle arrest involves the G1/S cyclins, Cln1 and Cln2 that recognize CDK substrates by specific docking motifs and promotes their phosphorylation (Bhaduri & Pryciak, 2011; Koivomagi *et al.*, 2011). Activated Far1 inhibits both the kinase activity and the substrate recognition by Cln1/2 (Pope *et al.*, 2014). In the presence of pheromone, Far1 relocates from the nucleus to the cytoplasm (Butty *et al.*, 1998). The level of Far1 is regulated by its proteosomal degradation; Far1 is degraded by the ubiquitin-dependent degradation system (Henchoz *et al.*, 1997) after being tagged by the Cdc28-Cln kinase that phosphorylates specific residues recognized by the G1/S degradation system (Henchoz *et al.*, 1997). Therefore, the level of Far1 is balanced by its expression during exposure to pheromone by Ste12 mediated increased transcription (Chang & Herskowitz, 1990) and stabilization by its Fus3 dependent phosphorylation (Peter *et al.*, 1993).

1.4.8 Polarization

The hallmark of pheromone response in yeast cells is morphological changes to form a polarized structure called a “shmoo”, named for cartoon character created by Al Capp in 1948. Yeast cells sense the pheromone concentration gradient from opposite mating partners and arrange their cytoskeletal structure to extend toward the most attractive prospective mate (Mackay & Manney, 1974; Segall, 1993). Polarization is chemotropic since it is directed towards the highest chemical gradient (Segall, 1993) and proteins involved in the polarization and the mating processes present themselves at the polarized moving front forming a patch (Bi & Park, 2012; Henderson *et al.*, 2018).

Mating projections are formed along a highly polarized structure along an axis in the direction of the shmoo tip. Organization of this structure requires redistribution of many

proteins, actin cytoskeleton, vesicular transport, such as exocysts, cytosolic differential protein localizations etc. (Narayanaswamy *et al.*, 2008). The protein Far1 is actively engaged in this process by interacting with the polarity establishment proteins. G β binds to the Far1–Cdc24 complex and pulls it towards the plasma membrane where Cdc24 exchanges GDP for GTP on Cdc42. GTP-bound active Cdc42 then binds Bem1, which is bound to Cdc24 and Cla4 (Kozubowski *et al.*, 2008). Polarization requires the formin Bni1, which gets phosphorylated and activated by Fus3 and helps in the polymerization of the actin filaments required for secretory vesicles to move to the growing shmoo tip (Evangelista *et al.*, 1997; Matheos *et al.*, 2004; Gao *et al.*, 2009). Cell polarity factors Spa2 and Pea2 are also involved in binding Bni1 at the site of polarization (Bidlingmaier & Snyder, 2004). The exocysts are also brought along with the secretory vesicles to the site of polarity and play a role in cell fusion (Guo *et al.*, 1999; Boyd *et al.*, 2004; Shen *et al.*, 2013; Liu & Novick, 2014).

1.5 Adaptor proteins

By definition, adaptors can be thought of protein molecules that connect two proteins together. In reality, they are not just passive connectors for molecules but possess regulatory properties for cellular information processing (Pawson & Scott, 1997). Although adaptors lack any enzymatic activity, they act in transducing upstream signaling to downstream components and are known to have signal amplification and signal specificity determinant properties. A general scenario of adaptor proteins is that they have modular domains that have docking sites for docking proteins with membrane targeting signals, such as PH domains, or a myristoylation site that is used to bring the complex near the membrane for activation (Pawson & Scott, 1997). By linking many proteins, adaptors generate a signaling complex that is required to elicit an appropriate response to environmental signals. The type of protein binding modules and the particular sequences in their motifs on the adaptor proteins guide the specificity of signaling, as well as their proximity to the binding partner and subcellular localization (Flynn, 2001).

In humans there are over 100 different adaptor proteins and an example are those that are upstream of RTK signaling, grouped according to their structures and functions (Gotoh, 2008). The first group is comprised of proteins that have multiple tyrosine phosphorylation sites and can bind downstream signaling components, often tethering them to the membrane through membrane localization domains. Once bound to the RTK the phosphorylation sites get phosphorylated and the adaptor can interact with SH2 domain containing proteins. Examples include GRB2 associated binding proteins (GAB), insulin receptor substrate (IRS), and Src homology 2 containing protein (SHC). The second group comprises of Src homology 3 (SH3) and SH2 domain containing proteins that have no phosphorylation sites and no membrane localization signals. Examples include GRB2, CRK and NCK (Gotoh, 2008). There are many adaptor proteins (<https://www.rndsystems.com/research-area/adaptor-proteins>) in human and describing them is beyond the scope of this thesis.

1.5.1 Ste50 adaptor protein

The adaptor protein Ste50 was identified in a genome-wide sequencing project of *S. cerevisiae* by Rad *et al.*, in 1991. It was characterized to be a protein essential for differentiation of cells when stimulated with pheromone. Critically, the C-terminus was found to be required for pheromone response signaling since deletion of its C-terminus suppressed cell cycle arrest induced by constitutively overexpressed *STE4* (Rad *et al.*, 1992). Ste50 is constitutively expressed in yeast and when overexpressed, increases Fus1 activity, whereas deletion causes reduced mating efficiency (Rad *et al.*, 1992) and attenuated cell cycle arrest in response to pheromone (Xu *et al.*, 1996); therefore, Ste50 is surmised to have an accessory role in pheromone response. Soon after, this protein was found to be required for filamentation (Rad *et al.*, 1998) and is also required to regulate Ste11 function in the Sho1 dependent HOG (high osmolarity glycerol) pathway (Posas *et al.*, 1998; Wu *et al.*, 1999; Raitt *et al.*, 2000; Rad, 2003). Ste50 is a 346 aa protein with a N-terminal sterile alpha motif (SAM) and a C-terminal Ras association (RA) domain linked by a Ser/Thr-rich region. Previous studies have established that the interaction of the Ste50 SAM domain with the SAM domain of Ste11 (MAP3K) is necessary for Ste11 function in all three yeast MAPK pathways - pheromone response, hyperosmolar stress regulation and pseudohyphal growth (Gustin *et al.*, 1998; Posas *et al.*, 1998; Wu *et al.*, 1999; Jansen *et al.*,

2001; O'Rourke *et al.*, 2002). Ste50 is phosphorylated on multiple serine/threonine residues by casein kinase and one of these phosphorylation sites, T42, has been found to regulate mating signaling (Wu *et al.*, 2003). Further, it was shown that under hyperosmolar condition Hog1 phosphorylates Ste50, which diminishes Kss1 activation and specifically activating the HOG signaling (Hao, *et al.*, 2008). Ste50 has homologous proteins in other fungal species. Although no proteins with sequence homology to Ste50 were found in other organisms, a human protein called Arap3, which is an effector of phosphoinositide (PI) 3 kinase is known to possess a RA domain and a SAM domain (Krugmann *et al.*, 2004). Arap3 acts as a GAP (GTPase activating protein) for Arf (ADP-ribosylation factor) and Rho G-proteins (Krugmann *et al.*, 2002). It is known that the RA domain of Arap3 interacts with Rap1 small G-protein (Krugmann *et al.*, 2004) and the SAM domain binds to the SAM domain of SHIP1 (SH2 domain-containing inositol 5' -phosphatase), which is a negative regulator of the PI3K signaling (Raaijmakers *et al.*, 2007).

1.5.1.1 SAM domain

The SAM domain of Ste50 is at the N-terminal region containing residues 27-109 (Grimshaw *et al.*, 2004) and the isolated SAM domain is monomeric in solution. The structure is quite similar to other SAM domains and also shows similarity to the Ste11 SAM domain (Bhattacharjya *et al.*, 2004; Kwan *et al.*, 2004; Grimshaw *et al.*, 2004); the Ste50 SAM domain is composed of five helices that form the core compact fold, and the specific hydrophobic residues that are required for homodimerization are buried in this SAM domain (Grimshaw *et al.*, 2004), suggesting that the molecule does not oligomerize. Kwan *et al.* 2004 showed that Ste50 couldn't interact with itself to form dimers. But this was contradicted later on by the work of Slaughter *et al.*, revealing that without pheromone stimulation, Ste50 oligomerizes *in vivo* and does not interact with Ste11, while pheromone stimulation decreases the size of this multimeric form (Slaughter *et al.*, 2008). The monomeric Ste50 SAM domain interacts with the dimeric Ste11 SAM domain through specific hydrophobic residues, and disrupting the hydrophobic interaction at residue I59, stops the binding to the Ste11 SAM domain and abolishes cellular response to pheromone (Kwan *et al.*, 2004). Ste50 appears to interact with Ste11 constitutively (Posas *et al.*, 1998).

1.5.1.2 RA domain

The RA domain of the Ste50 protein is in the C-terminal region and consists of 93 amino acids that span residues 235-327 (Schultz *et al.*, 1998; Kiel & Serrano, 2006; Letunic *et al.*, 2009). Among fungal species the RA domain of Ste50 protein is more conserved than its SAM domain (Truckses *et al.*, 2006). One of the documented functions of the RA domains is to act as an effector of small GTPases such as Ras by binding to its GTP-bound or activated form (Han *et al.*, 2017); however, the yeast Ste50-RA domain does not seem to bind Ras, but rather binds Cdc42 (Truckses *et al.*, 2006). RA domains are known to have a spectrum of partners other than Ras (Rodriguezviciana *et al.*, 1994; Morrison, *et al.*, 1988; Bhattacharya *et al.*, 2002; Sikai *et al.*, 2015). A structurally common feature among Ras association domains is their ubiquitin folds that has very little contact with the rest of the protein and possess sites for protein interactions through intermolecular beta sheets formed with Ras.

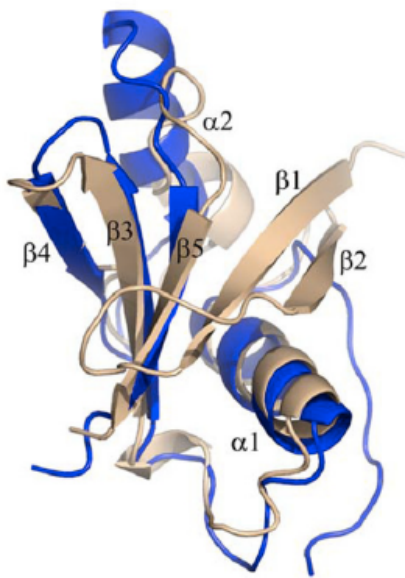


FIGURE 9: NMR solution structure of Ste50-RA domain. Ste50-RA domain (blue) overlaid on RalGDS RA domain (tan). Ref. Ekiel *et al.*, 2009 MBoC (with permission).

The structure of the Ste50-RA domain exhibits those signature ubiquitin folds and therefore categorized in the ubiquitin super fold family of proteins [Figure 9]. The NMR solution structure of this domain however shows a lack of two beta-sheets that are required for Ras interactions; these sheets are replaced by a more unstructured region (Ekiel *et al.*, 2009). This categorizes the Ste50-RA domain as a sub-family within the ubiquitin like superfamily. Detailed structural analysis found that the Ste50-RA domain can form a compact globular structure without the two canonical beta-sheets (Ekiel *et al.*, 2009). The amino acids between 250-261 are highly conserved among other Ste50 orthologues in fungi, whereas the amino acids 235-249 of the RA domain are highly variable (Ekiel *et al.*, 2009). The structure has the potential to bind

partners other than Ras-like small GTPases (Harjes *et al.*, 2006; Tong *et al.*, 2007). *In vitro* binding assays found this domain to interact with Rho-like small GTPases (Truckses *et al.*,

2006; Annan *et al.*, 2008). Deletion analysis showed that the core of this domain is required for signaling in the mating pathway (Ekiel *et al.*, 2009).

1.6 Specificity of signaling

Specificity of signaling is defined by how the input of a signal is selectively received and maintained during the transduction process to generate a specific output. To understand specificity we need to know how input signals are recognized, how components of one pathway shield themselves from other pathways, and what mechanisms control signaling through shared components. Due to the complexity of signaling networks, especially in higher organisms, many signals use common components and multiple signals could either converge on the common component giving rise to a single coordinated output or may diverge and give rise to differing outputs. A famous example involves the early studies on PC12 cells; these studies showed that stimulating the ERK MAPK pathway with nerve growth factor (NGF) caused a sustained activation of the ERK pathway, lead cells to differentiate and form neuronal cells, whereas stimulation with epidermal growth factor (EGF) caused a transient ERK pathway activation and resulted in the proliferation of PC12 cells (Marshall, 1995). Also, in *Drosophila melanogaster*, different tissues responded to the stimulation of the ERK MAPK pathway to elicit tissue specific differentiation (Brunner *et al.*, 1994; Madhani *et al.*, 1997a, 1998). Therefore, as early as these studies scientists suspected that there are other elements that help different signals retain their specific functions, while sharing signaling effector protein. Multiple mechanisms leading to signal specificity have been discovered since these pioneering studies, including sequestration, cross inhibition, kinetic insulation, combinatorial signaling, and preferred substrate interactions. An introduction to each of these strategies will be given below.

1.6.1 Mechanisms of signaling specificity

Sequestration

Sequestration is manifested by scaffolding, compartmentalization, and temporal separation (Smith & Scott, 2002; White & Anderson, 2005). Scaffold proteins sequester multiple components across its platform, thus forming distinct macromolecular complexes

(Whitmarsh & Davis, 1998) and can augment the reaction kinetics by facilitating information flow from one kinase to the other. In the pheromone response pathway in yeast, Ste5 is a great example of a scaffold protein that binds the Ste11, Ste7 and Fus3 kinases. Ste11 and Ste7 are common kinases shared by both the pheromone response and the filamentous growth pathways (Schwartz *et al.*, 2006). KSR is an equivalent example of mammalian scaffold protein, it binds the three kinases in the cascade and positively regulates ERK signaling pathway (Good *et al.*, 2009). Compartmentalization can achieve specificity by separating shared components in different subcellular compartments. Examples include ERK MAPK, which is activated by various extracellular stimuli; the temporal nature of ERK stimulation and its subcellular compartmentalization (nucleus) is required to achieve specificity of signaling needed in generating differential signaling responses (Ebisuya *et al.*, 2005). If different genes responsible for a MAPK pathway are expressed in a temporal fashion then it is possible to achieve specificity of signaling. Examples of temporal gene expression include genes that are expressed during the cell cycle and development. Cyclins and CDKs are expressed at different time points during the cell cycle and development, forming complexes that perform distinct functions (Cross, 1988; Nash *et al.*, 1988; Hadwiger *et al.*, 1989).

Cross Inhibition

Pathways with common components can inhibit each other; the two MAPK pathways controlling pheromone response and hyperosmolar glycerol response share components sequestered by scaffold proteins. Mutational analysis showed that HOG pathway represses the mating pathway under pheromone or HOG stimulation (Hall *et al.*, 1996; O'Rourke *et al.*, 1998). The HOG pathway is also inhibited by the pheromone response pathway (McClellan *et al.*, 2007). Fus3 negatively regulates the HOG pathway by expressing Fus1 that inhibits Sho1 (Nelson *et al.*, 2004). Fus3 also cross inhibits the filamentous growth pathway when under pheromone stimulation by lowering the magnitude and duration of Kss1 activation and by phosphorylating and targeting Tec1 for degradation (Bao *et al.*, 2004).

Kinetic insulation

The temporal nature of signal transduction pathways may contribute to pathway specificity. Pathways may exhibit very different kinase activity profiles [Figure 10]. In a scenario where pathways A and B share a common component C, the terminal kinases KA and KB may retain signaling specificity by kinetic insulation. If KA has a slow kinetics, then

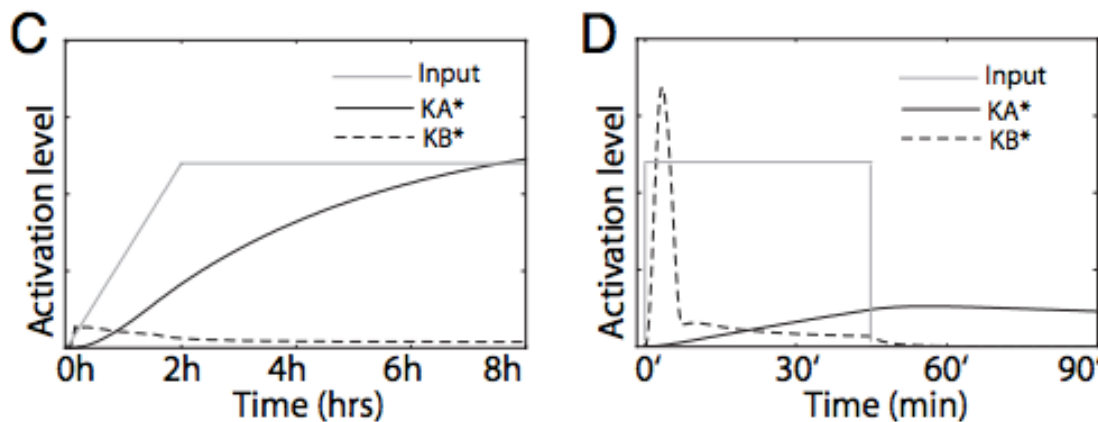


FIGURE 10: Kinetic insulation. Two different pathways A and B share a common component C. The kinetic profile of A (KA) with black solid line and the kinetic profile of B (KB) with black dashed line when a slowly increasing signal is received by the component C (C, Grey line indicates activation of component C) and the activation profile when signal is in a pulse of 45 min (D, activation is indicated by grey line). Ref. Behar *et al.*, 2007 (Copyright 2007, National Academy of Sciences, U.S.A, with permission.)

it would be prevented from getting activated by a transient short signal. On the other hand KB would not be activated by a signal that is slow and gradient. For example, the activity of the Hog1 MAPK is highly transient. Hog1 was found to be rapidly activated upon hyperosmolar stress within 30 min by quick deactivation (Klipp *et al.*, 2005). In contrast, pheromone response is graded, and even in saturating concentrations of pheromone, it takes about 60 min for Fus3 to achieve optimal MAPK activity, which slowly declines with time but remain active well over 90 min (Behar *et al.*, 2007).

Combinatorial signaling

Combinatorial signaling may contribute to signaling specificity. In combinatorial signaling two or more independent signals combine to form a composite signal that has a different

effect than the original signals. An example of combinatorial signaling specificity in yeast is observed in the case of Ste12 where both the mating and the filamentous signaling use the downstream Ste12 transcription factor. But in the case of filamentous signaling the Ste12 and Tec1 transcription factors bind cooperatively to the filamentous response enhancer (FRE) element to specifically promote filamentous growth (Madhani *et al.*, 1997b).

Kinase-substrate specificity

A kinase needs to recognize and interact with its specific substrate among thousands of potential phosphorylatable sites on various proteins. Therefore, protein phosphorylation has to be highly specific. Much of this is accomplished through mechanisms that include the actual kinase active site structure and the residues flanking the serine, threonine and tyrosine residues in its substrates (Ubersax & Ferrell, 2007). Docking interactions also

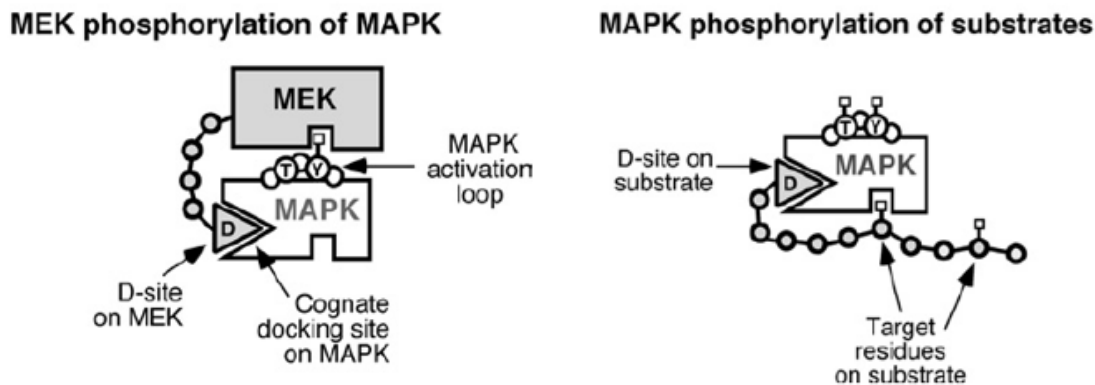


FIGURE 11: Kinase-substrate specificity. Ref. Bardwell, 2006 with permission.

enable a kinase to recognize and bind a substrate (Biondi & Nebreda, 2003; Bardwell, 2006; Goldsmith *et al.*, 2007) [Figure 11]. Many other mechanisms and factors are involved in kinase-substrate specificity, such as whether the kinase and its substrates are co-localized and co-expressed, and the local and distal interactions between them. In addition, adaptors and scaffolds play a role in mediating kinase actions (Faux & Scott, 1996a; Pawson & Scott, 1997). In case of co-localized kinases, distinct motifs are recognized by each enzyme to avoid unexpectedly phosphorylating non-target substrates (Faux & Scott, 1996b; Pinna & Ruzzene, 1996; Sim & Scott, 1999; Sharrocks *et al.*, 2000; Adams, 2001;

Biondi & Angel, 2003; Bhattacharyya et al., 2006; Remenyi et al., 2006; Shi et al., 2006; Alexander et al., 2011; Lai et al., 2016; Miller & Turk, 2018).

1.6.2 RA domain in MAPK signaling specificity

The Ste50-RA domain has been shown to regulate signaling specificity in two MAPK branches of *S. cerevisiae*, the filamentous growth and hyperosmolar stress pathways. In the filamentous growth pathway, the Ste50p-RA domain interacts with a Rho GTPase (Cdc42p) to specifically regulate the pathway (Truckses *et al.*, 2006). Residue I46 of Cdc42 was found to be critically required and is structurally located on the opposite side of the molecule to its switch I and II surface, which, in its GTP bound state, binds the effector Ste20. Cells containing an RA domain mutant I267A L268A that has reduced binding to Cdc42 either in its GTP or GDP bound state were found to be highly defective in filamentous growth. This interaction could be replaced by a plasma membrane targeting signal or a membrane localized Ste50 suppressing specifically the filamentous growth signaling Cdc42-interaction defective mutants. This suggests that Ste50-Cdc42 binding is essentially to tether Ste50-Ste11 to the plasma membrane to facilitate signaling.

The interaction of the Ste50-RA domain with the transmembrane protein Opy2 is required for the Sho1-branch of the HOG signaling pathway (Wu *et al.*, 2006). In the noncanonical ubiquitin fold of this RA domain the β 1 and β 2 strands are lacking; the unstructured peptide that corresponds to the sequence that would have formed the β 2-strand was found to be required for this interaction with the Opy2 (Ekiel *et al.*, 2009). Mutational studies showed that the regions interacting with Opy2 are involved in the α 1, α 2, β 5 and the intrinsically disordered region corresponding to the β 2 strand of the RA domain. Three peptide motifs in the intrinsically disordered region of the cytoplasmic tail of Opy2 are involved in this interaction (Ekiel *et al.*, 2009; Yamamoto *et al.*, 2010). These regions are functionally partially overlapping and collectively essential for HOG signaling. Ste50 RA domain mutants that are defective in HOG pathway signaling retain a normal functional signaling in the pheromone response pathway, suggesting that the RA domain is involved in differential connections with the shared MAP3K Ste11 to upstream component(s) to contribute to pathway signaling specificity.

1.7 Protein localization dynamics

The biological processes within a living cell are mostly regulated by changes in protein abundance and localization. Protein localization could indicate a protein's requirement at a place for executing its function. Many different mechanisms exist that control the presence of proteins in different cellular compartments, which include spatio-temporal gene expression regulation and protein turnover. But for cellular processes that are fast and require rapid use of proteins, trafficking of the functional proteins or their regulators is an effective method of control (i.e. importins, nuclear shuttling); by controlling the amount of protein at the target site a cellular process can be turned on or off. Many proteins in yeast have regulated localizations (Kumer *et al.*, 2002); the G1 cyclins Cln2 and Cln3 are differentially compartmentalized during the cell cycle (Edgington & Futcher, 2001); also, Cdc42 involved in cell polarization accumulates at the young bud tip (Smith *et al.*, 2013; Okada *et al.*, 2017) and Ste5 shuttling between nucleus and cytoplasm was also found to be necessary for pheromone signaling (Mahanty *et al.*, 1999). Such findings have revealed that a sizeable portion of yeast proteins, especially proteins involved in the MAPK pathways, is subject to controlled localization. Cells use many translocation methods to localize proteins; various transport systems exist, such as vesicular transport, nuclear transport, endomembrane system transport, peroxisomal transport, and mitochondrial transport (Rapoport *et al.*, 2017). Beyond these, the basic characteristics of a protein also dictate its localization, such as protein size, amino acid sequence, targeting signals, interaction domains, conformations and post-translational modifications. Since this dissertation describes wild type and mutant Ste50 cellular localizations in great detail, some of the factors that influence protein localization are presented below along with the transport mechanism involved in the nuclear localization of proteins.

Protein characteristics

The amino acid composition of a protein often dictates its localization, especially the surface exposed residues show correlation between different cellular compartments, suggesting that the proteins adapt to the environment of the residing compartments to be functional (Andrade *et al.*, 1998). In addition, the isoelectric points of proteins have been found to be very different among cytoplasmic, transmembrane and nuclear proteins

(Schwartz *et al.*, 2001). Protein size and hydrophobicity can also affect their distribution. For example, for nuclear localization, a protein of 40 kDa can pass through the nuclear membrane but larger molecules would be excluded. Many proteins possess targeting signals and these can vary considerably in length, composition and their position in the protein (Von Heijne, 1990). Examples include nuclear localization signals (NLS) and signal peptides required for entry into the endoplasmic reticulum.

Interaction domains

For a large number of proteins, their localization occurs due to binding to other proteins that either have particular localization signals or have other basic properties to reside in particular locations. These proteins usually have domains (Pawson, 2002) that can interact with other proteins, nucleic acids or lipids. Many of these domains have been discovered during molecular signaling studies where the function of these domains is to recruit pathway components to the membrane and also bring them in proximity for signal flow. Examples of domains include: SH2 and PTB domains that have recognition binding motifs for specific phosphotyrosine regions (Songyang *et al.*, 1993), SH3 and WW domains that bind to specific proline rich sequences and help form protein complexes, and PDZ domains that bind to specific C-terminal regions in the partner by beta-sheet augmentation (Cowburn, 1997).

Post-translational modifications

Many proteins undergo post-translational modifications (PTMs) to form the mature, functional proteins; these are covalent modifications usually mediated by enzymes. A common form of post-translational modification is phosphorylation since this can activate or inactivate an enzyme and control diverse biological pathways. Phosphorylation can regulate protein localization including transport to the nucleus (Jans, 1995); especially if the phosphorylation is close to a nuclear localization signal then it can affect the protein's nuclear localization. Thus by phosphorylating and dephosphorylating, the nuclear localization of protein can be regulated. Glycosylation is another type of PTM that promotes protein folding and stability; proteins that are not folded properly are translocated to the cytosol by the quality control machinery and are subjected to proteosomal degradation (Jakob *et al.* 1998). Attachment of lipids to proteins is yet another type of PTM that dictates

localization of proteins to the membranes. Common lipid modifications include myristoylation, palmitoylation and isoprenylation. Attaching GPI anchors to proteins while in the endoplasmic reticulum increases their hydrophobicity and results in membrane localization (Paulick & Bertozzi, 2008).

1.7.1 Protein transport

Very broadly, protein localization by transport can be grouped into three different categories: a) transport through large pores in the organelle membrane, such as traversing the nuclear membrane (Gorlich & Mattaj 1996) for nucleocytoplasmic shuttling; b) transport through membranes as translocation complexes (Rassow & Pfanner 2000; Meacock *et al.*, 2002) where the protein remains unfolded and is assisted through chaperones, such as transport through mitochondrial membrane, peroxisomes and ER; c) vesicular transport whereby proteins can be transported between compartments in vesicles (Rothman & Wieland, 1996). An invagination of the membrane in the donor compartment encloses the proteins. The vesicle moves from the donor to the receiving compartment, releasing the content. Lysosomes, secretory systems, plasma membrane and Golgi bodies use vesicle transport. I will describe here the nuclear transport system.

1.7.1.1 Nuclear transport

Protein translocation to the nucleus is well characterized, and tightly controlled by nuclear pore complexes. The nuclear pore complex is a large assembly consisting of nucleoporins (NUPs) that is embedded in and spans the nuclear envelope (Schwartz, 2005; Tran & Wente, 2006; Maco *et al.*, 2006; Schwartz, 2016). The NUPs are different nuclear pore proteins, and, in *S. cerevisiae*, there is around 30 of them present, most of which are conserved among eukaryotes (Doye & Hart, 1997; Rout *et al.*, 2000). The nuclear pore complex thus formed is recognized by the chaperon transport receptors, karyopherins (Ström & Weis, 2001; Pemberton & Paschal, 2005) that transiently bind to the complex and are required for the protein to traverse the nuclear pore. Other than karyopherins, the nuclear pore complex is impermeable to most macromolecules. Tiny molecules, such as water, amino acids, ions, and nucleotides can freely cross the pore complex, but larger molecules such as proteins require transporters called importins and exportins to enter and exit the nucleus. In the cytoplasm, importins bind their cargo either directly or

indirectly through adaptor proteins, anchor to the nucleoporins, and translocate to the other side of the nuclear envelope releasing their cargo. Release of cargo is achieved by binding with GTP-bound Ran GTPase, a Ras-related GTPase that regulates delivery of cargo by these systems (Moore & Blobel, 1993; Melchior *et al.*, 1993). Nuclear export involves cargo recognition inside the nucleus in the presence of RanGTP, exporting the cargo to the cytoplasm and then releasing it by GTP hydrolysis to GDP.

Nuclear proteins are usually tagged with a nuclear localization signal sequence (NLS) that binds to importins for entry into the nucleus. Proteins that exit the nucleus possess a nuclear export signal (NES) that binds to exportins. The NLS signal in a protein can be recognized by its characteristics; mainly these sequences are hydrophilic, some consists of a short stretch of basic residues that have sequence similarity with SV40 large T antigen NLS (Kalderon *et al.*, 1984). In others, there is a bipartite signal consisting of two portions of basic residues separated by a relatively short spacer of 10-12 residues (Dingwall *et al.*, 1988). Beside these, there are other nonclassical NLS that are composed of a mixture of polar and nonpolar residues, which are found in NLS of Mata2 and vRNPs proteins (Mattaj & Englmeier, 1998; Nakada, 2015). NES signals (Gorlich & Mattaj, 1996) consists of four hydrophobic residues with a sequence motif of LxxxLxxLxL, L=hydrophobic residue and X=any amino acid (la Cour *et al.*, 2004). NLSs interact by hydrogen bonding with a series of asparagine residues on the importin (Kunzler *et al.*, 2001; Cook *et al.*, 2007).

1.8 Genetic suppression of mutants

Genetic suppression is a classical strategy to identify genetic interactions between genes and assess their relationship and involvement in that biological process. The commonly employed approaches to suppress the phenotypic defect of the query mutant gene function are through either overexpression or deletion (loss-of-function) of other genes. For gene overexpression, there are three general ways to overproduce genes: (a) expression of open reading frames under a strong promoter, such as GAL1, GAL10, TDH3 and ADH1; b) transformation with plasmid vectors that replicate in multiple copies and contain the gene of interest; c) amplify gene copy numbers, for example Ty transposition vectors random insertion in the genome to amplify gene copy number (Rine, 1991). A specific type of

suppressor assay is routinely used, where the genetic interaction is identified through overexpressed library genes from a 2 μ plasmid vector that can suppress the phenotypic defect caused by mutation in the query gene (Prelich, 1999). In this approach a high copy plasmid, bearing a genomic library, is transformed into the strain to be suppressed. The selection is based on user specification but usually selection conditions are used that identifies growth due to promoter activity. High dosage gene suppression can result from direct interaction with the defective query mutant or it might be due to increasing the gene products that are activators of either upstream or downstream components that can compensate the query mutant in the pathway. One can dissect these possibilities genetically or biochemically determining if the proteins physically interact.

A clear advantage of genetic suppression assay over other methods in establishing the relationship between two genes results from its power of suppression to illuminate the molecular relationship between the genes that can occur through various mechanisms. These mechanisms include compensating for defective interactions, regulation by post-translational modifications, regulation by inhibiting or activating either upstream or downstream components in the same signaling pathway or through activation of other pathways (Rine, 1991). The suppressor assay is valuable in establishing relationships between gene products and can help decipher roles of uncharacterized genes in the genome. This dissertation sets to search and investigate cellular component(s) that when overexpressed can genetically suppress the Ste50-RA mutants specifically defective in pheromone signalling.

1.9 Objectives

Our objective is to understand the fundamentals of cellular signaling specificity. In a scenario where multiple signaling pathways share a common component, how do different stimuli retain the specificity of their responses? Yeast MAPK pathways present such a scenario and serve as a simple prototypical model, where multiple MAPK pathways share components and provide us with a simple system to study stimulus/response to decipher signaling specificity. One of the well-studied MAPK pathways in yeast is the mating MAPK pathway; this pathway has been extensively studied because of its simplicity and clear

input/output behaviour. Almost all the major components in this pathway have been identified and their activities during pheromone signal transduction from the receptor to the nucleus have been established. However, how the mating signal is specifically transduced through the MAPK3K Ste11, a shared component, is still poorly understood. The Ste50 adaptor protein is an interacting partner of Ste11. Previously, we have established that the structure of the Ste50-RA domain has unique features that may allow it to attain differential interaction modes to interact with specific partners (Ekiel *et al.*, 2009).

Therefore, the objective of this research was to determine the molecular role of Ste50 in the regulation of the pheromone signaling pathway. Based on previous findings, the RA domain appears to play a critical role in the regulation of the three major yeast MAPK pathways (Wu *et al.*, 2006). Because RA domain mutants defective in the interaction with the Opy2p protein only effect the HOG signaling pathway (Ekiel *et al.*, 2009) and RA domain interaction with Cdc42 effect the filamentous growth pathway (Truckses *et al.*, 2006), we hypothesized:

The RA domain will utilize a different region to specifically connect Ste11 to the mating-pheromone response-signaling pathway.

This hypothesis will be tested by generating libraries of Ste50 variants consisting of mutations in the RA domain introduced through error-prone-PCR-based random mutagenesis, and screening for variants that are specifically defective in mating-pheromone-response-siganling.

In order to understand the structural basis of the Ste50 function in specific regulation of pheromone signalling, we will utilize structural bioinformatics analyses of the *ste50* mutants using the solution structure of Ste50.

We will use live cell microscopy to study the localization profiles of the wild type and Ste50 mutants and perform single cell analysis of the cellular localization of Ste50 and its mutants in response to pheromone.

Specifically-pheromone-response-defective mutants obtained will be used to identify potential regulators of Ste50p in the mating pathway. This will be achieved through

identifying genetic suppressors of these mutants. We hypothesize:

Overexpressing certain regulators of Ste50p could functionally compensate these partially defective Ste50 mutants.

This hypothesis will be tested in a yeast strain (*MATa ste50Δ FUS1::HIS3 sst2::ura3 far1::hisG*) that has a pheromone signaling reporter and can only grow in a histidine-lacking medium when a functional pheromone signaling pathway is present.

Chapter II: Adaptor protein Ste50 directly modulates yeast MAPK signaling specificity through differential connections of its RA domain

Nusrat Sharmeen,^a Traian Sulea,^{b,c} Malcolm Whiteway,^{d,*} Cunle Wu^{a,b,*}

Mol Biol Cell 2019 Mar 15; 30(6): 794-807. doi: 10.1091/mbc.E18-11-0708.

^aDivision of Experimental Medicine
Department of Medicine
McGill University
Montreal, QC, Canada H4A 3J1

^bHuman Health Therapeutics Research Centre
National Research Council Canada
6100 Royalmount Avenue
Montreal, Quebec, Canada H4P 2R2

^cInstitute of Parasitology
McGill University
Sainte-Anne-de-Bellevue
QC, Canada H9X 3V9

^dDepartment of Biology,
Concordia University
Montreal, QC, Canada H4B 1R6

2.1 Preface

This article was published in *Molecular Biology of the Cell*. Here we addressed a fundamental question about eukaryotic systems - how multiple signaling pathways that share common components retain their signaling specificity. In the model yeast system, the Ste50-RA (Ras Association) domain has previously been shown to specifically direct MAPK signaling in the HOG and filamentous growth pathways, but a specific connection to the mating pathway had not been identified. In this manuscript we show that the RA domain has critical residues specifically directing signaling through the mating and HOG MAPK signaling pathways. These residues form distinct patches with residues specifically required for one pathway clustered together on the three-dimensional structure of the RA domain. These patches could be potential protein-protein interaction sites. The critical residues responsible for specific pheromone signaling are required for protein association and localization, GFP tagging and live cell imaging appear to support such a notion. Thus, our study shows that the RA domain of Ste50p uses different interaction modes for associating with different partner proteins conferring MAPK signaling specificity.

Author contributions:

Nusrat Sharmeen	Conceptualized, Methodology, Designed experiments, Performed investigations, Performed formal analysis, Wrote the original manuscript, and Edited manuscript extensively.
Traian Sulea	Performed mainly NMR modeling and analyzed its results, Figure S2, Table S2 and Figure 5 preparations and write up for Figure 5. Edited the manuscript.
Malcolm Whiteway	Conceptualization, Methodology, Edited the manuscript.
Cunle Wu	Conceptualization, Methodology, Edited the manuscript.

2.2 Abstract

Discriminating among diverse environmental stimuli is critical for organisms to ensure their proper development, homeostasis, and survival. *Saccharomyces cerevisiae* regulates mating, osmoregulation, and filamentous growth using three different MAPK signaling pathways that share common components and therefore must ensure specificity. The adaptor protein Ste50 activates Ste11p, the MAP3K of all three modules. Its Ras association (RA) domain acts in both hyperosmolar and filamentous growth pathways, but its connection to the mating pathway is unknown. Genetically probing the domain, we found mutants that specifically disrupted mating or HOG-signaling pathways or both. Structurally these residues clustered on the RA domain, forming distinct surfaces with a propensity for protein-protein interactions. GFP fusions of wild type (WT) and mutant Ste50p show that WT is localized to the shmoo structure and accumulates at the growing shmoo tip. The specifically pheromone response-defective mutants are severely impaired in shmoo formation and fail to localize ste50p, suggesting a failure of association and function of Ste50 mutants in the pheromone-signaling complex. Our results suggest that yeast cells can use differential protein interactions with the Ste50p RA domain to provide specificity of signaling during MAPK pathway activation.

Key words: RA domain, Ste50, MAPK signaling, Yeast, Specificity, Pheromone response.

2.3 Introduction

The development and survival of organisms depends on their ability to receive environmental stimuli and transduce them through signaling pathways to elicit specific responses that control cellular processes. This is accomplished by numerous modular signaling pathways (Mayer, 2015). Many signaling pathways share common component(s). A fundamental question in the field of signal transduction is how the myriads of inputs are sensed, integrated, and transduced accurately so that each elicits a specific and proper biological response.

A well-studied example of component overlap is found in the yeast *Saccharomyces cerevisiae*. Shared components are found in three major mitogen-activated protein kinase (MAPK) signaling pathways—the mating pheromone response pathway, which controls a developmental transition in response to pheromone, the high-osmolarity glycerol (HOG) pathway, which maintains homeostasis in response to environmental stress, and the pseudohyphal growth pathway, which controls cellular morphology in response to nutrient signals (Herskowitz, 1995). One of the shared components of these pathways, MAP3K Ste11, is part of the basic MAPK module consisting of MAP3K, MAP2K, and MAPK; this module is highly conserved among eukaryotes [Figure 1]. MAP3K Ste11, which is located at the top of these MAPK modules, serves as a critical point of regulation in MAPK signaling (Craig *et al.*, 2008). For normal function, Ste11 kinase must interact with the Ste50 adaptor protein, which is a small multidomain protein consisting of a conserved N-terminal SAM (sterile alpha motif) and a C-terminal RA (Ras association) domain connected by a linker region. Previous studies have established that the interaction of the Ste50 SAM domain with the SAM domain of Ste11 (MAP3K) is necessary for Ste11p function in all three pathways—pheromone response, hyperosmotic stress regulation, and pseudohyphal growth (Gustin *et al.*, 1998; Posas *et al.*, 1998; Wu *et al.*, 1999; Jansen *et al.*, 2001; O'Rourke *et al.*, 2002; see Figure 1). Studies have shown that costimulating individual yeast cells with pheromone and osmotic stress activates both pathways independently without interference, indicating sufficient insulation for pathway specificity (Patterson *et al.*, 2010).

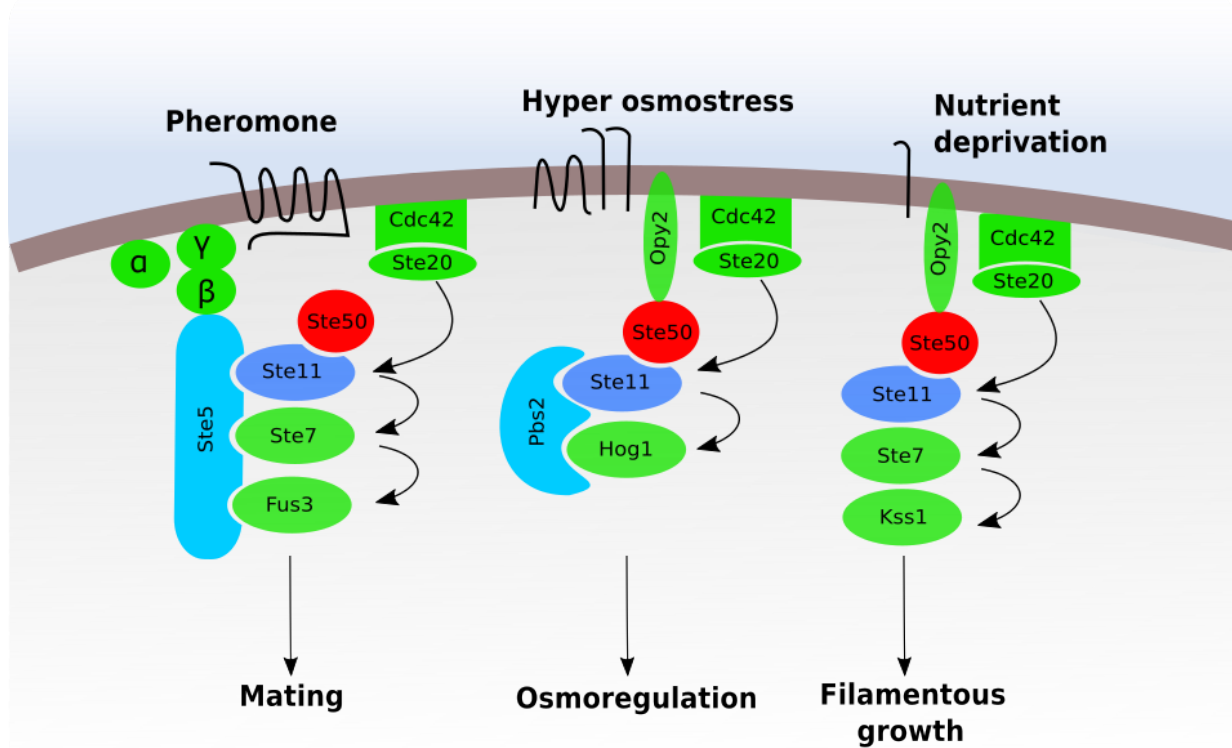


FIGURE 1: MAPK pathways with shared components in *Saccharomyces cerevisiae*. The pheromone, osmstress and nutrient deprivation are the three MAPK pathways that regulate mating, osmstress and filamentous growth. All three pathways share the MAP3K Ste11 and the adaptor protein Ste50 that interacts with Ste11p (Gustin *et al.*, 1998; Posas *et al.*, 1998; Wu *et al.*, 1999; Jansen *et al.*, 2001; O'Rourke *et al.*, 2002).

A general theme of adaptor protein recruitment in a signaling pathway is amplification of signaling through contribution of additional docking sites for modular signaling (Pawson and Scott, 1997). Adaptors involved in specificity of signaling have been extensively documented (Songyang *et al.*, 1993; Stein *et al.*, 2003; Qamra and Hubbard, 2013), and this specificity role appears to have been adopted by Ste50p through its C-terminal RA domain. The RA domain of Ste50p is absolutely required to ensure proper function of the three MAPK pathways in yeast. The Ste50-RA domain apparently does not bind Ras; rather it has been found to bind the related membrane-anchored Rho small GTPase family member Cdc42p (Tatebayashi *et al.*, 2006; Truckses *et al.*, 2006), as well as a transmembrane protein, Opy2p (Wu *et al.*, 2006). Binding of these proteins with the Ste50p RA domain

appears to direct Ste11p signaling in specific pathways: Opy2p in the HOG pathway (Tatebayashi *et al.*, 2006; Wu *et al.*, 2006) and Cdc42p in the pseudohyphal growth pathway (Truckses *et al.*, 2006). Pathway regulation by the Ste50p RA domain via interactions with various protein partners was found to facilitate Ste11p membrane localization, where it can be phosphorylated and activated by the PAK Ste20p. Detailed analysis of Ste50p and Opy2p interaction showed that specific peptide motifs in the disordered cytoplasmic tail of Opy2p interact with certain Ste50p RA domain residues to specifically regulate HOG signaling (Ekiel *et al.*, 2009; Yamamoto *et al.*, 2010). Interestingly, Opy2p is not required for pheromone response, as yeast cells deleted for *OPY2* show normal pheromone response (Wu *et al.*, 2006).

RA domains have been identified in many other organisms, including humans. Structurally, RA domains adopt a ubiquitin fold and are capable of interacting with a wide spectrum of partners, including the Ras small GTPase, the Raf serine/threonine protein kinase, PI3K families of lipid kinases, the Ral guanine nucleotide dissociation stimulator (RalGDS), and RASSF tumor suppressor family members (Morrison *et al.*, 1988; Rodriguez-Viciano *et al.*, 1994; Bhattacharya *et al.*, 2002; Sakai *et al.*, 2015). NMR solution structure analysis of the Ste50p RA domain indicated that it lacks the two canonical N-terminal beta-sheets required for Ras interaction, and this region is rather more unstructured (Kiel and Serrano, 2006; Ekiel *et al.*, 2009). Thus, the Ste50p RA domain defines a subfamily within the ubiquitin-like superfamily and exhibits the potential to bind partners other than Ras-like small GTPases (Harjes *et al.*, 2006; Tong *et al.*, 2007). Although it is established that the RA domain is necessary for Ste50p function in regulating the pheromone response pathway (mating), the molecular role of Ste50p function in this pathway remains unclear; specifically, whether the Ste50p RA domain is connected to the pheromone response pathway is unknown.

In this study, we have genetically probed the functioning of the RA domain of this Ste50p adaptor molecule shared by multiple MAPK pathways in yeast and analyzed how mutations affect signaling specificity. Most interestingly, mutants that are specifically defective in pheromone response provide new evidence that the Ste50-RA domain utilizes different residues to play vital roles in connecting the function of the Ste50 adaptor protein to ensure MAPK pathway signaling specificity.

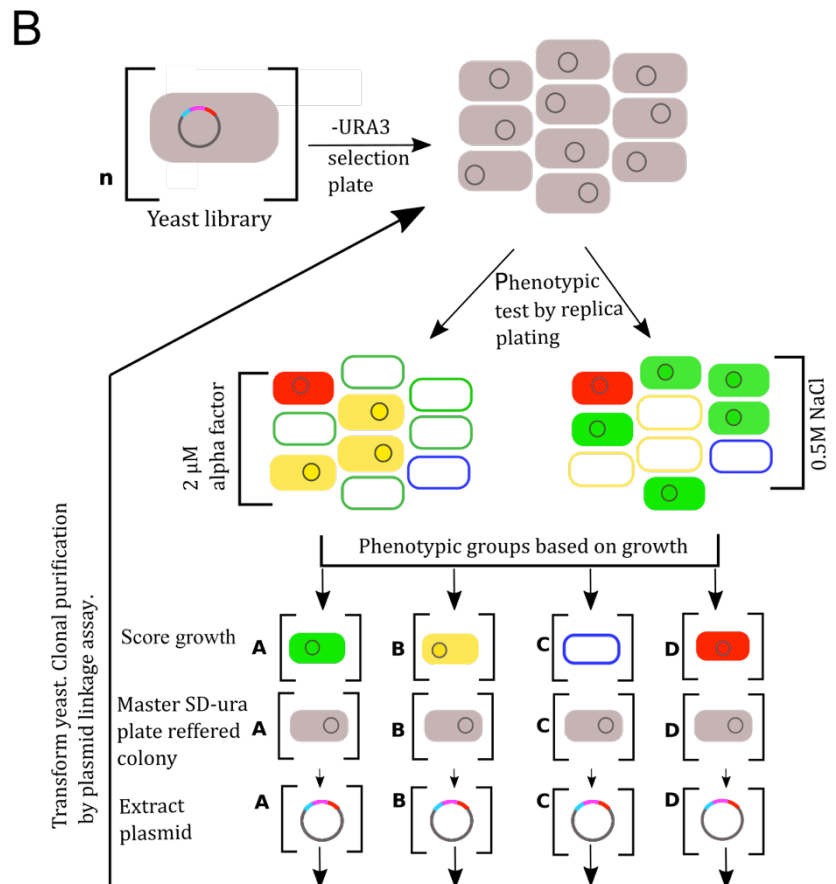
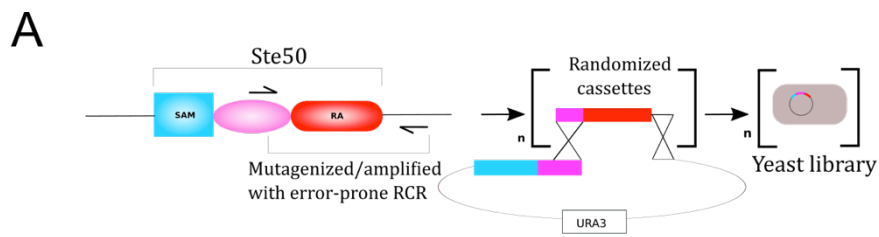
2.4 Results

Ste50-RA domain mutant libraries

The Ste50p adaptor protein is a 346 amino acid residue protein consisting of a N-terminal SAM and a C-terminal RA domain connected by a linker region [Figure 2A]. The RA domain consists of 93 amino acids, spanning residues 235-327 (Schultz *et al.*, 1998; Kiel and Serrano, 2006; Letunic *et al.*, 2009). We randomly mutagenized (as described in *Materials and Methods*) between residues 147-346 spanning the RA domain to introduce point mutations generating phenotypic changes. Three libraries were built under different PCR conditions to maximize the number of events causing a few (1 to 3) amino acid changes per clone. The resulting libraries consisting in total of ~72,000 primary *in vivo* recombination (IVR) transformants were subjected to phenotypic screening analysis.

Screening the mutant libraries revealed four distinct phenotypes

If the Ste50p RA domain functions differently in the pheromone response pathway and the HOG pathway, one would expect that the differential RA domain functions should be genetically separable. To delineate the amino acids in the RA domain that are important for distinctive signaling properties, we performed an extensive phenotypic screen [see Methods and Figure 2B] for mutants in the Ste50-RA domain. We studied the ability of these mutants to show specific phenotypes. Using the growth/no-growth screening conditions under pheromone and osmotic stress (see *Materials and Methods*), we anticipated four possible phenotypic combinations among the two chosen MAPK pathways [Figure 2C]; i) Wild type - no growth in the presence of pheromone, normal growth under hyperosmolar stress; ii) Mutants specifically defective in pheromone response - pheromone resistant growth, hyperosmolar stress resistant growth; iii) Mutants specifically defective in HOG pathway- no growth in the presence of pheromone, hyperosmolar stress sensitive; iv) Mutants that are defective in both pathways - pheromone resistant growth, hyperosmolar stress sensitive. We identified all of the four above mentioned expected phenotypes from the screens [Figure 2D]. In total 90,000



C

Groups	Ste50 alleles	Growth on pheromone	Growth on NaCl
A	WT	-	+
B	Mating & HOG signal defective	+	-
C	Specifically HOG signal defective	-	-
D	Specifically mating defective	+	+

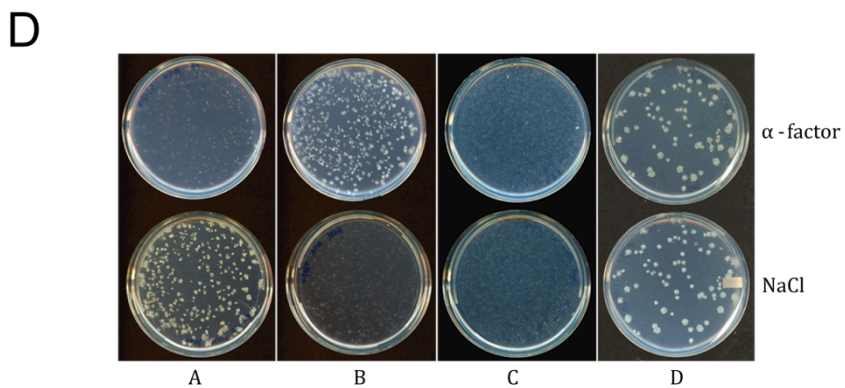


FIGURE 2: Ste50-RA domain mutant library construction and screening. A) Random mutagenesis of Ste50-RA domain with error-prone PCR and homologous recombination in yeast was used to create the mutant libraries. B) Library was plated on SD-ura, replicated onto selective media containing 2 μ M α -factor or 0.5M NaCl. Phenotypes scored on both plates and grouped according to their growth patterns by comparing both plates. Library clones conferring a growth phenotype: wt green, specifically pheromone signal defective red, specifically HOG signal defective blue, defective in both pheromone and HOG signaling yellow. Colored filled and hollow shapes represent growth and no growth respectively of the corresponding phenotypes (same color codes). Plasmids were extracted from colonies of each phenotypic group by referring back to the master SD-ura plates. Rescued plasmids were reintroduced into yeast to recapitulate the originally observed phenotypes (plasmid linkage assay). C) All four expected possible phenotypes grouped as A, B, C and D. Growth (+) and no growth (-). D) Phenotypes of the representative candidates obtained from the library screens.

colonies were screened (equivalent to \sim 1.25X of the combined mutant libraries) and the candidates obtained were put through further confirmations by rigorous plasmid linkage assays (see Methods) [Figure 2B]. Finally, 108 clones possessing the different phenotypic properties were selected for further analysis.

Critical residues in the Ste50-RA domain specifically control pheromone and HOG signaling pathways

To identify the mutation(s) in the final 108 clones, we performed Sanger sequencing and analysed their sequences (see Methods). Sequencing revealed that 57 clones either had frame-shift mutations or introduction of stop codons leading to truncated proteins. The remaining 51 mutant clones bearing mostly 1-4 point mutations fell into the four different categories, with some recurrent hits. These mutants included 7 specifically pheromone signal defective mutants [Table 1A]; 9 (non-redundant) specifically HOG signal defective mutants [Table 1B] and 3 (non-redundant) pheromone and HOG signal doubly defective mutants [Table 1C]. Sequencing also identified clones showing wild type function bearing point mutations, suggesting that alterations of these residues had no detectable defect in

signaling in either of the MAPK pathways investigated [Table S1]. Altogether, these mutations altered 62 unique residues in the Ste50p region amplified by PCR. Within the RA domain [Figure 3, boxed], 39 residues were changed [Figure 3, red] (a total of 48 different replacements were made on these residues) generating ~42% amino acid replacements; some of these changes causing specific phenotypes supported observations made in a previous study (Ekiel *et al.*, 2009). Our results suggest that the specific amino acid substitution for a particular residue could be a crucial determinant of its functionality, for example, changing H275 from histidine to proline yielded a strong specific HOG signaling defective phenotype, while changing it to alanine caused only a weak phenotypic effect [Table 1B and Ekiel *et al.*, 2009]. Mutants showed variability in the number of amino acid substitutions and the strength of phenotypes displayed. In the specifically-pheromone-response-defective class, the strongest phenotypic mutants included M_w_1 (R283G Q294L) and H3N_3 (R296G); while the triple mutants R6 (A242G N270D I289T) and G4 (K260N L300V I307K), as well as the double mutant M10N_2_2 (V288D D328V) also showed significant pheromone response defects [Table 1A]. L182P L277S mutant was isolated from multiple independent specifically-HOG-signal-defective clones. We wanted to identify the mutations responsible for the phenotypic effects in clones with multiple mutations, so we dissected them.

STE50 YCL032W SGDID:S00000537
MEDGKQAINEGSNDASPDLDVNGTILMNNEDFSQWSVDDVITWCISTLEVEETDPLCQ
RLRENDIVGDLLELPELCLQDCQDLCDGDLNKAIFKILINKMRDSKLEWKDDKTQEDMI
TVLKNLYTTTSAKLQEFQSQYTRLRMDVLDVMKTSSSSPINTHGVSTTPSSNNTII
PSSDGVSLSQTDYFDTVHNRQSPSRRESPTVTVFRQPSLSHKSLSLHKDSKPKVPQISTN
QSHPSAVSTANTPGPSPNEALKQLRASKEDSCERILKNAMKRHNLADQDWRQYVLVIC
YGDQERLLELNEKPVIFKRLKQQGLHPAIMLRRGDFEEVAMMNGSDNVTTPGGRL

FIGURE 3: Ste50p amino acid sequence showing point mutations. The protein contains 346 amino acid residues. RA domain spans 235-327 residues (shown boxed, dark blue) (Schultz, 1998; Kiel and Serrano, 2006; Letunic, 2009). Error-prone mutagenic PCR has led to random changes in the region shown in light blue, which includes 62 residues that are in red.

For the dissections, we selected clones based on their strong phenotypic traits. From the specifically-pheromone-response-defective group we selected a number of clones since we were most interested in this new class; therefore, clones R6, G4 and M_w_1 were dissected. The R6 & G4 mutants were analyzed by gBlocks DNA synthesis (Integrated DNA technology) while M_w_1 was dissected by site-directed mutagenesis (see *Materials and Methods*). Recombinant plasmids of the variants were sequence verified and re-tested in pheromone and osmotic stress assays [Table 2 and Figure S1]. For the R6 mutant, the single mutation I289T was found to be the driver mutation [Table 2, Figure S1A]. For the G4 triple mutant, the single mutants showed only weak phenotypes, but the strong

TABLE 1: Ste50-RA domain desired mutants from library screens

A. Ste50 specifically pheromone signal defective mutants			
Clones	Mutations	Growth on α -factor	Growth on NaCl
H3N_3	R296G	+++++	++++
M_w_1	R283G Q294L	+++++	++++
R6	A242G N270D I289T	++++	++++
G4	K260N L300V I307K	++++	++++
M10N_2_2	V288D D328V	++++	++++
H11N_2	I289V R323G	+++	++++
M1N	I289T	+++	+++
B. Ste50 specifically HOG signal defective mutants			
M6_2	K149R H219Y N250I L277S I320M	-	-
O2-1	K223N K225E R274S H275Y L322F V340G	+	-
H16	L182P L277S	-	-
M6	H219Y L277S I320M	-	-
H1N_2	S154Y H275P	-	-
H4N_2	A271T L277S	-	-
H7N_2	H275R	-	-
H8N_2	N250S L277S N310S	-	-
H9N_2	V180E L277S K303R N335S	-	-
C. Ste50 pheromone and HOG signal defective mutants			
3-7	L322S	+++++	-
Mol. Bio. 2009	I320K	+++++	-
M2N_2_1	K260E C290S P304S	++++	-

Note: ++++++ is 100% functional in HOG signaling and - is 100% functional in pheromone response. Mutations causative for the observed phenotypes are in bold.

phenotype was almost fully retained by the double mutants containing the I307K mutation [Table 2 and Figure S1B]. In the case of M_w_1 (R283G Q294L) interestingly, the double mutations were critical; both single mutants appeared WT [Table 2 and Figure S1C]. To further investigate the complex multiple mutational phenotypic behavior, we performed transcriptional activation assays with G4 and M_w_1 mutants and their mutational dissects using a FUS1-LacZ promoter-reporter system (see Methods) [Figure 4]. The double mutant M_w_1 (R283G Q294L) showed severe defect, only ~14% of the wild type pheromone response. Interestingly, the dissected single mutation could not recapitulate the transcriptional output of the double mutant; R283G and Q294L showed almost 80% and

TABLE 2: Mutational dissections of multiple mutations to find causal mutation(s)

Clones	Mutations	Growth on 2 μ M α -factor	Growth on 0.5M NaCl
R6	A242GN270DI289T	++++	+++
Dissects	A242GN270D	-	+++++
	N270D	-	+++++
	A242G	-	+++++
	I289T	++++	++++
	N270DI289T	++++	++++
	A242GI289T	++++	+++
G4	K260NL300VI307K	++++	++++
Dissects	K260N	-	+++++
	L300V	-	+++++
	I307K	-	+++++
	K260NL300V	-	+++++
	K260NI307K	++++	++++
	L300VI307K	++++	++++
M_w_1	R283G Q294L	+++++	++++
Dissects	R283G	-	++++
	Q294L	-	++++
H16	L182P L277S	-	-
Dissects	L182P	-	+++++
	L277S	-	-

39% of the wild type pheromone response respectively, where Q294L appears as the driver mutation. For the triple mutant G4 (K260N L300V I307K), all three mutations are needed for the strong pheromone response defect [Figure 4] although, I307K seems to be the mutation effecting the most.

In addition, the HOG specific double mutant L182P L277S was subjected to site-directed mutagenesis to identify the driver mutation(s); the single mutation L277S was found to cause the observed phenotypic effects [Table 2 and Figure S1D]. The other multiple-point mutants causing strong phenotypes with defects specific to HOG signaling include at least one mutation at positions R274, H275, L277 as seen here and previously (Ekiel *et al.*, 2009); these positions were predicted to harbor the driver mutation in these cases [Table 1B].

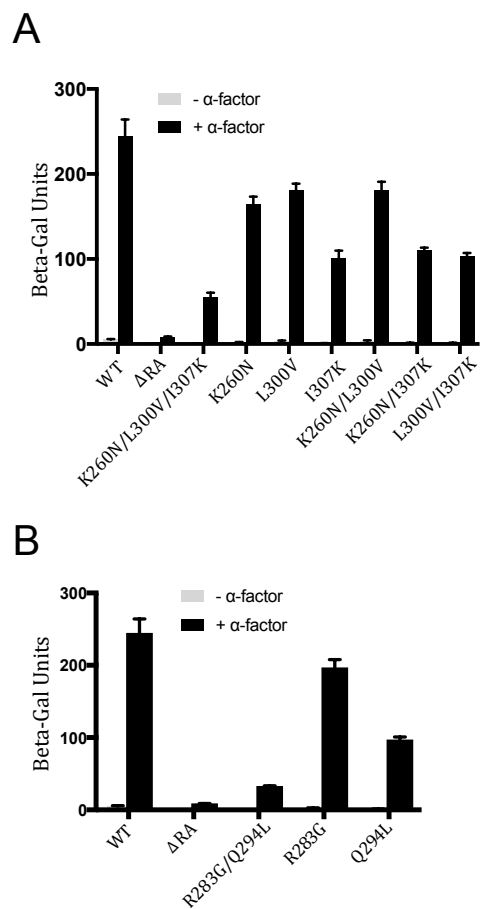


FIGURE 4: Transcriptional activation of Ste50-RA domain mutants. Yeast strain ($\Delta ste50$, *FUS1-LacZ*) harboring Ste50-RA domain mutant G4 (K260N/L300V/I307K) and its mutational dissected derivatives (A) or mutant M_w_1 (R283G/Q294L) and its mutational dissected derivatives (B) assayed for their ability to activate the pheromone response pathway using a *FUS1-LacZ* promoter-reporter. (n=5) bar represents standard deviations. Beta-Gal= β -galactosidase.

Residues specifically involved in the pheromone response or the HOG signaling pathway have distinct structural localizations within the Ste50-RA domain

We have generated three groups of Ste50-RA domain mutants displaying different MAPK signaling defects. In order to find how these mutant residues are differentially controlling the MAPK activities we mapped the residues onto the solution structure (Ekiel *et al.*, 2009) of the folded RA domain (residues 251-327). The mapping showed clear structural clustering of the residues according to their phenotypic traits [Figure 5, A and B]. The structural clusters responsible for controlling specific pheromone response and HOG signals reside at a distance from each other on opposite sides of the RA domain structure. Also, residues affecting both pathways are located between those pathway-specific clusters.

According to functional data for single mutants and dissected out multiple mutants [Tables 1A and Table 2, Figure 4], five residues from the pheromone signaling group include R283, I289, Q294, R296 and I307. These belong mainly to the β -sheet and face away from the α 1-helix and more towards the α 2-helix of this peculiar RA-domain fold [Ekiel *et al.*, 2009]. Among these residues, R283, Q294, R296 and I307 are exposed at the protein surface and, with the exception of R283, are also predicted by a structural bioinformatics meta-prediction approach to have a high propensity for engagement in protein-protein interactions [Figure 5C]. Residue R283 is also the most structurally isolated from this group. Interestingly, R283G had only a marginal effect in the transcriptional activation assay [Figure 4], but it showed consistently a synergistic effect when combined with the Q294L by all assays [Table 2, Figure 4 and Figure S1C]. Two computational methods employed to predict stability changes upon mutations [Table S2] indicated that I289 mutations could lead to moderate destabilization of the Ste50-RA fold, suggesting localized conformational changes and not unfolding or significant misfolding of the domain as a result of conservative mutations of this buried residue. This is supported by the fact that the I289T mutant is functional in the HOG pathway. It is significant that the buried residue I289 is located directly underneath the surface-exposed residues belonging to the pheromone signaling cluster, emphasizing its structural role in supporting the shape of the putative protein-protein interface required for pheromone signaling.

FIGURE 5: Structural clustering of Ste50-RA domain residues according to their functional phenotypes. Residues affecting the pheromone, hyperosmolar signaling, or both pathways are colored in red, blue and yellow, respectively, and are represented as atomic spheres (A) and the molecular surface (B) of the NMR structure of the Ste50-RA domain (Ekiel *et al.*, 2009). The pathway-specific cluster residues are located at a distance from each other on opposite sides of the domain structure, and residues affecting both pathways located between those pathway-specific clusters. (C) Structural bioinformatics meta-prediction based on 9 different algorithms (see *Materials and Methods*) showing the propensity of Ste50-RA domain residues to engage in protein-protein interactions. Color-coding of functional residues is as in panels (A) and (B).

Localized at the C-terminal end of the α 1-helix and away from the pheromone signaling-associated cluster is another group of residues that, in Tables 1B & 2 and in a previous study (Ekiel *et al.*, 2009), have been shown to affect specifically the HOG signaling pathway: R274, H275, N276 and L277. These residues are surface-exposed and their mutations are predicted to be very well tolerated structurally especially in the case of the former three, while a minor destabilizing effect is predicted for the L277S mutant relative to wild type [Table S2]. Interestingly, residues N276 and L277 are predicted not to have a high propensity for participating in interactions with other proteins [Figure 5C].

Based on the single-point mutation data in Table 1C, residues I320 and L322 emerge as being engaged in both pathways. These two residues are located on the structure of the RA domain in an area that bridges the above-mentioned pathway-specific distinct clusters [Figure 5, A and B]. Like the residues implicated specifically in pheromone signaling, these functionally nonspecific residues belong to the domain's β -sheet but face towards the α 1-helix where the HOG pathway-specific cluster is located. These residues also belong to regions predicted to represent potential protein-protein interaction sites [Figure 5C].

In order to further delineate the structural boundaries of these functional clusters, we have probed several other residues by site directed mutagenesis based on structural analysis. None of these single mutations alone seem to have significant phenotypic effects [Table S3], with minor defects observed only for I306E and A319E in the pheromone signaling. This

additional targeted mutagenesis data may indicate relatively weak contribution from residues at these positions, which nevertheless may be amplified by combinations of several mutations as seen earlier, leading to possible expansions of the mapped functional-structural clusters. Further functional and structural work will be required in order to more accurately define the boundaries of these clusters.

To investigate how Ste50-RA domain functional interfaces relate to the canonical interaction mode of the RA domain with small GTPases, we overlaid the structure of the Ste50-RA domain on to the RalGDS RA domain bound to the Ras small GTPase (Huang *et al.*, 1998) [Figure S2]. Interestingly, the surface responsible for the specific-pheromone-signaling on the Ste50-RA domain was not located near the small GTPase interaction site but rather positioned completely opposite in the structure, suggesting the possibility of binding partners for pheromone signaling that are not small GTPases.

Specifically-pheromone-response defective clones show strong quantitative growth phenotypes

We focused on the strong and the structurally interesting R283G Q294L and R296G mutants belonging to the pheromone-response-defective class. For a quantitative assessment of the mutants' growth properties compared to the controls, mutants were tested in parallel by both liquid and solid growth assays. As expected, the wild type Ste50 bearing strains showed severe growth retardation due to cell cycle arrest in the quantitative liquid growth assay. In contrast, the RA null mutant was clearly defective in pheromone-induced cell cycle arrest [Figure 6A] with ~4.5X more pheromone resistant growth than the wild type. Mutants R283G Q294L and R296G had a similar growth pattern to Ste50 Δ RA, confirming the strong pheromone response defects of these mutants. Parallel growth assays on hyperosmolar media confirmed Ste50 Δ RA to have severe growth defect while the WT could withstand the hyperosmolar stress and grow ~3X more [Figure 6B]. Similarly, mutant R296G and R283G Q294L had normal growth pattern on hyperosmolar stress as it paralleled the wild type, confirming their specific pheromone response defects [Figure 6B]. Weaker alleles of specifically-pheromone-response-defective mutants had comparatively lower pheromone resistance growth while keeping their HOG response normal [Figure S3].

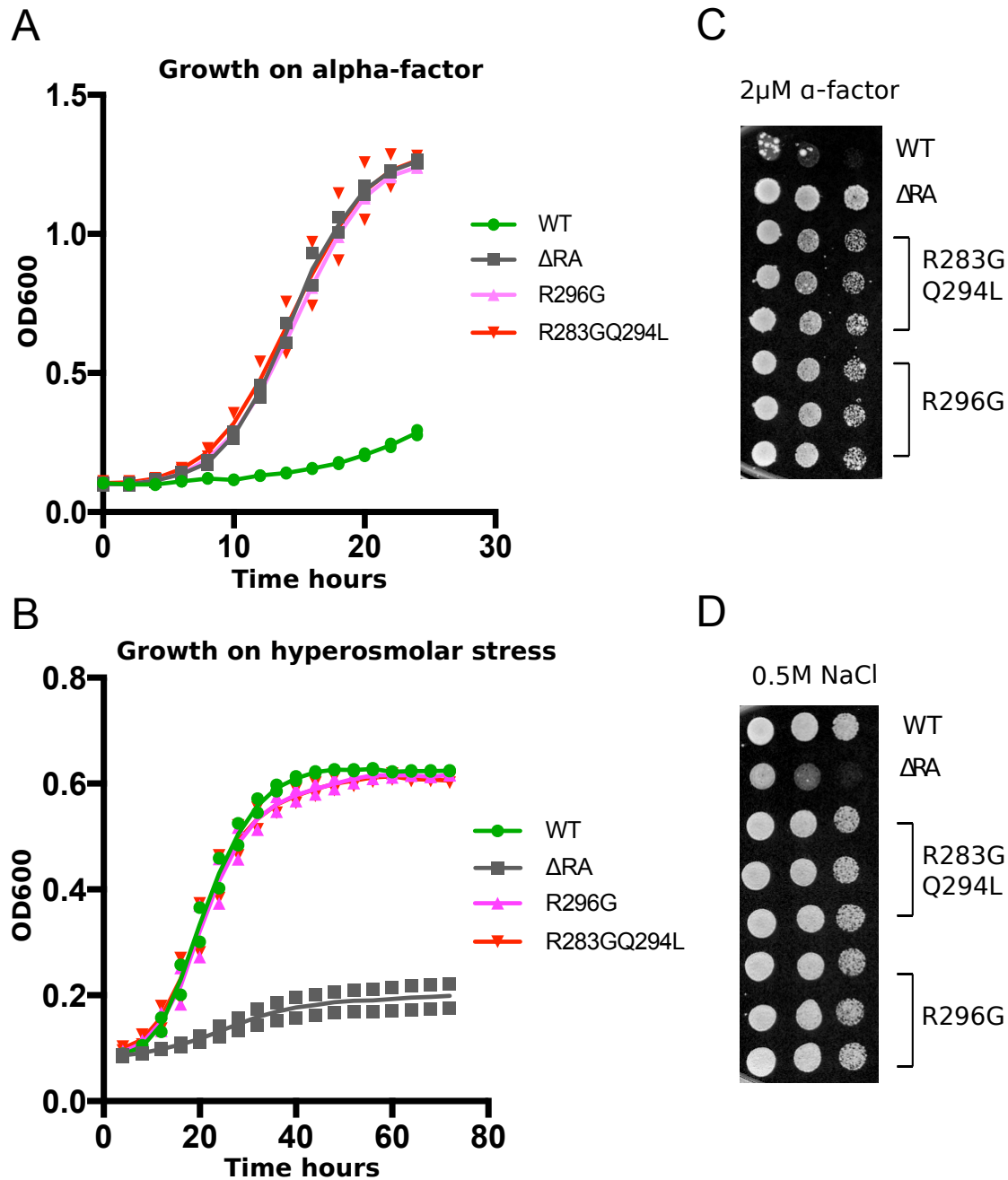


FIGURE 6: Growth characterization of Ste50-RA domain mutants specifically defective in pheromone response showing growth in both alpha factor and hyperosmolar stress. A) & B) Growth curves for ste50-RA domain mutants. Yeast strain YCW1886 transformed with Ste50-RA domain mutants indicated or with WT or RA domain deletion constructs at OD₆₀₀ of ~0.1 were stimulated with either A) 2µM α -factor for 24 hours or B) 0.5M NaCl for 72 hours and OD measured at 10 and 15 minutes intervals by TECAN machine on SD-ura selection media (*Materials and Methods*) for pheromone response and hyperosmolar stress

respectively. Figures representing two trials. C) & D) Growth assay on solid media for the clones indicated of serial dilutions on SD-ura with 2 μ M α -factor or 0.5M NaCl plates scored after 2 days.

We also assessed the phenotypic growth properties for the above mutants under the same pheromone and hyperosmolar conditions by spot assays on test plates. The results for the spot assay corroborated the liquid culture assays showing growth for R283G Q294L and R296G on pheromone [Figure 6C] while both mutant strains retained their ability to grow on hyperosmolar stress [Figure 6D]. Together, our results suggest that the Ste50-RA domain contains residues that are specifically required for pheromone response signaling.

Further, we tested specifically HOG signal defective mutants, S154Y H275P, H275R and L277S, as well as mutants that are defective in both pathways, L322S and I320K, by spot assay on test plates (see methods) [Figure S4, A and B]. S154Y H275P and L277S showed WT phenotype on pheromone but were unable to withstand hyperosmolar stress. On the other hand, L322S and I320K showed defective response phenotypes under both conditions.

Ste50-RA domain mutants specifically defective in pheromone response are severely defective in shmoo formation

Since prior work showed the adaptor protein Ste50 with deleted regions confers reduced mating ability (Rad *et al.*, 1992), we speculated that the severe loss of pheromone response observed in our mutants might have also compromised some biological functions causing morphological effects.

Differential interference contrast (DIC) microscopy studies with WT and R283G Q294L bearing strains showed no apparent morphological differences without pheromone treatment, but indeed gross morphological differences were observed when cells were treated with pheromone. We stimulated cells with pheromone and monitored them over a time-course (see methods). After as little as 1 hour of stimulation, cells with wild type Ste50 started to show morphological changes generating readily detectable pointed polarized structures called shmoos [Figure 7A1]. Under similar conditions the pheromone

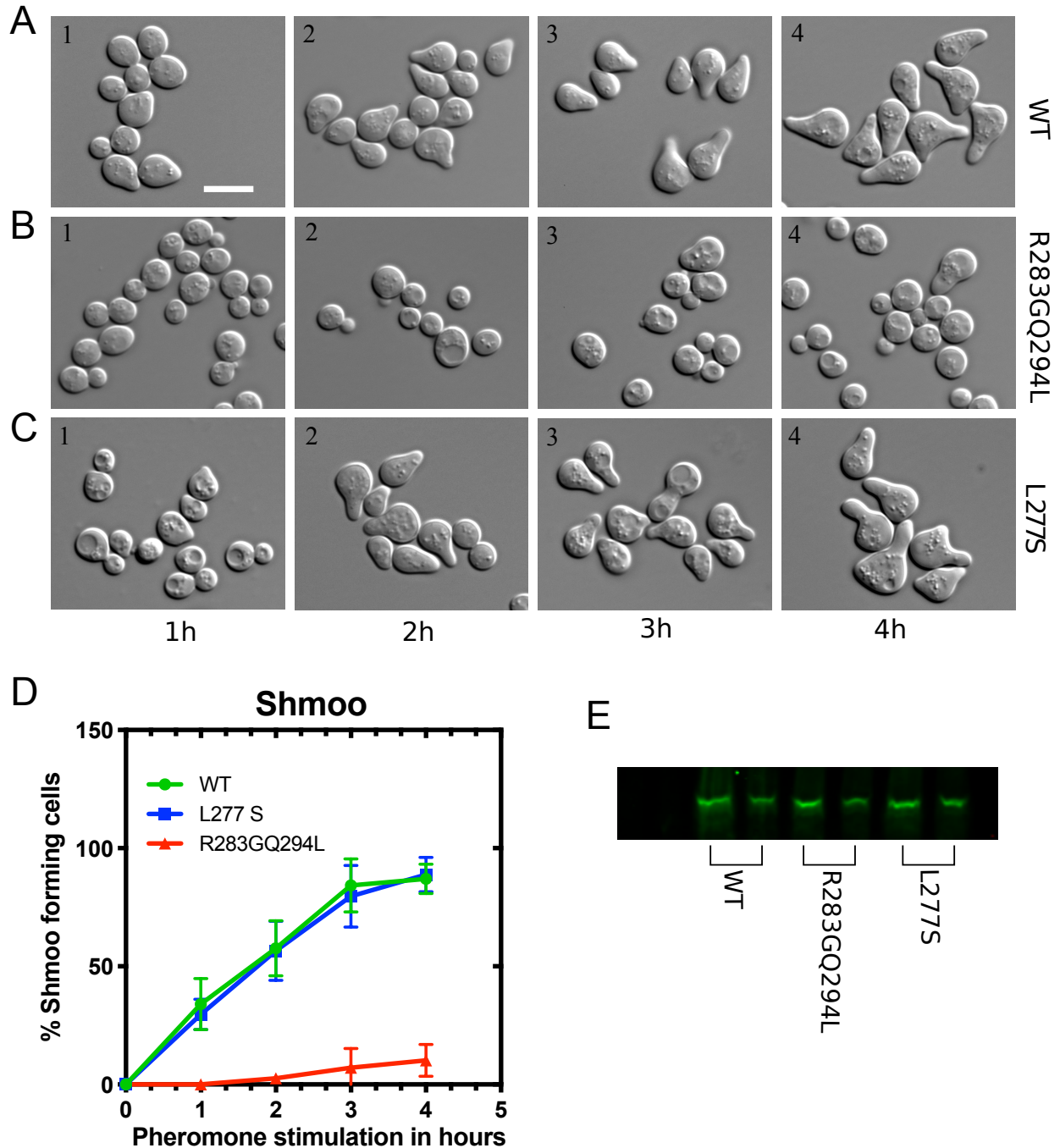


FIGURE 7: Residues 283 and 294 are critically required for shmoo formation. A-C) Yeast cells bearing GFP tagged WT, mutant R283G Q294L and L277S Ste50 were stimulated with $2\mu\text{M}$ α -factor and samples collected at 1, 2, 3, and 4 hours. Cells were morphologically examined under the microscope. D) Quantitative and time-course analysis of the ability of Ste50p for shmoo formation in response to pheromone as described in *Materials and*

Methods. Standard deviations were calculated from five independent experiments of at least 200 cells at each time point. E) Western blot analysis of WT Ste50p and mutants as indicated and described in *Materials and Methods*. For each Ste50 allele, lanes represent 200 μ g and 150 μ g of proteins. Bar represents 10 μ m.

response defective mutant, R283G Q294L failed to form polarized structures and retained its unstimulated morphology [Figure 7B1]. The morphological differences were more pronounced at 2 hours of pheromone stimulation; R283G Q294L failed to form shmoo while almost ~60% of the WT cells showed distinct shmoos [Figure 7, A2, B2 and D]. The percentage of shmoo formation increased with time [Figure 7A3] and reached to ~87% for the wild type at 4hrs; in contrast R283G Q294L showed shmoos on average of only ~10% of cells (almost 6 fold < WT) [Figure 7, A4, B4 and D], providing evidence that residues 294 and 283 are critically involved in the polarized growth aspect of pheromone signaling.

To reinforce our finding that lack of shmooing is a feature of the specifically pheromone-response-defective mutants, we also examined shmoo forming ability of the specifically HOG signal defective mutant L277S. The shmoo formation of the L277S mutant showed no significant difference from the wild type at 1, 2, 3 and 4 hours of pheromone stimulations [Figure 7, C1-4 and D]. Thus in support of our growth assays, the shmoo assay also showed severe defect in the specifically pheromone response defective mutant R283G Q294L, while the HOG signal defective mutant L277S showed no impairment. To determine whether the shmoo forming ability was due to the differential expression of these alleles, we performed expression analysis of GFP tagged mutants and wild type Ste50p by immunoblotting. Our results show that the levels of protein expression of these ste50 alleles relative to the WT were unchanged [Figure 7E].

RA domain residues responsible for specific-pheromone-response are required for shmoo tip localization of Ste50p

Our microscopic studies established that mutant R283G Q294L has a grossly reduced ability to form shmoos. To examine the cellular localization of this class of mutants compared to wild type Ste50p, we used fluorescent GFP tagged Ste50-WT, R283G Q294L

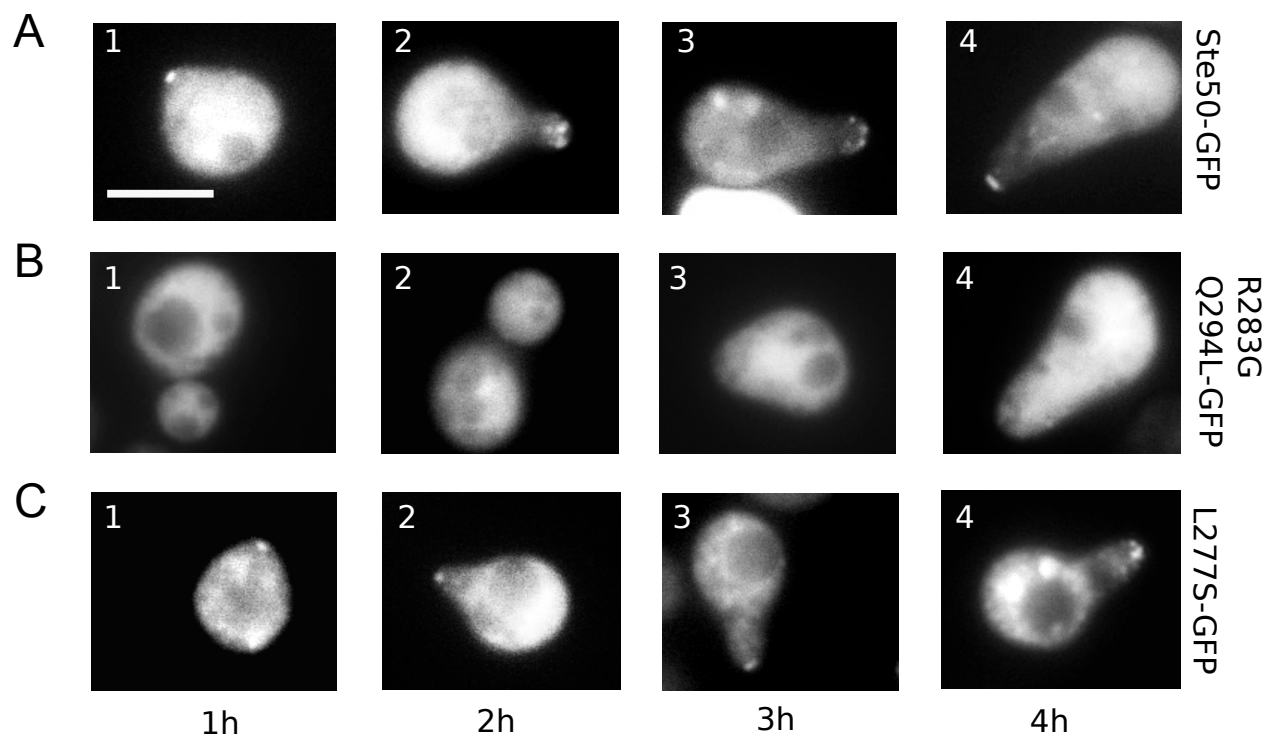


FIGURE 8: Ste50-GFP localization profile. Yeast strains expressing either wild type (A), the R283GQ294L (B) or the L277S (C) RA domain mutant Ste50-GFP fusion proteins were studied microscopically to determine cellular GFP protein localization after pheromone treatment for the indicated time. Wild type or L277S Ste50-GFP protein localizes to the shmoo tip within 1 hour of pheromone treatment (A1, C1 and D) and show increased localization with time (A2-4, C2-4 and D). The RA domain mutant R283G Q294L shows no and L277S to study their localizations (see Methods). Yeast cells were transformed with

these fusion constructs and were verified for Ste50p functionality by testing pheromone responsive cell cycle arrest [Figure S5]. Previously, studies have shown Ste50p to be mainly cytoplasmic (Huh *et al.*, 2003) with a fraction in the mitochondria (CYCLOPs – Collections of Yeast Cells and Localization Patterns). We undertook a detailed study of Ste50p localization by cellular imaging both in the absence and in the presence of pheromone. In the absence of pheromone we observed WT Ste50p to be mainly cytoplasmic confirming the previously reported observation. However, we observed that Ste50-GFP accumulated in more than shmoo up to two hours (B1-2) and fails to localize to the shmoo tip (B3-4). Results of three independent experiments at each time point, at least 100 shmoos were analyzed for shmoo accumulations (D). Bar, 5 μ m.

80% of cells at the shmoo tip within 1 hour of pheromone stimulation [Figure 8, A1 and D]. The accumulation appeared punctate and visually quite different from the master regulator of polarization, Cdc42p (Smith *et al.*, 2013). Increased accumulation was observed with the growth of the shmoo structure [Figure 8, A2-4] and in the population level the number of shmoo with accumulation peaked around 2 hours [Figure 8D].

To explore the cellular localization of the R283G Q294L mutant cells when treated with pheromone, we examined the behavior of the mutant GFP fusion protein under the same conditions and also examined L277S-GFP fusion as a reference. Microscopic studies revealed that under pheromone treatment and over a course of 4hrs, R283G Q294L not only formed markedly reduced shmoos (as discussed above) but also failed to accumulate Ste50-GFP signal at the tips that did form [Figure 8, B1-4]. Up to two hours of pheromone stimulation, generally no observable shmoos or GFP signal accumulation were detected for R283G Q294L [Figure 8, B2]. Longer pheromone stimulation showed a few shmoos for R283G Q294L with barely any accumulations at the tip. Therefore, even in the presence of shmoo structures, R283G Q294L failed to accumulate Ste50-GFP at the shmoo tip, suggesting residues 283 and 294 are required for shmoo tip localization of Ste50. In contrast, mutant L277S-GFP accumulated at the shmoo tip like the wild type [Figure 8, C1-4]. Therefore, Ste50 shmoo-tip accumulation was unaffected by the mutation at position 277 that influences osmotic response.

2.5 Discussion

Signaling pathways that share common components require mechanisms to ensure specificity of information transfer, and this specificity is often provided by adaptor molecules. Key features of such adaptors include domains (for example SH2, SH3) containing protein-binding modules that orchestrate specific protein-protein interactions (PPIs) generating larger signaling complexes; examples of such adapters include Grb2, MYDDB and SHC1. In several yeast MAPK pathways, the SAM domain of the adaptor protein Ste50 connects to the SAM domain of a common MAPKKK termed Ste11 (Jansen *et al.*, 2001), which is a homolog of mammalian MEKKs; all are situated at the same level as Raf in their corresponding pathways. As well, the Ste50 protein contains an RA domain that controls the specificity of Ste11 signaling (Truckses *et al.*, 2006, Wu *et al.*, 2006). We previously uncovered a role of the Ste50-RA domain specifically directing signaling through the HOG pathway; the present study builds on these findings by identifying a role for the Ste50-RA domain in pheromone signaling and establishing the region required for interaction in the pheromone response pathway. This work shows that the RA domain of Ste50p uses distinct surfaces to specifically connect to either the mating pheromone pathway or to the HOG signaling pathway.

We randomly mutagenized the Ste50-RA domain by error-prone PCR and screened for mutants with specific MAPK signaling phenotypes and obtained several classes [Table 1]. Among them the class I mutants generated cells that specifically showed pheromone-response-defective signaling; these cells were blocked in undergoing pheromone-dependent cell cycle arrest but remained functional in response to hyperosmolar stress. We found that the positions of the functionally important residues that are specifically involved in the pheromone response pathway (R283, I289, Q294, R296 and I307) are distinct from the residues that are involved in the HOG signaling pathway, (R274, H275, N276 and L277) [Tables 1 and 2]. Mapping these residues onto the three-dimensional RA domain NMR structure showed that they clustered around distinct patches [Figure 5]. Residues that affected both pathways (I320 and L322) were found to be located between these two pathway-specific clusters. This clustering suggests distinct epitopes on the protein surface that may be required for interacting with partner proteins (Kiel and

Serrano, 2006). Although the RA domain has a non-canonical ubiquitin fold (Ekiel *et al.*, 2009), the topology of the core still resembles the canonical ubiquitin fold, with three β sheets and two α helices. The patches identified in this study belong to the stable, well-folded core of the domain encompassing amino acids 262-326 (Ekiel *et al.*, 2009). Structurally, the specifically-pheromone-response defective residues belong to the β -sheet and are facing away from the α 1-helix where the specifically-HOG-signal-defective residues are positioned [Figure 5A], showing that these binding epitopes are on different secondary structure elements that provide different interfaces and interaction modes. A computational analysis further indicated that mutations introduced in these surface patches maintain this well-folded structure [Table S2], suggesting that the associated phenotypic effects observed in this study were not a result of major conformational changes. The data presented here identifies the structural basis of the Ste50p RA domain that differentially connects to the different MAPK pathways and potentially modulates signaling specificity.

Interestingly, we found that in two cases more than one mutation were required to bring out the desired phenotypic effect(s), for example R283G Q294L and K260N L300V I307K, where pheromone stimulation caused a stronger phenotypic response with the combined mutations than with the dissected component ones [Table 2]. It seems that simultaneous modification of various residues may have coherently amplified individually weak structural and dynamic perturbations into stronger effects (Tripathi *et al.*, 2016).

We established by GFP tagging and live cell imaging that the wild type Ste50-GFP accumulates to the shmoo tip upon pheromone stimulation, while the specifically-pheromone-response-defective mutants failed to localize. Generally, mutations affecting protein localization indicate loss of a transient interaction and are identified as loss-of-function kinds (Yates and Sternberg, 2013). In the wild type, this accumulation at the shmoo tip strengthens with time and is punctate in nature. Since this accumulation is at the growing shmoo tip, Ste50p may be a member of the polarization complex. We carefully examined whether there is Ste50 accumulation at the young bud tip, since this was found in the case of Cdc42p (Smith *et al.*, 2013; Okada *et al.*, 2017), which is a core member of the polarization patch. We were unable to find such bud accumulation of Ste50p. Proteins

unique to bud or shmoo tips have been suggested before (Narayanaswamy *et al.*, 2008). We speculate that the shmoo tip accumulation of Ste50p could define a specific pheromone dependent polarization module, resulting from a complex formed between Ste50p and other protein(s) unique to pheromone response. This was supported by the fact that the specifically-pheromone-response-defective mutants found here showed gross inability in shmoo formation and failed to accumulate at the shmoo tip but were budding normally. This was also reinforced by the fact that the specific HOG signal defective class was wild type-like with regards to shmoo accumulation. These combined results suggest that these residues are critical for pheromone specific response and mutating these residues may have caused loss of partner interaction(s), hence lack of complex formation with Ste50p and localization at the pheromone-induced polarized structure - the shmoo tip.

The C-terminal RA domain of Ste50 appears to have a function in the yeast MAPK pathways similar to the mammalian N-terminal RA domain of Raf that interacts with Ras and is required for its delivery to the membrane. Although the RA domain of Ste50 does not bind Ras, it has been shown to bind the membrane-anchored small Rho-like GTPase Cdc42 (Tatebayashi *et al.*, 2006; Truckses *et al.*, 2006), as well as the transmembrane protein Opy2p (Wu *et al.* 2006), potentially for facilitating Ste11p membrane localization where it can be phosphorylated and activated by the PAK like Ste20p. Interestingly, these two interactions are required for Ste50 function in two different MAPK pathways, Opy2p for the HOG pathway (Wu *et al.*, 2006), and Cdc42p for the filamentous growth pathway (Truckses *et al.*, 2006). In the HOG signaling pathway it was shown previously that the Ste50-RA domain requires all three residues, R274 H275 N276 for its specific interaction with Opy2p (Ekiel *et al.*, 2009); here we found that a single residue H275 when changed from histidine to proline can alone yield a strong specific HOG signaling defect. Logically, replacement with proline instead of alanine (previous study) is likely to cause a more drastic disturbance to abrogate HOG signaling. In the filamentous growth pathway, it was shown that residues I267 and L268 of the Ste50-RA domain are required for interaction with Cdc42p small GTPase (Truckses *et al.*, 2006). Based on a structural comparison of the Ste50-RA domain using as guide the RalGDS RA domain bound to the Ras small GTPase [Figure S2], our data shows that the specifically-pheromone-response-defective surface on the Ste50-RA domain is located on the opposite face relative to the canonical binding site

for small GTPases. This finding implicates a possible PPI between the Ste50-RA domain and a binding partner for pheromone response that is not a small GTPase.

The PPIs for signaling pathways are usually transient (Gibson, 2009), and the interfaces are typically smaller than permanent interfaces (Perkins *et al.*, 2010). Chavali *et al.*, 2010 has proposed that a protein causing various phenotypically different diseases is usually centrally located in the PPI network, whereby it is involved with multiple biological pathways. In human, binding of Ras association domain with effector Ras appears to act as molecular switch controlling large number of pathways (Wohlgemuth, *et al.*, 2005). Structurally, a common feature among Ras binding domains is their ubiquitin fold and their ability to interact with different partners. In humans, RA domains have been found to interact with a variety of partners (see Introduction); in yeast, previous studies found two proteins interacting with the Ste50-RA domain. Two possibilities for engagement into PPI are: i) the RA domain may have different surfaces and interact with many interaction partners; or ii) it may have multiple partners that share the same or overlapping interfaces, allowing only one partner to bind at a time (Kim *et al.*, 2006). Based on our study here, the Ste50-RA domain shows unique structural patches for differential MAPK signaling, indicating the possibility of engaging in PPI through scenario i). It is possible that the structurally overlapping region between the pathway-specific clusters of the Ste50-RA domain may also be a site for protein binding, as indicated by our structural meta-prediction study [Figure 5C]. Cooperative binding was found for Fus1 that binds both promiscuous and selective ligands in distinct conformational modes (Reményi *et al.*, 2005).

This work identifies two distinct surface regions containing pathway specific mutations. These regions are consistent with potential binding sites for proteins involved in specific interactions for mating and osmoregulatory signaling. Although Opy2 represents the HOG pathway interacting protein, a candidate for a pheromone pathway protein associating through the RA domain remains to be elucidated. Suppression studies and protein-protein association assays directed by these specificity-defining mutations represent promising avenues for identifying such a protein.

Thus, the functional repertoire of Ste50 is expanding into signal discrimination using distinct structural interaction modes. Given the structurally conserved nature and repeated employment of RA domains in signaling molecules in higher eukaryotes, the implication of this work goes beyond the yeast model system in terms of our understanding of the RA domain and the mechanisms of action of this versatile protein module.

2.6 Materials and Methods

Yeast strains, plasmids and yeast manipulations

The yeast strain used in this study was: YCW1886 (*MATa ste50Δ::Kan^R ssk1Δ::Nat^R sst1::hisG FUS1-LacZ::LEU2 his3 leu2 ura3 trp1 ade2*). The plasmids used in this study are listed in Table S5. The *E. coli* strain used in this study was MC1061 (*F- Δ(ara-leu)7697 [araD139]B/r Δ(codB-lacI)3 galk16 galE15 λ- e14-mcrA0 relA1 rpsL150(strR) spoT1 mcrB1 hsdR2(r-m+)*) from Invitrogen. Standard manipulations of yeast strains, culture conditions and media were as described (Dunham *et al.*, 2015). Yeast transformations were carried out by the lithium acetate method (Chen *et al.*, 1992). Benchling was used for the design of plasmids and primers.

Plasmid construction

Plasmid pNS101 containing a *HIS3* stuffer marker was constructed by cloning the *HIS3* marker from pCW606 as a *SalI* fragment into the *SalI* site of pCW463, which contains *STE50* lacking the RA domain. Mutant *ste50*-GFP plasmids were constructed by PCR amplification of the mutation using the pNS102 plasmids (see below) bearing the mutation(s) as templates with primers OCW551 and ONS30 to amplify the region plus the flanking sequences on both ends for *in vivo* recombination (IVR) in yeast into the *Bpu10I* linearized *Ste50*-GFP. The desired recombinants were confirmed by DNA sequencing.

Construction of *ste50* RA domain mutant libraries

Three *STE50* RA domain libraries were constructed using different mutagenic conditions to optimize the frequency of mutations in the RA region by mutagenic PCR (polymerase chain reaction). Briefly, PCR reactions were performed using plasmid pCW572 as template with

primers OCW80 and OCW164 to amplify the *STE50 RA* region plus flanking sequences on both ends for *in vivo* recombination (IVR) in yeast. All primers used in this study are listed in Table S6. Three separate PCR reactions were carried out with Taq DNA polymerase (New England Biolab, Montreal, Canada) under the following conditions: 1x Taq DNA polymerase buffer (New England Biolab), 0.2mM dNTP (each) mix, 0.2 μ M of each primers, ~100ng of template DNA for 30 cycles, included in each different mutagenic stress, such as 5mM MgCl₂ or 7mM MgCl₂ or 7mM MgCl₂ + 0.5mM MnCl₂. The PCR products were cloned into *EcoRI* and *Sall* digested plasmid pNS101 by *in vivo* recombination in yeast (YCW1886) to generate the mutant plasmids pNS102 (pRS-*STE50*¹⁻³⁴⁶::*URA3/AmpR*) containing libraries. The IVR clones were selected on agar plates lacking uracil; clones were counted, pooled and titers were determined.

All site-directed modifications of *STE50* were performed with site-directed mutagenesis kit (QuikChange II XL; Agilent Technologies, Montreal, Canada) according to manufacturer's protocol. The oligonucleotides used for generating the site directed *ste50* mutants are listed in Table S6. Plasmids were purified from several independent *E. coli* colonies from each mutagenesis and sequenced to verify the introduction of only the correct substitution(s). Verified plasmids were then used for phenotypic characterization.

Mutant *ste50* library screening

Conditions for screening mutant libraries were established using the wild type Ste50 (pCW267) and Ste50 RA domain deletion (pCW463) plasmids; challenging with α -factor for pheromone response and NaCl for hyperosmolar stress. The libraries were screened by initially plating ~200 cells/plate on synthetic defined (SD) media lacking uracil. Plates were incubated for 2 days at 30° C for colonies to grow, then replica plated in parallel at low density onto SD-Ura plates containing 2 μ M α -factor (Sigma-Aldrich, Oakville, Canada) and SD-Ura plates with 0.5M NaCl in galactose. After 1 day of incubation for the α -factor and 2 days for NaCl at 30° C, the four different phenotypes: (i) non growers on α -factor plates and growers on hyperosmotic medium plates, (ii) growers on both α -factor plates and hyperosmotic medium plates, (iii) non growers on α -factor plates and hyperosmotic medium plates, (iv) growers on α -factor plates and non growers on hyperosmotic plates, - were identified, picked from the master plate and patched separately on SD-Ura plates.

Plasmid rescue, plasmid linkage test and sequencing analysis

STE50 plasmids were recovered from the selected yeast strains with desired phenotypes, and used for transformation and propagation in *E. coli*. Plasmids were extracted from *E. coli*, and DNA concentrations were determined using NanoQuant Infinite Pro 200 (TECAN, Switzerland) according to manufacturer's protocol. Plasmid DNAs were then retransformed into yeast strain YCW1886 to ensure recapitulation of the desired phenotypes. *STE50* alleles that satisfied the selection criteria were sequenced with primers OCW93 and OCW164. All sequencing reactions were performed at the McGill University Génome Québec Innovation Centre. Nucleic and amino acid sequences were analyzed with Clustal Omega, ExPASy, and Bioinformatics.org; and compared with fungal genome database (<http://seq.yeastgenome.org/>) to identify mutations.

Mutational dissections with site-directed mutagenesis and gBlocks synthesis

Selected clones containing multiple mutations were dissected to find the driver mutation(s). This was achieved with designed gBlock DNA synthesis (IDT, Coralville, Iowa) [Table 1S] containing the permutation-combinations of mutation(s). The gBlocks were cloned into *EcoRI* and *SalI* digested plasmid pNS101 by *in vivo* recombination in yeast (YCW1886) to introduce the dissected mutation(s). Site-directed mutagenesis using QuikChange (Agilent Technology) were also performed to dissect mutants *ste50*^{L182PL277S} and *ste50*^{R283GQ294L} to find the causal mutation(s). To dissect *ste50*^{R283GQ294L}, primers ONS21 and ONS22 were used to revert the mutation at residue 283; ONS23 and ONS24 to change residue 294. For *ste50*^{L182PL277S}, primers ONS25 and ONS26 were used to revert the mutation at residue 182 and primers ONS27 and ONS28 were used to revert the mutation at residue 277. Plasmids extracted from five independent *E. coli* clones were sequence verified and then tested on alpha-factor and hyperosmolar stress to confirm the driver mutation(s).

Growth assay

For growth on solid media analysis, overnight cultures in synthetic defined media with amino acid dropout selection were diluted to OD₆₀₀ of 1 followed by 6-fold serial dilutions in multi well plates. Five micro liters of each dilution was spotted on pre-warmed agar

plates with respective selections using the indicated concentrations of alpha factor and NaCl in glucose. Plates were incubated in 30° C for 2-4 days and scored for growth.

For quantitative growth in liquid media assays, yeast strain YCW1886 was transformed with *ste50* mutants and control plasmids. Three different colonies from each transformation were grown until saturation. Fresh medium was re-inoculated from the saturated cultures in 1:1000 dilutions to obtain overnight cultures at exponential growth phase. Cultures were serially diluted in a 96 well plate to obtain OD₆₀₀ around 0.05-0.1, treated either with 2µM alpha factor or 0.5M NaCl in glucose, and the OD₆₀₀ measured on TECAN machine every 10 and 15 minutes respectively. Alpha factor treated cultures were measured for 24 hours and NaCl treated cultures were monitored for 72 hours. Replicate OD₆₀₀ plotted every 4 hours for analysis.

Microscopy and live-cell imaging

Before imaging, YCW1886 strains bearing *STE50* WT and mutants on plasmids were grown to saturation in selective SD-His liquid media then diluted 1:1000 in fresh media and incubated overnight to generate mid-exponential stage cultures next morning. Each culture was then divided into eight tubes, half of which received 2µM alpha-factor. Cells were incubated for several time points, samples collected and then prepared for viewing. Imaging was performed on a DM6000 Epifluorescent Microscope (Leica Biosystems, Wetzlar, Germany) with Volocity acquisition software (PerkinElmer, MA, USA) using 100x Leica Plan Fluotar (NA 1.3) lens. Both the Differential Interference Contrast (DIC) and the Fluorescein isothiocyanate (FITC) images were obtained for the pheromone and no pheromone treated cells. Single time point images of live or fixed cells were collected and ImageJ software (v. 1.37; National Institutes of Health) was used to process the images. For cell counting and image analysis of morphological studies, budding cells were counted as single cells and dead cells were omitted from the count. Generally, at least 200 cells were counted for each data point from 3-5 biological replicates.

Immunoblotting

From freshly streaked plates containing yeast strains bearing GFP fusions to either WT or mutant *STE50*, a single colony per strain was picked and cultured overnight in-His media

then diluted 1:1000 in 50 ml media and incubated at 30°C to OD of 0.8-1.0 next morning. Total protein was extracted by bead beating in IP150 buffer (50mM Tris-HCl pH 7.4, 150mM NaCl, 2mM MgCl₂, 0.1% Nonidet P-40) that had Complete Mini protease inhibitor cocktail tablet and Phosphatase inhibitor cocktail tablet (Roche Applied Sciences, Penzberg, Germany). Cell lysing was done by vortexing with glass beads in microcentrifuge. To avoid heating the samples, cells were disrupted for 30-60 sec with 20-30 sec pauses on ice for a total of 3 minutes. The lysates were centrifuged at 14,000 rpm for 10 min at 4°C in a bench top centrifuge (Heraeus Biofuge, Cambridge, MA) to pellet the cell debris and the cleared supernatants were transferred to fresh eppendorf tubes. The Bradford assay was used to estimate the protein concentrations of the lysates. Samples were then boiled with SDS-PAGE sample buffer and 150µg and 200µg of proteins for each sample were applied to prepared polyacrylamide gels (4-20%). Proteins were transferred to a nitrocellulose membrane and subsequently probed with anti-GFP primary antibody 1:1000 mouse monoclonal (ABCAM, Cambridge, MA) and secondary antibody 1:10,000 IRDye800 conjugated goat anti-mouse IgG (polyclonal) from LI-COR (Lincon, NE). Blots were visualized by LI-COR Odyssey imaging platform (Lincon, NE) to detect the fluorescent secondary antibody.

Structural bioinformatics

The minimized average NMR structure of the Ste50 RA domain residing in E251-D327 (Ekiel *et al.*, 2009) was used for structural bioinformatics analysis in this study. Molecular structure display, rendering and examination were done in PyMol (Schroedinger, Inc., New York, NY). Predictions of change in stability (folding free energy) upon mutations of the wild type protein were carried out with the mCSM (Pires *et al.*, 2014) and FoldX (Guerois *et al.*, 2002) methods using default settings, as well as, those implemented in ADAPT (Vivcharuk *et al.*, 2017) for FoldX stability calculations. Predictions of protein-protein interaction (PPI) sites were done with 9 structure-based methods benchmarked against a set of known protein-protein complexes with experimentally determined crystal structures (Maheshwari & Brylinski, 2015). Predictions for probable PPI residues were based on the default score thresholds for each method or, in the absence of a recommended threshold, as follows: residues predicted by at least 9 servers for SPPIDER; positive scores for WHISCY; scores greater than 10 for PIER; scores greater than 0.7 for VORFFIP. InterProSurf

predictions were based on combined patch and cluster analyses. The species homologs alignment of Ste50 RA domain from Figure S1 of (Ekiel *et al.*, 2009) was used as input in WHISCY.

β -galactosidase assay

Quantitative β -galactosidase reporter assays for the pheromone response was performed as described (Wu *et al.*, 1999; Tatebayashi *et al.*, 2006). YCW1886 cells bearing Ste50 WT, mutants and control vector were grown in selective SD-Ura medium at 30°C to late-exponential phase and then induced with 2 μ M α -factor for 4 h at 30°C. Beta-galactosidase activities were measured and expressed as $(OD_{420} \times 1000)/(OD_{600} \times t \times v)$ (Miller, 1972) where t is in minutes and v is in milliliters.

Acknowledgments: This research was supported by the Natural Sciences and Engineering Research Council (NSERC) of Canada grant (CW), NSERC CRC Tier 1 950-22895 (MW) and McGill University. We thank Dr. Brian Slaughter for sharing the wild type Ste50-GFP plasmid.

2.7 References

- Bhattacharya M, Anborgh PH, Babwah AV, Dale LB, Dobransky T, Benovic JL, Feldman RD, Verdi JM, Rylett RJ, Ferguson SS (2002). β -Arrestins regulate a Ral-GDS-Ral effector pathway that mediates cytoskeletal reorganization. *Nat Cell Biol* 4, 547-555.
- Chavali S, Barrenas F, Kanduri K, Benson M (2010). Network properties of human disease genes with pleiotropic effects. *BMC Syst Biol* 4, 78.
- Chen D, Yang B, Kuo T (1992). One-step transformation of yeast in stationary phase. *Curr Genet* 21, 83-84.
- Craig EA, Stevens MV, Vaillancourt RR, Camenisch TD (2008). MAP3Ks as central regulators of cell fate during development. *Dev Dyn* 237, 3102-3114.

- Dunham MJ, Gartenberg MR, Brown GW (2015). *Methods in Yeast Genetics and Genomics* 2015 Edition: A CSHL Course Manual
- Ekiel I, Sulea T, Jansen G, Kowalik M, Minailiuc O, Cheng J, Harcus D, Cygler M, Whiteway M, Wu C (2009). Binding the atypical RA domain of Ste50p to the unfolded Opy2p cytoplasmic tail is essential for the high-osmolarity glycerol pathway. *Mol Biol Cell* 20, 5117-5126.
- Gibson TJ 2009. Cell regulation: determined to signal discrete cooperation. *Trends Biochem Sci* 34, 471-482.
- Guerois R, Nielsen JE, Serrano L (2002). Predicting Changes in the Stability of Proteins and Protein Complexes: A Study of More Than 1000 Mutations. *J Mol Biol* 320, 369-387.
- Gustin MC, Albertyn J, Alexander M, Davenport K (1998). MAP Kinase Pathways in the Yeast *Saccharomyces cerevisiae*. *Microbiol Mol Biol Rev* 62, 1264-1300.
- Harjes E, Harjes S, Wohlgemuth S, Muller KH, Krieger E, Herrmann C, Bayer P (2006). GTP-Ras disrupts the intramolecular complex of C1 and RA domains of Nore1. *Struct* 14, 881-888.
- Herskowitz I (1995). MAPK kinase pathways in yeast: for mating and more. *Cell* 80, 187-197.
- Huang L, Hofer F, Martin GS, Kim SH (1998). Structural basis for the interaction of Ras with RaIGDS. *Nat Struct Mol Biol* 5, 422.
- Huh WK, Falvo JV, Gerke LC, Carroll AS, Howson RW, Weissman JS, O'shea EK (2003). Global analysis of protein localization in budding yeast. *Nature* 425, 686-691.
- Jansen G, Bühring F, Hollenberg CP, Rad MR (2001). Mutations in the SAM domain of STE50 differentially influence the MAPK-mediated pathways for mating,

- filamentous growth and osmotolerance in *Saccharomyces cerevisiae*. *Mol Genet Genomics* 265, 102-117.
- Kiel C & Serrano L (2006). The ubiquitin domain superfold: structurebased sequence alignments and characterization of binding epitopes. *J Mol Biol* 355, 821–844.
- Kim PM, Lu LJ, Xia Y, Gerstein MB (2006). Relating three-dimensional structures to protein networks provides evolutionary insights. *Science* 314, 1938-1941.
- Letunic I, Doerks T, Bork P (2009). SMART6, recent updates and new developments. *Nucleic Acids Res* 37, D229–D232.
- Maheshwari S & Brylinski M (2015). Predicting protein interface residues using easily accessible on-line resources. *Brief Bioinform* 16, 1025-1034.
- Mayer BJ (2015). The discovery of modular binding domains: building blocks of cell signalling. *Nat Rev Mol Cell Biol* 16, 691-698.
- Miller JH (1972). *Experiments in Molecular Genetics*. Cold Spring Harbor, NY Cold Spring Harbor Laboratory.
- Morrison DK, Kaplan DR, Rapp U, Roberts TM (1988). Signal transduction from membrane to cytoplasm: growth factors and membrane-bound oncogene products increase Raf-1 phosphorylation and associated protein kinase activity. *Proc Natl Acad Sci USA* 85, 8855-8859.
- Narayanaswamy R, Moradi EK, Niu W, Hart GT, Davis M, McGary KL, Ellington AD, Marcotte, EM (2008). Systematic definition of protein constituents along the major polarization axis reveals an adaptive reuse of the polarization machinery in pheromone-treated budding yeast. *J Proteome Res* 8, 6-19.

Okada S, Lee ME, Bi E, Park HO (2017). Probing Cdc42 polarization dynamics in budding yeast using a biosensor. In: *Methods in Enzymology*, ed. J. Abelson, M. Simon, G. Verdine, A. Pyle, Academic Press 589, 171-190.

O'Rourke SM, Herskowitz I, O'Shea EK (2002). Yeast go the whole HOG for the hyperosmotic response. *Trends Genet* 18, 405-412.

Patterson JC, Klimenko ES, Thorner J (2010). Single-cell analysis reveals that insulation maintains signaling specificity between two yeast MAPK pathways with common components. *Sci Signal* 3, ra75-ra75.

Pawson T & Scott JD (1997). Signaling through scaffold, anchoring, and adaptor protein. *Science* 278, 2075-2080.

Perkins JR, Diboun I, Dessailly BH, Lees JG, Orengo C (2010). Transient protein-protein interactions: structural, functional, and network properties. *Structure* 18, 1233-43.

Pires DE, Ascher DB, Blundell TL (2014). mCSM: predicting the effects of mutations in proteins using graph-based signatures. *Bioinformatics* 30, 335-342.

Posas F, Witten EA, Satio H (1998). Requirement of STE50 for osmostress-induced activation of the STE11 mitogen-activated protein kinase kinase kinase in the high-osmolarity glycerol response pathway. *Mol Cell Biol* 18, 5788-5796.

Qamra R & Hubbard SR (2013). Structural basis for the interaction of the adaptor protein grb14 with activated ras. *PloS one* 8, e72473.

Rad MR, Xu G, Hollenberg CP (1992). STE50, a novel gene required for activation of conjugation at an early step in mating in *Saccharomyces cerevisiae*. *Mol Gen Genet* MGG 236, 145-154.

- Reményi A, Good MC, Bhattacharyya RP, Lim WA (2005). The role of docking interactions in mediating signaling input, output, and discrimination in the yeast MAPK network. *Mol Cell* 20, 951-962.
- Rodriguezviciano P, Warne PH, Dhand R, Vanhaesebroeck B, Gout I, Fry MJ, Waterfield MD, Downward J (1994). Phosphatidylinositol-3-OH Kinase as a Direct Target of Ras. *Nature* 370, 527-532.
- Sakai N, Saito Y, Fujiwara Y, Shiraki T, Imanishi Y, Koshimizu TA, Shibata K (2015). Identification of protein arginine N-methyltransferase 5 (PRMT5) as a novel interacting protein with the tumor suppressor protein RASSF1A. *Biochem Biophys Res Commun* 467, 778-784.
- Schultz J, Milpetz F, Bork P, Ponting CP (1998). SMART, a simple modular architecture research tool: identification of signaling domains. *Proc Natl Acad Sci USA* 95, 5857-5864.
- Smith SE, Rubinstein B, Pinto IM, Slaughter BD, Unruh JR, Rong Li. (2013). Independence of symmetry breaking on Bem1-mediated autocatalytic activation of Cdc42. *J Cell Biol* 202.7, 1091-1106.
- Songyang Z, Shoelson SE, Chaudhuri M, Gish G, Pawson T, Haser WG, King F, Roberts T, Ratnofsky S, Lechleider RJ, Neel BJ, Birge RB, Fajardo JE, Chou MM, Hanafusa H, Schaffhausen B, Cantley LC (1993). SH2 domains recognize specific phosphopeptide sequences. *Cell* 72, 767-778
- Stein EG, Ghirlando R, Hubbard SR (2003). Structural Basis for Dimerization of the Grb10 Src Homology 2 Domain. Implications for ligand specificity. *J Biol Chem* 278, 13257-13264
- Tatebayashi K, Yamamoto K, Tanaka K, Tomida T, Maruoka T, Kasukawa E, Saito H (2006). Adaptor functions of Cdc42, Ste50, and Sho1 in the yeast osmoregulatory HOG

MAPK pathway. EMBO 25, 3033-3044.

- Tong Y, Chugha P, Hota PK, Alviani RS, Li M, Tempel W, Shen L, Park HW, Buck M (2007). Binding of Rac1, Rnd1, and RhoD to a novel Rho GTPase interaction motif destabilizes dimerization of the plexin-B1 effector domain. J Biol Chem 282, 37215–37224.
- Tripathi A, Gupta K, Khare S, Jain PC, Patel S, Kumar P, Pulianmackal AJ, Aghera N, Varadarajan R (2016). Molecular determinants of mutant phenotypes, inferred from saturation mutagenesis data. Mol Biol Evol 33, 2960-2975.
- Truckses DM, Bloomekatz JE, Thorner J (2006). The RA domain of Ste50 adaptor protein is required for delivery of Ste11 to the plasma membrane in the filamentous growth signaling pathway of the yeast *Saccharomyces cerevisiae*. Mol Cell Biol 26, 912-928.
- Vivcharuk V, Baardsnes J, Deprez C, Sulea T, Jaramillo M, Corbeil CR, Mullick A, Magoon J, Marcil A, Durocher Y, O'Connor-McCourt MD (2017). Assisted Design of Antibody and Protein Therapeutics (ADAPT). PloS One 12, e0181490.
- Wohlgemuth S, Kiel C, Kramer A, Serrano L, Wittinghofer F, Herrmann C (2005). Recognizing and Defining True Ras Binding Domains I: Biochemical Analysis. J Mol Biol 348, 741-58.
- Wu C, Jansen G, Zhang J, Thomas DY, Whiteway M (2006). Adaptor protein Ste50p links the Ste11p MEKK to the HOG pathway through plasma membrane association. Genes Dev 20, 734-746.
- Wu C, Leberer E, Thomas DY, Whiteway M (1999). Functional characterization of the interaction of Ste50p with Ste11p MAPKKK in *Saccharomyces cerevisiae*. Mol Biol Cell 10, 2425-2440.

Yamamoto K, Tatebayashi K, Tanaka K, Saito H (2010). Dynamic control of yeast MAP kinase network by induced association and dissociation between the Ste50 scaffold and the Opy2 membrane anchor. *Mol Cell* 40, 87-98.

Yates CM & Sternberg MJ (2013). The effects of non-synonymous single nucleotide polymorphisms (nsSNPs) on protein-protein interactions. *J Mol Biol* 425, 3949-3963.

2.8 Supplementary Materials

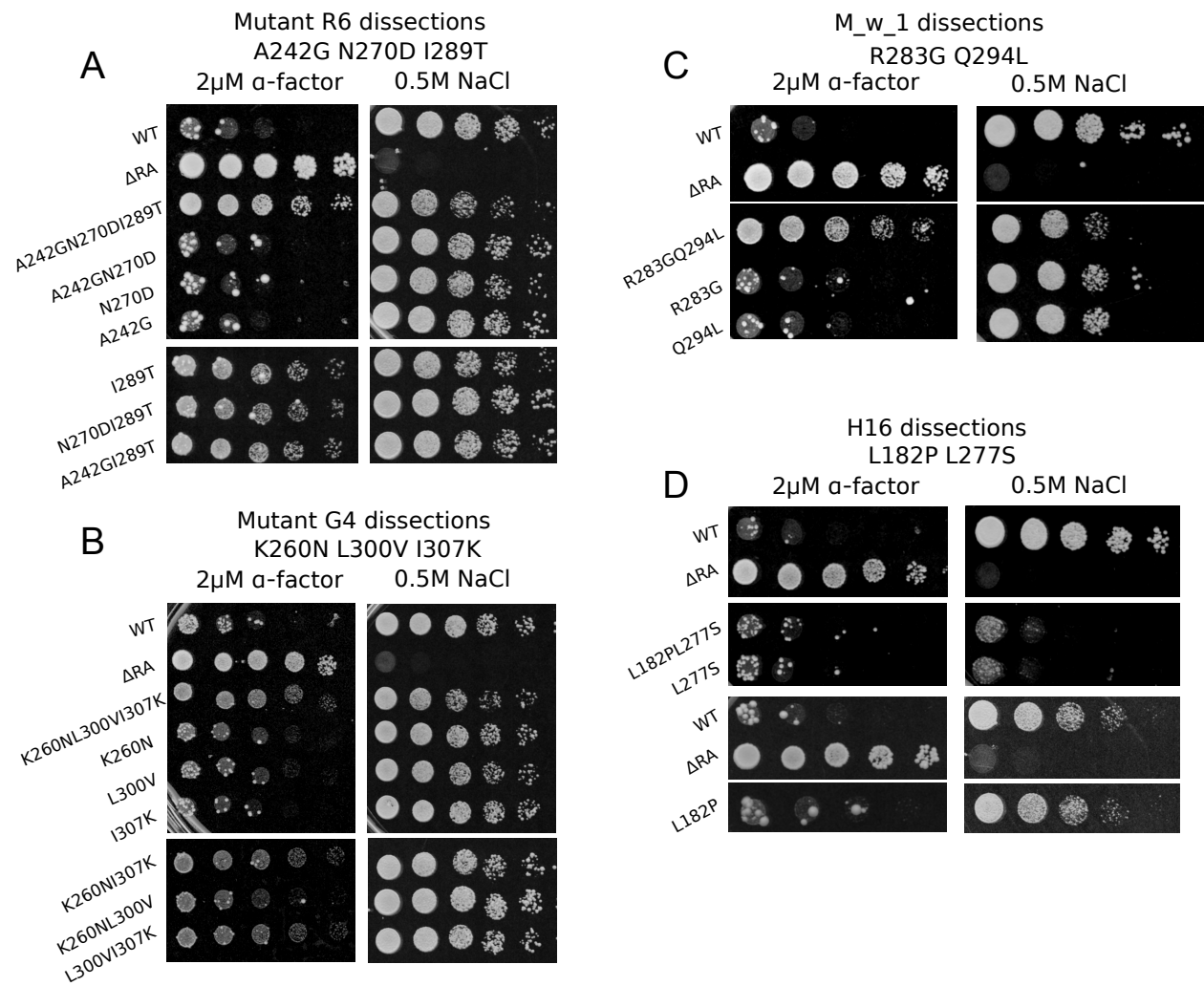


FIGURE S1: Dissection of multiple mutations to find the causal mutation(s). A, B and C) Mutants specifically defective in pheromone response with multiple mutations were dissected. Mutant R & G each containing 3 mutations and mutant M_w_1 containing two mutations were dissected into variants containing any possible combinations of mutations. Clones were tested on alpha factor and NaCl selection plates. D) HOG signal defective mutant H16 containing two mutations were also dissected.

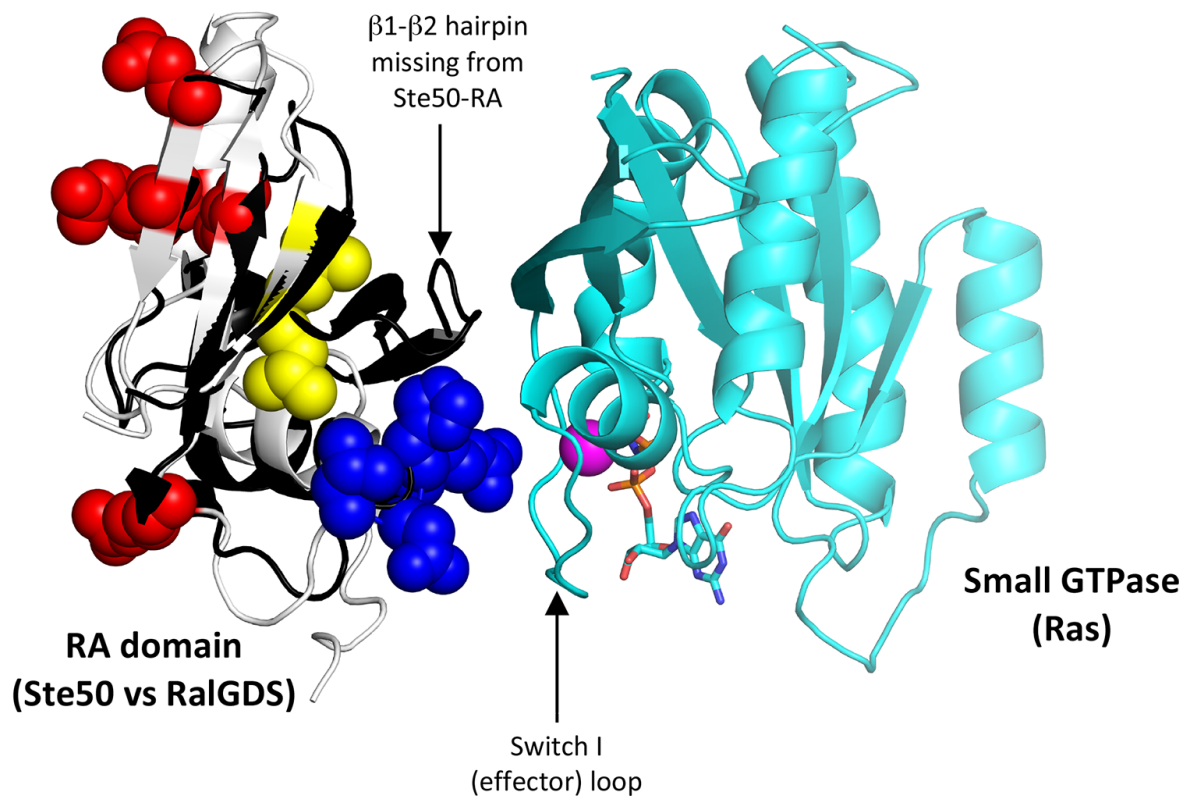


FIGURE S2: Location of the functional interfaces of Ste50-RA domain mapped in this study relative to the canonical interaction mode of RA domain with small GTPases. The image was generated by an overlay of the Ste50-RA domain structure (Ekiel *et al.*, 2009) with the structure of the RalGDS-RA domain bound to the Ras small GTPase (Husang *et al.*, 1998). The Ste50-RA domain structure is rendered as in Fig. 5A, with the pheromone signaling specific cluster in red and HOG signaling specific cluster in blue. The backbone of the overlaid RalGDS-RA domain is rendered in black. The structure of the small GTPase is rendered in cyan, with bound GTP analog (sticks) and Mg²⁺ ion (magenta sphere).

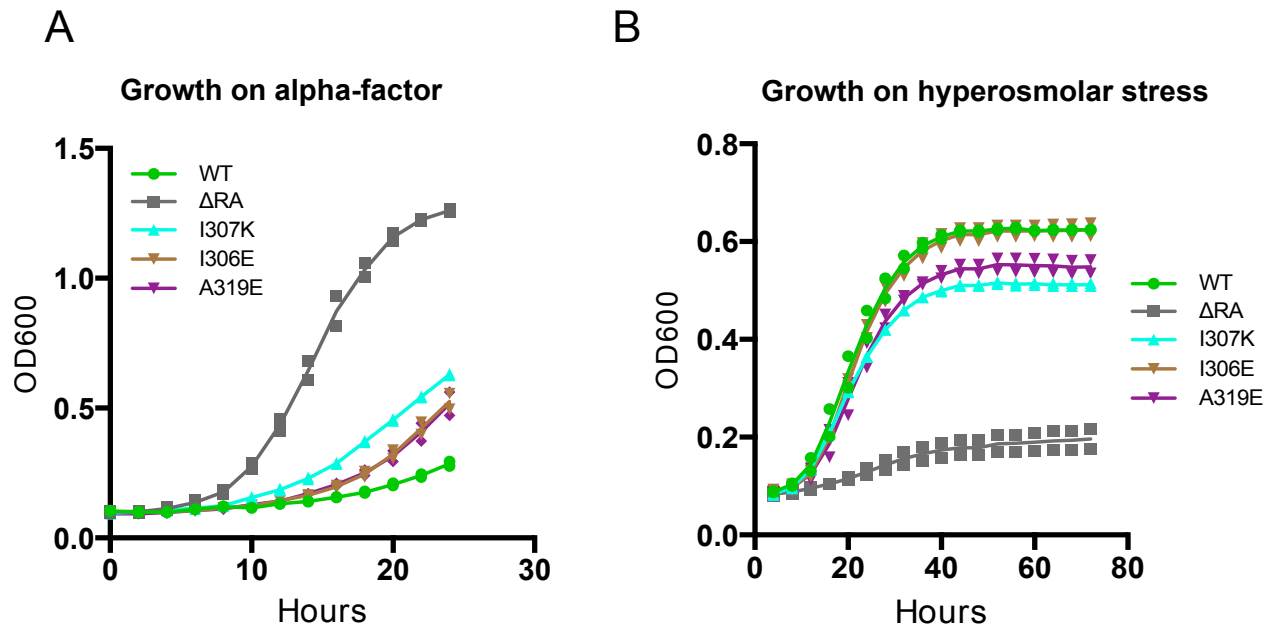


FIGURE S3: Growth assay of Ste50-RA domain mutant weak alleles specifically defective in pheromone response. A & B) Growth curves for yeast strain YCW1886 transformed with ste50 RA domain mutants indicated or with WT or RA domain deletion constructs at OD600 of ~0.1 were incubated in SD-ura selective media with either A) 2 μ M alpha factor for 24 hours or B) 0.5M NaCl for 72 hours and OD600 measured at 10 and 15 minutes intervals for pheromone and hyperosmolar stress respectively by TECAN machine. Data representative of two trials.

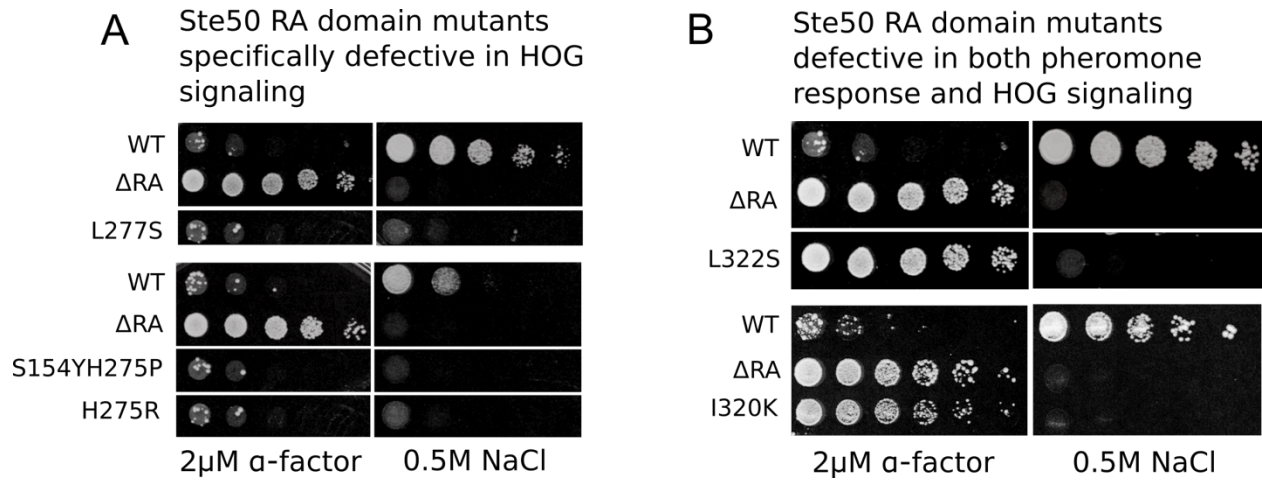
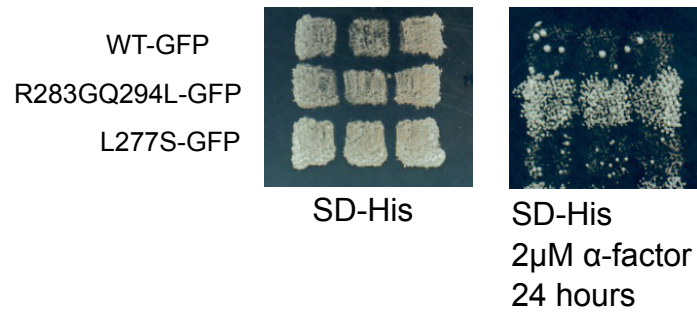


FIGURE S4: Growth assay of *ste50* mutants defective specifically in HOG pathway or in both HOG and pheromone response pathway signaling. Ste50 RA domain mutants indicated were transformed together with the control plasmids into selective plates containing either 2 μ M alpha factor or 0.5 M NaCl. A) Specifically HOG defective mutants. B) Mutants defective in both the HOG and pheromone response pathways.

A



B

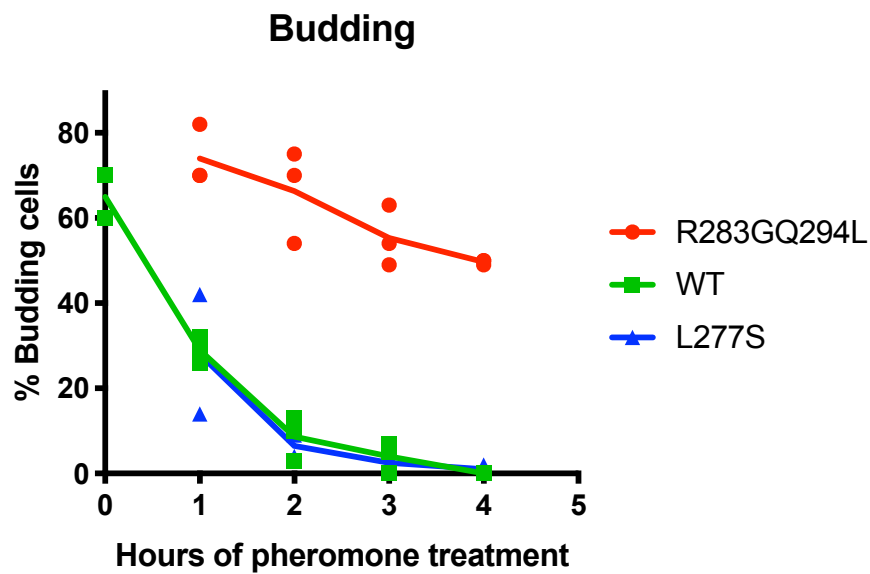


FIGURE S5: GFP tagged proteins retain their respective phenotypic cell cycle arrest. A) Yeast strain bearing WT, R283GQ294L and L277S were grown on SD-ura and replicated onto the test alpha-factor plate. B) Same strains grown on SD-ura in liquid cultures to exponential phase and treated with 2µM alpha factor. Samples were collected at different time points and microscopically analyzed. Scored for the percentage of cells bearing different alleles of Ste50 for budding cells at different times of pheromone treatment. At least two biological replicates and 200 cells par sample were analyzed.

TABLE S1: Ste50-RA domain point mutants with no selectable phenotypes.

Clone	Growth on α -factor	Growth on NaCl	Mutations	Pathway disrupted
Clone 3	-	+++++	G246R ³	None
M3	-	+++++	E261V ⁴	None
M4	-	+++++	L297V ²	None
M8	-	+++++	G343S	None
H15N	-	+++++	R325S	None
H6N_2	-	+++++	E302V	None
H2N_3	-	+++++	R323G E329G A332G	None
M8N	-	+++++	L316V	None
M11N	-	++++	A242T W282R	None
M12N	-	+++++	L212P K309Q	None
M15N_2	+	++++	Y285C E329D	None
3-1	-	+++++	H219Y N276S	None

Note: Superscripts denote number of recurrent hits.

TABLE S2: Stability analysis of Ste50-RA domain mutants.

Ste50 mutation	$\Delta\Delta G_{\text{folding}}(\text{Mut-WT})$	
	mCSM	FoldX
S259A	0.42	-0.12
K260N	-0.06	0.40
K260E	0.17	-0.35
E261V	-0.21	0.50
N270A	0.56	-1.08
R274A	-0.02	0.02
H275A	-0.41	0.60
H275P	-0.88	N/A
H275R	0.24	0.00
N276A	0.23	0.35
L277S	1.11	1.96
D281A	0.46	1.44
W282R	1.96	2.23
R283G	0.87	1.15
R283A	0.60	0.58
V288D	3.02	4.57
I289V	2.01	0.80
I289T	2.99	3.45
C290S	1.75	1.42
Q294L	-0.12	0.45
E295A	0.81	0.30
E295R	0.08	-0.15
R296G	1.09	3.32
L297V	0.74	0.37
L297A	1.28	1.86
L297E	0.85	1.25
E299A	0.69	-0.01
E299R	0.04	0.04
L300V	1.34	0.68
E302V	0.12	0.14
P304S	2.12	2.96
V305T	1.11	0.59
I306E	0.86	-0.69
I307K	1.57	0.80
K309A	0.27	0.40
K309Q	0.35	-0.31
L316V	1.10	0.44
A319E	0.98	-0.38
I320K	1.14	0.83
M321E	0.43	0.37
L322S	2.61	2.74
R323G	1.40	1.96
R325S	0.60	0.70

TABLE S3: Site-directed mutagenesis of Ste50-RA domain

SDM Mutants	Alpha factor	NaCl
E295R	-	+
L297E	±	+
E299R	-	+
I306E	+	+
A319E	+	+
E295A	±	+
L297A	±	+
E299A	±	+
M321E	±	+

- - Means no growth on alpha factor. Normal pheromone response.
- ± Means very low pheromone response defect.
- + Means detectable differential pheromone response defect compared to WT.
- + HOG means normal HOG signaling

TABLE S4: List of plasmids used in this study

Plasmids	Descriptions	Sources
pCW463(Δ RA)	pRS316-ste501-218::URA3/AmpR	Wu et al., 1999
pCW572	pRS313-ste50 ¹¹⁵⁻³⁴⁶ ::HIS3/AmpR	This study
pCW267(WT)	pRS316-STE50 ^{wt} ::URA3/AmpR	Wu et al., 1999
pCW700	pRS313-ste50 ^{I320K} ::URA3/AmpR	Ekiel et al., 2009
pCW701	pRS313-ste50 ^{R274AH275AN276A} ::URA3/AmpR	Ekiel et al., 2009
pCW702	pRS313-ste50 ^{H275AN276A} ::URA3/AmpR	Ekiel et al., 2009
pCW606	pYEX-4T2-ste50 ¹⁻²⁵⁷ HIS3::URA3::LEU2/AmpR	This study
pNS101	pRS316-ste50 ¹⁻²¹⁸ HIS3::URA3/AmpR	This study
pNS102	pRS316-ste50 ¹⁻³⁴⁶ ::URA3/AmpR	This study
pNS103	pRS316-ste50 ^{A242GN270DI289T} ::URA3/AmpR	This study
pNS104	pRS316-ste50 ^{A242G} ::URA3/AmpR	This study
pNS105	pRS316-ste50 ^{N270D} ::URA3/AmpR	This study
pNS106	pRS316-ste50 ^{I289T} ::URA3/AmpR	This study
pNS107	pRS316-ste50 ^{A242GN270D} ::URA3/AmpR	This study
pNS108	pRS316-ste50 ^{N270DI289T} ::URA3/AmpR	This study
pNS109	pRS316-ste50 ^{A242GI289T} ::URA3/AmpR	This study
pNS110	pRS316-ste50 ^{I307KL300VK260N} ::URA3/AmpR	This study
pNS111	pRS316-ste50 ^{I307K} ::URA3/AmpR	This study
pNS112	pRS316-ste50 ^{L300V} ::URA3/AmpR	This study
pNS113	pRS316-ste50 ^{K260N} ::URA3/AmpR	This study
pNS114	pRS316-ste50 ^{I307KL300V} ::URA3/AmpR	This study
pNS115	pRS316-ste50 ^{L300VK260N} ::URA3/AmpR	This study
pNS116	pRS316-ste50 ^{I307KK260N} ::URA3/AmpR	This study
pNS117	pRS316-ste50 ^{R283GQ294L} ::URA3/AmpR	This study
pNS118	pRS316-ste50 ^{R283G} ::URA3/AmpR	This study
pNS119	pRS316-ste50 ^{Q294L} ::URA3/AmpR	This study
pNS120	pRS316-ste50 ^{L182PL277S} ::URA3/AmpR	This study
pNS121	pRS316-ste50 ^{L182P} ::URA3/AmpR	This study
pNS122	pRS316-ste50 ^{L277S} ::URA3/AmpR	This study
pNS123	pRS316-ste50 ^{L322S} ::URA3/AmpR	This study
pNS124	pRS316-ste50 ^{H275R} ::URA3/AmpR	This study
pNS125	pRS316-ste50 ^{S154YH275P} ::URA3/AmpR	This study
pNS126	pRS316-ste50 ^{V288DD338V} ::URA3/AmpR	This study
pNS127	pRS316-ste50 ^{R296G} ::URA3/AmpR	This study
pNS128	pRS316-ste50 ^{I289VR323G} ::URA3/AmpR	This study
pNS129	pRS316-ste50 ^{I289VR323G} ::URA3/AmpR	This study
pNS130	pRS316-ste50 ^{K260EC290S P304S} ::URA3/AmpR	This study
pRS313-GFP	pRS313-STE50-GFP::HIS3/AmpR	Slaughter <i>et al.</i> , 2008
pNS131	pRS313-ste50 ^{R283GQ294L} -GFP::HIS3/AmpR	This study
pNS132	pRS313-ste50 ^{L277S} -GFP::HIS3/AmpR	This study
pNS133	pRS313-ste50 ^{R296G} -GFP::HIS3/AmpR	This study
pNS134	pRS316-ste50 ^{E295R} ::URA3/AmpR	This study
pNS135	pRS316-ste50 ^{L297E} ::URA3/AmpR	This study
pNS136	pRS316-ste50 ^{E299R} ::URA3/AmpR	This study
pNS137	pRS316-ste50 ^{I306E} ::URA3/AmpR	This study
pNS138	pRS316-ste50 ^{A319E} ::URA3/AmpR	This study
pNS139	pRS316-ste50 ^{E295A} ::URA3/AmpR	This study
pNS140	pRS316-ste50 ^{L297A} ::URA3/AmpR	This study
pNS141	pRS316-ste50 ^{L297E} ::URA3/AmpR	This study
pNS142	pRS316-ste50 ^{E299A} ::URA3/AmpR	This study
pNS143	pRS316-ste50 ^{M321A} ::URA3/AmpR	This study
pNS144	pRS316-ste50 ^{M321E} ::URA3/AmpR	This study

TABLE S5: List of oligonucleotides used in this study.

Name	Size	Sequence	Purpose
OCW80 (forward)	26	eggatccATGAAGACCAGCTCAAGC	Error-prone PCR
OCW164 (reverse)	21	AGCTATGACCATGATTACGCC	Error-prone PCR/sequencing
OCW93 (forward)	20	ACAGCCTGCTCCACTTATTC	Sequencing
OCW551 (forward)	21	GCCATAAAAATTCAAGATACTG	PCRout GFP+Colony PCR
OCW552R (reverse)	21	CAAGATCCGTTCCGAGGAGTC	Colony PCR
ONS01 (forward)	32	GCTATGGGGATCAAGcGAGGCTGTAGAAATTG	Site directed mutagenesis
ONS02 (reverse)	32	CAATTCTAACAGCCTCgCTTGATCCCCATAGC	Site directed mutagenesis
ONS03 (forward)	31	GGGATCAAGAGAGGgcGTTAGAAATTGAACG	Site directed mutagenesis
ONS04 (reverse)	31	CGTTCAATTCTAACgcCCTCTCTTGATCCCC	Site directed mutagenesis
ONS05 (forward)	42	GGGATCAAGAGAGGCTGTAGcATTGAACGAAAAGCCTGTG	Site directed mutagenesis
ONS06 (reverse)	42	CACAGGCTTTTCGTTCAAAtgCTAACAGCCTCTCTTGATCCCC	Site directed mutagenesis
ONS07 (forward)	36	GGGTTTGCACCCCCGCCATTgcGTTAAAGAAAGAGAGG	Site directed mutagenesis
ONS08 (reverse)	36	CCTCTTCTTCTTAAcgcAAATGGCGGGGTGCAAAACCC	Site directed mutagenesis
ONS09 (forward)	32	GCTATGGGGATCAaagGAGGCTGTTAGAAATTG	Site directed mutagenesis
ONS10 (reverse)	32	CAATTCTAACAGCCTCetTTGATCCCCCATAAGC	Site directed mutagenesis
ONS11 (forward)	31	GGGATCAAGAGAGGgaGTTAGAAATTGAACG	Site directed mutagenesis
ONS12 (reverse)	31	CGTTCAATTCTAACtcCCTCTCTTGATCCCC	Site directed mutagenesis
ONS13 (forward)	42	GGGATCAAGAGAGGCTGTTagATTGAACGAAAAGCCTGTG	Site directed mutagenesis
ONS14 (reverse)	42	CACAGGCTTTTCGTTCAAAtctTAACAGCCTCTCTTGATCCCC	Site directed mutagenesis
ONS15 (forward)	45	GAAACGAAAAGCCTGTGagATATTCAAGAACTTAAAGCAACAGGG	Site directed mutagenesis
ONS16 (reverse)	45	CCCTGTTGCTTTAAAGTTCTTGAATAATctCACAGGCTTTTCGTTT	Site directed mutagenesis
ONS17 (forward)	32	CAGGGTTTGCACCCCCGaaATTATGTTAAGAAG	Site directed mutagenesis
ONS18 (reverse)	32	CTTCTTAAACATAAAttCGGGGTGCAAAACCCCTG	Site directed mutagenesis
ONS19 (forward)	36	GGGTTTGCACCCCCGCCATTgaGTTAAAGAAAGAGAGG	Site directed mutagenesis
ONS20 (reverse)	36	CCTCTTCTTCTTAAcAcAAATGGCGGGGTGCAAAACCC	Site directed mutagenesis
ONS21 (forward)	37	CTTAGCAGATCAGGATTGgaGACAATAIGTCTTtaGTC	Site directed mutagenesis
ONS22 (reverse)	37	GACtAAGACATATTGTcCCCAATCCTGATCTGTGCTAAG	Site directed mutagenesis
ONS23 (forward)	37	CAATTGCTATGGGGATCaAGAGAGGCTGTTAGAAATTG	Site directed mutagenesis
ONS24 (reverse)	37	CAATTCTAACAGCCTCTcTGATCCCCCATAAGCAAAATG	Site directed mutagenesis
ONS25 (forward)	38	GTAGTGACGGTGTGTCTctTTCACAAACAGACTATTTT	Site directed mutagenesis
ONS26 (reverse)	38	GAAATAGTGTGTTTGTGAAaGAGACACACCCGTCACCTAC	Site directed mutagenesis
ONS27 (forward)	35	CAATGAAAAGACATAACThAGCAGATCAGGATTGG	Site directed mutagenesis
ONS28 (reverse)	35	CCAAATCCTGATCTGCTaAGTTATGTCTTTTTCATTTG	Site directed mutagenesis
ONS29 (forward)	18	CGATTAAGTTGGGTAACG	Colony PCR
ONS30 (reverse)	19	GTGATTTTCGAAGAAGTAGC	PCRout GFP+Colony PCR

Chapter III: Proper pheromone signaling requires spatiotemporally dynamic cellular localization of the adaptor protein Ste50

Nusrat Sharmeen,^a Chris Law,^b Malcolm Whiteway,^c Cunle Wu^{a,d}

^aDivision of Experimental Medicine
Department of Medicine
McGill University
Montreal, QC, Canada H4A 3J1

^bCentre for Microscopy and Cellular Imaging
Department of Biology
Concordia University
Montreal, QC, Canada H4B 1R6

^cDepartment of Biology,
Concordia University
Montreal, QC, Canada H4B 1R6

^dHuman Health Therapeutics Research Centre
National Research Council Canada
6100 Royalmount Avenue
Montreal, Quebec, Canada H4P 2R2

3.1 Preface

Previously we have shown that Ste50 adaptor protein localizes to the polarized shmoo tip and this tip localization is required for proper shmoo formation. With a continued effort to understand the tip localization dynamics and other localization functions of the adaptor protein that may be linked to pheromone signaling specificity, in the following chapter we performed detailed microscopic studies. Here we first describe how Ste50 polarity patch formation correlates with the polarized shmoo growth and pheromone stimulus. We describe that Ste50 has no involvement in the vegetative bud polarization, while enhanced bud-neck localization prior to cytokinesis requires Ste50-RA domain pheromone specific residues, which may prime the polarization of shmoo formation that is required for the pheromone signaling. We also describe that Ste50 localizes to the nucleus and this localization is impaired in cells with a specifically pheromone response defective mutant of Ste50, indicating that nuclear translocation of the protein may be involved in pheromone signaling function.

Author contributions:

Nusrat Sharmeen	Conceptualized, Designed experiments, Performed investigations, Performed formal analysis, Image processing, Wrote the original manuscript and Edited.
Chris Law	Set-up the microscope and carried out the microscopic time-lapse imaging, help with image analysis and Wrote the FIJI macros.
Malcolm Whiteway	Reviewed and Edited the manuscript.
Cunle Wu	Manuscript writing, Review and Editing; Data analysis and orientation

3.2 Abstract

Dynamic spatial-temporal protein translocation is necessary for the delivery of proteins to the site of their function and modifications to critically control diverse biological processes. In the yeast *Saccharomyces cerevisiae*, the adaptor protein Ste50 is required for the functions of three MAPK pathways that control pheromone response, osmoregulation, and filamentous growth. Previously we found that Ste50 localized to the polarized front of the shmoo structure in response to pheromone, and specific RA domain mutations caused loss of this localization function with an associated severe defect in the pheromone signaling. Here we show that Ste50 polarization patches form early on in response to pheromone and demarcate shmoo sites on the cell cortex. Patches are formed in the cytoplasm, and move toward their shmoo tip destination where their presence correlates with the shmoo maturation time, this appearance of Ste50 polarity patch at the shmoo tip is also pheromone concentration dependent. Ste50 showed no localization in the polarized bud front suggesting no Ste50 function in polarized bud growth. However, striking Ste50 localization was observed in the polarized bud-neck in the presence of pheromone that coincided around cytokinesis. A strain containing a Ste50-RA domain mutant, R296G, failed in this enhanced bud-neck localization, indicating a localization defect possibly due to loss of association. Wild type Ste50 also translocated to the nucleus during vegetative growth, as well as when cells were stimulated with pheromone. The Ste50 RA domain mutant R296G showed significantly reduced nuclear localization, suggesting a possible link with the pheromone signaling dependent polarization function of Ste50p. Our results suggest that spatiotemporal cellular localizations of Ste50 are required for proper pheromone signaling in yeast.

3.3 Introduction

Protein translocation during cellular signaling is a mechanism that ensures organisms can efficiently regulate pathway components eliciting specific responses. Many proteins in the MAPK pathway undergo reorganization in a stimulus dependent way to relocate at sites where they can exert their functions, often by forming multimeric complexes (Alberts *et al.*, 1998). Complex formation needs proximity and this organization provides a positional cue that is required for protein activity, thereby influencing signaling specificity and efficacy. For example, protein kinase A (PKA) and protein kinase C (PKC) use adaptor proteins “A kinase adaptor proteins” (AKAPs) and “receptors for activated C kinase” (RACKs) to achieve substrate specificity through modifying their subcellular localizations and thus protein-protein interactions (Faux & Scott, 1996; Pawson & Scott, 1997; Mochly-Rosen & Gordon, 1998). Often components translocate to the membrane, this is a general phenomenon found among all organisms, from unicellular bacteria to humans (Fanger *et al.*, 1999; Widmann & Gibson, 1999; Laub & Goulian 2007; Driessen *et al.*, 2008; Lemmon & Schlessinger, 2010; Maik-Rachline *et al.*, 2019).

Saccharomyces cerevisiae MAPK signaling pathways control important biological processes, such as growth, differentiation and environmental stress regulation through response to pheromone, nutritional conditions and osmolarity changes, respectively (Herskowitz, 1995). The component proteins of these MAPK pathways show many translocation dynamics during their activation and inactivation. The well-studied mating-pheromone response pathway has many proteins that translocate during signaling. For example, the upstream MAP4K Ste20 has been found at the polarized front of the bud during vegetative growth, and the shmoo tip after activation by pheromone (Peter *et al.*, 1996; Leberer *et al.*, 1997). MAP3K Ste11 is localized in the cytoplasm and translocated near the membrane upon pheromone stimulation (Pryciak *et al.*, 1998). Scaffold protein Ste5 was found to continuously undergo nucleocytoplasmic shuttling and remains mostly in the cytoplasm after pheromone treatment (Pryciak *et al.*, 1998; Mahanty *et al.*, 1999). Ste5 nuclear export is facilitated by the exportins Msn5/Ste21 and is required for pheromone response

(Mahanty *et al.*, 1999). Ste5 also localizes to the shmoo tip after pheromone treatment (Pryciak *et al.*, 1998). The MAPK Fus3 is also found to translocate to the nucleus upon activation to activate the transcription factor Ste12 (Choi *et al.*, 1999). The bifunctional protein Far1 is required for cell cycle arrest and shmoo formation. To achieve these two functions, Far1 localizes between two different cellular compartments, the cytoplasm and the nucleus. Nuclear Far1 is responsible for pheromone dependent cell cycle arrest and its translocation to the nucleus is by its bipartite NLS signals (Blondel *et al.*, 1999) while export from the nucleus is with the help of the exportins Msn5/Ste21 (Blondel *et al.*, 1999). In response to pheromone Far1 redistributes to the cytoplasm where it is sequestered by Ste4 to tether it to the membrane (Blondel *et al.*, 1999).

The adaptor protein Ste50 works at the level of MAP3K Ste11 in the pheromone response pathway with its N-terminal SAM domain interacting with the SAM domain of the Ste11 protein. This interaction is critically required for proper pheromone response (Wu *et al.*, 1999). The C-terminal RA domain of this protein interacts with plasma membrane localized proteins Opy2p and Cdc42p to function in the HOG and pseudohyphal growth signaling pathways respectively (Wu *et al.*, 2006; Truckses *et al.*, 2006). GFP tagged Ste50p showed its presence mainly in the cytoplasm (Huh *et al.*, 2003) during vegetative growth.

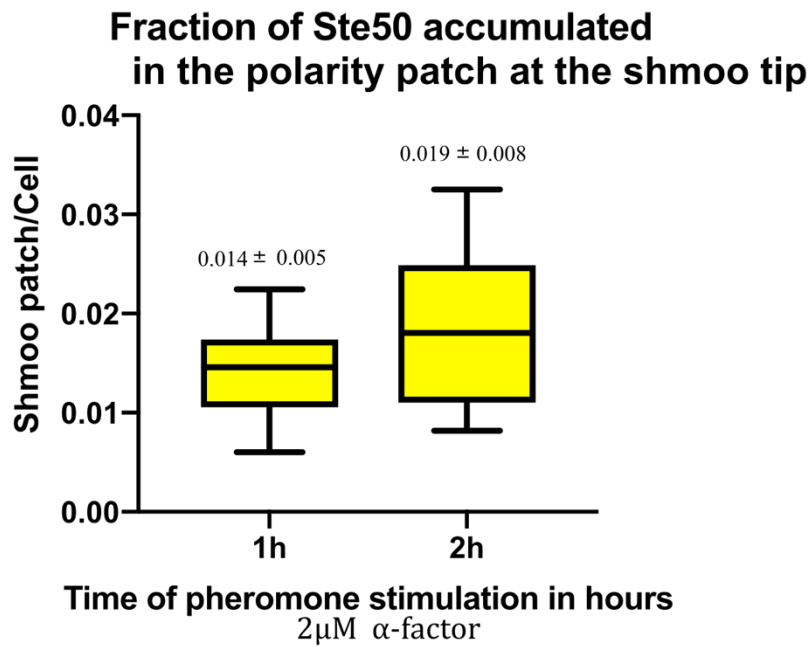
Our recent work revealed the localization profile of Ste50p in response to pheromone. Ste50p localizes to the polarized shmoo tip under pheromone stimulation and this tip localization is critical for shmoo formation (Sharmeen *et al.*, 2019). Here we performed a detailed microscopic study of this protein to uncover its localization profile. Our study revealed new evidence of the dynamic localization profile of Ste50p to cellular sites during vegetative growth and under pheromone stimulation, while the specifically pheromone response defective RA domain mutant protein failed to translocate properly, indicating a molecular link may be broken that is required for its involvement in many cellular processes geared towards the success of a robust mating signaling.

3.4 Results

Pheromone-signaling dependent shmoo tip localization of Ste50p

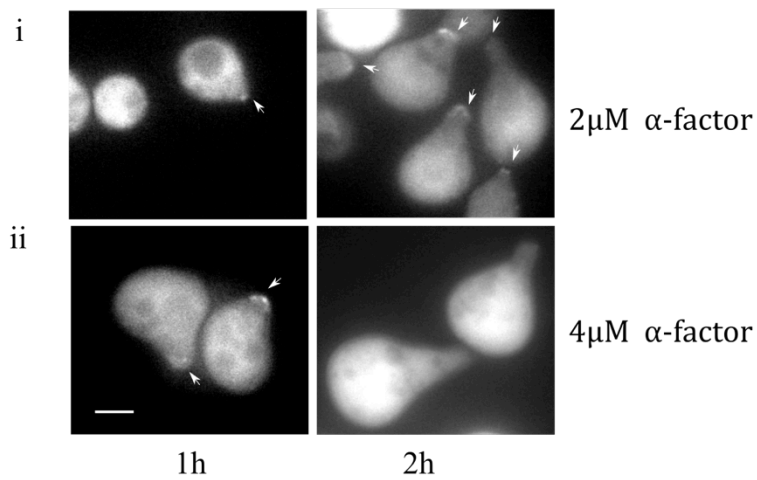
Previously we demonstrated that wild type Ste50p localizes to the shmoo tip upon pheromone treatment and that RA domain of Ste50p is required for this localization (Sharmeen *et al.*, 2019). However, in our time-course experiments with exponentially growing cells treated with 2 μ M pheromone, dense shmoo tip localizations of Ste50-GFP could be visualized usually within 20-30 min of pheromone treatment and peaked around 2h. The characteristics of this shmoo tip localization were investigated in more detail here by microscopic studies. Since Ste50 was mainly cytoplasmic, the fraction of Ste50-GFP that was mobilized to the tip during pheromone stimulation was calculated. This was plotted for different durations of pheromone stimulation for individual cells in Figure 1A. On average the estimated fraction of Ste50-GFP at the shmoo tip (mean shmoo patch/mean cell) was 0.014 ± 0.005 and 0.019 ± 0.008 at 1h and 2h of pheromone stimulations respectively. Interestingly, although significantly different sizes of Ste50p polarization patches were observed at the shmoo tip at 1h and 2h of pheromone stimulations, cells mobilized on average similar fractions (1.4% and 1.9%) to the tip. To investigate whether shmoo tip accumulation of Ste50p is pheromone dose-dependent, cells were stimulated with different amounts of pheromone and followed by microscopic analysis. At 1h of pheromone stimulation, the percentage of cells undergoing shmoo formation between 2 μ M and 4 μ M treatments were 34% and 52% and the percentage of cells with Ste50-GFP accumulated at the shmoo tip were 60% and 84%, respectively. While at 2h of pheromone stimulation, shmoo formation was 57% and 98% and accumulation was 80% and 5% respectively. Increasing the pheromone concentration (4 μ M) caused gross Ste50-GFP accumulation at the shmoo tip that appeared sooner and disappeared faster [Figure 1B], while at a lower pheromone level (0.2 μ M, data not shown) although cells were able to form some shmoos, the polarization patches were mostly wandering around the cell cortex, as observed before (Dyer, 2013). These results demonstrate that the appearance of a sizeable polarization patch of Ste50 at the tip is dependent on pheromone concentration and the length of pheromone exposure.

A



B

**Shmoo tip accumulation of Ste50
at different pheromone concentrations**



C

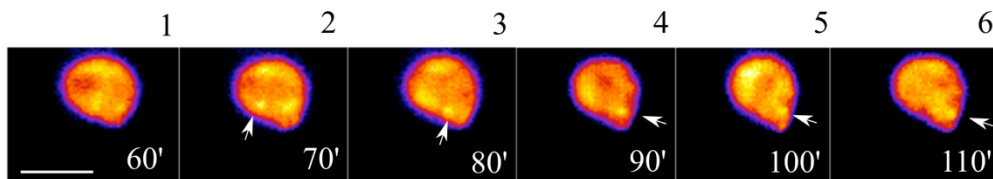


FIGURE 1: Characterization of the shmoo tip localization of Ste50. Yeast strain YCW1886 bearing wild type Ste50-GFP was stimulated with alpha-factor and imaged by microscopy. (A) Ste50 accumulation at the shmoo tip quantified with respect to the cytoplasmic amount ($n > 20$). (B) Cells were stimulated with the indicated concentrations of alpha factor for the indicated time, bar 10 μm . (C) Single cell analysis with time-lapse microscopy shows Ste50 polarity patch (punctate) travelling from the cytoplasm towards the shmoo tip. Used the imagej LUT fire tool. Bar 5 μm . Frames every 10 min. Bar 2 μm . All results are based on live cell imaging by fluorescent microscopy.

To study the details of the appearance and the disappearance of Ste50p polarization patches at the shmoo tip, single cells were followed after stimulating with 2 μM pheromone by time-lapse microscopy using an automated image analysis platform (Nikon Ti, see *Materials and Methods*) and generated long time-lapse movies. By imaging cells over a period of time we were able to detect punctate polarity patch movements in the cytoplasm of single cells, these patches are beadlike and show highly intense GFP signals, and showed a track of movement towards the shmoo tip, an example is shown in Figure 1C. These results demonstrate that polarity patches are formed within the cytoplasm and translocate to the shmoo tip.

Single cell analysis revealed that Ste50p is an early indicator of shmoo formation in response to pheromone

Our population level time-course microscopic studies with live yeast cells bearing Ste50-GFP treated with 2 μM pheromone showed foci of accumulated Ste50p on the cell cortex. These accumulations were readily detectable usually after 3 hours of pheromone treatment [Figure 2A]. To confirm that the foci are the locations for the future shmoo development, we performed time-lapse microscopy (see *Materials and Methods*). By tracking single cells over time we confirmed that Ste50-GFP localized foci are sites for future shmoo development [Figure 2B]. This phenomenon could be observed more readily for the second

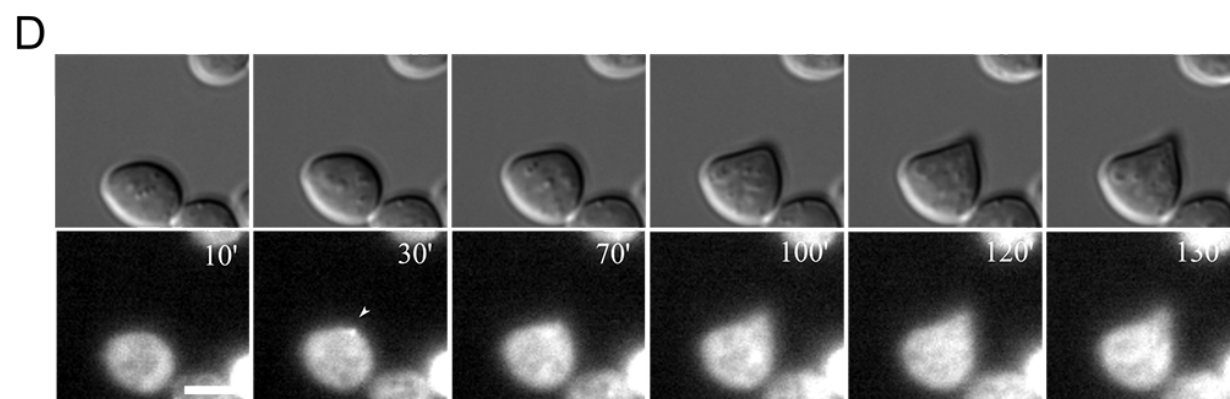
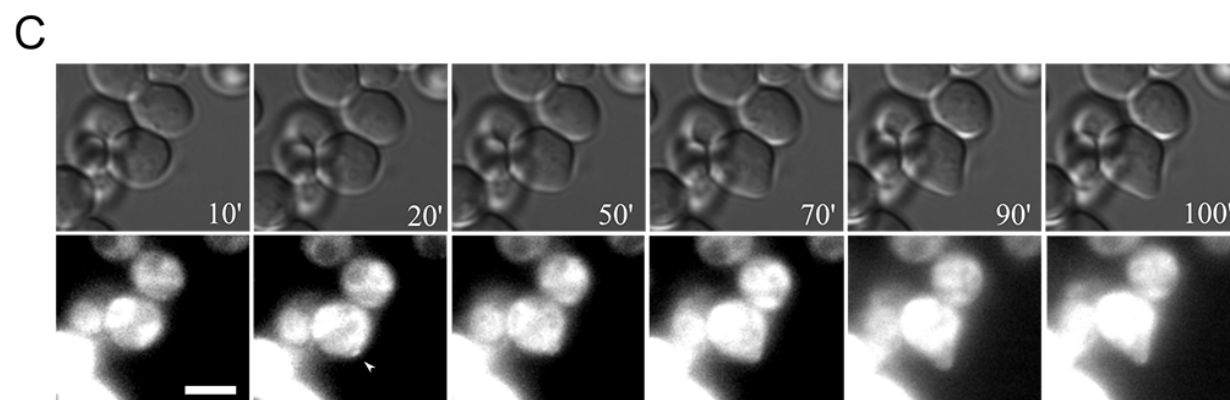
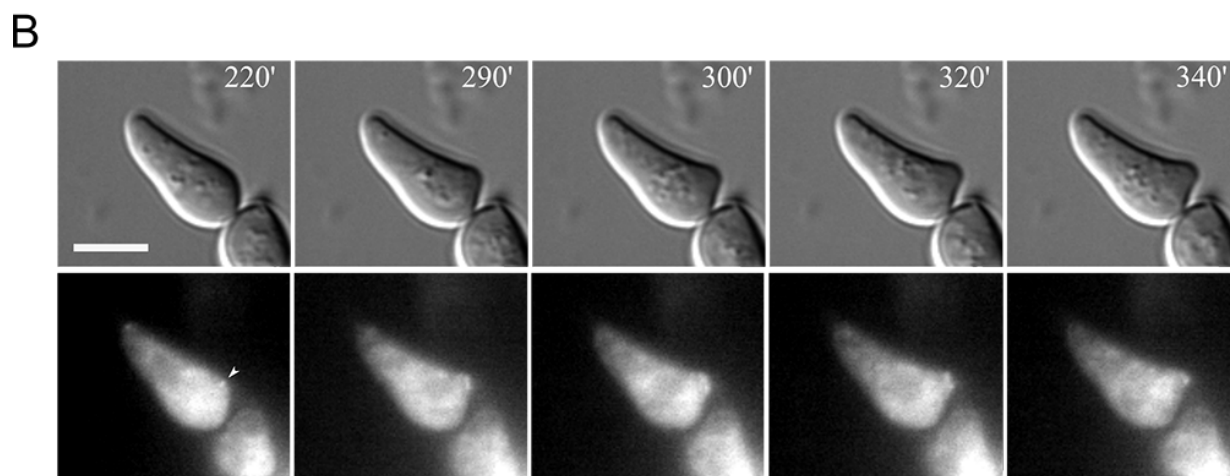
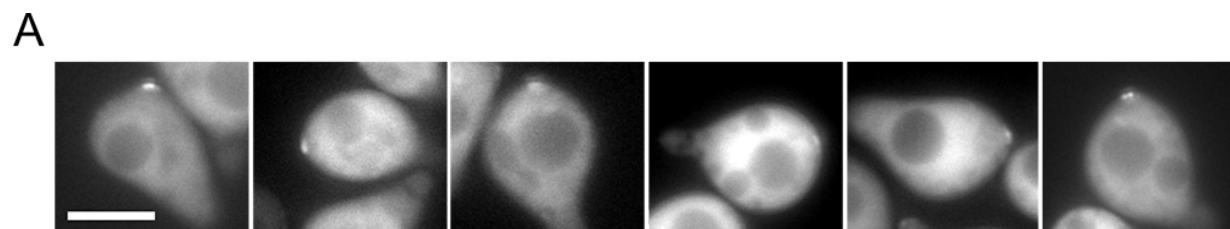


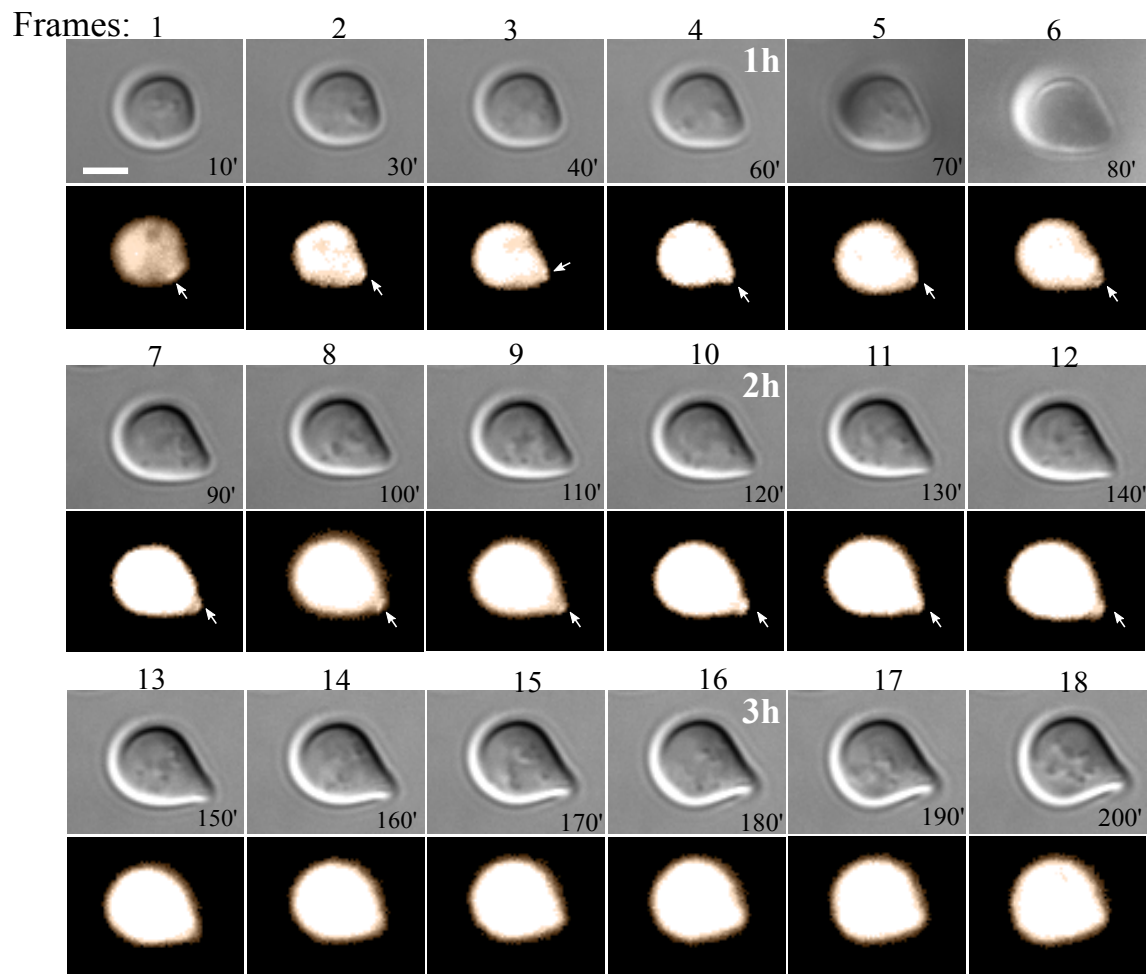
FIGURE 2: Ste50 polarity patch on the cell cortex is an early indicator of shmoo formation. Yeast strain YCW1886 expressing Ste50-GFP was studied microscopically after 2 μ M alpha-factor treatment. Time-course microscopic studies showing cells with Ste50-GFP foci after 3h pheromone treatment (A). Time-lapse microscopic studies with Ste50-GFP showing nucleation of Ste50-GFP as an early indicator (arrow) of future shmoo development sites for secondary shmoo (B) and primary shmoo (C) & (D). Bar indicates 5 μ m.

shmoo since the foci were large, possibly due to the readily available existing Ste50 polarization punctate patches, but was also observed for the primary shmoo as early as 20 minutes after pheromone treatment [Figure 2C & D]. Thus our time-lapse studies showed that Ste50 nucleates into foci on the cell surface, an early indication for shmoo polarization.

Ste50 localization at the shmoo tip correlates with shmoo maturation but not shmoo maintenance

Single cell studies by time-lapse microscopy over a long period showed details of Ste50-GFP translocations within the cell and novel findings. The cytoplasmic Ste50-GFP moved dramatically and rapidly and punctate polarity patch also polarized/depolarized. Examining single cell revealed that Ste50-GFP polarity patch was formed at the future polarization site as an early indicator of shmoo formation (as also found before and discussed above) at ~10 min [Figure 3A, Frame 1]. The dynamics of Ste50-GFP polarity patch showed that the time for peak appearance of the polarity patch at the shmoo tip was 2h [Figure 3A, Frame 10], supporting our previous findings from time-course microscopic observations (Sharmeen *et al.*, 2019), followed by its gradual disappearance within the next 20min [Figure 3A, Frame 11, 12]. The above scenario was also observed in other cells that were examined. To find if there is a relationship between polarized shmoo growth and Ste50 polarization patch at the tip, we measured the shmoo growth by measuring the long axis of the cell in each frame and plotted against time [Figure 3B]. This analysis showed that shmoo polarization increased linearly with time when Ste50 polarity patch were observed at the shmoo tip [Figure 3A, Frames 1-12 and Figure 3B] and stopped when the polarity patch disappeared [Figure 3A, Frame 13 and 3B]. Therefore, it supports the

A



B

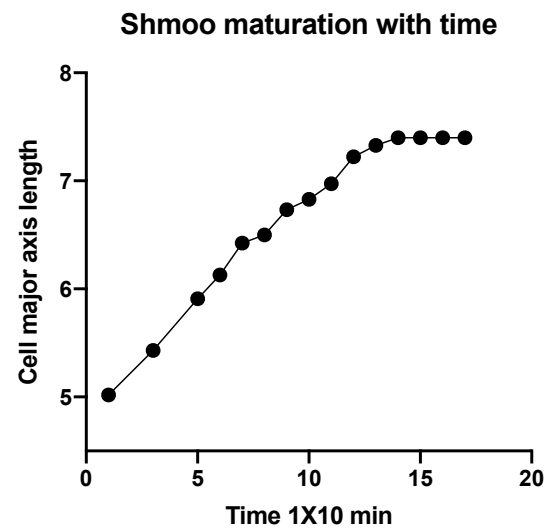


FIGURE 3: Ste50 localizes to the shmoo tip until shmoo maturation. Punctate, shmoo polarization patches of Ste50-GFP in yeast cell. (A) Time-lapse microscopy with frames at indicated intervals in minutes. Arrow shows Ste50-GFP polarity patch accumulation over time. Accumulation appears at the shmoo polarization front in frame 1, 10 minutes after pheromone stimulation. Peak accumulation is observed at 2h, accumulation starts to disappear in frames 11-12. Thereafter, accumulation disappears. Imagej LUT tool was utilized with thresholding. (B) Correlation of Ste50 polarity patch at the shmoo tip with polarized growth. Data represents the cell in (A) and shown for frame 1-15 (until 170 min). The major cell axis (μm) versus time in min has been plotted. The shmoo tip polarization patch starts to disappear after frame 10 (120 min) that corresponds to the termination of the polarized shmoo growth.

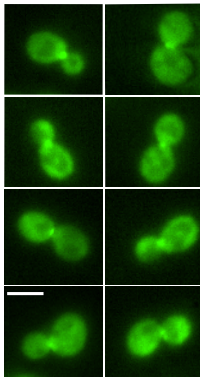
hypothesis that the residence time of Ste50 at the shmoo tip is required for shmoo maturation; as the shmoo reaches its maturation, Ste50 disappears. Similar correlation between the residence of bud polarization patch and bud maturation was also reported before (Waddle *et al.*, 1996). Thus, Ste50 is required at the tip until the shmoo matures and not needed for shmoo maintenance.

Pheromone triggers enhanced bud-neck localization of Ste50

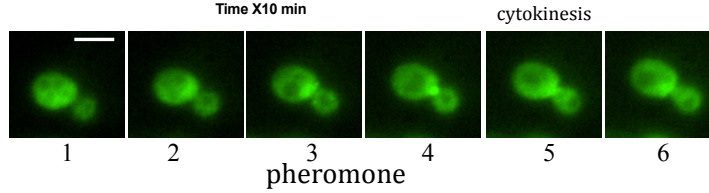
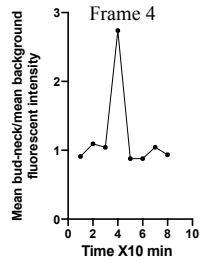
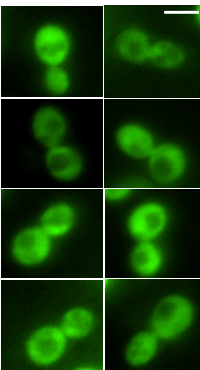
Vegetatively growing yeast cells reproduce through budding. With the progression of cell cycle, cells invaginate and separate by cytokinesis in telophase (Hartwell *et al.*, 1974; Elliott *et al.*, 1983). During the Ste50-GFP localization studies by time-lapse microscopy with pheromone-stimulated cells, single cells were followed and unexpectedly found striking transient localization of Ste50-GFP at the bud-neck prior to cytokinesis [Figure 4A]. Ste50-GFP localization at the bud-neck could be detected in 100% of cells under pheromone stimulation, although the intensity of localization varied among the population of cells. From single cell analysis, as an example, the cell showing the most bud-neck localized Ste50-GFP was quantified, and the mean GFP signal (see *Materials & Methods*) showed a sharp localization of Ste50-GFP in the bud-neck $\sim 10\text{min}$ prior to cytokinesis, which disappeared quickly in the preceding step [Figure 4B, Frame 4]. To find if this phenomenon

exclusively occurred in the pheromone treated cells, time-lapse movies were carried out with pheromone untreated cells. In the absence of pheromone stimulation Ste50-GFP was still detectable at the bud-neck just before cytokinesis, similar to the pheromone treated cells, but only found in ~10% of cells [Figure 4C]. As an example, the cell showing the most Ste50-GFP at the bud-neck was quantified, the GFP signal at the bud-neck for the untreated cell showed ~2X less intensity than the pheromone treated cells [Figure 4D, Frame 4].

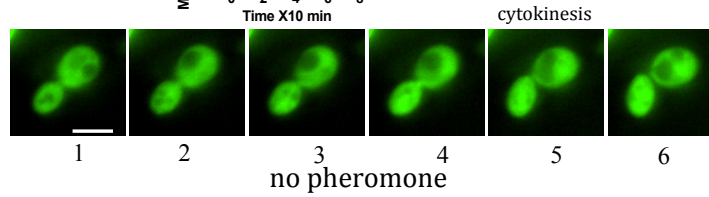
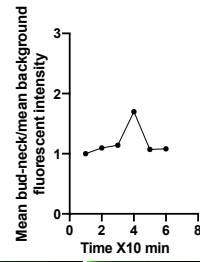
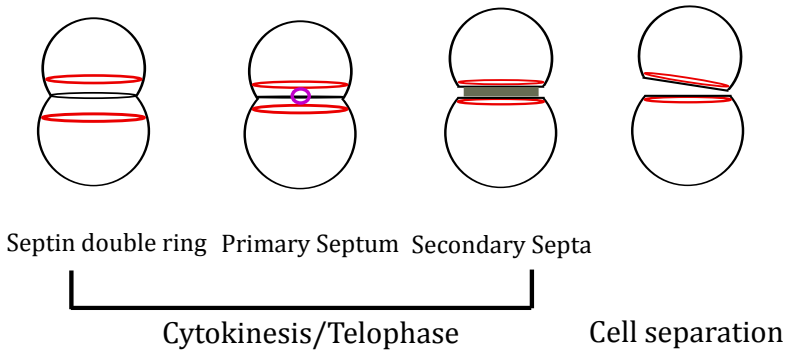
Cytokinesis consists of 3 different stages, septin double ring formation, primary septum formation and secondary septum formation [Figure 4E] (Wloka & Bi, 2012). During secondary septum formation, cells break up and are held only by the secondary septum, here, by cytokinesis we specifically focus on the cell break up and not cell separation. Our time-lapse movies detected the cell break up [Figure 4F] and subsequent loss of Ste50-GFP from the bud-neck. Interestingly, some of the mother-daughter cells retained a remnant of the accumulated Ste50 even after cytokinesis that became a site for shmoo growth later on [Figure 4F, straight arrow]. Vasen *et al.*, 2018 also reported similar observation that the polarity patch involved during cytokinesis remained after cytokinesis and was used to form shmoo polarization. We found in ~85% of the cells shmoo projection grew just next to the previous bud site and in ~15% the position could not be positively identified, supporting previous observations (Madden & Snyder, 1992). We previously created Ste50-RA domain mutants that are specifically defective in pheromone signaling (Sharmeen *et al.*, 2019). These mutants lost their ability to accumulate at the polarized shmoo tip. To find if these mutations also cause a loss of bud-neck localization, we examined Ste50-RA domain mutant R296G under pheromone stimulation and followed the mutant's localization by time-lapse movies. The mutant did not show any enhanced bud-neck Ste50p localization in response to pheromone as observed for the wild type [Figure 4G]. It is however, difficult to conclude whether the mutant completely lost its ability for bud-neck localization under pheromone treatment, since WT Ste50p bud-neck localization could only be detected in ~10% of the vegetatively growing cells at a very low level of Ste50-GFP signal. Therefore, the mutant may have very low levels of localized Ste50-GFP, which may not have been detected. The mutant's budding pattern was found to be similar to the

A WT Ste50-GFP

+alpha-factor

B Bud-neck localization of Ste50 in response to pheromone**C** WT Ste50-GFP

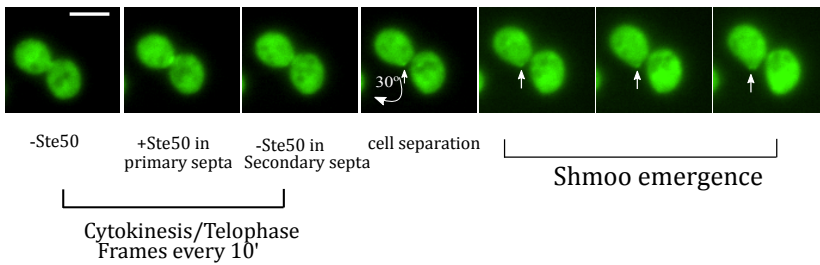
-alpha-factor

D Bud-neck localization of Ste50 in vegetatively growing cells**E**

Septin double ring Primary Septum Secondary Septa

Cytokinesis/Telophase

Cell separation

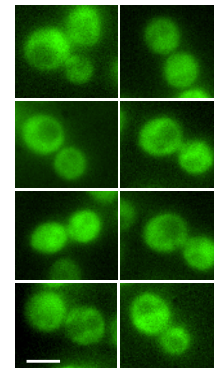
F

-Ste50

+Ste50 in
primary septa-Ste50 in
Secondary septa

cell separation

Shmoo emergence

Cytokinesis/Telophase
Frames every 10'**G** Ste50-R296G-GFP

+alpha-factor

FIGURE 4: Ste50 localizes to the bud-neck. Yeast strain YCW1886 with bud-neck localization of WT Ste50 with and without pheromone treatment (A & C). Quantified bud-neck localization of WT Ste50 with and without pheromone treatment in time-lapse movies (frame every 10 min) (B & D). Cartoon, showing yeast cytokinesis (E). Time-lapse movie showing stages of cytokinesis and cell separation in WT type Ste50 after pheromone treatment. Curved arrow showing 30° movement. Straight arrow showing shmoo emergence (F). RA domain mutant of Ste50 (R296G) showing reduced to undetectable levels of bud-neck localization (G).

vegetatively growing wild type cells. These results suggest that mutation in the RA domain of Ste50p causes loss of enhanced localization at the bud-neck during pheromone stimulation, reinforcing our previous results identifying the loss of this mutant's ability to localize at the shmoo tip.

Ste50 localizes to the nucleus

Our microscopic observation showed a dual subcellular localization of Ste50p. It is generally accepted that in dividing cells Ste50 is localized in the cytoplasm. However, in the process of the detailed microscopic study of the cellular localization of Ste50p, we noticed that a fraction of cells showed increased Ste50-GFP localization in the nucleus in yeast cultures. This was confirmed with DAPI nuclear staining of the cells and dual fluorescence channel visualizations (*Materials and Methods*) [Figure 5A]. Interestingly, this observation is similar to what had been described for the scaffold protein Ste5 (Mahanty *et al.*, 1999). In order to examine if there is any change in the WT Ste50p nuclear localization with time, exponentially growing cells were used to determine Ste50p nuclear localizations over different time points under the vegetative growth conditions (*Materials and Methods*). This resulted in a variable Ste50p nuclear localization in between ~13% to 25% of cells at the

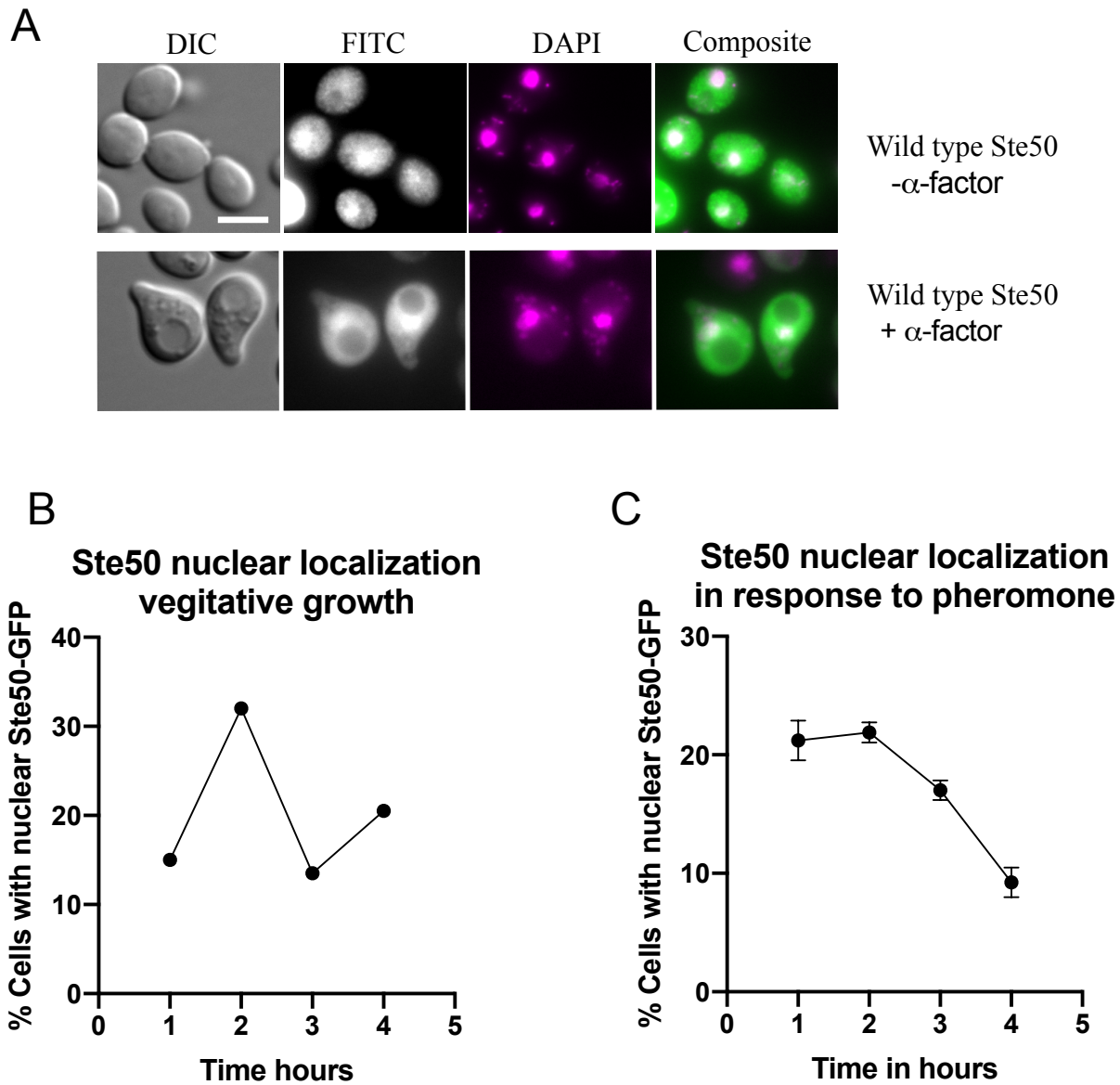


FIGURE 5: Ste50 localizes to the nucleus. Yeast cells transformed with wild type Ste50-GFP with and without pheromone stimulation treated with DAPI nuclear stain (*Materials and Methods*) for microscopic visualization. Ste50-GFP localizes to the nucleus (A). Time-course nuclear Ste50-GFP localization in the vegetatively growing cells (B) and in response to pheromone (represents four independent experiments) (C). Bar represents 5 μ m.

population level over four hours. Results of independent experiments showed a random nature of Ste50 localization with time [Figure 5B]. During microscopic examination many cells under pheromone stimulation also showed clear Ste50-GFP nuclear localization [Figure 5A]; to determine if pheromone causes increased nuclear localization of Ste50-GFP, time-course studies were performed. Cells under pheromone stimulation showed very consistent nuclear localization profile with a loss over time [Figure 5C], this observation may indicate nuclear exit of Ste50, or alternatively it may be due to changing Ste50 protein abundance levels during the different time points of investigation due to either protein expression levels or protein degradation.

Cell cycle dependent nuclear localization of Ste50

The random nature of Ste50 nuclear localization under vegetative growth conditions indicated that the localization could be cell cycle dependent, which has been observed for many nuclear shuttling proteins (Koch *et al.*, 1993; Costanzo *et al.*, 2004; Kosugi *et al.*, 2009; Taberner *et al.*, 2009). To investigate, detailed microscopic examinations were performed of the cellular morphological changes and nuclear structural modifications that occurred during the different cell cycle phases, and broadly categorized cells in different cell cycle phases in the time-course experiments (*Materials and Methods*). The proportion of cells showing nuclear Ste50-GFP in the binned groups was obtained as a ratio of the total number of cells in their respective groups.

The different cell cycle phases were set as G1 - stages with no bud and undivided nucleus; S - stages when bud starts but undivided nucleus; anaphase – nuclear division into mother-daughter cells but nucleus is not separated; telophase – separated nucleus between mother-daughter cells; cell separation – mother-daughter separates (Delobel *et al.*, 2014) [Figure 6A]. This undertaking showed a clearer picture of the localization profile of Ste50-GFP during the different cell cycle phases. Ste50 could be identified in the nucleus in all the different cell cycle phases but their relative proportions were variable [Figure 6B]; Ste50-GFP was mainly found to accumulate in the nucleus during the G1 and S phase, with loss of localization during anaphase and telophase when the nucleus is segregating between the

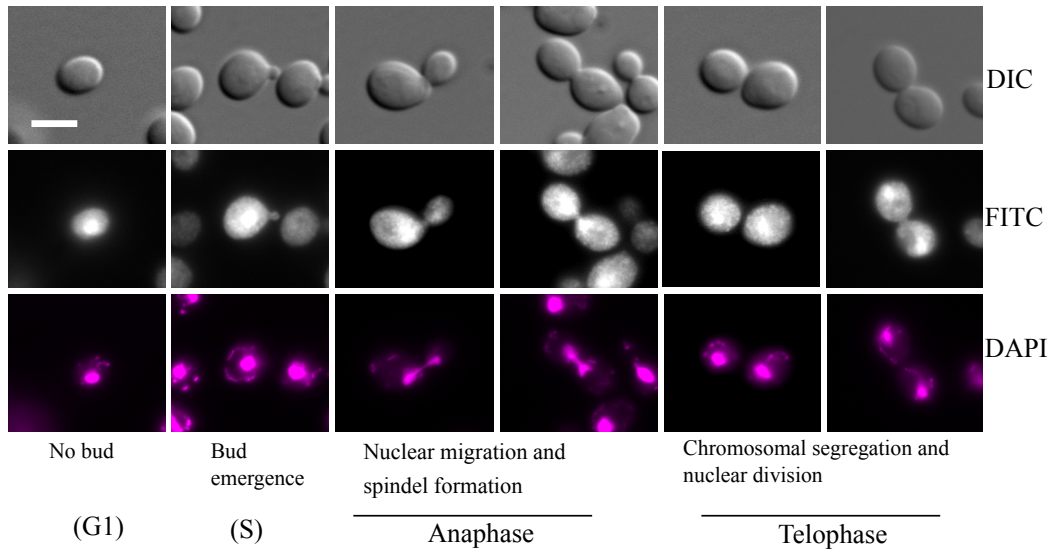
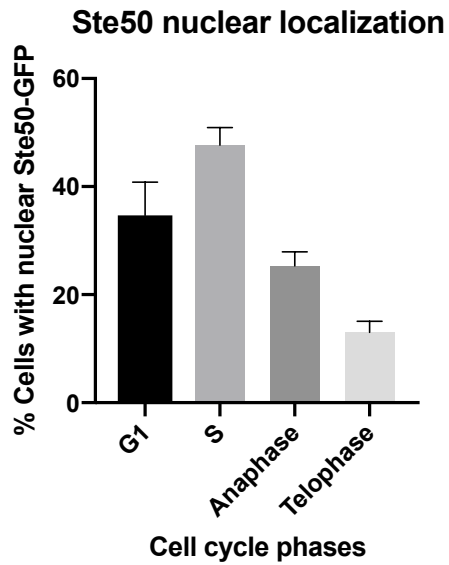
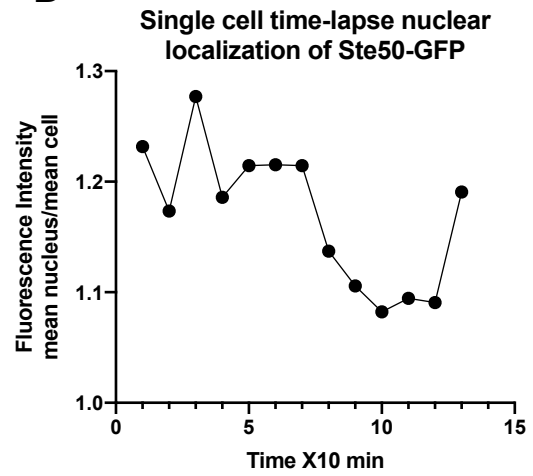
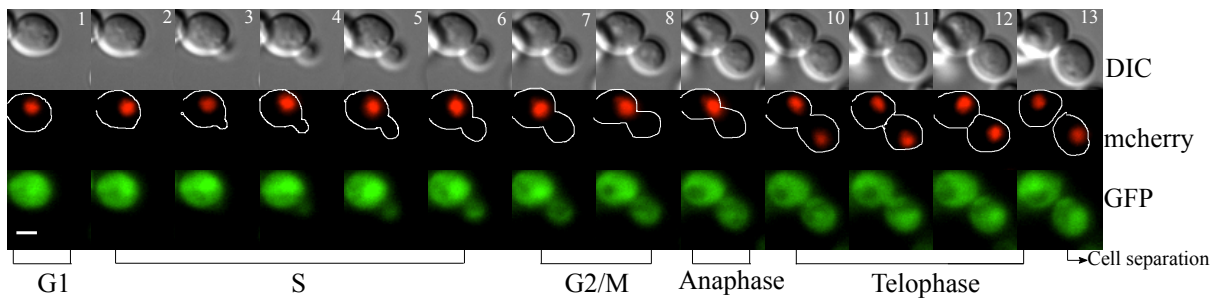
A**B****D****C**

FIGURE 6: Ste50 localizes to the nucleus in a cell cycle dependent manner. Accumulation at different cell cycle phases in reference to cell and nuclear morphology, visualized in DAPI treated cells as indicated (A) (see results section). The percentage of cell at different cycle phases showing nuclear Ste50-GFP localization (B). Time-lapse movie showing the appearance and disappearance of Ste50 nuclear localization at different cell cycle phases with Hta2-mcherry and Ste50-GFP (C). Frames every 10 min and bar 5 μ m. Proportion of Ste50-GFP at the nucleus quantified from (C) in (D).

mother and daughter cells. These results demonstrate that Ste50p localizes to the nucleus in variable abundance during different cell cycle phases.

To confirm Ste50 nuclear localization during the different cell cycle phases, single cells were followed by time-lapse microscopy. The movies thus generated were manually processed to align the cell cycle events in different cells. A complete cell cycle was designated as the time of the bud emergence till cell separation, when mother and daughter cells separate. When the movies were processed, a few frames were taken before the start of the bud appearance that signified the G1 phase. Single cell analysis showed a general trend of nuclear localization of Ste50 starting from the end of G1 into S phase [Figure 6C]. In all the cells that were analyzed, the S phase, when cells were undergoing DNA replication, was highly enriched with nuclear localized Ste50-GFP [Figure 6C, Frame 1-8], while nuclear localization dropped during telophase [Figure 6C, Frame 14 & 15]. We quantified the Ste50-GFP nuclear localization by measuring the fluorescent intensities (mean nucleus/mean cell) of the different cell cycle phases from the time-lapse movies of many cells, an example is shown in Figure 6D, which corresponds to Figure 6C. Of the 25 different cells analyzed for nuclear GFP intensities, 21 showed a drop around telophase. The decrease in nuclear Ste50 level during telophase in the single cell time-lapse study corresponded with the decrease observed in the population level time-course study. These results show that nuclear Ste50 levels change in a cell cycle dependent manner in yeast.

Ste50-RA domain mutant defective in pheromone signaling is also defective in nuclear localization

To examine whether there is any correlation between the nuclear localization of Ste50 and pheromone signaling, the specifically-pheromone-response-defective Ste50-RA domain mutant R296G (Sharmeen *et al.*, 2019), was tested. Its pheromone signaling capability measured by a transcriptional activation assay showed a gross pheromone response defect [Figure S1]. To find if this mutation has any effect in the nuclear localization of the protein, the nuclear localization of R296G with and without pheromone stimulation was microscopically examined. Results show that the mutant had an impaired ability to localize into the nucleus during the vegetative growth, as well as to respond to pheromone [Figure 7A]. Quantification of the nuclear localization of R296G under those conditions clearly revealed its impaired nuclear localization pattern [Figure 7B]. Compared to the WT, R296G showed ~10X less nuclear localization during vegetative growth [Figure 7C]; and under pheromone stimulation the mutant's localization profile remained unchanged relative to the vegetative growth, showing gross difference with the WT [Figure 7D]. These results demonstrate that the Ste50-RA domain is required for its nuclear localization in yeast cells.

3.5 Discussion

Previously we discovered that the adaptor protein Ste50 localizes to the polarized shmoo tip in response to pheromone, and the RA domain of Ste50 is required for its delivery to the tip (Sharmeen *et al.*, 2019). We also showed that the RA domain mutants that are defective in pheromone signaling show impaired localization and cause a severe defect in shmoo formation. Here we show a dynamic, spatiotemporal cellular localization profile of Ste50p, which is dependent on the integrity of its RA domain, and required for the success of shmoo formation in response to mating-pheromone signaling.

We characterized the shmoo tip localization of Ste50p and established that the cell mobilizes a small fraction (~2%) of the cytoplasmic Ste50p to the shmoo tip, which is quite

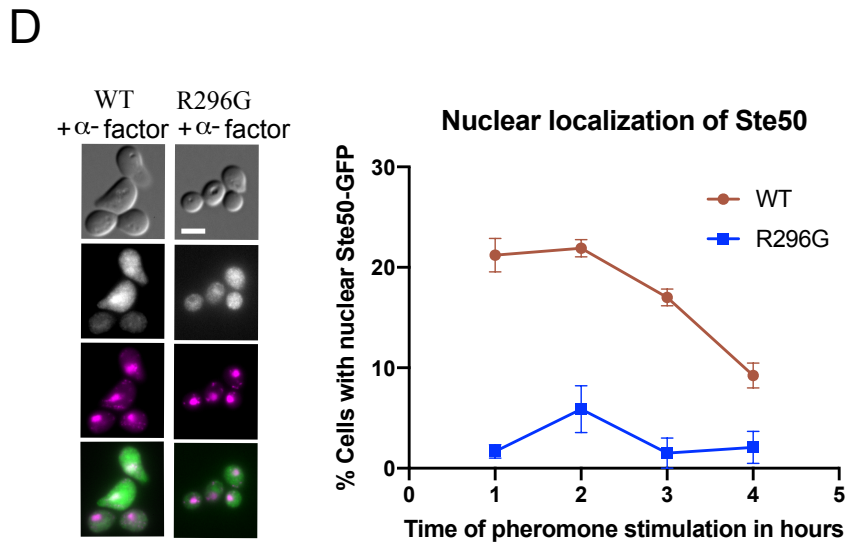
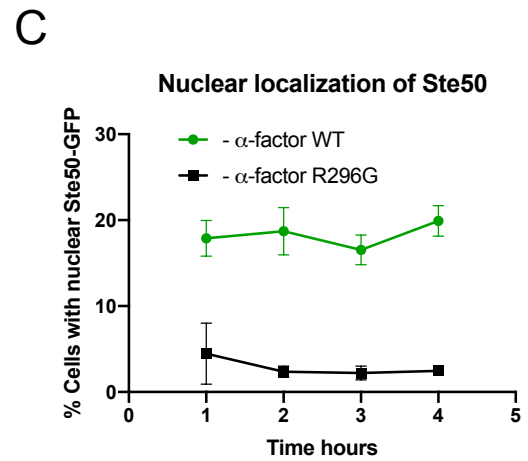
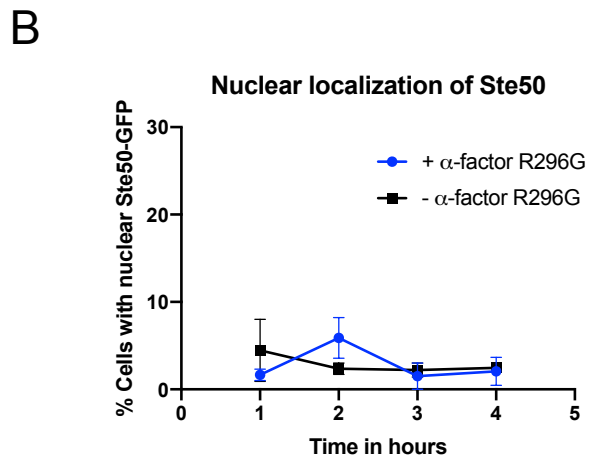
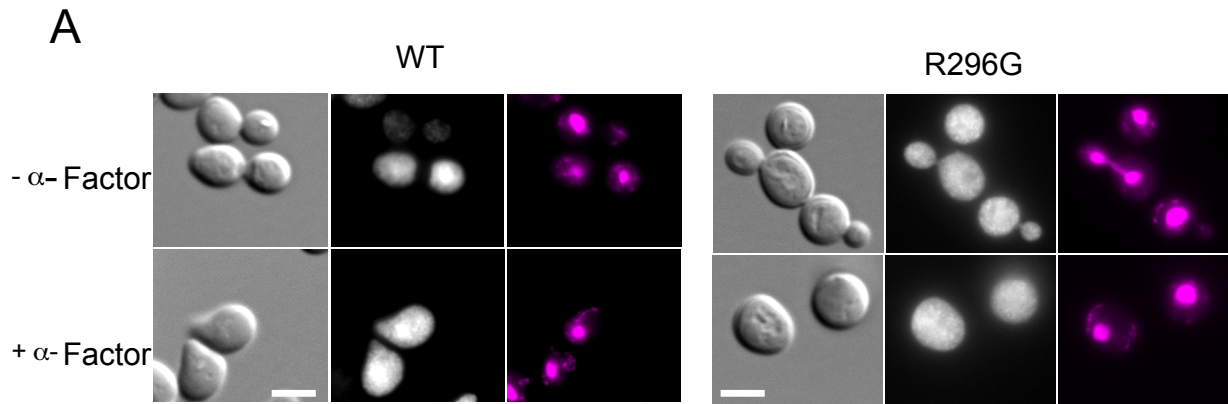


FIGURE 7: Nuclear localization of different Ste50 alleles. The yeast strain YCW1886 was transformed with a CEN plasmid bearing either the WT or the R296G Ste50 alleles. Strains were cultured for 4h hours for a time-course study of Ste50 nuclear localization with or without pheromone. Nuclear localization of R296G during vegetative growth and pheromone treatment (A); and its impaired nuclear translocation (B). In comparison to wild type, the mutant's nuclear localization during vegetative growth (C) and under pheromone stimulation (D). Bar represents 5 μ m.

consistent between different lengths of pheromone stimulation. This observation suggests that cell size, as well as the net amount of Ste50p are not the dominant parameters in the pheromone associated shmoo tip localization kinetics of Ste50p. Cells also showed sensitivity to the pheromone concentrations for projection formation, as observed previously (Segall *et al.*, 1993) and Ste50-GFP had a concentration dependent tip localization pattern [Figure 1B]; at low pheromone concentration, scanty accumulation, while at higher concentrations a dramatically larger amount of Ste50p accumulated that both appeared sooner and disappeared faster. This suggests that tip accumulation could be driven by Ste50 involvement in the polarized shmoo structure formation.

We discovered that Ste50 is an early indicator of the presumptive shmoo site in the G1 arrested cells. Microscopic time-lapse studies identified nucleation of Ste50-GFP at the cell surface upon pheromone stimulation at a site that later developed into a shmoo structure. Results showed that punctate structures of the polarity patches are found in the cytoplasm that moved to the location of polarization. Time-lapse movies showed wandering punctate polarity patches during the initial stages of the polarity establishment that relocated to the site of polarization. Relocation of polarity patches is known in *S. cerevisiae* (Arkowitz *et al.*, 2013). These observations indicate that Ste50p becomes localized, directly or indirectly, in G1 arrested cells by recognizing the landmark of a presumptive shmoo site. There could be a molecular link that brings Ste50 to this site. Whatever brings the polarization patch together, the interactions appear to be transient and flexible because patches polarize/depolarize sometimes within short time frames. Shmoo site demarcation by

Ste50p should be through interaction with proteins necessary for the shmoo site assembly; known proteins involved in polarity site selection include Cdc24 that later forms a complex intertwined network with Cdc42, Bem1, Ste5 and Far1 (Slaughter *et al.*, 2009). The integration of Ste50 into the polarity patch is shown here to be early on around 10 min, quite similar to the time frame of 12 min for actin polarity patch (Waddle *et al.*, 1996).

The shmoo patch dynamics uncovered by the time-lapse microscopy that demonstrated the appearance and disappearance of Ste50p from the shmoo tip constitute new findings. The Ste50p shmoo polarity patch appeared at around 10 min after pheromone stimulation, peaked at 120 min and disappeared approximately after 140 min. This timing of shmoo patch appearance/disappearance could not be compared with the Cdc24/Cdc42 dependent actin patch at the shmoo tip, since no relevant data have been documented. But some data could be traced for actin bud patch appearance/disappearance (Waddle *et al.*, 1996), which determined that patch appears at the beginning of the cell cycle at the incipient bud site at around 6-12 min and seems to completely disappear at 112 min. Although this timing is not for shmoo polarity patch establishment, in general the timing of actin patch appearance/disappearance seems to be in the range of Ste50p polarity patch assembly/disassembly, suggesting that polarity patch establishment timing in cells in general may be similar.

In addition to the shmoo tip, another polarity site localization of Ste50-GFP was observed in the bud-neck just ~10 min prior to cytokinesis and disappeared after cytokinesis. This transient localization was very striking and could be readily detected in the time-lapse microscopic movies. This spatiotemporal localization was observed generally in all cells after pheromone stimulation, while only seen in ~10% of the cells at a very low level in the vegetatively growing cells. In an unsynchronized population, cells that are at G1 start to form shmoos after pheromone stimulation, while cells that are not at G1 have to finish the cell cycle and reach the G1 phase before they can form shmoos [Figure 4F]. Can cycling cells respond to pheromone? It is known that cycling cells in the late G1-S phase are unable to respond to pheromone since Cdc28p prevents plasma membrane localization of Ste5

(Strickfaden *et al.*, 2007), however in the G2-M phase the pheromone response driven transcription becomes fully active, generating all the necessary proteins required for pheromone response to help cells get into the next decision point of entry into conjugation (Zanolari & Riezman 1991; Oehlen & Cross, 1994, 1998; Wassmann & Ammerer, 1997; Strickfaden *et al.*, 2007). However, the drastic cytoskeletal changes do not take place during the G2-M phases. Since the observed bud-neck localization of Ste50 was around telophase, it may imply that the wild type cells at telophase are pheromone responsive to some extent and Ste50 localizes to the bud-neck before cytokinesis to help in the process, since cells formed shmoos right after cytokinesis and the specifically-pheromone-response-defective mutants of the Ste50-RA domain failed to enhance localization to the bud-neck under pheromone stimulation. The function of bud-neck localization of Ste50 is unknown and needs to be explored further.

Our results suggest that the Ste50 polarity patch may have dual functions, involvement at the bud-neck during cytokinesis and for the shmoo polarization. Components of the pheromone response pathway, such as Bem1 and Ste4 were also observed to be present at the bud-neck and polarized shmoo tip, reported by a recent study (Vasen *et al.*, 2018). A similar example is the actin polarization patch that contains the same component proteins forming the shmoo and the bud polarization (Smith *et al.*, 2001). Our results also demonstrate clearly that Ste50 is not involved in the bud polarization of the vegetatively growing cells, in that respect Ste50 plays a different role than Cdc42 in the polarization of yeast cells since Cdc42 localizes both to the incipient bud site and to the growing bud tip (Smith *et al.*, 2013; Okada *et al.*, 2017).

There has been no previous work defining a nuclear localization of the Ste50 adaptor protein. In this study, we showed for the first time that a fraction of the adaptor protein localizes to the nucleus both during vegetative growth and under pheromone stimulation. In the vegetatively growing cells, ~13-25% of cells showed nuclear Ste50p localization, similar to the scaffold protein Ste5p (Mahanty *et al.*, 1999). Interestingly, stimulating with pheromone did not change the upper limit of nuclear localization for Ste50p, on average

~20% of cells showed nuclear localization that consistently declined after 3h of pheromone stimulation. The fluctuation of nuclear localization between samples in the vegetatively growing cells prompted us to investigate whether the localization is cell cycle dependent. In the population level studies there was a significant decrease in nuclear localization during anaphase and telophase. We concluded through single cell analysis that cells actually showed a similar level of nuclear localized Ste50p during the cell cycle with a drop in the telophase. These interesting results should prompt further investigations on Ste50 protein abundance in different cellular locations during the different phases of cell cycle. Testing a Ste50-RA domain mutant that has a mutation in the putative Ste50 nuclear localization signal (NLS) [Figure S3] showed a gross inability to translocate the protein to the nucleus during either vegetative growth or pheromone signaling. Since the protein is larger than molecules that can passively enter into the nucleus through the nuclear pore, it is possible that the protein is actively transported, whether using its own NLS or binding with another nuclear protein is unknown. Further studies will be needed to test whether the putative nuclear localization signals (NLS) from Ste50p are functional to facilitate nuclear transport.

The fact that the specifically-pheromone-defective Ste50p RA mutant R296G is also impaired in nuclear localization indicates that nuclear localization of Ste50 may have a critical role in pheromone signaling. The mutant may have impaired some interaction(s) that may directly or indirectly affect the nuclear localization of Ste50p. This kind of regulated import has been observed in many nuclear proteins that shuttle between the nucleus and cytoplasm during response to extracellular stimuli (Flach *et al.*, 1994; Mahanty *et al.*, 1999). Our finding of Ste50 nuclear localization leads to several possible scenarios, one of which could be that Ste50 may undergo some modification in the nucleus and then translocate to the cytoplasm where it interacts and regulates a cytoplasmic pheromone-signaling component, Ste11 MAP3K.

3.6 Materials and Methods

Yeast strain, plasmids and transformations

The yeast strains used in this study were: YCW1886 (*MATa ste50Δ::Kan^R ssk1Δ::Nat^R sst1::hisG FUS1-LacZ::LEU2 his3 leu2 ura3 trp1 ade2*) and ySP269 (W303 *MATa leu2-3, 112 trp1-1 can1-100 ura3-1 ade2-1 his3-11, 15 Hta2-CFP:URA3*) (a generous gift from Dr Serge Pelet from University of Lausanne, Switzerland). The plasmids used in this study are listed in Table S1. All yeast transformations were carried out using the lithium acetate method (Chen *et al.*, 1992). Standard manipulations of yeast strains, culture conditions and media were as described (Dunham *et al.*, 2015). *E. coli* strain DH10B: *F⁻ mcrA Δ(mrr-hsdRMS-mcrBC) φ80lacZΔM15 ΔlacX74 recA1 endA1araD-139 Δ(ara-leu)7697 galU galK λ⁻ rpsL(Str^R) nupG* (Invitrogen) was used for plasmid maintenance.

Beta-galactosidase assay

Yeast cells bearing WT Ste50, Ste50ΔRA and Ste50^{R296G} were cultured overnight in SD-Ura media at 30°C and diluted the following day to 1:1000 in fresh media to obtain an exponential culture next morning. Cultures were split to have pheromone treated and untreated samples, were stimulated with 2μM alpha-factor for 4h and processed for quantitative β-galactosidase reporter assays for pheromone response as described in (Wu *et al.*, 1999; Tatebyashi *et al.*, 2006). β-galactosidase activities were measured and expressed as $(OD_{420} \times 1000)/(OD_{600} \times t \times v)$ (Miller, 1972) where t is in minutes and v is in milliliters.

Time-course microscopy of live yeast cells

Yeast cells bearing Ste50-GFP on a centomeric plasmid were grown to saturation on synthetic defined media without histidine, and then diluted to 1:1000 in fresh media for overnight growth to get exponential cultures the next day. Cells were then treated with 2μM alpha-factor and samples collected at 1 hour intervals up to 4 hours and prepared for

imaging. Still images were captured using a Leica DM6000 equipped with DIC optics, a mercury lamp, and a GFP filter cube (480/20nm ex - 510/20nm em) using Volocity software (Perkin-Elmer, MA, USA), a Hamamatsu Orca ER camera and a 100x PLAN FLUO lens (NA 1.3). The DIC (Differential Interference Contrast) and the FITC (Fluorescein isothiocyanate) images were viewed and analyzed and processed by ImageJ software (v. 1.37; National Institutes of Health).

Time-lapse microscopy of live cells

For time-lapse experiments, yeast strains (YCW1886, ySP269) bearing plasmids were cultured in SD-His media to saturation then diluted into fresh media to obtain exponential culture next morning. One ml of overnight culture was concentrated and cells were loaded onto a multiwell glass-bottom dish (Mattek, MA, USA) pre-coated with concanavalin A (1mg/ml) (Sigma-Aldrich, Oakville, Canada). After cell attachment, cells were covered with 1% agarose (Sigma-Aldrich, Oakville, Canada) at 30°C containing 2 μ M alpha-factor in thin layer and supplemented on top with 1 ml of SD-His media. Just before viewing, 1 ml of SD-His media with alpha-factor was added to a final concentration of 2 μ M. Cells were viewed from the bottom with an inverted microscope. Images were captured on a Nikon Ti microscope equipped with a TIRF arm, DIC optics, a GFP filter cube (480/40nm ex - 520/75nm em), 488nm laser (50mW), a Photometrics Evolve 512 EMCCD camera and a 100x APO TIRF objective lens (NA 1.49). The TIRF arm was adjusted to generate a highly inclined laminated optical sheet (Tokunaga M, *et al.*, 2008), and images were captured at multiple XY positions every 10 minutes for 8-12 hours; imaging was performed at room temperature.

Nuclear Ste50 localization quantitation

For time-course experiments the nuclear Ste50-GFP localization was quantified for the % of cells having increased nuclear localization of GFP over the cytoplasmic mean GFP intensity. Overnight exponential cultures at OD₆₀₀ around 0.4 in SD-His were split and half were treated with 2 μ M alpha-factor and incubated with shaking at 30°C. Samples were withdrawn at 0 hour and subsequently every hour for 4 hours. Cells were fixed in 4%

paraformaldehyde and stained with DAPI (for fixed cells). Imaging was performed with Leica DM6000 as described above for still imaging. Cells visually showing a distinct GFP fluorescence signal that overlapped reference nuclear DAPI signal were counted as positives. Images were analyzed by ImageJ software (v. 1.37; National Institutes of Health). At least three independent experiments were used and 200 or more cells were counted. The % was calculated as the number of cells having nuclear Ste50-GFP accumulation over the total number of cells. For binning of cell cycle dependent nuclear localization analysis, 100 cells in each category (see results) were analysed for the nuclear localization of Ste50-GFP and plotted as percentages.

Image analysis

The ratio of intensity between the shmoo patch and the whole cell was determined by measuring the mean intensity of each compartment using FIJI. Briefly, the boundaries of the cell were determined using an automatic thresholding method, verified by the investigator, while the boundary of the shmoo was selected by the investigator using the ellipse tool; mean intensities were measured for each area and a ratio was calculated [macro S4]. Multiple cells were measured per field of view, and all cells were imaged using the same exposure times and fluorescent lamp intensities. Macros used for this analysis is attached in the supplementary data. Bud-neck intensity analysis: a 4-5 micro meter area was selected by hand around the bud joint. Then the mean intensity of this area was measured, and a ratio was calculated against the mean GFP intensity of a similar size area of the mother cell.

For the time-lapse microscopy to examine nuclear translocation of Ste50, an ImageJ macro was used (macro S3). Briefly, at each timepoint the cell of interest was manually outlined in the GFP channel using the ellipse tool, then the location of the nucleus was determined using thresholding of the mCherry channel. The mean intensity of the nuclear signal was determined by measuring the GFP signal in the region corresponding to the nucleus, while the mean cytoplasmic GFP signal was determined by calculating the mean GFP intensity of the cell excluding the area corresponding to the nucleus. Shmoo length was calculated by

using the ellipse tool in ImageJ to encompass the whole cell of interest, then measuring the long axis of the ellipse; this analysis was repeated across multiple timepoints.

3.7 References

- Alberts B (1998). The cell as a collection of protein machines: preparing the next generation of molecular biologists. *Cell* 92, 291-294.
- Arkowitz RA (2013). Cell polarity: wonderful exploration in yeast sex. *Curr Biol* 23(1), R10-R12.
- Bhavsar-Jog YP, Bi E (2017, June). Mechanics and regulation of cytokinesis in budding yeast. In *Seminars in cell & developmental biology* 66, 107-118. Academic Press.
- Bi E & Park HO (2012). Cell polarization and cytokinesis in budding yeast. *Genetics* 191, 347-87.
- Blondel M, Alipuz PM, Huang LS, Shaham S, Ammerer G, Peter M (1999). Nuclear export of Far1p in response to pheromones requires the export receptor Msn5p/Ste21p. *Gen Dev* 13, 2284-2300.
- Choi KY, Kranz JE, Mahanty SK, Park KS, Elion EA (1999). Characterization of Fus3 localization: active Fus3 localizes in complexes of varying size and specific activity. *Mol Biol Cell* 10, 1553-1568.
- Costanzo M, Nishikawa JL, Tang X, Millman JS, Schub O, Breitkreuz K, ... & Tyers M (2004). CDK activity antagonizes Whi5, an inhibitor of G1/S transcription in yeast. *Cell* 117, 899-913.

- Delobel P & Tesnière C (2014). A simple FCM method to avoid misinterpretation in *Saccharomyces cerevisiae* cell cycle assessment between G0 and sub-G1. PLoS One 9(1), e84645.
- Diener C, Schreiber G, Giese W, del Rio G, Schröder A, Klipp E (2014). Yeast mating and image-based quantification of spatial pattern formation. PLoS comp biol 10(6),e1003690.
- Dingwall C, Robbins J, Dilworth SM, Roberts B, Richardson WD (Sep 1988). The nucleoplasmin nuclear location sequence is larger and more complex than that of SV-40 large T antigen. J Cell Biol 107 (3), 841-9.
- Driessen AJ & Nouwen N (2008). Protein translocation across the bacterial cytoplasmic membrane. Annu Rev Biochem 77, 643-667.
- Dyer JM, Savage NS, Jin M, Zyla TR, Elston TC, Lew DJ (2013). Tracking shallow chemical gradients by actin-driven wandering of the polarization site. Curr Biol 23(1), 32-41.
- Elliott SG (1983). The yeast cell cycle: coordination of growth and division rates. In Prog Nucleic Acid Res Mol biol 28, 143-176.
- Errede BL, Vered L, Ford E, Pena MI, Elston TC (2015). Pheromone induced morphogenesis and gradient tracking are dependent on the MAPK Fus3 binding to G α . Mol Biol Cell 26, 3343-3358.
- Fanger GR (1999). Regulation of the MAPK family members: role of subcellular localization and architectural organization. Histol Histopathol 14, 887-894.

Faux MC & Scott JD (1996). Molecular Glue: kinase anchoring and scaffold proteins. *Cell* 85, 9-12.

Flach J, Bossie M, Vogel J, Corbett A, Jinks T, Willins DA, Silver PA (1994). A yeast RNA-binding protein shuttles between the nucleus and the cytoplasm. *Mol Cell Biol* 14(12), 8399-8407.

Hartwell LH (1974). *Saccharomyces cerevisiae* cell cycle. *Bact Rev*, 38(2), 164.

Herskowitz I (1995). MAPK kinase pathways in yeast: for mating and more. *Cell* 80, 187-197.

Huh WK, Falvo JV, Gerke LC, Carroll AS, Howson RW, Weissman JS, O'shea EK (2003). Global analysis of protein localization in budding yeast. *Nature* 425, 686-691.

Jackson CL, Konopka JB, Hartwell IH (1991). *S. cerevisiae* alpha pheromone receptors activate a novel signal transduction pathway for mating partner discrimination. *Cell* 67, 389-402

Kalderon D, Roberts BL, Richardson WD, Smith AE (1984). A short amino acid sequence able to specify nuclear location. *Cell* 39, 499-509.

Kobayashi J & Matsuura Y (2013). Structural basis for cell-cycle-dependent nuclear import mediated by the karyopherin Kap121p. *J mol biol* 425(11), 1852-1868.

Koch C, Moll T, Neuberg M, Ahorn H, Nasmyth K (1993). A role for the transcription factors Mbp1 and Swi4 in progression from G1 to S phase. *Science* 261, 1551-1557.

- Kosugi S, Hasebe M, Tomita M, Yanagawa H (2009). Systematic identification of cell cycle-dependent yeast nucleocytoplasmic shuttling proteins by prediction of composite motifs. *Proc Natl Acad Sci* 106(25), 10171-10176.
- Laub MT & Goulian M (2007). Specificity in two-component signal transduction pathways. *Annu rev genet* 41, 121-145
- Leberer E, Wu C, Leeuw T, Fourest-Lieuvin A, Segal JE, Thomas DY (1997). Functional characterization of the Cdc42p-binding domain of yeast Ste20p protein kinase. *EMBO J* 16, 83-97.
- Lemmon MA & Schlessinger J (2010). Cell signaling by receptor tyrosine kinases. *Cell* 141(7), 1117-1134.
- Madden K & Snyder M (1992). Specification of sites for polarized growth in *Saccharomyces cerevisiae* and the influence of external factors on site selection. *Mol biol cell* 3(9), 1025-1035.
- Mahanty SK, Wang W, Farley FW, Elion EA (1999). Nuclear shuttling of yeast scaffold Ste5 is required for its recruitment to the plasma membrane and activation of the mating MAPK cascade. *Cell* 98(4), 501-512
- Maik-Rachline G, Hacoheh-Lev-Ran A, Seger R (2019). Nuclear ERK: Mechanism of Translocation, Substrates, and Role in Cancer. *Int J Mol Sci* 20(5), 1194.
- Makkerh JP, Dingwall C, Laskey RA (August 1996). Comparative mutagenesis of nuclear localisation signals reveals the importance of neutral and acidic amino acids. *Curr Biol* 6 (8), 1025-7.

- Mochly-Rosen D (1995). Localization of protein kinases by anchoring proteins: a theme in signal transduction. *Science* 268, 247-251 ,
- Muranen T, Grönholm M, Renkema GH, Carpen O (2005). Cell cycle-dependent nucleocytoplasmic shuttling of the neurofibromatosis 2 tumour suppressor merlin. *Oncogene* 24(7), 1150.
- Nern A & Arkowitz RA (2000). Nucleocytoplasmic shuttling of the Cdc42p exchange factor Cdc24p. *J cell biol* 148(6), 1115-1122.
- Newmeyer DD, Forbes DJ (March 1988). Nuclear import can be separated into distinct steps in vitro: nuclear pore binding and translocation". *Cell* 52 (5), 641–53.
- Oehlen LJ, & Cross FR (1994). G1 cyclins CLN1 and CLN2 repress the mating factor response pathway at Start in the yeast cell cycle. *Genes Dev* 8, 1058 – 1070.
- Oehlen LJ, & Cross FR (1998). Potential regulation of Ste20 function by the Cln1 Cdc28 and Cln2-Cdc28 cyclin-dependent protein kinases. *J Biol Chem* 273, 25089 – 25097.
- Okada S, Lee ME, Bi E, Park HO (2017). Probing Cdc42 polarization dynamics in budding yeast using a biosensor. *Methods in Enzymology*, ed. J. Abelson, M. Simon, G. Verdine, A. Pyle, Academic Press 589, 171-190.
- Pawson T & Scott JD (1997). Signaling through scaffold, anchoring and adaptor proteins. *Science* 278, 2075-2080.
- Peter M, Neiman AM, Park HO, vanLohuizen M, Herskowitz I (1996). Functional analysis of the interaction between the small GTP-binding protein Cdc42 and the Ste20 protein kinase in yeast. *EMBO J* 15, 7046–7059.

- Pryciak PM & Huntress FA (1998). Membrane recruitment of the kinase cascade scaffold protein Ste5 by the G β γ complex underlies activation of the yeast pheromone response pathway. *Gen Dev* 12(17), 2684-2697.
- Segall JE (1993). Polarization of yeast cells in spatial gradients of alpha mating factor. *Proc Natl Acad of Sci* 90, 8332-8336.
- Slaughter BD, Smith SE, Li R (2009). Symmetry breaking in the life cycle of the budding yeast. *Cold Spring Harbor perspectives in biology* 1(3), a003384.
- Smith SE, Rubinstein B, Pinto IM, Slaughter BD, Unruh JR, Rong Li. (2013). Independence of symmetry breaking on Bem1-mediated autocatalytic activation of Cdc42. *J Cell Biol* 202 7, 1091-1106.
- Smith MG, Swamy SR, Pon LA (2001). The life cycle of actin patches in mating yeast. *J Cell Sci* 114(8), 1505-1513.
- Strickfaden SC, Winters MJ, Ben-Ari G, Lamson RE, Tyers M, Pryciak PM (2007). A mechanism for cell-cycle regulation of MAP kinase signaling in a yeast differentiation pathway. *Cell* 128, 519 – 531.
- Taberner FJ, Quilis I, Igual JC (2009). Spatial regulation of the start repressor Whi5. *Cell Cycle* 8(18), 3013-3022.
- Tokunaga M, Imamoto N, Sakata-Sogawa K (2008). Highly inclined thin illumination enables clear single-molecule imaging in cells. *Nat methods* Feb5(2), 159.
- Truckses DM, Bloomekatz JE, Thorner J (2006). The RA domain of Ste50 adaptor protein is required for delivery of Ste11 to the plasma membrane in the filamentous growth signaling pathway of the yeast *Saccharomyces cerevisiae*. *Mol Cell Biol* 26, 912-928.

- Vasen G & Lerner AC (2018). Intrinsic polarization cues interfere with pheromone gradient sensing in *S. cerevisiae*. bioRxiv, 502856.
- Waddle JA, Karpova TS, Waterston RH, Cooper JA (1996). Movement of cortical actin patches in yeast. *J cell biol* 132(5), 861-870.
- Wassmann K, & Ammerer G (1997). Overexpression of the G1-cyclin gene CLN2 represses the mating pathway in *Saccharomyces cerevisiae* at the level of the MEKK Ste11. *J Biol Chem* 272, 13180 – 13188.
- Wloka C & Bi E (2012). Mechanisms of cytokinesis in budding yeast. *Cytoskeleton*, 69(10), 710-726.
- Widmann CS, Gibson S, Jarpe MB, Johnson GL (1999). Mitogen-activated protein kinase: conservation of a three-kinase module from yeast to human. *Physiol rev* 79(1), 143-180
- Wu C, Leberer E, Thomas DY, Whiteway M (1999). Functional characterization of the interaction of Ste50p with Ste11p MAPKKK in *Saccharomyces cerevisiae*. *Mol Biol Cell* 10, 2425-2440.
- Wu C, Jansen G, Zhang J, Thomas DY, Whiteway M (2006). Adaptor protein Ste50p links the Ste11p MEKK to the HOG pathway through plasma membrane association. *Genes Dev* 20, 734-746
- Yan H, Merchant AM, Tye BK (1993). Cell cycle-regulated nuclear localization of MCM2 and MCM3, which are required for the initiation of DNA synthesis at chromosomal replication origins in yeast. *Gen Dev* 7(11), 2149-2160.

Zanolari B & Riezman H (1991). Quantitation of alpha-factor internalization and response during the *Saccharomyces cerevisiae* cell cycle. *Mol Cell Biol* 11(10), 5251-5258.

3.8 Supplementary Materials

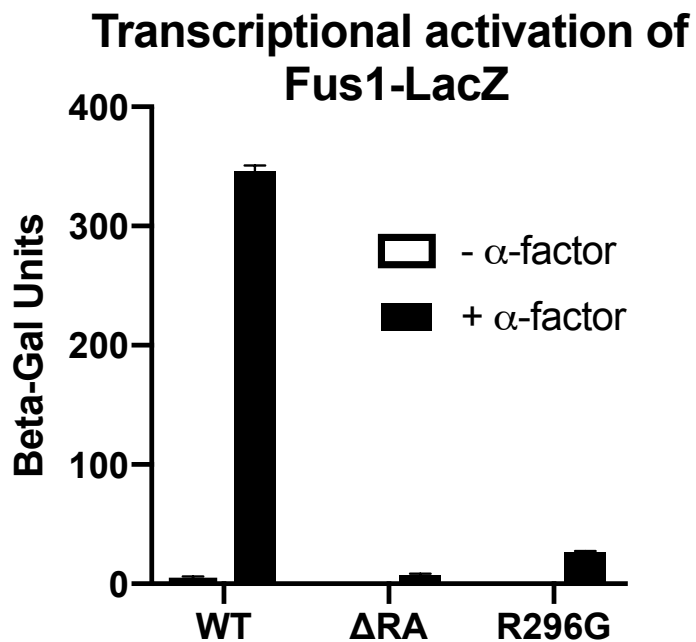


FIGURE S1: Transcriptional activation assay of the Ste50-RA domain mutant R296G. Yeast strain YCW1886 was transformed with different alleles of Ste50, WT, RA deletion and mutant R296G. Cells were grown to late exponential phase and stimulated with 2 μ M alpha-factor for 4h. Promoter reporter activity was measured by Fus1-LacZ activity. Beta-galactosidase activity was measured colorimetrically as described (Wu *et al.*, 1999; Tatebayashi *et al.*, 2006).

>STE50 YCL032W SGDID:S000000537
MEDGKQAINEGSNDASPDLDVNGTILMNNEDFSQWSVDDVITWCISTLEVEETDPLCQRL
RENDIVGDLLPELCLQDCQDLCGDLNKAIFKILINKMRDSKLEWKDDKTQEDMITVLK
NLYTTTSAKLQEFQSQYTRLRMDVLDVMKTSSSSSPINTHGVSTTVPSSNNTIIPSSDGV
SLSQTDYFDTVHNRQSPSRRESPVTVFRQPSLSHSLHKDSKNKVPQISTNQSHPSAVS
TANTPGPSPNEALKQLRASKEDSCERILKNAMKRHNLADQDWRQYVLVICYGDQERLLELNEKP
VIIFKNLQQGLHPAIMLRRRRGDFEEVAMMNGSDNVTPGGRL

Predicted bipartite NLS:

LINKMRDSKLEWKDDKTQEDMITVLKNLYTTT: Score 4.1
RDSKLEWKDDKTQEDMITVLKNLYTTTSAKLQEF: Score 3.1
RQSPSRRESPVTVFRQPSLSHSLHKDSKNK: Score 3.3
RILKNAMKRHNLADQDWRQYVLVICYGDQERLLE: Score 3.8

FIGURE S2: Potential NLS of Ste50 (http://nls-mapper.iab.keio.ac.jp/cgi-bin/NLS_Mapper_form.cgi)

1-299 are the residues that include the NLS signal. And the NLS signal include the mutations that are specifically mating disruptive, Q294L and R296G.

MACRO S3: Nuclear localization of Ste50-GFP intensity measurement

```
//Get Everything Set Up  
imList=getList("image.titles");  
name = imList[0];  
fPath = getInfo("image.directory");  
run("Channels Tool...");  
Stack.getDimensions(width, height, channels, slices, frames);  
run("Set Measurements...", "area mean centroid integrated redirect=None decimal=3");  
cellSignal=newArray();  
cellIntSignal=newArray();  
cellSize=newArray();  
nuclearSignal=newArray();  
nuclearIntSignal=newArray();
```

```

nuclearSize=newArray();
if(roiManager("count")>0){
    roiManager("deselect");
    roiManager("delete");
}
roiManager("Associate", "true");
roiManager("Centered", "false");
roiManager("UseNames", "false");
roiManager("Show All");
w=getWidth();
h=getHeight();
wh=Array.concat(w,h);
winSize = 100;
Array.getStatistics(wh, min, max, mean, stdDev);
if (winSize>min){
    winSize = min;
}

//Let the user set parameters
waitForUser("Assay the movie: \n Which time frames do you want to analyse?");
Dialog.create("Time Frames");
Dialog.addNumber("Start: ",1);
Dialog.addNumber("End: ",frames);
Dialog.addNumber("Is the Green channel 1 or 2: ",1);
Dialog.addNumber("Window Size (Pixels): ",winSize);
Dialog.show();
t1=Dialog.getNumber();
t2=Dialog.getNumber();
gChannel =Dialog.getNumber();
winSize=Dialog.getNumber()/2;

```

```

tLast= t2 - t1 + 1;

if (winSize>min){
    winSize = min;
}
if (gChannel == 1){
    rChannel = 2;
} else {
    rChannel = 1;
}

//Let the user outline the cell of interest
Stack.setFrame(t1);
Stack.setChannel(gChannel)
setTool("Ellipse");
Stack.setDisplayMode("color");
for (frm=0;frm<tLast;frm++){
    Stack.setFrame(t1+frm);
    waitForUser("Draw around the cell of interest");
    roiManager("add");
}
setBatchMode(true);

count1 = roiManager("Count");
for (frm=0;frm<count1;frm++){
    Stack.setFrame(t1+frm); //go to the right frame
    Stack.setChannel(gChannel); //go to the green channel
    roiManager("Select",frm); //select the right ROI
    roiManager("Measure"); //measure in the green channel
    temp=getResult("Mean",nResults-1); //store the mean green intensity

```

```

cellSignal=Array.concat(cellSignal,temp);
temp=getResult("RawIntDen",nResults-1); //store the whole cell signal
cellIntSignal=Array.concat(cellIntSignal,temp);
temp=getResult("Area",nResults-1); //store the whole cell area
cellSize=Array.concat(cellSize,temp);
Stack.setChannel(rChannel); //go the the red channel
run("Duplicate...", " "); //duplicate it *this duplicate is the size of the cell ROI
setAutoThreshold("Li dark"); //threshold it
run("Convert to Mask"); //mask it
run("Analyze Particles...", "size=1-Infinity add"); //find the nucleus
count2 = roiManager("Count"); //count the ROIs
close(); //close the red channel duplicate
if (count1 == count2){ //if a nuclear ROI has not been found
    setBatchMode(false);
    Stack.setChannel(rChannel); //go the the red channel
    run("Duplicate...", " "); //duplicate it *this duplicate is the size of the cell ROI
    setTool("freehand");
    waitForUser("Draw around the nucleus, the click OK");
    roiManager("Add");
    setBatchMode(true)
}
roiManager("Select",frm); //select the cell ROI
Stack.setChannel(gChannel); //in the green channel
run("Duplicate...", " "); //duplicate the cell
roiManager("Select",roiManager("Count")-1); //select the nuclear ROI
roiManager("Measure"); //measure the nuclear intensity
temp=getResult("Mean",nResults-1); // get the measurements
nuclearSignal=Array.concat(nuclearSignal,temp);
temp=getResult("RawIntDen",nResults-1);
nuclearIntSignal=Array.concat(nuclearIntSignal,temp);

```

```

temp=getResult("Area",nResults-1);
nuclearSize=Array.concat(nuclearSize,temp);
roiManager("Select",roiManager("Count")-1); //select the nuclear ROI (rather, the
last in the list)
roiManager("Delete"); //delete it
close(); //close the duplicated green window
}
run("Clear Results");
updateResults();
setBatchMode(false);
print(winSize,width,height);
for (frm=0;frm<tLast;frm++){
    selectWindow(name);
    Stack.setFrame(t1+frm);
    Stack.setChannel(gChannel);
    roiManager("Select",frm);
    getSelectionBounds(x, y, width, height);
    xInit = x + (width*0.5);
    yInit = y + (height * 0.5);
    xInit = xInit - winSize;
    yInit = yInit - winSize;
    makeRectangle(xInit,yInit,winSize*2,winSize*2);
    run("Duplicate...", "duplicate channels=1-3 frames="+ (t1+frm));
    setResult("Mean Cell GFP",nResults,cellSignal[frm]);
    setResult("Mean Nuclear GFP",nResults-1,nuclearSignal[frm]);
    setResult("Mean Cell Size (µm)",nResults-1,cellSize[frm]);
    setResult("Mean Nuclear Size (µm)",nResults-1,nuclearSize[frm]);
    setResult("Total Cell GFP",nResults-1,cellIntSignal[frm]);
    setResult("Total Nuclear GFP",nResults-1,nuclearIntSignal[frm]);
}

```

```
selectWindow(name);
close();
run("Concatenate...", "all_open open");
saveAs("tif");
saveAs("results");
```

MACRO S4: Shmoo localization of Ste50-GFP intensity measurement

```
nameArray = newArray(0);
shmooMean_array = newArray(0);
cellMean_array = newArray(0);
shmooInt_array = newArray(0);
cellInt_array = newArray(0);
setTool("ellipse");
count = roiManager("count");
name = getInfo("image.filename");
path = getInfo("image.directory");
if (count>0){
    roiManager("Select All");
    roiManager("Delete");
}
resetThreshold();
setBackground(0,0,0);
fin = "No";
while (fin != "Yes"){
    setTool("ellipse");
    waitForUser("Select a cell to analyse. \n Include as much background as you can");
    run("Duplicate...", " ");
    rename("Cell");
```

```

run("Clear Outside");
run("Select None");
run("Duplicate...", " ");
rename("Mask");
setAutoThreshold("Yen dark");
run("Convert to Mask");
run("Close-");
run("Open");
Dialog.create("Threshold Satisfaction");
Dialog.addMessage("Does this threshold look good?");
Dialog.addChoice(" ", newArray("Yes", "No"), "Yes");
Dialog.show()
thresh = Dialog.getChoice();
if (thresh == "No"){
    close();
    run("Select None");
    selectWindow("Cell");
    run("Duplicate...", " ");
    rename("Mask");
    setTool("freehand");
    waitForUser("Draw around the cell");
    run("Fill");
    run("Clear Outside");
    run("Select None");
    setAutoThreshold("Yen dark");
    run("Convert to Mask");
    run("Close-");
    run("Open");
}

```

```

run("Analyze Particles...", "include add");
close();
selectWindow("Cell");
roiManager("Select",0);
run("Measure");
wholeCell_mean = getResult("Mean", nResults-1);
wholeCell_int = getResult("RawIntDen", nResults-1);
run("Select None");
setTool("ellipse");
waitForUser("Select the Shmoo tip");
run("Measure");
shmoo_mean = getResult("Mean", nResults-1);
shmoo_int = getResult("RawIntDen", nResults-1);
close();
nameArray = Array.concat(nameArray,name);
shmooMean_array = Array.concat(shmooMean_array,shmoo_mean);
cellMean_array = Array.concat(cellMean_array,wholeCell_mean);
shmooInt_array = Array.concat(shmooInt_array,shmoo_int);
cellInt_array = Array.concat(cellInt_array,wholeCell_int);
Dialog.create("Status");
Dialog.addMessage("Have you analysed all cells in this image?");
Dialog.addChoice(" ", newArray("Yes", "No"), "No");
Dialog.show()
fin = Dialog.getChoice();
}

run("Clear Results");
updateResults();

for (i=0;i<lengthOf(nameArray);i++){

```

```

    setResult("Image Name", nResults, nameArray[i]);
    setResult("Cell Integrated Signal", nResults-1, cellInt_array[i]);
    setResult("Shmoo Integrated Signal", nResults-1, shmooInt_array[i]);
    setResult("Shmoo Integrated Proportion", nResults-1,
(shmooInt_array[i]/cellInt_array[i]));
    setResult("Cell Mean Signal", nResults-1, cellMean_array[i]);
    setResult("Shmoo Mean Signal", nResults-1, shmooMean_array[i]);
    setResult("Shmoo:Cell Signal Ratio", nResults-1,
shmooMean_array[i]/cellMean_array[i]);
}

```

TABLE S1: List of plasmids used in this study

Plasmids	Descriptions	Sources
pCW463(Δ RA)	pRS316- <i>ste50</i> ¹⁻²¹⁸ ::URA3/AmpR	Wu <i>et al.</i> , 1999
pCW267(WT)	pRS316- <i>STE50</i> ^{wt} ::URA3/AmpR	Wu <i>et al.</i> , 1999
pNS127	pRS316- <i>ste50</i> ^{R296G} ::URA3/AmpR	This study
pRS313-GFP	pRS313- <i>STE50</i> -GFP:: <i>HIS3</i> /AmpR	Slaughter <i>et al.</i> , 2008
pNS131	pRS313- <i>ste50</i> ^{R283GQ294L} GFP:: <i>HIS3</i> /AmpR	This study
pNS133	pRS313- <i>ste50</i> ^{R296G} -GFP:: <i>HIS3</i> /AmpR	This study

Chapter IV: Multicopy suppressor analysis with Ste50 mutants identified *RIE1* as a component of the mating signalling process in *Saccharomyces cerevisiae*

Nusrat Sharmeen,^a Malcolm Whiteway,^b Cunle Wu^{a,c}

^aDivision of Experimental Medicine
Department of Medicine
McGill University
Montreal, QC, Canada H4A 3J1

^bDepartment of Biology,
Concordia University
Montreal, QC, Canada H4B 1R6

^cHuman Health Therapeutics Research Centre
National Research Council Canada
6100 Royalmount Avenue
Montreal, Quebec, Canada H4P 2R2

4.1 Preface

In the previous two chapters, we proposed that the Ste50-RA domain is required to regulate the pheromone signaling pathway in yeast, and we generated RA domain mutants that are specifically defective in pheromone signaling. This gave us the opportunity to take advantage of the mutants' distinct phenotype and isolate high-copy genetic suppressors of the mating signaling defect. Our genetic screens isolated *RIE1* as a suppressor gene. Further gene deletion studies established that *RIE1* is a component of the mating-pheromone-signaling pathway.

Author contributions:

Nusrat Sharmeen	Conceptualized, Designed experiments, Performed investigations, Performed formal analysis, Image processing, Wrote the original manuscript, and Edited the manuscript.
Malcolm Whiteway	Conceptual/Technical guidance, Reviewed and Edited the manuscript.
Cunle Wu	Conceptualized and Experimental design, Reviewed and Edited the manuscript.

4.2 Abstract

The pheromone response pathway in the yeast *Saccharomyces cerevisiae* uses a shared MAP3K Ste11 with two other MAPK pathways that control osmotic response and filamentous growth. The Ste50 adaptor protein controls the functions of Ste11 in all the three pathways. We previously found that distinct residues of the Ste50-RA domain specifically disrupted mating signaling suggesting possible loss of a protein interaction. To understand how the Ste50-RA domain is specifically connected to the mating pathway, we designed a multicopy suppressor screen to identify high copy suppressors of the specifically-pheromone-response-defective Ste50-RA domain mutants. The screens identified known multicopy suppressors of the mating pathway, such as *STE11*, *STE5*, *STE4* that are *STE50* mutant-independent. The screens also identified *RIE1* as a multi-copy Ste50 mutant-dependent suppressor. Yeast cells with a *RIE1* deletion showed defective pheromone response, aberrant shmoo morphology and defective cell cycle arrest. These results suggest that *RIE1* is a new component of the mating-pheromone response pathway.

4.3 Introduction

Living cells are ubiquitously exposed to a plethora of stimuli in their environment, which are sensed and integrated to generate precise responses that drive vital cellular processes such as growth, differentiation, and apoptosis. Pathways form complex networks within the cell, posing serious challenges as to the proper internal transduction of messages. The scenario is even more perplexing when multiple pathways share common components.

Signal transduction and regulation is well understood from the mating signaling pathway in the haploid yeast cells in *Saccharomyces cerevisiae*. Haploid yeast cells exist in two mating forms - *MATa* cells and *MAT α* cells. The result of mating is the fusion of the two mating forms to create a zygote, a *MATa/MAT α* diploid. The haploid *MATa* and *MAT α* cells secrete a-factor and α -factor respectively, which are recognized by the opposite mating partner through their specific membrane bound G-protein coupled receptors, Ste2 and Ste3 respectively. The pheromone signal is transduced from the receptor to the down-stream components of the mating signaling pathway by a heterotrimeric G-protein that is activated by the exchange of GDP for GTP, and dissociates into $G\alpha$ and $G\beta\gamma$. The γ -subunit connects the $G\beta\gamma$ unit to the membrane and the β -subunit transmits signals through binding with Ste5 and Far1. Ste11 is a shared MAP3K component among the three yeast MAPK pathways; these pathways control the mating process in response to pheromone, filamentous growth (FG) in response to nutrient deprivation, and glycerol production in response to hyperosmotic stress (Herskowitz, 1995). The kinase domain is located in the C-terminal region of Ste11 and the regulatory region is located in the N-terminus. The regulatory region comprises three domains, the SAM domain that binds to Ste50 adaptor protein (Wu *et al.*, 1999; Jansen *et al.*, 2001), a domain that binds Ste5 (Yerko *et al.*, 2013), followed by a small domain that is responsible for binding and inhibiting the catalytic domain located in the C-terminus (Tu *et al.*, 1997; Bauman and Albright 1998; van Drogen *et al.*, 2000). The inhibition of the catalytic domain by the catalytic binding domain (CBD) is required to stop constitutive activation of Ste11. Upon pheromone stimulation, Ste20 phosphorylates specific serine threonine residues (Ser302 and/or Ser306 and Thr307)

present in the CBD, this weakens its inhibition of the Ste11 catalytic domain thereby activating Ste11 (van Drogen *et al.*, 2000).

Another regulation of Ste11 is through the adaptor protein Ste50. The N-terminal SAM domain of Ste50 interacts with the N-terminal SAM domain of Ste11 (Wu *et al.*, 1999; Jansen *et al.*, 2001). Without this interaction mating is inefficient, and in some strains reduced about 100-fold. The mechanism by which Ste50 regulates Ste11 is not entirely clear; it is thought that binding with Ste50 loosens the inhibitory action of the CBD on the catalytic domain thereby increasing the accessibility of the serine threonine residues in the CBD to be phosphorylated by Ste20 (Wu *et al.*, 1999; Bardwell, 2005). Another possibility is that Ste50 interaction with Ste11 could enable Ste11 to remain in a phosphorylated open conformation for an extended period (Wu *et al.*, 1999; Bardwell, 2005).

Studies on Ste50 regulation of Ste11 have revealed that the RA domain of Ste50 is responsible for conferring MAPK signaling specificity by regulating signal transduction through the Ste11 protein. In the HOG signaling pathway a transmembrane protein Opy2p is required to interact with certain Ste50-RA domain residues to specifically direct the hyperosmolar stress signal through Ste11 (Wu *et al.*, 2006). The RA domain has also been associated with specifically directing signaling through the filamentous growth pathway by interacting with the Rho-like GTPase Cdc42 (Truckses *et al.*, 2006).

Our recent study revealed that the Ste50-RA domain uses distinct amino acid residues to specifically regulate the pheromone signaling pathway in yeast (Sharmeen *et al.*, 2019). These residues cluster on the NMR structure and structural meta-prediction studies showed a propensity for protein-protein interactions. Here we performed a genetic screen against these specifically-pheromone-signaling-defective Ste50-RA domain mutants to identify suppressor(s), which can compensate for the functional defects of the Ste50 mutants when overexpressed. This genetic suppressor study will provide a better understanding of how the Ste50-RA domain specifically connects to the pheromone response pathway.

4.4 Results

Yeast high copy genomic library screen for suppressor(s) that suppress the specifically-pheromone-signaling defect of the Ste50-RA domain mutants

Previously we genetically probed the Ste50-RA domain and found a number of mutants that are specifically defective in pheromone response (Sharmeen *et al.*, 2019). We showed by bioinformatics that the pheromone-signaling-specific residues were localized on the opposite surface from where the HOG-signaling-specific residues resided in the RA domain NMR structure. Bioinformatics prediction also showed that these residues are potential protein interaction sites, and live cell imaging further confirmed that the mutants were unable to associate and localize to the growing shmoo tip upon pheromone stimulation suggesting a potential loss of protein-protein interaction.

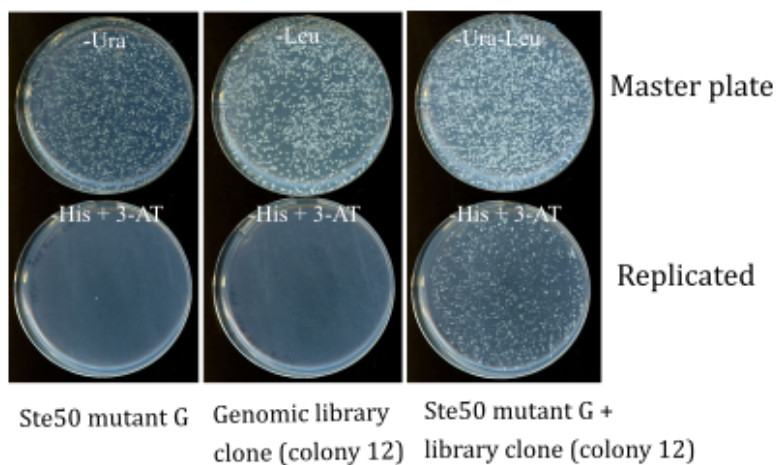
Here we undertook to identify genetic suppressor(s) of these Ste50-RA domain mutants whose gene product(s) might interact with the Ste50p mutants and compensate for their defect in pheromone signaling. The screen would identify Ste50 dependent components of the pheromone signaling pathway along with other elements that are not Ste50 dependent. The yeast strain YCW311, $\Delta ste50$ with a *FUS1-HIS3* reporter, should grow in histidine deficient media only if a functional pheromone signaling pathway is present. In this yeast strain carrying the *ste50* mutant allele on a *CEN* plasmid with an *URA3* marker, we screened a high-copy yeast genomic tiling collection (GE Dharmacon, CO). The library collection was on a high copy 2 μ plasmid with a *LEU2* marker. The suppressor screens were carried out with the initially isolated Ste50-RA domain triple mutants G (I307K L300V K260N) and R (A242G N270D I289T). In total, 20,500 transformants (~10X the library size coverage) were screened for suppression of mutants R and G and 270 initial hits were obtained.

Characterization of initial library hits revealed suppressors of the pheromone response pathway

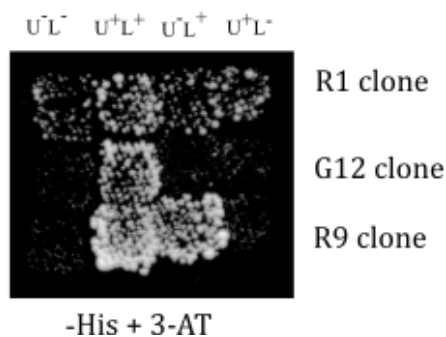
Initial hits were characterized by genetically dissecting them through plasmid linkage test; this was done through random loss of either the *LEU2* or *URA3* marked plasmids (see

methods), which resulted in 4 populations: *Ura⁺leu⁻*, *Leu⁺ura⁻*, *leu⁻ura⁻*, *Leu⁺Ura⁺* [Figure 1A and Table 1]. This analysis identified *ste50* mutant plasmid dependent growth specifically due to the presence of the suppressor plasmid (*Leu⁺Ura⁺*). Overall we identified 56 suppressor hits by this analysis, among them 28 showed background strain related growth; 26 showed *ste50* mutant independent, while 2 showed *ste50* mutant dependent, suppression of the pheromone signaling defect [Table S1]. The identified *ste50* mutant dependent suppression was found in clones G12 and G13 isolated from the genomic screens. One of the hits, colony 12, was used to show Ste50 dependent growth on selection media [Figure 1B]. The suppression was confirmed for colonies G12 by the plasmid linkage assay [Figure 1C] and the identity of all the suppressors were revealed by DNA sequencing and by comparison with the yeast genomic database (see *Materials and Methods*).

A



B



C

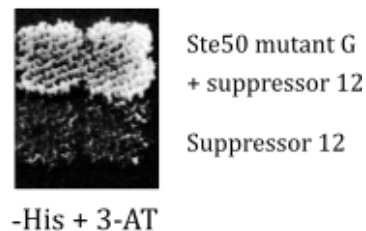


FIGURE 1: Yeast genomic library clone 12 is a genetic suppressor of the Ste50-RA domain mutant G (K260N L300V I307K). Yeast strain YCE311 (see *Materials and Methods*) bearing Ste50 RA domain mutant G was transformed with yeast genomic library (Dharmacon, CO, USA) and screened for suppressor(s) of the mutant G. (A) Showing growth on the selection media, as indicated, of colony 12, bearing genomic library clone. (B) YCW311 bearing mutant G with different library clones that were subjected to genetic dissection (see *Materials and Methods*) to reveal all the possible growth patterns on the selection media. (C) Confirmation of colony 12 as a suppressor after reintroduction of the suppressor by plasmid linkage assay.

TABLE 1: Suppression growth characterization

Genetic dissections		Suppression
U-L-	No library plasmid/ No ste50 plasmid	Nonspecific strain related growth
U+L+	Library plasmid/ste50 plasmid	Ste50 mutant dependent suppression by library clone
U+L-	No library plasmid/ ste50 plasmid	Ste50 mutant plasmid related growth (background)
U-L+	Library plasmid/ No ste50 plasmid	Ste50 independent suppression by library clone

Suppressor identification revealed a genomic fragment containing the *MGA1-RIE1* genes as a Ste50 dependent suppressor of defective pheromone signaling

Table 2 provides a list of the library plasmids recovered and the open reading frames in their genomic fragments. We obtained multiple recurring hits of known regulators of pheromone signaling from the screens that included Ste4 (4X), Ste11 (7X) and Ste5 (4X), confirming that the screens worked. Sequence analysis of the two independently screened Ste50 dependent suppressor clones revealed in each a 5903 base pair fragment in chromosome VII containing two open reading frames that were identified as *MGA1-RIE1* [Figure 2]. Identification of the ORFs of other suppressors obtained showed possible general transcriptional activation [Table 2]. We were most interested in ste50 mutant

dependent suppressor *MGA1-RIE1*, where *MGA1* is a known suppressor of the pseudohyphal growth defects of ammonium permease mutants (Lorenz *et al.*, 1988), and *RIE1* is a putative RNA binding protein (Feroli *et al.*, 1997) that was also found to genetically interact with *STE50* in a SGA (synthetic genetic array) study (Costanzo *et al.*, 2016). Further dissection by sub-cloning was required to identify the gene responsible for the suppression function.

***RIE1* is a genetic suppressor of the specifically-pheromone-signaling-defective Ste50-RA domain mutants**

The two ORFs found from the suppressor screen were dissected by sub-cloning (see *Materials and Methods*) in the parental 2 μ vector pGP546 to delineate the gene responsible Ste50 independent regulators of pheromone signaling we used overexpressed *STE4* in the pGP546 2 μ vector. Of the two ORFs, we found *RIE1* caused suppression of the pheromone signaling defect due to the Ste50-RA domain mutations [Figure 3].

TABLE 2: Yeast genomic library clones that suppressed pheromone signaling defect of the STE50 mutant

Genetic interaction with Ste50	Times found	Gene(s)	Feature type	Description
Ste50 independent	1	tC(GCA)P2	tRNA gene	Cysteine tRNA
		YPRCdelta1	LTR	Ty1LTR
		5	LTR	Ty1LTR
		YPRWdelta14	ARS	Autonomously replicating unit
Ste50 independent	3	<i>UGA3</i>	ORF	Utilization of GABA
		<i>UGX2</i>	ORF	Unknown function
		<i>SFA1</i>	ORF	Alcohol dehydrogenase and formaldehyde dehydrogenase.
		<i>NRP1</i>	ORF	Putative RNA binding protein.

		<i>FAP7</i>	ORF	NTPase for small ribosome synthesis.
		<i>CDC36</i>	ORF	Regulate mRNA levels.
Ste50 independent	4	<i>RPB10</i>	ORF	RNA polymerase subunit.
		<i>MGM1</i>	ORF	Mitochondrial GTPase
		<i>STE4</i>	ORF	G protein beta subunit
		<i>SAS5</i>	ORF	Subunits of SAS complex
		<i>SPR2</i>	ORF	Putative spore wall protein
		<i>AIM41</i>	ORF	Unknown function
		<i>RUD3</i>	ORF	Golgi matrix protein
Ste50 independent	7	<i>STE11</i>	ORF	Signal transducing MEK kinase
Ste50 independent	4	<i>STE5</i>	ORF	MAPK scaffold protein
Ste50 independent	1	<i>MDM36</i>	ORF	Mitochondrial protein
		<i>YPR084W</i>	ORF	unknown function
		<i>ASA1</i>	ORF	Subunit of ASTRA complex
Ste50 independent	1	<i>DOC1</i>	ORF	Processivity factor
		<i>CSE1</i>	ORF	Chromosome segregation
		<i>YGL239C</i>	ORF,	Heme activator protein
		<i>HAP2</i>	Dubious ORF	Transcriptional activator and global regulator of respiratory genes
		<i>YGL235W</i>	Uncharacterized ORF	Putative protein of unknown function, potential Cdc28 substrate
Ste50 dependent	2	<i>MGA1</i>		Suppressor of filamentous growth
		<i>RIE1</i>		RNA binding protein

for this suppression. Dissected genes were tested by the suppressor assay to find the causal gene for the *ste50* mutant-dependent-suppression. The two genes, *MGA1* and *RIE1* were tested against the strongest Ste50-RA domain specifically-pheromone-signaling-defective mutants R283G Q294L and R296G (Sharmeen *et al.*, 2019). As a positive control for the Ste50 independent regulators of pheromone signaling, overexpressed *STE4* open reading frame in the pGP546 2 μ vector was used. Of the two ORFs, *RIE1* caused suppression of the pheromone signaling defect due to the Ste50-RA domain mutations [Fig. 3].

C chromosome VII

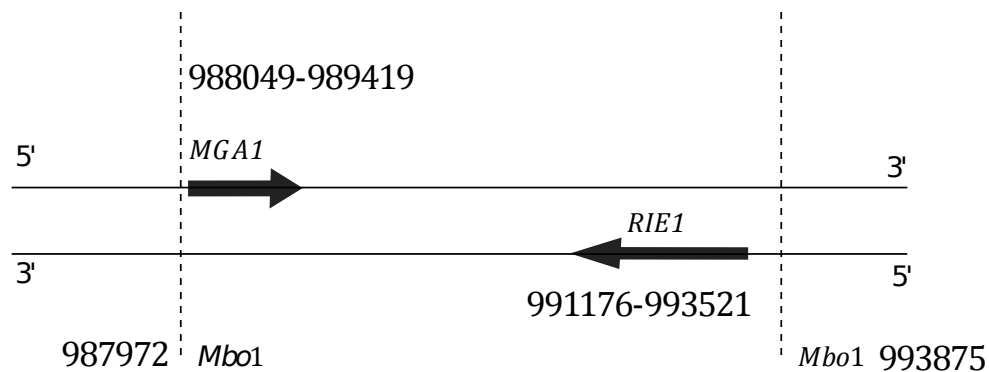


FIGURE 2: *MGA1* and *RIE1* chromosomal location. *Saccharomyces cerevisiae* genomic library fragment (between dashed lines) containing *MGA1* and *RIE1* ORFs in chromosome VII. Inserted in BamH1 site of the plasmid pGP564.

Phenotypic analysis of *RIE1* deletion suggests a role for this gene in the pheromone signaling pathway

To confirm if either *RIE1* or *MGA1* acts in the pheromone signaling pathway, yeast strains containing independent deletion of either *RIE1* or *MGA1* were studied microscopically. We also tested the wild type BY4741 in parallel. We found that in the absence of pheromone stimulation, none of the yeast strains exhibited any detectable phenotype; *RIE1* deletion causing no morphological effect on the vegetatively growing cells has been reported before (Feroli *et al.*, 1997) [Figure 4A]. When stimulated with pheromone, the wild type strain

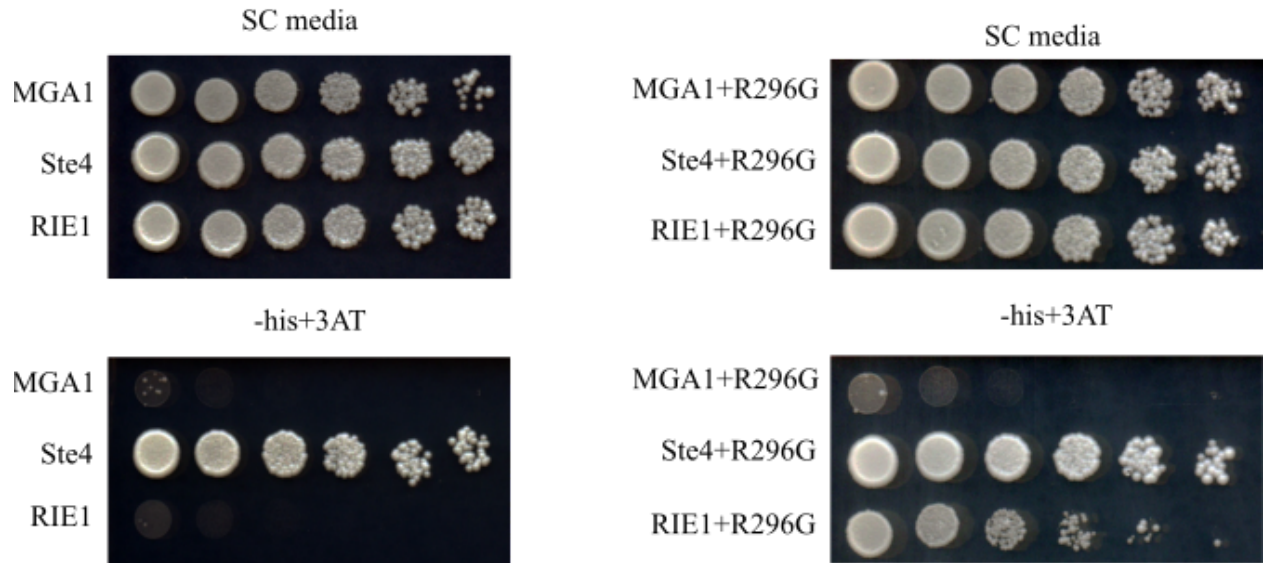


FIGURE 3: Multicopy *RIE1* can suppress pheromone signaling defect of Ste50 mutant R296G. Yeast strain YCW311 bearing different alleles as indicated were transformed with either *MGA1* or *RIE1* and tested on selected plates by spot assay.

showed shmoo formation, with shmoo devoid of a properly defined neck region. Both the wild type and the $\Delta mga1$ presented cells with similar morphology, suggesting that deletion of *MGA1* has no effect in pheromone signaling. However deletion of *RIE1* blocked typical shmoo formation, showing an aberrant morphology of elongated cells with a bud at the tip [Figure 4A]. We analyzed the shmoo forming ability among the three strains and Figure 4B shows that $\Delta mga1$ had similar morphology and level of shmoo formation as the wild type, but gross inability of $\Delta rie1$ to form any typical shmoo [Figure 4B]. Interestingly, $\Delta rie1$ showed increased budded cells (includes all cells showing bud) [Figure 4C]. Shmoo structure is considered as found in the wild type. There is a significant difference in terms of budded cells between the wt and *Rie1*-deletion upon pheromone stimulation [Figure 4D]. The proportion of un-budded cells decreased in this strain upon pheromone stimulation [Figure 4E]. These results suggest that *RIE1* may have a role in the pheromone response pathway.

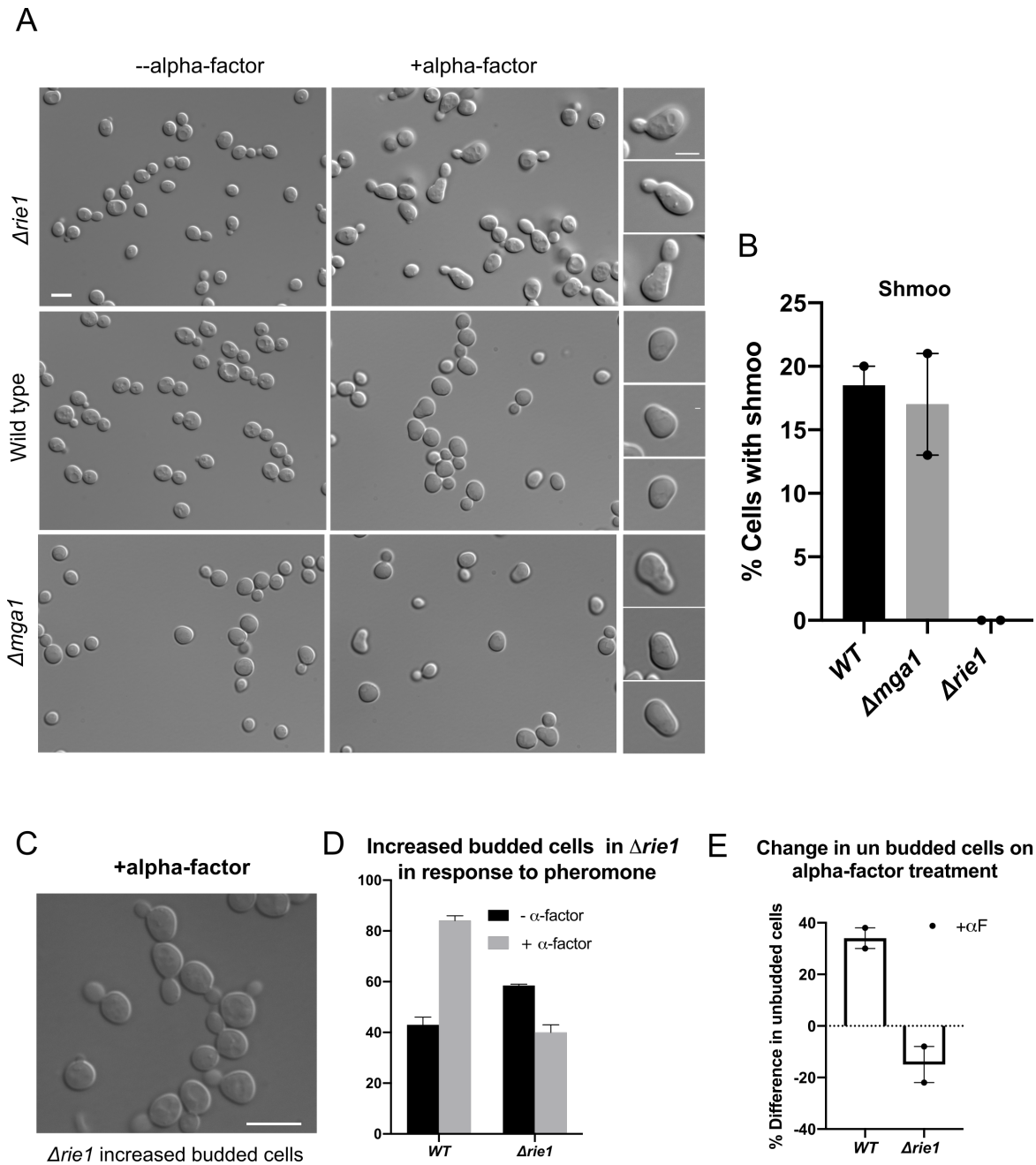


FIGURE 4: Phenotype of *RIE1* suppressor deletion strain. Yeast strains, BY4741 derivatives with different alleles, as indicated, were cultured up to exponential phase and either stimulated/unstimulated with pheromone. (A) Phenotypes of the indicated alleles. (B) Relative typical shmoo formation among the different alleles. (C) and (D), increased budding in $\Delta rie1$. (E) Decrease in un-budded cells upon pheromone stimulation.

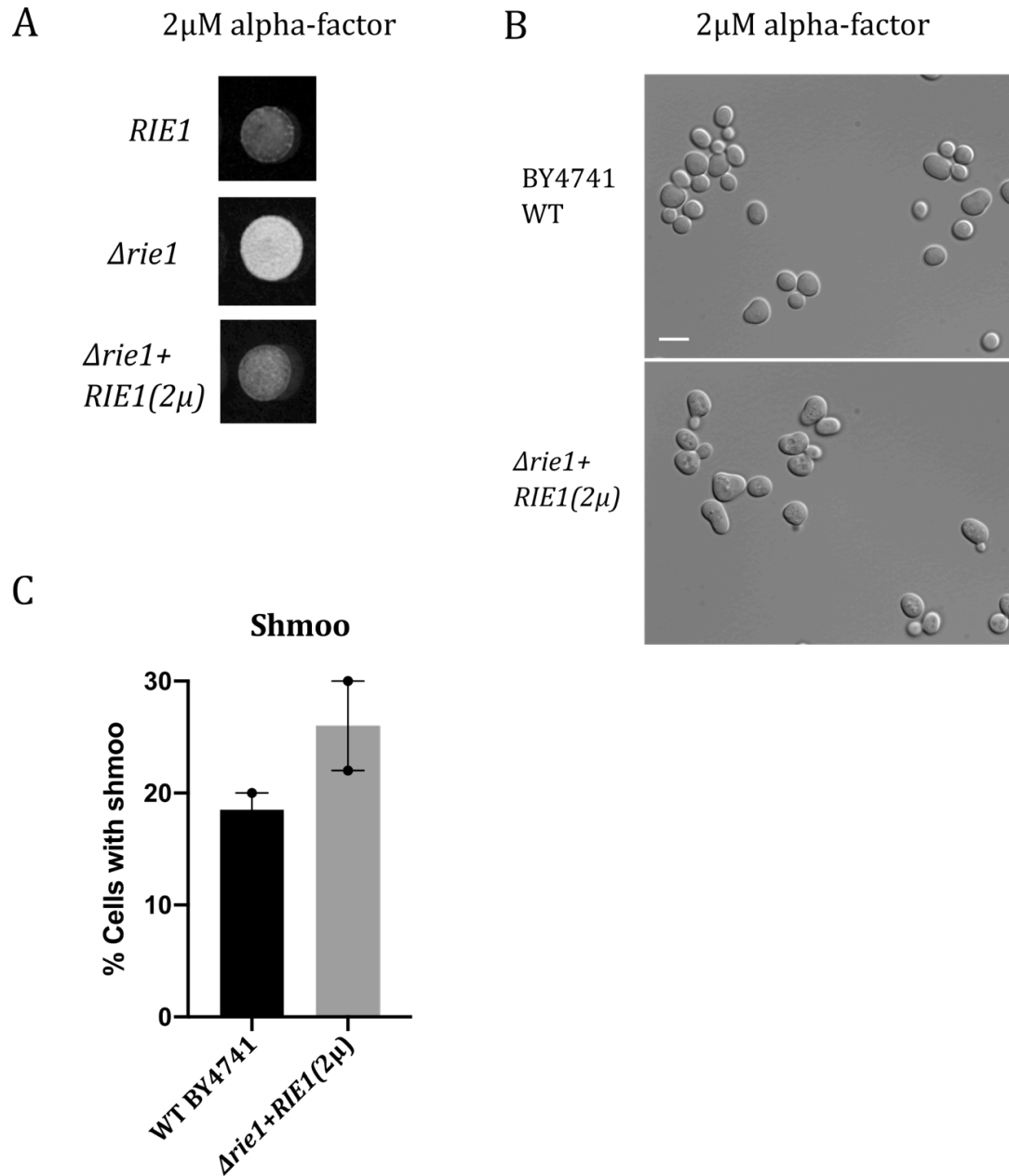


FIGURE 5: Characterization of Δ *rie1* yeast strain. BY4741 derived yeast strains with the indicated genotypes were cultured overnight and spotted on selective media containing 2 μ M alpha-factor (see *Materials and Methods*) to assay their function of pheromone signalling (A). Complementation of Δ *rie1* with *RIE1* on 2 μ plasmid (B) and the proportion of cells with shmoo formation (C). Bar 5 μ m.

Characterization of *RIE1* in pheromone signaling

To characterize *RIE1* function in pheromone signaling, we tested $\Delta rie1$ cells for their ability to grow under pheromone stimulation by spot assay on the selective solid media designed to analyze cell cycle arrest (see *Materials and Methods*). $\Delta rie1$ was also transformed with an overexpressed *RIE1* open reading frame on a 2 μ plasmid to find whether complementation happens and can recapitulate, on a test plate, the wild type cell cycle arrest due to pheromone treatment. Results show that $\Delta rie1$ had alpha-factor resistant growth on theselective plate suggestive of impaired ability to undergo cell cycle arrest due to pheromone stimulation, indicating defective pheromone signaling [Figure 5A]. This pheromone signaling defect could be complemented by a plasmid-bearing allele of *RIE1* - the $\Delta rie1 + 2\mu\text{-}RIE1$ strain [Figure 5A]. The $\Delta rie1$ strain that was transformed with 2 $\mu\text{-}RIE1$ was also assessed for complementation by examining the recapitulation of shmoo formation [Figure 5B]. Results show that the $\Delta rie1 + 2\mu\text{-}RIE1$ strain regained a higher level of shmoo forming ability as the WT strain [Figure 5C] suggesting that $\Delta rie1$ when complemented with 2 $\mu\text{-}RIE1$ recapitulated the wild type pheromone signaling. Together these results show that *RIE1* is a component of the pheromone signaling pathway.

4.5 Discussion

The mating MAPK pathway in *S. cerevisiae* shares many components with other MAPK pathways; one of these shared components is the MAP3K Ste11. The role of the Ste50 adaptor protein in the regulation of signaling specificity for the different extracellular signals sharing Ste11 has been investigated for the hyperosmolar glycerol and the filamentous growth pathways (Wu *et al.*, 2006; Truckses *et al.*, 2006), but its role in mating-specific signaling is poorly understood. We previously demonstrated that specific residues in the RA domain of Ste50 are involved in the regulation of mating signaling (Sharmeen *et al.*, 2019). Changing these residues abrogates pheromone signaling, while keeping HOG signaling functional. These residues were involved in the pheromone-signaling-related Ste50 patches required for shmoo polarization, were required for the Ste50 patches at the

bud-neck before cytokinesis and were also further involved in the nuclear localization of the protein. That changing these residues resulted in loss of localization and pheromone signaling could be due to a loss of protein interaction with Ste50 that is specifically required for pheromone signaling.

Based on the above findings we designed a genetic suppressor screen strategy utilizing a high copy genomic library to find effectors of the mating signaling function of the Ste50-RA domain mutants. Some of the genomic fragments were known to cause lethality as listed in the Prelich yeast genomic tiling collection database (GE Dharmacon, CO). However, it was not possible to cross check them since the screen was random so the lethal gene bearing plasmids will not be assessed in the screen. We identified genes that are known components of the pheromone response pathway and when overexpressed bypassed the requirement for Ste50, such as *STE11*, *STE5* and *STE4*. This supports previous understandings that adaptor protein recruitment in a signaling pathway is required for amplification of signaling (Pawson and Scott, 1997). We also identified a gene, *RIE1* that showed suppression of the growth defect in the presence of the mating-pathway-specific Ste50 mutants. *RIE1* has been shown to genetically interact with Ste50 (Costanzo *et al.*, 2016). The study conducted SGA analysis to map genetic interactions among gene pairs in *S. cerevisiae*. *RIE1* was found to have a negative genetic interaction with Ste50, a negative genetic interaction was noted when a double mutant exhibited a fitness defect, the double mutant with *RIE1* was found not as lethal but somewhat sick.

Phenotypic tests with strains deleted for *RIE1* or *MGA1*, the other gene found on the suppressing fragment, established that *RIE1* has a genetic connection with the pheromone response pathway. Cells with a *RIE1* deletion showed abnormal shmooing when cells were stimulated with pheromone. The treated cells had an increased number of budded cells compared to the wild type. In the cell cycle arrest testing, *RIE1* showed increased pheromone resistant growth relative to the wild type.

RIE1 is a putative RNA binding protein (Feroli *et al.*, 1997) with a domain that has characteristics present in many poly A binding proteins (Query *et al.*, 1989; Burd *et al.*, 1991). It interacts with a specific domain of a polyA binding protein (PAB1) (Richardson *et al.*, 2012). Poly A binding (PAB) proteins are typically involved in RNA metabolic functions, and therefore interact with a number of different proteins. Since the PAB1 proteins have both nuclear and the cytoplasmic functions, these proteins probably require interactions with many other proteins and complexes (Kuhn *et al.*, 1996; Mangus *et al.* 2003; Kuhn & Wahle 2004; Hosoda *et al.* 2006). However the revelation of the molecular role of *RIE1* gene is still rudimentary, it has been found to localize mainly in the P-bodies that are rich in enzymes involved in mRNA turnover (Buchan *et al.*, 2008). A GFP tagged fusion protein of *RIE1* was found localized diffusely in the cytoplasm under the vegetative growth conditions (Kojima *et al.*, 2016).

We established here that *RIE1* regulates pheromone signaling through its genetic interactions with *STE50*, whether there is a physical interaction involved is not known. Further protein interaction studies by Co-IP could reveal its physical involvement and further our knowledge in the mechanism of this regulation.

4.6 Materials and Methods

Yeast Strains and Yeast Manipulations

The genotypes and sources of the yeast and bacterial strains used in this study are listed in Table 3. Yeast strains were grown in YPD (yeast peptone dextrose) and plasmid-bearing strains were grown in SD (synthetic defined) media with appropriate auxotrophic requirements. The yeast high-copy genomic tiling collection was obtained from GE-Dharmacon (CO, USA). The standard manipulation of yeast strains, culture conditions and media were as described (Dunham *et al.*, 2015). Yeast transformations were carried out by the lithium acetate method (Chen *et al.*, 1992).

Plasmids

The plasmids used in this study are: pRS316-*STE50*^{wt}::*URA3*/AmpR; pRS316-*ste50*^{I307KL300VK260N}::*URA3*/AmpR; pRS316^{A242GN270DI289T}; pRS316-*ste50*^{R296G}::*URA3*/AmpR and pRS316-*ste50*^{R283GQ294L}::*URA3*/AmpR. The parental vector of the yeast 2 μ library, pGP546 was used to construct plasmids containing the dissected genes from the identified suppressor genomic fragment. The genes were PCR amplified with primers having flanking sequences on both ends for *in vivo* recombination (IVR) in yeast into the *Bam*HI linearized pGP546 and selected on SD-Leu plates. Transformants were confirmed by PCR.

TABLE 3: Strains used in this study

Strain	Genotype	Reference
YCW311	<i>MATa ste50Δ::TRP1 FUS1-HIS3 far1::hisG sst2::ura3 his3 ura3 leu2 trp1</i>	This study
BY4741	<i>MATa his3 leu2 ura3 met15</i>	Yeast knockout collection ATCC
<i>Δmga1</i>	<i>MATa YGR249wΔ::Kan^Rhis3 leu2 ura3 met15</i>	Yeast knockout collection ATCC
<i>Δrie1</i>	<i>MATa YGR250CΔ::Kan^Rhis3Δ1 leu2Δ0 ura3Δ0 met15Δ0</i>	Horizon-Dharmacon
<i>E.coli</i>	F- Δ (<i>ara-leu</i>)7697 [<i>araD139</i>]B/r Δ (<i>codB-lacI</i>)3 <i>galK16 galE15</i> λ - e14- <i>mcrA0 relA1 rpsL150</i> (StrR) <i>spoT1 mcrB1 hsdR2</i> (r-m+)	Invitrogen

3-AT Titration Assay

Yeast strain YCW311 was transformed with plasmids containing WT, *ste50ΔRA*, and *ste50* mutants and grown on SD-Ura for two days. Transformants were then replicated onto SD-Ura-His with different concentrations of 3-AT (3-amino triazole) in the absence of pheromone. The replicates were incubated at 30°C for 2-3 days before growth was scored. The 3-AT minimum concentration needed to knock off a mutant's basal pathway activity was set at 0.1mM in the absence of pheromone.

Yeast high copy genomic library screen for suppressor(s)

Suppressor screens were performed using a 2 μ plasmid-based multi-copy yeast genomic library (Dharmacon, CO) for genes that suppresses the growth defect of *ste50* mutants. The *ste50* plasmids were transformed independently into yeast strain YCW311 and plated on SD-Ura for selection. The resulting strains were used for transformation with the genomic library (*LEU2*). The transformants were plated on media lacking uracil and leucine (SD-Ura-Leu) and incubated for two days at 30°C. The transformants were then replicated on SD-Ura-Leu-His + 0.1mM 3-AT and incubated for 2-3 days at 30°C. Plates were then scored for growth.

Characterization of the initial suppressor hits

The initial hits from the suppressor screens were subjected to genetic analysis to characterize *ste50* mutant dependent or independent suppressors. Each suppressor was streaked on YPD for single colony, grown in 30°C for 2 days and replicated sequentially onto SD-Ura, SD-Leu, SD-His + 0.1mM 3-AT different selective media plates. The replicates were incubated in 30°C for 2-3 days and differential growth under different selection conditions were assessed for *ste50* dependent suppression(s). Two growth patterns suggest random strain related growth: (i) No growth on SD-ura and SD-leu but growth on SD-his + 0.1mM 3-AT. (ii) Growth on SD-ura and no growth on SD-leu but growth on SD-his + 0.1mM 3-AT. No growth on SD-ura but growth on SD-leu and growth on SD-his + 0.1mM 3-AT determines general suppressor for the pheromone response pathway since it is independent of the *Ste50* mutant. Simultaneous requirement of both URA3-based and LEU2-based plasmids for growth on SD-his + 0.1mM 3-AT identifies a hit of *Ste50* plasmid dependent suppressor.

Identification of the genomic insert

Yeast genomic fragment contained in the library plasmid pGP546 was identified by Sanger sequencing using primers 5' TAAGTTGGGTAACGCCAGGG 3' and 5' AGCGG-ATAACAATTTACACAGGA 3'. All sequencing was carried out at the McGill University Génome Québec Innovation Centre. The identified nucleic acid sequences were then used to

retrieve the genomic fragment using “yeast genome browser” in the fungal genome database (<http://seq.yeastgenome.org/>).

Dissection of genes in the suppressor

The identified Ste50 RA domain mutant suppressor contained two genes, *MGA1* and *RIE1*. To find the causal mutation, we dissected the genes using primers F-MGA1 ACGCCAAGCGCGCAATTAACCCTCACTAAAGGGAACAAAAGCTGGAGCTCCACCGCGGTGGCGGC CGCTCTAGAAGTAGTCCGGAATGAAAAAGGCCAT/RTAAGTTGGGTAACGCCAGG and F-YGR5-0CCGCAATTAATGTGAGTTACC/R-TATAGGGAATTGGGTACCGGGCCCCCCTCGAGGTTCGAC-GGTATCGATAAGCTTGATATCGAATTCCTGCAGCCCGGAATTGTTTATCTATCCTTTGC containing flanking sequences on both ends for in vivo recombination (IVR) in yeast into the *Bam*HI linearized pGP546 and selected on SD-Leu plates. Transformants were confirmed by PCR.

Microscopy and live-cell imaging

Morphological studies by microscopy was done as described (Sharmeen *et al.*, 2019). Briefly, yeast strains with or without plasmids were grown to saturation and then diluted in their respective media. Cells at ~0.4 OD₆₀₀ were then stimulated with 2μM alpha-factor and prepared for viewing. A DM6000 Epifluorescent Microscope (Leica Biosystems, Wetzlar, Germany) with Velocity acquisition software (PerkinElmer, MA, USA) using 100x Leica Plan Fluotar (NA 1.3) lens was used for imaging. ImageJ software (v. 1.37; National Institutes of Health) was used to process the images. For all imaging analysis at least 200 cells were counted in triplicate.

Spot assay

Spot assay was done on solid media with appropriate selections. Briefly, cultures were grown over night and diluted to OD₆₀₀ of 1 then serially diluted to 6-fold in a 96 well plate. Five micro liters were spotted on the plates for each dilution and grown at 30°C for 2 days.

Acknowledgments: Financial supports from Natural Sciences and Engineering Research Council (NSERC) of Canada grant (C.W.), NSERC CRC Tier 1 950-22895 (M.W.), and McGill University.

4.7 References

- Bardwell L (2005). A walk-through of the yeast mating pheromone response pathway
Peptides, 26(2), 339-350.
- Bauman P & Albright CF (1998). Functional analysis of domains in the Byr2 kinase.
Biochimie 80, 621–625.
- Buchan JR, Muhlrاد D, Parker R (2008). P bodies promote stress granule assembly in
Saccharomyces cerevisiae. *J Cell Biol* 183, 441–455.
- Burd CG, Matunis EL, Dreyfuss G (1991). The multiple RNA-binding domains of the mRNA
poly(A)-binding protein have different RNA-binding activities. *Mol Cell Biol* 11,
3419–3424.
- Costanzo M, VanderSluis B, Koch EN, Baryshnikova A, Pons C, Tan G, ... & Pelechano, V
(2016). A global genetic interaction network maps a wiring diagram of cellular
function. *Science* 353(6306), aaf1420.
- Feroli F, Carignan I G, Pavanello A, Guerreiro P, Azevedo D, Rodrigues-Pousada C,
Melchiorretto P, Panzeri L, Carbone MLA (1997). Analysis of a 17.9 kb region from
Saccharomyces cerevisiae chromosome VII reveals the presence of eight open
reading frames, including BRF1 (TFIIB70) and GCN5 genes. *Yeast* 13(4), 373-7.

- Herskowitz I (1995). MAP kinase pathways in yeast: for mating and more. *Cell* 80(2), 187-197.
- Hosoda N, Lejeune F, Maquat LE (2006). Evidence that poly(A) binding protein C1 binds nuclear pre-mRNA poly(A) tails. *Mol Cell Biol* 26, 3085–3097.
- Jansen G, Buhring F, Hollenberg CP, Ramezani Rad M (2001). Mutations in the SAM domain of STE50 differentially influence the MAPK-mediated pathways for mating, filamentous growth and osmotolerance in *Saccharomyces cerevisiae*. *Mol Genet Genomics* 265, 102–117.
- Kojima R, Kajiura S, Sesaki H, Endo T and Tamura Y (2016). Identification of multi-copy suppressors for endoplasmic reticulum-mitochondria tethering proteins in *Saccharomyces cerevisiae*. *FEBS letters* 590(18), 3061-3070.
- Kuhn U & Pieler T (1996). *Xenopus* Poly(A) binding protein: functional domains in RNA binding and protein–protein interaction. *J Mol Biol* 256, 20–30.
- Kuhn U & Wahle E (2004). Structure and function of poly(A) binding proteins. *BBA* 1678, 67–84.
- Lorenz MC & Heitman J (1998) Regulators of pseudohyphal differentiation in *Saccharomyces cerevisiae* identified through multicopy suppressor analysis in ammonium permease mutant strains. *Genetics* 150(4), 1443-57.
- Mangus DA, Evans MC, Jacobson A (2003). Poly (A)-binding proteins: multifunctional scaffolds for the posttranscriptional control of gene expression. *Genome Biol* 4, 223–246.

- Query C, Bentley RC, Keene JD (1989). A common RNA recognition motif identified within a defined U1 RNA binding domain of the 70K U1 snRNP protein. *Cell* 57, 89.
- Richardson R, Denis CL, Zhang C, Nielsen ME, Chiang YC, Kierkegaard M, ... & Yao G (2012). Mass spectrometric identification of proteins that interact through specific domains of the poly (A) binding protein. *Mol Genet Genom* 287(9), 711-730.
- Truckses DM, Bloomekatz JE, Thorner J (2006). The RA domain of Ste50 adaptor protein is required for delivery of Ste11 to the plasma membrane in the filamentous growth signaling pathway of the yeast *Saccharomyces cerevisiae*. *Mol Cell Biol* 26, 912-928.
- Tu H, Barr M, Dong DL, Wigler M (1997). Multiple regulatory domains on the Byr2 protein kinase. *Mol Cell Biol* 17, 5876-5887.
- van Drogen F, O'Rourke SM, Stucke VM, Jaquenoud M, Neiman AM, Peter M (2000). Phosphorylation of the MEKK Ste11p by the PAK-like kinase Ste20p is required for MAP kinase signaling in vivo. *Curr Biol* 10, 630-639.
- Wu C, Leberer E, Thomas DY, Whiteway M (1999). Functional characterization of the interaction of Ste50p with Ste11p MAPKKK in *Saccharomyces cerevisiae*. *Mol Biol Cell* 10, 2425-2440.
- Wu C, Jansen G, Zhang J, Thomas DY, Whiteway M (2006). Adaptor protein Ste50p links the Ste11p MEKK to the HOG pathway through plasma membrane association. *Genes Dev* 20(6), 734-746.

Chapter V: Discussion and future studies

Role of Ste50 as a MAPK signal discriminator

Specificity of signaling suggests that a single input stimulus perceived by a cell can be transduced into a destined output. Various mechanisms have been proposed for establishing specificity of cellular signaling (Smith & Scott, 2002; Schwartz & Madhani, 2004; White & Anderson, 2005). This investigation involved an attempt to understand how specificity of a signal is maintained when multiple signals are transduced through a common component. The yeast pheromone response pathway, which shares pathway modules with several other pathways, was taken as a prototype in this study. Specificity posits that adaptor proteins can be instrumental in specificity function by having the capacity to interact with other proteins incurring control mechanisms (Songyang *et al.*, 1993; Stein *et al.*, 2003; Qamra *et al.*, 2013). Such an adaptor, Ste50, controls the function of Ste11 to specifically regulate the hyperosmolar glycerol and the filamentous growth pathways. Because Ste50 with deleted regions confers reduced mating ability (Rad *et al.*, 1992) and the RA domain had been proposed to have structurally different interfaces (Ekiel *et al.*, 2009), it is conceivable that the RA domain may have specificity determinants for the mating pathway. Data presented here reports that the adaptor Ste50 functions as a signal discriminator that specifically regulates either pheromone or HOG signal transduction. Briefly, Ste50-RA domain mutant libraries were generated with random error-prone PCR and homologous recombination in a yeast vector. The mutants were screened for specific MAPK signaling phenotypes and three different classes of mutants were obtained [Chapter II, Table 1]: Class I mutants were specifically pheromone response defective; their pheromone response is blocked and they thus were unable to undergo pheromone dependent cell cycle arrest, although they remained functional in the hyperosmolar glycerol signaling pathway. These included mutations in the RA domain residues R283, I289, Q294, R296 and I307. Class II mutants were specifically defective in the hyperosmolar glycerol signaling pathway, while keeping normal cell cycle arrest under

pheromone treatment, these included mutations in the RA domain residues R274, H275, N276 and L277. Class III mutants were impaired in both pheromone and HOG signaling and included mutations in the RA domain residues I320 and L322. Mutants having multiple mutations were dissected to reveal the causal mutation, this process generated in some cases a single driver mutation but in some others multiple mutations were needed to generate the strong phenotypes. The phenomenon behind multi-mutations generated phenotypes is speculative that might result from cumulative individual weak structural and dynamic perturbations of the individual mutation into stronger effects (Tripathi *et al.*, 2016).

Phenotype-causing residues cluster on Ste50-RA domain NMR structure

The NMR structure of the Ste50-RA domain has been described in Ekiel *et al.*, 2009. Interestingly, different classes of phenotype-causing residues of the Ste50-RA domain showed distinct clustering on the NMR structure, suggesting that these residues form surfaces as potential sites for protein-protein interaction. Residues involved in specifically pheromone signaling were clustered at a distance opposite to the residues specifically involved in HOG signaling, and the residues that are involved in both pheromone and HOG signaling were located in between them. A similar mapping was reported by Reményi *et al.*, 2005 for Far1 in the pheromone response pathway that associates with Fus3 and Kss1 and was explained as specificity of signaling due to cooperative binding. Structurally the RA domain has a non-canonical ubiquitin fold (Ekiel *et al.*, 2009) but the core still maintains the canonical ubiquitin fold containing three β sheets and two α helices. The distinct patches for the different phenotypes were found within the core ubiquitin fold encompassing residues 262-326 (Ekiel *et al.*, 2009). Further computational analysis indicated that the structure of the well-folded core was not disrupted by the introduction of these mutations [Chapter II, Table S2], which indicates that the different phenotypic effects found were not due to any major conformational changes. Residues involved in the specificity of pheromone signaling were located in the β sheet and were facing away from the α 1-helix where the HOG signaling specific residues were positioned [Chapter II, Figure 5A]. These results revealed that the binding sites are located on different secondary

structure elements providing different protein-protein interaction interfaces and interaction modes. Thus, these data provide the structural basis for the RA domain of the adaptor Ste50; it has genetically separable surfaces that potentially connects to the different MAPK signaling pathway and differentially modulate signaling specificity.

Further structural and functional analysis will be required to accurately define the boundaries of these surfaces of protein-protein interaction. To have a more comprehensive mutagenesis profile, saturation mutagenesis combined with deep sequencing would be a very powerful way to identify mutants when hooked up to a convenient automated phenotypic screen, such as a reporter assay (Tripathi, 2014).

Distinct clusters of phenotype-causing residues have a propensity for protein-protein interaction

The several epitopes formed due to the different phenotypic clustering discovered on the Ste50 NMR structure were further analyzed by 9 different algorithms that revealed the propensity of the Ste50-RA domain residues to engage in protein-protein interactions [Chapter II, Figure 5C]. Further microscopic live cell imaging discovered that the specifically-pheromone-response-defective mutants were severely impaired in shmoo formation, supporting the defective pheromone signal in these mutants. Additional microscopic studies with the GFP tagged wild type Ste50 and mutants revealed that the wild type Ste50 localized to the growing shmoo tip upon pheromone stimulation, while the specifically-pheromone-response-defective Ste50 mutants failed to localize. Failure to localize due to mutation usually indicates a loss of a transient interaction (loss of obligate interaction causes complete loss of function) causing loss of function (Yates & Sternberg, 2013). The present finding suggests that Ste50 is a member of the polarization complex and is specific for pheromone dependent polarization module resulting from the association with other pheromone response related proteins. Thus the data here suggests that Ste50 forms functional protein-protein interactions to mediate pheromone signaling, supporting the previous findings from the computational analysis.

The Ste50 polarity patch formation could be studied in more detail in future to identify the associating proteins in the polarity complex. Microscopic studies could include probing with different fluorescent-tagged known polarity factors, such as Cdc42, Bem1, Ste20, Ste5, Ste4, Far1 etc. to elucidate co-localization or the timing of the differential congregations of the polarity patch establishment factors. Further, interactions with each could be verified by FRET (fluorescence resonance energy transfer) (Sun *et al.*, 2012), which could be very beneficial to study the spatial-temporal regulation of protein-protein interactions in the natural environment of the living cells.

Ste50-RA domain expected to interact with a non-small GTPase protein to connect pheromone signaling

The RA domain of Ste50p has been previously shown to specifically interact with Opy2p in the HOG signaling pathway (Wu *et al.*, 2006) and Cdc42 small GTPase in the filamentous growth pathway (Truckses *et al.*, 2006). Binding with Opy2p and Cdc42p were found to be required for membrane translocation of Ste50 facilitating signaling. This function of the Ste50-RA domain is analogous to the mammalian N-terminal RA domain of Raf interacting with the small GTPase Ras to direct membrane translocation of the protein. The RA domain residues required for specific Opy2p interaction includes R274 H275 N276 and the Cdc42p specific interactions involve I267 and L268. The present discovery of the RA domain surface required for the specific pheromone response was found to be located on the opposite face of the RalGDS RA domain-binding site for small GTPases [Chapter II, Figure S2] suggesting pheromone signaling may involve a non-small GTPase binding target for the Ste50-RA domain.

The present work identifies genetically separable distinct surfaces containing pathway specific mutations. Data presented herein consistently showed potential binding sites for interacting with specific surfaces in the pheromone and HOG signaling pathway. Opy2p being already identified for the HOG signaling pathway, future studies with suppressor analysis and protein-protein association investigations of the pheromone specificity defined mutations will be informative for identifying interacting proteins.

Characteristics of the Ste50 polarity patch

As demonstrated in chapter II, pheromone stimulation causes Ste50p to form a punctate patch at the growing shmoo tip. The patch appearance is found to increase with the growth of the shmoo structure [Chapter II, Figure 8 A2-4] and at the population level was found to peak around two hours after pheromone treatment based on the number of cells with patches [Chapter II, Figure 8D]. Further studies with microscopic time-lapse analysis at the single cell level revealed that the peak appearance of the Ste50 shmoo patch is also at 2h after pheromone stimulation [Chapter III, Figure 3A]. Cells mobilized on average about 2% of the cytoplasmic Ste50 to the tip and this percentage does not change significantly with time [Chapter III, Figure 1A]. Yeast cells are known to have pheromone-concentration-dependent shmoo formation (Segall *et al.*, 1993). However, the polarity patch mobilization varied drastically due to the concentration of pheromone treatment, at lower pheromone concentration patch wandered along the cell cortex as also reported previously (Dyer, 2013); at higher pheromone concentrations, the shmoo matured early and the Ste50 polarity patch exhibited early appearance/disappearance [Chapter III, Figure 1B] indicating possible Ste50 involvement in the shmoo structure formation. Further data supports this observation where the Ste50 polarity patch was found to appear as an early indicator of shmoo structure formation and to disappear upon shmoo maturation [Chapter III, Figure 3A-B]. Examples of this phenomenon have been described for actin polarization during vegetative budding in yeast cells in the case of bud maturation (Waddle *et al.*, 1996). The present data found a timing of Ste50 polarity patch appearance/disappearance that was similar to actin patch appearance/disappearance. Additional findings showed that the Ste50 polarity patch travels from the cytoplasm towards the shmoo polarization site. The Ste50 patch movement could be driven by actin and myosin in yeast cells.

It is known that actin polarity patches are formed at the site of polarization (Smith *et al.*, 2001). The two major components of the polarization are actin cables and actin patches. Actin patches are formed at cortical membrane zones together with regulatory proteins that bind actin (Smith *et al.*, 2001). Studies with Cdc42 in polarity establishment during budding showed evidence that Cdc42 patch formation at the presumptive bud site is

independent of the localization or integrity of the actin cytoskeleton (Park *et al.*, 2007). Whether Ste50 presumptive shmoo site localization is actin dependent/independent could be investigated in detail in future with Latrunculin-B treatment to inhibit formation of actin cytoskeleton.

Pheromone specific residues are required for the bud-neck localization of Ste50

When an asynchronous population of wild type Ste50 bearing yeast cells were treated with pheromone, striking Ste50 localization was observed in the bud neck just before cytokinesis of cycling cells that are beyond G1 phase of the cell cycle. The localization transient appearance seems to be involved with cytokinesis. Cells under pheromone treatment that are beyond the G1 stage of the cell cycle have to finish the rest of the cycle to be at G1 and then develop shmoos. Previous studies found that when cells that are not in G1 are treated with pheromone, they do not form shmoos since Cdc28p phosphorylates Ste5p and prevents its plasma membrane localization, inhibiting the pheromone response pathway (Strickfaden *et al.*, 2007). However, all the transcription due to a pheromone-dependent response becomes totally active when cells are in the G2/M phase (Oehlen & Cross, 1994, 1998; Wassmann and Ammerer, 1997; Strickfaden *et al.*, 2007). Therefore, during and after the G2/M phase, the proteins required for the mating-pheromone response are present, although morphological modification due to cytoskeleton changes does not take place.

The localization of Ste50 to the cycling cells at the bud-neck is observed near telophase, that is past G2/M phase, when the proteins for the pheromone response are present. Actin-myosin ring forms in G2 and then maturation happens, at this point Ste50 localizes and the secondary septum and cytokinesis takes place. The septum markers will be helpful to elucidate whether the Ste50 localization happens before or after the septum formation. Rho1 is needed for the activation of actin/myosin, similar to Cdc42 it regulates lots of polarized events as well, but there is a second wave of Rho requirements for the septum formation. That could be interesting since Rho is a polarity determinant and at that point

other factors also come together for cell wall assembly, as well as Ste50. Permeable dyes can be used as markers to tell the timing of Ste50 localization, such as calcofluor white for primary septum since it stains with chitin (Utsugi *et al.*, 2002) and Aniline blue for staining glucan to mark the secondary septum. So is mcherry fluorescence tagged septin, which can be used to mark the timing of cell division (Yadenburg & Rose, 2009).

This spatiotemporal localization was observed generally in all cells after pheromone stimulation, while only seen in ~10% of the cells at a very low level in the vegetatively growing cells. This shows that pheromone signaling augments Ste50p bud-neck localization. It is tempting to speculate that cells may be programmed to have increased bud-neck localization of Ste50p for a faster exit from the vegetative state to shmoo formation. Interestingly, time-lapse movies revealed that in some cells a remnant of Ste50p patch remained at the bud-neck junction of the separated mother-daughter cells even after cytokinesis, and the sites quickly developed into shmoos [Figure 5F]. This has two implications; first, evidence shows that the polarity patch that assembles in the bud-neck is the same polarity patch that can drive shmoo polarization. Second, it may suggest that under pheromone stimulation cells have a greater need to have faster exit from budding and enter into the shmoo creation and Ste50 promotes this exit. The observation that pheromone signaling defective RA domain mutant failed in enhanced localization of Ste50p at the bud-neck in response to pheromone supports this view and suggests that a molecular link has been broken with this mutant that is required for patch formation at the bud-neck. Since our results show that the patch has dual functions, at the bud-neck and shmoo polarization, also supported by a recent study (Vasen *et al.*, 2018; Madden and Snyder, 1992) this link could be the same for the shmoo patch. A similar example is the actin polarization patch that contains the same component proteins forming the shmoo and bud polarization complexes (Smith *et al.*, 2001). These results indicate that the RA domain may have a molecular link that plays roles in both the polarization states. However, this theory is constrained by the fact that although Ste50p localizes to the bud-neck, it did not localize to the growing bud tip [Figure 6C]. This is in contrast to Cdc42 that localizes to the incipient bud site and growing bud tip (Smith *et al.*, 2013; Okada *et al.*, 2017). It is very

clear from these observations that Ste50 is not required for bud formation in yeast; rather its function is to facilitate exit from budding through cytokinesis in the vegetatively growing cells, and this function may have been pronounced in response to pheromone.

The nuclear localization of Ste50 and its potential role in pheromone response signaling

Ste50 has been reported previously and also observed by us as a cytoplasmic protein. However, this study consistently observed clear nuclear localization of the protein as a novel finding. Under vegetative growth condition Ste50p was found localized in the nucleus in ~13-25% of cells in the population level studies. This localization of Ste50 resembles Ste5 as reported by Mahanty *et al.*, 1999. In the vegetative growth conditions a pool of Ste50 is always present in the nucleus, since if there was no nuclear Ste50-GFP cells should show an empty nuclear zone, similar to the vacuole. The nuclear Ste50-GFP is only evident when its nuclear localization is over and above the cytoplasmic level. Similar localization was also found during pheromone stimulation. Pheromone treatment did not increase the upper limit of Ste50 nuclear localization and showed consistent decrease over time. One of the reasons for lower nuclear localization could be more rapid export than import (Kim & Chen, 2000). However, the decrease of Ste50 nuclear localization upon pheromone treatment is not rapid like Ste5 (Mahanty *et al.*, 1999). The nuclear localization of Ste50 varied with the cell cycle and was found to decrease during telophase, both at the population level and in single cell analysis. Ste50-RA domain mutant specifically defective in pheromone response had impaired ability to translocate to the nucleus in the DAPI treated cells, and when quantified showed 10X less nuclear localization [Chapter III, Figure 7] indicating the requirement of the RA domain for the nuclear translocation of Ste50 protein. This mutant has a mutation in the putative NLS of the protein. Since the size of the protein precludes it from passive diffusion into the nucleus, it is possible that the protein is actively transported to the nucleus. However, loss of nuclear localization due to mutation supports a binding partner for nuclear localization that may have a critical role in pheromone signaling and could be linked to Ste50's capacity to go to the shmoo or be involved in the shmoo formation. How Ste50 is localized in the nucleus is not known but

shuttling proteins undergo modifications in the nucleus and are key factors in relaying messages between the nucleus and cytoplasm (Mahanty *et al.*, 1999, Gama-Carvalho & Carmo-Fonseca, 2001). Generally, cell cycle dependent nuclear localization of yeast proteins is CDK dependent (Kosugi *et al.*, 2009). Interestingly, the yeast pheromone signaling scaffold protein, Ste5, has also been shown to have cell cycle dependent nuclear localization (Garrenton *et al.*, 2009). Its nuclear localization is mediated by CDK1 depended phosphorylation, and in the nucleus, it is degraded by the proteosomal system. This apparently controls the level of Ste5 in the cytoplasm and prevents spurious activation of the pheromone signaling pathway.

Future studies could include Ste50 protein abundance experiments during the different cell cycle by taking samples at different time points after cell synchronization and determining expression levels. This will tell us whether nuclear localization reflects the amount of protein. Active translocation can be probed by fusing the NLS signal with GFP and measure the nuclear GFP localization. Nuclear export can be studied by blocking exit and *de novo* synthesis of Ste50. A *cdc*-mutant could be useful to allow cell synchronization. *De novo* synthesis can be blocked by cycloheximide. These could be all studied in single cells.

***RIE1* genetically interacts with Ste50 and affects pheromone signaling**

Genetic suppressor analysis with specifically-pheromone-response-defective Ste50 mutants obtained *RIE1* as a Ste50 dependent suppressor. *RIE1* deletion caused defective cell cycle arrest and no shmoo formation. *RIE1* encodes a putative RNA binding protein (Feroli *et al.*, 1997). *RIE1* was found also to genetically interact with *STE50* in a SGA assay (Costanzo *et al.*, 2016). The SGA score for *Rie1 - ste50* [SGA score = -0.2012, P-value = 2.763E-6]. If the SGA score < -0.12 and p-value < 0.05, it is considered a significant negative genetic interaction. Although *RIE1* is found to interact genetically with *STE50*, whether there is any physical interaction is not known. How *Rie1* can mediate pheromone signaling specificity can only be determined empirically. In an ideal scenario, one would expect *Rie1* to physically interact with Ste50-RA domain to bring this module near the membrane,

either directly or interacting with other signaling molecules to facilitate pheromone signaling. Rie1, although has been found to be a RNA binding protein with RNA binding motifs (Feroli *et al.*, 1997) was also found to bind other proteins (<https://string-db.org/network/4932.YGR250C>). Many of these proteins are involved in RNA translation; therefore, Rie1 may have a role in RNA translation. Localized RNA translation has been shown for Fus3 at the shmoo tip (Gelin-Licht *et al.*, 2012).

To investigate physical interactions between Rie1 and Ste50 future work includes protein-protein interaction studies with Co-IP that would provide answers. In future deletion of *RIE1* in the YCW1886 yeast background strain used for the study of the RA domain mutants would be useful to have proper morphological and phenotypic assessments. The cell cycle arrest function could also be studied in more detail by the halo assay with a *ste50* deletion strain and mutants side by side along with wild type, which would be informative. Also, a double deletion of *RIE1* and *STE50* would be useful for the microscopic analysis involving different fluorescent-tagged version of the proteins for expression and co-localization studies. Whether Rie1, a putative RNA binding protein has any function in the nuclear localization of Ste50 can be investigated by overexpression/deletion of *RIE1* and analyzing Ste50 nuclear translocation. The defective signaling pathway specific mutants of the Ste50-RA domain could be further useful for identification of additional components of the MAPK pathway defective in both pheromone and HOG signaling.

Concluding remarks

This thesis presents some novel discoveries; it encompasses research that investigated how signals retain specificity when they share a common pathway module. The specificity of signaling is certainly an important issue for understanding how signals are transduced and integrated properly to elicit a destined biological response. This fundamental inquiry is important since many pathways, such as the classical mammalian ERK MAPK pathway, are activated by numerous extracellular stimuli. Molecular signaling is at the heart of organismal function, therefore knowledge about the various mechanisms cells use to

achieve proper signaling will increase our understanding of diseases and help us to come up with solutions.

Saccharomyces cerevisiae represents an outstanding model to study this, since many of the basic principals of the MAPK pathways are conserved in more complex eukaryotes. In spite of all the discoveries made in the regulation of MAPK signaling specificity in yeast, how mating-pheromone response pathway is specifically regulated through a common MAP3K Ste11 is poorly understood. I have revealed several aspects of an adaptor protein involved in regulating the specificity of the pheromone signaling in the yeast *Saccharomyces cerevisiae*. This adaptor was known to be required for proper mating signaling - the present study finds that the localization profile of this adaptor protein acts to make sure that proper polarization happens and mating is ensured. The discovery that a distinct surface of the RA domain of the Ste50 protein is required for pheromone signal specificity is intertwined with the polarized shmoo structure formation function and positions it as an important control node for the mating MAPK signaling pathway. The dynamic role of this adaptor protein in the different yeast MAPK pathways through interacting with the different proteins could be spatiotemporal or simultaneous, and the nature of which needs to be further investigated. The implication of this study goes beyond just yeast system since RA domain is conserved and exists in all higher eukaryotes including humans.

Bibliography

- Adams JA (2001). Kinetic and catalytic mechanisms of protein kinases. *Chem Rev* 101, 2271–2290.
- Adler J (1966). Chemotaxis in bacteria. *Science* 153(3737), 708-716.
- Aguilar-Uscanga B, Francois JM (2003). A study of the yeast cell wall composition and structure in response to growth conditions and mode of cultivation. *Lett Appl Microbiol* 37, 268–274.
- Alberts B, Johnson A, Lewis J, et al. (2002). General Principles of Cell Communication. In NCBI bookshelf (ed.). *Molecular biology of the cell* (4th ed.). New York: Garland Science.
- Albertyn J, Hohmann S, Thevelein JM, Prior BA (1994). GPD1, which encodes glycerol-3-phosphate dehydrogenase, is essential for growth under osmotic stress in *Saccharomyces cerevisiae*, and its expression is regulated by the high-osmolarity glycerol response pathway. *Mol Cell Biol* 14, 4135–44.
- Alepuz PM, Jovanovic A, Reiser V, Ammerer G (2001). Stress-induced MAP kinase Hog1 is part of transcription activation complexes. *Mol Cell* 7, 767–777.
- Alexander J, Lim D, Joughin BA, Hegemann B, Hutchins JR, Ehrenberger T, ... & Fry AM (2011). Spatial exclusivity combined with positive and negative selection of phosphorylation motifs is the basis for context-dependent mitotic signaling. *Sci Signal* 4(179), ra42-ra42.

- Andersson J, Simpson DM, Qi M, Wang Y, Elion EA (2004). Differential input by Ste5 scaffold and Msg5 phosphatase route a MAPK cascade to multiple outcomes. *EMBO J* 23, 2564–2576.
- Andrade MA, O'Donoghue SI, Rost B (1998). Adaptation of protein surfaces to subcellular location. *J Mol Biol* 276, 517-525.
- Annan RB, Wu C, Waller DD, Whiteway M, Thomas DY (2008). Rho5p is involved in mediating the osmotic stress response in *Saccharomyces cerevisiae*, and its activity is regulated via Msi1p and Npr1p by phosphorylation and ubiquitination. *Eukaryot Cell* 7(9), 1441-1449.
- Arancibia SA, Beltrán CJ, Aguirre IM, Silva P, Peralta AL, Malinarich F, Hermoso MA (2007). Toll-like receptors are key participants in innate immune responses. *Biol Res* 40 (2), 97–112.
- Bao MZ, Schwartz MA, Cantin GT, Yates JR, Madhani HD (2004). Pheromone dependent destruction of the Tec1 transcription factor is required for MAP kinase signaling specificity in yeast. *Cell* 119, 991–1000.
- Bardwell L (2006). Mechanisms of MAPK signalling specificity. *Biochem Soc Trans* 34(Pt 5), 837-841.
- Behar M, Dohlman HG, Elston TC (2007). Kinetic insulation as an effective mechanism for achieving pathway specificity in intracellular signaling networks. *Proc Nat Acad Sci* 104(41), 16146-16151.
- Bhaduri S & Pryciak PM (2011). Cyclin-specific docking motifs promote phosphorylation of yeast signaling proteins by G1/S Cdk complexes. *Curr Biol* 21, 1615–1623.

- Bhattacharjya S, Xu P, Gingras R, Shaykhutdinov R, Wu C, Whiteway M, Ni F (2004). Solution structure of the dimeric SAM domain of MAPKKK Ste11 and its interactions with the adaptor protein Ste50 from the budding yeast: Implications for Ste11 activation and signal transmission through the Ste50–Ste11 complex. *J Mol Biol* 344(4), 1071-1087.
- Bhattacharya M, Pieter HA, Babwah AV, Dale LB, Dobransky T, Benovic JL, Feldman RD, Verdi JM, Rylett RJ, Ferguson SSG (2002). β -Arrestins regulate a Ral-GDS–Ral effector pathway that mediates cytoskeletal reorganization. *Nat Cell Biol* 4(8), 547.
- Bhattacharyya RP, Reményi A, Good MC, Bashor CJ, Falick AM, Lim WA (2006). The Ste5 scaffold allosterically modulates signaling output of the yeast mating pathway. *Science* 311(5762), 822-826.
- Bhattacharyya RP, Remenyi A, Yeh BJ, Lim WA (2006). Domains, motifs, and scaffolds: the role of modular interactions in the evolution and wiring of cell signaling circuits. *Annu Rev Biochem* 75, 655–680.
- Bi E & Park HO (2012). Cell polarization and cytokinesis in budding yeast. *Genetics* 191, 347–387.
- Bidlingmaier S & Snyder M (2004). Regulation of polarized growth initiation and termination cycles by the polarisome and Cdc42 regulators. *J Cell Biol* 164, 207–218.
- Bilsland-Marchesan E, Arino J, Saito H, Sunnerhagen P, Posas F (2000). Rck2 kinase is a substrate for the osmotic stress-activated mitogen-activated protein kinase Hog1. *Mol Cell Biol* 20, 3887–3895.
- Biondi RM & Nebreda AR (2003). Signalling specificity of Ser/Thr protein kinases through docking-site-mediated interactions. *Biochem J* 372, 1–13.

- Blackwell E, Halatek IM, Kim HJ N, Ellicott AT, Obukhov AA, Stone DE (2003). Effect of the pheromone-responsive G α and phosphatase proteins of *Saccharomyces cerevisiae* on the subcellular localization of the Fus3 mitogen-activated protein kinase. *Mol Cell Biol* 23(4), 1135-1150.
- Blackwell E, Kim HJN, Stone DE (2007). The pheromone-induced nuclear accumulation of the Fus3 MAPK in yeast depends on its phosphorylation state and on Dig1 and Dig2. *BMC Cell Biol* 8(1), 44.
- Blomberg A & Adler L (1998). Roles of glycerol and glycerol-3-phosphate dehydrogenase (NAD⁺) in acquired osmotolerance of *Saccharomyces cerevisiae*. *J Bacteriol* 171(2), 1087-92. PMID: 2644223.
- Bohm SK, Grady EF, Bunnett NW (1997). Regulatory mechanisms that modulate signalling by G-protein-coupled receptors. *Biochem J* 322(Pt 1), 1-18.
- Borhan B, Souto ML, Imai H, Shichida Y, Nakani-shi K (2000). Movement of retinal along the visual trans-duction path. *Science* 288, 2209-2212.
- Botstein D, Chervitz SA, Cherry M (1997). Yeast as a model organism. *Science* 277 (5330), 1259-1260.
- Botstein D & Fink GR (2011). Yeast: an experimental organism for 21st century biology. *Genetics* 189, 695-704.
- Boyd CT, Hughes MP, Novick P (2004). Vesicles carry most exocyst subunits to exocytic sites marked by the remaining two subunits, Sec3p and Exo70p. *J Cell Biol* 167, 889-901.

- Brewster JL, de Valoir T, Dwyer ND, Winter E, Gustin MC (1993). An osmosensing signal transduction pathway in yeast. *Science* 259, 1760–1763.
- Brown AJ, Dyos SL, Whiteway MS, White JHM, Watson MAEA, Marzioch M, Clare JJ, Cousens DJ, Paddon C, Plumpton C, Romanos MA, Dowell SJ (2000). Functional coupling of mammalian receptors to the yeast mating pathway using novel yeast/mammalian G protein α -subunit chimeras. *Yeast* 16, 11– 22.
- Brunner D, Oellers N, Szabad J, Biggs III WH, Zipursky SL, Hafen E (1994). A gain-of-function mutation in *Drosophila* MAP kinase activates multiple receptor tyrosine kinase signaling pathways. *Cell* 76(5), 875-888.
- Butty AC, Pryciak PM, Huang LS, Herskowitz I, Peter M (1998). The role of Far1p in linking the heterotrimeric G protein to polarity establishment proteins during yeast mating. *Science* 282(5393), 1511-1516.
- Byers B & Goetsch L (1975). Behaviors of spindles and spindle plaques in the cell cycle and conjugation in *Saccharomyces cerevisiae*. *J Bacteriol* 124, 5 1 1-23.
- Cairns BR, Ramer SW, Kornberg RD (1992). Order of action of components in the yeast pheromone response pathway revealed with a dominant allele of the STE11 kinase and the multiple phosphorylation of the STE7 kinase. *Gen Dev* 6(7), 1305-1318.
- Carpenter G (1983). The biochemistry and physiology of the receptor-kinase for epidermal growth factor. *Mol Cell Endo* 31(1), 1-19.
- Chang F & Herskowitz I (1990). Identification of a gene necessary for cell cycle arrest by a negative growth factor of yeast: FAR1 is an inhibitor of a G1 cyclin, CLN2. *Cell* 63(5), 999-1011.

- Chen M, Chory J, Fankhauser C (2004). Light signal transduction in higher plants. *Annu Rev Genet* 38, 87-117.
- Chen RE & Thorner J (2007). Function and regulation in MAPK signaling pathways: lessons learned from the yeast *Saccharomyces cerevisiae*. *Biochimica et Biophysica Acta (BBA)-Mol Cell Res* 1773(8), 1311-1340.
- Choi KY, Satterberg B, Lyons DM, Elion EA (1994). Ste5 tethers multiple protein kinases in the MAP kinase cascade required for mating in *S. cerevisiae*. *Cell* 78, 499-512.
- Conklin BR & Bourne HR (1993). Structural elements of G[alpha] subunits that interact with G[beta][gamma], receptors, and effectors. *Cell* 73(4), 631-641.
- Cook A, Bono F, Jinek M, Conti E (2007). Structural biology of nucleocytoplasmic transport. *Annu Rev Biochem* 76, 647-671.
- Cook JG, Bardwell L, Kron SJ, Thorner J (1996). Two novel targets of the MAP kinase Kss1 are negative regulators of invasive growth in the yeast *Saccharomyces cerevisiae*. *Gen Dev* 10, 2831-2848.
- Cooper JA & Hunter T (1981). Changes in protein phosphorylation in Rous sarcoma virus-transformed chicken embryo cells. *Mol Cell Biol* 1, 165-178.
- Costanzo M, Nishikawa JL, Tang X, Millman JS, Schub O, Breitkreuz K, ... & Tyers M (2004). CDK activity antagonizes Whi5, an inhibitor of G1/S transcription in yeast. *Cell* 117, 899-913.
- Cowburn D (December 1997). Peptide recognition by PTB and PDZ domains. *Curr Opin Struct Biol* 7 (6), 835-838.

- Cross F, Hartwell LH, Jackson C, Konopka JB (1988). Conjugation in *Saccharomyces cerevisiae*. *Annu Rev Cell Biol* 4, 429-457.
- Cross FR (1988). DAFI, a mutant gene affecting size control, pheromone arrest, and cell cycle kinetics of *Saccharomyces cerevisiae*. *Mol Cell Biol* 8, 4675-4684.
- Cuatrecasas P (1974). Membrane receptors. *Ann Rev Biochem* 43, 169-214.
- Cullen PJ & Sprague GF Jr (2002). The roles of bud-site selection proteins during haploid invasive growth in yeast. *Mol Biol Cell* 13, 2990-3004.
- Cullen PJ, Sabbagh W, Graham E, Irick MM, van Olden EK, Neal C, ... & Sprague GF (2004). A signaling mucin at the head of the Cdc42- and MAPK-dependent filamentous growth pathway in yeast. *Genes Dev* 18(14), 1695-1708.
- Cullen PJ & Sprague GF (2012). The regulation of filamentous growth in yeast. *Genetics* 190(1), 23-49.
- Dan I, Watanabe NM, Kusumi A (2001). The Ste20 group kinases as regulators of MAP kinase cascades. *Trends Cell Biol* 11(5), 220-230.
- De Felice FG, & Ferreira ST (2014). Inflammation, defective insulin signaling, and mitochondrial dysfunction as common molecular denominators connecting type 2 diabetes to Alzheimer disease. *Diabetes* 63(7), 2262-2272.
- de Nadal E, Alepuz PM, Posas F (2002) Dealing with osmotic stress through MAP kinase activation. *EMBO Rep* 3, 735-740.
- de Nadal E, Real FX, Posas F (2007). Mucins, osmosensors in eukaryotic cells? *Trends Cell Biol* 17, 571-574.

- Dietzel C & Kurjan J (1987). The yeast SCG1 gene: a G α -like protein implicated in the a- and α -factor response pathway. *Cell* 50(7), 1001-1010.
- Dohlman HG & Thorner J (1997). RGS Proteins and Signaling by Heterotrimeric G Proteins. *J Biol Chem* 272(7), 3871-3874.
- Dohlman HG & Thorner JW (2001). Regulation of G protein-initiated signal transduction in yeast: paradigms and principles. *Annu Rev Biochem* 70, 703–754.
- Douzery EJ, Snell EA, Baptiste E, Delsuc F, Philippe H (2004). The timing of eukaryotic evolution: does a relaxed molecular clock reconcile proteins and fossils? *Proc Natl Acad Sci U S A* Oct 26; 101(43), 15386-15391.
- Doye V & Hurt E (1997). From nucleoporins to nuclear pore complexes. *Curr Opin Cell Biol* 9, 401–411.
- Dyer JM, Savage NS, Jin M, Zyla TR, Elston TC, Lew DJ (2013). Tracking shallow chemical gradients by actin-driven wandering of the polarization site. *Curr Biol* 23(1), 32-41.
- Ebisuya M, Kondoh K, Nishida E (2005). The duration, magnitude and compartmentalization of ERK MAP kinase activity: mechanisms for providing signaling specificity. *J Cell Sci* 118(14), 2997-3002.
- Edgington NP & Futcher B (2001). Relationship between the function and the location of G1 cyclins in *S. cerevisiae*. *J Cell Sci* 114, 4599–4611.
- Ekiel I, Sulea T, Jansen G, Kowalik M, Minailiuc O, Cheng J, Harcus D, Cygler M, Whiteway M, Wu C (2009). Binding the atypical RA domain of Ste50p to the unfolded Opy2p cytoplasmic tail is essential for the highosmolarity glycerol pathway. *Mol Biol Cell* 20, 5117–5126.

- Elion EA, Satterberg B, Kranz JE (1993). FUS3 phosphorylates multiple components of the mating signal transduction cascade: evidence for STE12 and FAR1. *Mol Biol Cell* 4, 495–510.
- Elion EA (1995). Ste5: a meeting place for MAP kinases and their associates. *Trends in cell biology*, 5(8), 322-327.
- Elion EA (2001). The Ste5p scaffold. *J Cell Sci* 114, 3967–33978.
- Elliott SG (1983). The yeast cell cycle: coordination of growth and division rates. In *Prog Nucleic Acid Res Mol Biol* 28, 143-176.
- Erdman S & Snyder M (2001). A filamentous growth response mediated by the yeast mating pathway. *Genetics* 159(3), 919-928.
- Errede B, Gartner A, Zhou Z, Nasmyth K, Ammerer G (1993). MAP kinase-related FUS3 from *S. cerevisiae* is activated by STE7 in vitro. *Nature* 362(6417), 261.
- Evangelista M, Blundell K, Longtine MS, Chow CJ, Adames N, Pringle JR, Peter M, Boone C (1997). Bni1p, a yeast formin linking cdc42p and the actin cytoskeleton during polarized morphogenesis. *Science* 276, 118–122.
- Fairweather I (2004). Cell signalling in prokaryotes and lower metazoa, School of Biology and Biochemistry The Queen's University of Belfast Belfast, Northern Ireland.
- Faux MC & Scott JD (1996a). More on target with protein phosphorylation: conferring specificity by location. *Trends Biochem Sci* 21, 312–315.
- Faux MC & Scott JD (1996b). Molecular Glue: Kinase Anchoring and Scaffold Proteins. *Cell* 85 (1), 9–12.

- Feng Y, Song LY, Kincaid E, Mahanty SK, Elion EA (1998). Functional binding between Gbeta and the LIM domain of Ste5 is required to activate the MEKK Ste11. *Curr Biol* 8, 267–278.
- Ferreira C, van Voorst F, Martins A, Neves L, Oliveira R, Kielland-Brandt MC, et al. (2005). A member of the sugar transporter family, Stl1p is the glycerol/H⁺ symporter in *Saccharomyces cerevisiae*. *Mol Biol Cell* 16(4), 2068–76.
- Feroli F, Carignan I G, Pavanello A, Guerreiro P, Azevedo D, Rodrigues-Pousada C, Melchiorretto P, Panzeri L, Carbone MLA (1997). Analysis of a 17.9 kb region from *Saccharomyces cerevisiae* chromosome VII reveals the presence of eight open reading frames, including BRF1 (TFIIIB70) and GCN5 genes. *Yeast* 13(4), 373-7.
- Ferrigno P, Posas F, Koepp D, Saito H, Silver PA (1998). Regulated nucleo/cytoplasmic exchange of HOG1 MAPK requires the importin beta homologs NMD5 and XPO1. *EMBO J* 17, 5606–5614.
- Flatauer LJ, Zadeh SF, Bardwell L (2005). Mitogen-activated protein kinases with distinct requirements for Ste5 scaffolding influence signaling specificity in *Saccharomyces cerevisiae*. *Mol Cell Biol* 25(5), 1793-1803.
- Fields S (1990). Phermone response in yeast. *Trends Biochem Sci* 15(7), 270-273.
- Ford CE, Skiba NP, Bae H, Daaka Y, Reuveny E, Shekter LR, Rosal R, et al. (1998). Molecular basis for interactions of G protein $\beta\gamma$ subunits with effectors. *Science* 280(5367), 1271-1274.
- Frumkes TE, Sekuler MD, Reiss EH (1972). Rod-cone interaction in human scotopic vision. *Sci* 175(4024), 913-914.

- Furukawa K, Hoshi Y, Maeda T, Nakajima T, Abe K (2005). *Aspergillus nidulans* HOG pathway is activated only by two-component signaling pathway in response to osmotic stress. *Mol Microbiol* 56, 1246–1261.
- Gama-Carvalho M, & Carmo-Fonseca M (2001). The rules and roles of nucleocytoplasmic shuttling proteins. *FEBS letters* 498(2-3), 157-163.
- Gao L & Bretscher A (2009). Polarized growth in budding yeast in the absence of a localized formin. *Mol Biol Cell* 20, 2540– 2548.
- Garrenton LS, Young SL, Thorner J (2006). Function of the MAPK scaffold protein Ste5 requires a cryptic PH domain. *Genes Dev* 20, 1946–1958.
- Garrenton LS, Braunwarth A, Irniger S, Hurt E, Künzler M, Thorner J (2009). Nucleus-specific and cell cycle-regulated degradation of mitogen-activated protein kinase scaffold protein Ste5 contributes to the control of signaling competence. *Mol Cell Biol* 29(2), 582-601.
- Gartner A, Nasmyth K, Ammerer G (1992). Signal transduction in *Saccharomyces cerevisiae* requires tyrosine and threonine phosphorylation of FUS3 and KSS1. *Gen Dev* 6(7), 1280-1292.
- Gelin-Licht R, Paliwal S, Conlon P, Levchenko A, Gerst JE (2012). Scp160-dependent mRNA trafficking mediates pheromone gradient sensing and chemotropism in yeast. *Cell Rep* 1(5), 483-494.
- Gillespie PG & Walker RG (2001). Molecular basis of mechanosensory transduction. *Nature* 413 (6852), 194–202.

- Gimeno CJ, Ljungdahl PO, Styles CA, Fink GR (1992). Unipolar cell divisions in the yeast *S. cerevisiae* lead to filamentous growth: regulation by starvation and RAS. *Cell* 68, 1077–1090.
- Goldsmith EJ, Akella R, Min X, Zhou T, Humphreys JM (2007). Substrate and Docking Interactions in Serine/threonine Protein Kinases. *Chem Rev* 107 (11), 5065–81.
- Good M, Tang G, Singleton J, Reményi A, Lim WA (2009). The Ste5 scaffold directs mating signaling by catalytically unlocking the Fus3 MAP kinase for activation. *Cell* 136(6), 1085-1097.
- Gorlich D & Mattaj IW (1996). Nucleocytoplasmic transport. *Science* 271, 1513-1518.
- Gotoh N (2008). Regulation of growth factor signaling by FRS2 family docking/scaffold adaptor proteins. *Cancer Sci* 99, 1319-1325.
- Grimshaw SJ, Mott HR, Stott KM, Nielsen PR, Evetts KA, Hopkins LJ, Nietlispach D, Owen D (2004). Structure of the sterile α motif (SAM) domain of the *Saccharomyces cerevisiae* mitogen-activated protein kinase pathway-modulating protein Ste50 and analysis of its interaction with the Ste11 SAM. *J Biol Chem* 279(3), 2192-2201.
- Guo W, Roth D, Walch-Solimena C and Novick P (1999). The exocyst is an effector for Sec4p, targeting secretory vesicles to sites of exocytosis. *EMBO J* 18, 1071–1080.
- Gustin MC, Albertyn J, Alexander M, Davenport K (1998). MAP Kinase Pathways in the Yeast *Saccharomyces cerevisiae*. *Microbiol Mol Biol Rev* 62, 1264-1300.
- Haber JE (2012). Mating-type genes and MAT switching in *Saccharomyces cerevisiae*. *Genetics* 191, 33–64.

- Hadwiger JA, Wittenberg C, Richardson HE, de Barros-Lopes M, Reed SI (1989). A novel family of cyclin homologs that control G1 in yeast. *Proc Natl Acad Sci USA* 86, 6255–6259.
- Hall JP, Cherkasova V, Elion E, Gustin MC, Winter E (1996). The osmoregulatory pathway represses mating pathway activity in *Saccharomyces cerevisiae*: isolation of a FUS3 mutant that is insensitive to the repression mechanism. *Mol Cell Biol* 16, 6715–6723.
- Han CW, Jeong MS, Jang SB (2017). Structure, signaling and the drug discovery of the Ras oncogene protein. *BMB reports* 50(7), 355-360.
- Han J, Lee JD, Bibbs L, Ulevitch RJ (1994). A MAP kinase targeted by endotoxin and hyperosmolarity in mammalian cells. *Science* 265(5173), 808-811.
- Hao N, Zeng Y, Elston TC, Dohlman HG (2008). Control of MAPK specificity by feedback phosphorylation of shared adaptor protein Ste50. *J Biol Chem* 283(49), 33798-33802.
- Harjes E, Harjes S, Wohlgemuth S, Muller KH, Krieger E, Herrmann C, Bayer P (2006). GTP-Ras disrupts the intramolecular complex of C1 and RA domains of Nore1. *Struct* 14, 881–888.
- Harrison R & DeLisi C (2002). Condition specific transcription factor binding site characterization in *Saccharomyces cerevisiae*. *Bioinformatics* 18, 1289–1296.
- Hartwell LH, Culotti J, Pringle JR, Reid BJ (1974). Genetic control of cell division cycle in yeast. *Science* 183, 46–51.

- Hartwell LH (1980). Mutants of *Saccharomyces cerevisiae* unresponsive to cell division control by polypeptide mating hormone. *J Cell Biol* 85, 811–822.
- Henchoz S, Chi Y, Catarin B, Herskowitz I, Deshaies RJ, Peter M (1997). Phosphorylation- and ubiquitin-dependent degradation of the cyclin-dependent kinase inhibitor Far1p in budding yeast. *Gen Dev* 11(22), 3046-3060.
- Henderson, NT, Clark-Cotton MR, Zyla TR, Lew DJ (2018). How yeast cells find their mates. *BioRxiv* (2018): 422790.
- Hersen P, McClean MN, Mahadevan L, Ramanathan S (2008). Signal processing by the HOG MAP kinase pathway. *Proc Nat Acad Sci* 105(20), 7165-7170.
- Hohmann S (2002). Osmotic stress signaling and osmoadaptation in yeasts. *Microbiol Mol Biol Rev* 66, 300–372.
- Hohmann S (2009). Control of high osmolarity signaling in the yeast *Saccharomyces cerevisiae*. *FEBS Lett* 583, 4025-4029.
- Horn F, Weare J, Beukers MW, Horsch S, Bairoch A, Chen W, Edvardsen O, Campagne F, Vriend G (1998). GPCRDB: an information system for G protein-coupled receptor. *Nucleic Acids Res* 26, 275–279.
- Huang LS, Doherty HK, Herskowitz I (2005). The Smk1p MAP kinase negatively regulates Gsc2p, a 1,3-beta-glucan synthase, during spore wall morphogenesis in *Saccharomyces cerevisiae*. *Proc Natl Acad Sci U S A* 102(35), 12431-12436.
- Hunter T & Plowman GD (1997). The protein kinases of budding yeast: six score and more. *Trends Biochem Sci* 22(1), 18-22.

- Inouye C, Dhillon N, Thorner J (1997). Ste5 RING-H2 domain: role in Ste4-promoted oligomerization for yeast pheromone signaling. *Science* 278, 103–106.
- Jackson CL & Hartwell LH (1990a). Courtship in *S. cerevisiae*: both cell types choose mating partners by responding to the strongest pheromone signal. *Cell* 63(5), 1039-1051.
- Jackson CL & Hartwell LH (1990b). Courtship in *Saccharomyces cerevisiae*: an early cell-cell interaction during mating. *Mol Cell Biol* 10(5), 2202-2213.
- Jacoby T, Flanagan H, Faykin A, Seto AG, Mattison C, Ota I (1997). Two protein-tyrosine phosphatases inactivate the osmotic stress response pathway in yeast by targeting the mitogen-activated protein kinase, Hog1. *J Biol Chem* 272, 17749–17755.
- Jakob CA, Burda P, Roth J, Aebi M (1998). Degradation of misfolded endoplasmic reticulum glycoproteins in *Saccharomyces cerevisiae* is determined by a specific oligosaccharide structure. *J Cell Biol* 142, 1223-1233.
- Jans DA (1995). The regulation of protein transport to the nucleus by phosphorylation. *Biochem J* 311(Pt 3), 705-716.
- Jansen G, Bühring F, Hollenberg CP, Rad MR (2001). Mutations in the SAM domain of STE50 differentially influence the MAPK-mediated pathways for mating, filamentous growth and osmotolerance in *Saccharomyces cerevisiae*. *Mol Genet Gen* 265(1), 102-117.
- Kachroo AH, Laurent JM, Yellman CM, Meyer AG, Wilke CO, Marcotte EM (2015). Systematic humanization of yeast genes reveals conserved functions and genetic modularity. *Science* 348(6237), 921-925.

- Kang YS, Kane J, Kurjan J, Stadel JM, Tipper DJ (1990). Effects of expression of mammalian G alpha and hybrid mammalian-yeast G alpha proteins on the yeast pheromone response signal transduction pathway. *Mol Cell Biol*, 10(6), 2582-2590.
- Kataoka T, Powers S, Cameron S, Fasano O, Goldfarb M, Broach J, Wigler M (1985). Functional homology of mammalian and yeast RAS genes. *Cell* 40(1), 19-26.
- Kiel C & Serrano L (2006). The ubiquitin domain superfold: structurebased sequence alignments and characterization of binding epitopes. *J Mol Biol* 355, 821-844.
- Kim JE & Chen J (2000). Cytoplasmic-nuclear shuttling of FKBP12-rapamycin-associated protein is involved in rapamycin-sensitive signaling and translation initiation. *Proc Nat Acad Sci* 97(26), 14340-14345.
- Kleene SJ (2008). The electrochemical basis of odor transduction in vertebrate olfactory cilia. *Chem Senses* 33, 839-859.
- Kleerebezem M, Quadri LE, Kuipers OP, De Vos WM (1997). Quorum sensing by peptide pheromones and two-component signal-transduction systems in Gram-positive bacteria. *Mol Microbiol* 24(5), 895-904.
- Klein S, Reuveni H, Levitzki A (2000). Signal transduction by a nondissociable heterotrimeric yeast G protein. *Proc Natl Acad Sci USA* 97, 3219-3223.
- Klipp E, Nordlander B, Kruger R, Gennemark P, Hohmann S (2005). Integrative model of the response of yeast to osmotic shock. *Nat Biotechnol* 23, 975-982.
- Koivomagi M, Valk E, Venta R, Iofik A, Lepiku M, Morgan DO, Loog M (2011). Dynamics of Cdk1 Substrate Specificity during the Cell Cycle. *Mol Cell* 42, 610-623.

- Kosugi S, Hasebe M, Tomita M, Yanagawa H (2009). Systematic identification of cell cycle-dependent yeast nucleocytoplasmic shuttling proteins by prediction of composite motifs. *Proc Nat Acad Sci* 106(25), 10171-10176.
- Kozubowski L, Saito K, Johnson JM, Howell AS, Zyla TR, Lew DJ (2008). Symmetry-breaking polarization driven by a Cdc42p GEF-PAK complex. *Curr Biol* 18, 1719–1726.
- Krisak L, Strich R, Winters RS, Hall JP, Mallory MJ, Kreitzer D, Winter E (1994). SMK1, a developmentally regulated MAP kinase, is required for spore wall assembly in *Saccharomyces cerevisiae*. *Gen Dev* 8(18), 2151-2161.
- Krugmann S, Anderson KE, Ridley SH, Risso N, McGregor A, Coadwell J, ...& Maniava M (2002). Identification of ARAP3, a novel PI3K effector regulating both Arf and Rho GTPases, by selective capture on phosphoinositide affinity matrices. *Mol Cell* 9(1), 95-108.
- Krugmann S, Williams R, Stephens L, Hawkins PT (2004). ARAP3 is a PI3K- and rapamycin-regulated GAP for RhoA. *Curr Biol* 14(15), 1380-1384.
- Kumar A, Agarwal S, Heyman JA, Matson S, Heidtman M, Piccirillo S, ... & Cheung KH (2002). Subcellular localization of the yeast proteome. *Gen Dev* 16(6), 707-719.
- Kunzler M & Hurt E (2001). Targeting of Ran: variation on a common theme? *J Cell Sci* 114, 3233–3241.
- Kwan JJ, Warner N, Pawson T, Donaldson LW (2004). The solution structure of the *S. cerevisiae* Ste11 MAPKKK SAM domain and its partnership with Ste50. *J Mol Biol* 342(2), 681-693.

- Kwan JJ, Warner N, Maini J, Chan Tung KW, Zakaria H, Pawson T, Donaldson L (2006). *Saccharomyces cerevisiae* Ste50 binds the MAPKKK Ste11 through a head-to-tail SAM domain interaction. *J Mol Biol* 356, 142–154.
- la Cour T, Kiemer L, Mølgaard A, Gupta R, Skriver K, Brunak S (June 2004). Analysis and prediction of leucine-rich nuclear export signals. *Protein Eng Des Sel* 17 (6), 527–536.
- Lai S, Winkler DF, Zhang H, Pelech S (2016). Determination of the substrate specificity of protein kinases with peptide micro- and macroarrays. In *Kinase Screening and Profiling* (pp. 183-202). Humana Press, New York, NY.
- Lambrechts MG, Bauer FF, Marmur J, Pretorius IS (1996). Muc1, a mucin-like protein that is regulated by Mss10, is critical for pseudohyphal differentiation in yeast. *Proc Natl Acad Sci USA* 93, 8419–8424.
- Lan KL, Zhong H, Nanamor M, Neubig RR (2000). Rapid Kinetics of Regulator of G-protein Signaling (RGS)-mediated G α i and G α o Deactivation. *J Biol Chem* 275(43), 33497-33503.
- Leberer E, Dignard D, Thomas DY, Leeuw T (2000). A conserved G binding (GBB) sequence motif in Ste20p/PAK family protein kinases. *Biol Chem* 381, 427–431.
- Lee J, Reiter W, Dohnal I, Gregori C, Beese-Sims S, Kuchler K, Ammerer G, Levin DE (2013). MAPK Hog1 closes the *S. cerevisiae* glycerol channel Fps1 by phosphorylating and displacing its positive regulators. *Genes Dev* 27, 2590–601.
- Leeuw T, Fourest-Lieuvin A, Wu C, Chenevert J, Clark K, Whiteway M, Thomas DY, Leberer E (1995). Pheromone response in yeast: association of Bem1p with proteins of the MAP kinase cascade and actin. *Science* 270, 1210–1213.

- Leivar P, Monte E, Oka Y, Liu T, Carle C, Castillon A, ...& Quail PH (2008). Multiple phytochrome-interacting bHLH transcription factors repress premature seedling photomorphogenesis in darkness. *Curr Biol* 18(23), 1815-1823.
- Letunic I, Doerks T, Bork P (2009). SMART6, recent updates and new developments. *Nucleic Acids Res* 37, D229–D232.
- Levin DE (2011). Regulation of cell wall biogenesis in *Saccharomyces cerevisiae*: The cell wall integrity signaling pathway. *Genetics* 189, 1145–1175.
- Liu CC, Tsai CW, Deak F, Rogers J, Penuliar M, Sung YM, ... & Estus S (2014). Deficiency in LRP6-mediated Wnt signaling contributes to synaptic abnormalities and amyloid pathology in Alzheimer's disease. *Neuron* 84(1), 63-77.
- Liu D & Novick P (2014). Bem1p contributes to secretory pathway polarization through a direct interaction with Exo70p. *J Cell Biol* 207, 59-72.
- Lo WS & Dranginis AM (1998). The cell surface flocculin Flo11 is required for pseudohyphae formation and invasion by *Saccharomyces cerevisiae*. *Mol Biol Cell* 9, 161–171.
- Lord KA, Hoffman-Liebermann B, Liebermann DA (1990). Nucleotide sequence and expression of a cDNA encoding MyD88, a novel myeloid differentiation primary response gene induced by IL6. *Oncogene* 5 (7), 1095–7.
- Lowenstein EJ, Daly RJ, Batzer AG, Li W, Margolis B, Lammers R, Ullrich A, Skolnik EY, Bar-Sagi D, Schlessinger J (1992). The SH2 and SH3 domain-containing protein GRB2 links receptor tyrosine kinases to ras signaling. *Cell* 70 (3), 431–42.

- Mackay V & Manney TR (1974). Mutations affecting sexual conjugation and related processes in *Saccharomyces cerevisiae*. I. Isolation and phenotypic characterization of nonmating mutants. *Genetics* 76, 255–271.
- MacKay VL (1993). a's, α 's and shmoos: mating pheromones and genetics. In: Hall, MN; Linder, P., editors. *The Early Days of Yeast Genetics*. Plainview (NJ): Cold Spring Harbor Laboratory Press; p. 273-290.
- Maco B, Fahrenkrog B, Huang NP, Aebi U (2006). Nuclear pore complex structure and plasticity revealed by electron and atomic force microscopy. In *Xenopus Protocols* pp. 273-288. Humana Press.
- Madden K & Snyder M (1992). Specification of sites for polarized growth in *Saccharomyces cerevisiae* and the influence of external factors on site selection. *Mol Biol Cell* 3(9), 1025-1035.
- Madhani HD, Styles CA, Fink GR (1997a). MAP kinases with distinct inhibitory functions impart signaling specificity during yeast differentiation. *Cell* 91, 673–684.
- Madhani HD & Fink GR (1997b). Combinatorial control required for the specificity of yeast MAPK signaling. *Science* 275(5304), 1314–1317.
- Madhani HD & Fink GR (1998). The riddle of MAP kinase signaling specificity. *Trends Genet* 14(4), 151-155.
- Maeda T, Wurgler-Murphy SM, Saito H (1994). A two-component system that regulates an osmosensing MAP kinase cascade in yeast. *Nature* 369, 242–245.
- Maeda T, Takekawa M, Saito H (1995). Activation of yeast PBS2 MAPKK by MAPKKKs or by binding of an SH3-containing osmosensor. *Science* 269, 554–558.

- Mager WH & Siderius M (2002). Novel insights into the osmotic stress response of yeast. *FEMS Yeast Res* 2(3), 251-257.
- Mahanty SK, Wang Y, Farley FW, Elion EA (1999). Nuclear shuttling of yeast scaffold Ste5 is required for its recruitment to the plasma membrane and activation of the mating MAPK cascade. *Cell* 98(4), 501-512.
- Mainwaring WIP (1976). Steroid hormone receptors: a survey. *Vitamin Hormon Vol.* 33, pp. 223-245. Academic Press.
- Marcus S, Polverino A, Barr M, Wigler M (1994). Complexes between STE5 and components of the pheromone-responsive mitogen-activated protein kinase module. *Proc Natl Acad Sci USA* 91, 7762-7766.
- Marshall CJ (1995). Specificity of receptor tyrosine kinase signaling: transient versus sustained extracellular signal-regulated kinase activation. *Cell* 80(2), 179-185.
- Mashima T & Tsuruo T (2005). Defects of the apoptotic pathway as therapeutic target against cancer. *Drug Resist Updates*, 8(6), 339-343.
- Mas G, Nadal ED, Dechant R, Concepcion MLR, Logie C, Jimeno-Gonzalez S, Chavez S et al. (2009). Recruitment of a chromatin remodelling complex by the Hog1 MAP kinase to stress genes. *EMBO J* 28, 326-336.
- Masuda K, Shima H, Katagiri C, Kikuchi K (2003). Activation of ERK induces phosphorylation of MAPK phosphatase-7, a JNK specific phosphatase, at Ser- 446. *J Biol Chem*, 278(34), 32448-32456.

- Matheos D, Metodiev M, Muller E, Stone D, Rose MD (2004). Pheromone-induced polarization is dependent on the Fus3p MAPK acting through the formin Bni1p. *J Cell Biol* 165, 99–109.
- Mattaj IW & Englmeier L (1998). Nucleocytoplasmic transport: the soluble phase. *Annu Rev Biochem* 67 (1), 265–306.
- Mattison CP & Ota IM (2000). Two protein tyrosine phosphatases, Ptp2 and Ptp3, modulate the subcellular localization of the Hog1 MAP kinase in yeast. *Genes Dev* 14, 1229–1235.
- McClellan MN, Mody A, Broach JR, Ramanathan S (2007). Cross-talk and decision making in MAP kinase pathways. *Nat genet* 39(3), 409-414.
- Meacock SL, Lecomte FJ, Crawshaw SG, High S (2002). Different transmembrane domains associate with distinct endoplasmic reticulum components during membrane integration of a polytopic protein. *Mol Biol Cell* 13, 4114-4129.
- Melchior F, Paschal B, Evans J, Gerace L (1993). Inhibition of nuclear protein import by nonhydrolyzable analogues of GTP and identification of the small GTPase Ran/TC4 as an essential transport factor. *J Cell Biol* 123, 1649–1659.
- Metodiev MV, Matheos D, Rose MD, Stone DE (2002). Regulation of MAPK function by direct interaction with the mating-specific G α in yeast. *Science*, 296(5572), 1483-1486.
- Michael J, Osborn J, Ross Miller (2007). Rescuing yeast mutants with human genes. *Brief Funct Genomics*, Volume 6, Issue 2, June 2007, Pages 104–111.

- Miller CJ & Turk BE (2018). Homing in: mechanisms of substrate targeting by protein kinases. *Trends Biochem Sci* 43(5), 380-394.
- Moore MS & Blobel G (1993). The GTP-binding protein Ran/TC4 is required for protein import into the nucleus. *Nature* 365, 661–663.
- Morrison DK, Kaplan DR, Rapp U, Roberts TM (1988). Signal transduction from membrane to cytoplasm: growth factors and membrane-bound oncogene products increase Raf-1 phosphorylation and associated protein kinase activity. *Proc Natl Acad Sci USA* 85, 8855-8859.
- Nakada R, Hirano H, Matsuura Y (2015). Structure of importin- α bound to a non-classical nuclear localization signal of the influenza A virus nucleoprotein. *Sci Rep* 5, 15055.
- Nakafuku M, Obara T, Kaibuchi K, Miyajima I, Miyajima A, Itoh H, ... & Kaziro Y (1988). Isolation of a second yeast *Saccharomyces cerevisiae* gene (GPA2) coding for guanine nucleotide-binding regulatory protein: studies on its structure and possible functions. *Proc Nat Acad Sci* 85(5), 1374-1378.
- Nakayama N, Miyajima A, Arai K (1985). Nucleotide sequences of STE2 and STE3, cell type-specific sterile genes from *Saccharomyces cerevisiae*. *EMBO J* 4, 2643–2648.
- Nakayama N, Kaziro Y, Arai KL, Matsumoto K (1988). Role of STE genes in the mating factor signaling pathway mediated by GPA1 in *Saccharomyces cerevisiae*. *Mol Cell Biol* 8(9), 3777-3783.
- Narayanaswamy R, Moradi EK, Niu W, Hart GT, Davis M, McGary KL., ... & Marcotte EM (2008). Systematic definition of protein constituents along the major polarization axis reveals an adaptive reuse of the polarization machinery in pheromone-treated budding yeast. *J Prot Res* 8(1), 6-19.

- Nash R, Tokiwa G, Anand S, Erickson K, Futcher AB (1988). The WHI1_ gene of *Saccharomyces cerevisiae* tethers cell division to cell size and is a cyclin homolog. *EMBO J* 7, 4335–4346.
- Neiman AM (2011). Sporulation in the budding yeast *Saccharomyces cerevisiae*. *Genetics* 189(3), 737-765.
- Nelson B, Parsons AB, Evangelista M, Schaefer K, Kennedy K, Ritchie S, Petryshen TL, Boone C (2004). Fus1p interacts with components of the Hog1p mitogen-activated protein kinase and Cdc42p morphogenesis signaling pathways to control cell fusion during yeast mating. *Genetics* 166, 67–77.
- Nern A & Arkowitz RA (1999). A Cdc24p-Far1p-G-protein complex required for yeast orientation during mating. *J Cell Biol* 144, 1187–1202.
- Nomoto SN, Nakayama KA, Matsumoto K (1990). Regulation of the yeast pheromone response pathway by G protein subunits. *EMBO J* 9, 691–696.
- Nouraini S, Xu D, Nelson S, Lee M, Friesen JD (1997). Genetic evidence for selective degradation of RNA polymerase subunits by the 20S proteasome in *Saccharomyces cerevisiae*. *Nucleic Acids Res* 25, 3570–3579.
- O'Brien KP, Remm M, Sonnhammer EL (2005). Inparanoid: a comprehensive database of eukaryotic orthologs. *Nucleic Acids Res* 33, D476–D480.
- Oehlen LJ, & Cross FR (1994). G1 cyclins CLN1 and CLN2 repress the mating factor response pathway at Start in the yeast cell cycle. *Genes Dev* 8, 1058 – 1070.
- Oehlen LJ, & Cross FR (1998). Potential regulation of Ste20 function by the Cln1 Cdc28 and Cln2-Cdc28 cyclin-dependent protein kinases. *J Biol Chem* 273, 25089 – 25097.

- Ogura K, Tandai T, Yoshinaga S, Kobashigawa Y, Kumeta H, Ito T, Sumimoto H, Inagaki F (2009). NMR structure of the heterodimer of Bem1 and Cdc24 PB1 domains from *Saccharomyces cerevisiae*. *J Biochem* 146, 317–325.
- Okada S, Lee ME, Bi E, Park HO (2017). Probing Cdc42 polarization dynamics in budding yeast using a biosensor. In: *Methods in Enzymology*, ed. J. Abelson, M. Simon, G. Verdine, A. Pyle, Academic Press 589, 171-190.
- Olson KA, Nelson C, Tai G, Hung W, Yong C, Astell C, Sadowski I (2000). Two regulators of Ste12p inhibit pheromone-responsive transcription by separate mechanisms. *Mol Cell Biol* 20, 4199–4209.
- Oppenheimer JH, Schwartz HL, Surks MI, Koerner D, Dillmann WH (1976, January). Nuclear receptors and the initiation of thyroid hormone action. In *Proceedings of the 1975 Laurentian Hormone Conference* (pp. 529-557). Academic Press.
- O'Rourke SM & Herskowitz I (1998). The Hog1 MAPK prevents cross talk between the HOG and pheromone response MAPK pathways in *Saccharomyces cerevisiae*. *Genes Dev* 12(18), 2874–2886.
- O'Rourke SM, Herskowitz I, O'Shea EK (2002). Yeast go the whole HOG for the hyperosmotic response. *TRENDS Genet* 18(8), 405-412.
- O'Rourke SM & Herskowitz I (2004). Unique and redundant roles for HOG MAPK pathway components as revealed by whole-genome expression analysis. *Mol Biol Cell* 15, 532–542.
- Osumi M, Shimoda C, Yanagishima N (1974). Mating reaction in *Saccharomyces cerevisiae*. *Arch Microbiol* 97(1), 27-38.

- Pan X, Harashima T, Heitman J (2000). Signal transduction cascades regulating pseudohyphal differentiation of *Saccharomyces cerevisiae*. *Curr Opin Microbiol* 3(6), 567–572.
- Park HO & Bi E (2007). Central roles of small GTPases in the development of cell polarity in yeast and beyond. *Microbiol Mol Biol Rev* 71(1), 48-96.
- Paulick MG & Bertozzi CR (July 2008). The glycosylphosphatidylinositol anchor: a complex membrane-anchoring structure for proteins. *Biochem* 47 (27), 6991–7000.
- Pawson T & Scott JD (1997). Signaling through Scaffold, Anchoring, and Adaptor Proteins. *Science* 278 (5346), 2075–2080.
- Pawson T, Raina M, Nash P (2002). Interaction domains: from simple binding events to complex cellular behavior. *FEBS letters* 513(1), 2-10.
- Pelicci G, Lanfrancone L, Grignani F, McGlade J, Cavallo F, Forni G, Nicoletti I, Grignani F, Pawson T, Pelicci PG (1992). A novel transforming protein (SHC) with an SH2 domain is implicated in mitogenic signal transduction. *Cell* 70 (1), 93–104.
- Pemberton LF & Paschal BM (2005). Mechanisms of receptor-mediated nuclear import and nuclear export. *Traffic* 6, 187-198.
- Pestova EV, Håvarstein LS, Morrison DA (1996). Regulation of competence for genetic transformation in *Streptococcus pneumoniae* by an auto-induced peptide pheromone and a two-component regulatory system. *Mol Microbiol*, 21(4), 853-862.
- Peter M, Gartner A, Horecka J, Ammerer G, Herskowitz I (1993). FAR1 links the signal transduction pathway to the cell cycle machinery in yeast. *Cell* 73(4), 747-760.

- Peter M & Herskowitz I (1994). Direct inhibition of the yeast cyclindependent kinase Cdc28-Cln by Far1. *Science* 265, 1228–1231.
- Piekarska I, Rytka J, Rempola B (2010). Regulation of sporulation in the yeast *Saccharomyces cerevisiae*. *Acta Biochimica Polonica*, 57(3), 241-50.
- Pinna LA & Ruzzene M (1996). How do protein kinases recognize their substrates? *Biochim Biophys Acta* 1314, 191–225.
- Pope PA, Bhaduri S, Pryciak PM (2014). Regulation of cyclin-substrate docking by a G1 arrest signaling pathway and the Cdk inhibitor Far1. *Curr Biol* 24(12), 1390-1396.
- Posas F, Wurgler-Murphy SM, Maeda T, Witten EA, Thai TC, Saito H (1996). Yeast HOG1 MAP kinase cascade is regulated by a multistep phosphorelay mechanism in the SLN1-YPD1-SSK1 “two-component” osmosensor. *Cell* 86, 865–875.
- Posas F, Witten EA, Saito H (1998). Requirement of STE50 for osmostress-induced activation of the STE11 mitogen-activated protein kinase kinase kinase in the high-osmolarity glycerol response pathway. *Mol Cell Biol* 18(10), 5788-5796.
- Posas F & Saito H (1998a). Activation of the yeast SSK2 MAP kinase kinase kinase by the SSK1 two-component response regulator. *EMBO J* 17, 1385–1394.
- Prelich G (1999). Suppression mechanisms: themes from variations. *Trends Genet* 15, 261–266.
- Price LA, Kajkowski EM, Hadcock JR, Ozenberger BA, Pausch MH (1995). Functional coupling of a mammalian somatostatin receptor to the yeast pheromone response pathway. *Mol Cell Biol* 15, 6188–6195.

- Printen JA & Sprague GF (1994). Protein-protein interactions in the yeast pheromone response pathway: Ste5p interacts with all members of the MAP kinase cascade. *Genetics* 138, 609–619.
- Proft M & Struhl K (2004). MAP kinase-mediated stress relief that precedes and regulates the timing of transcriptional induction. *Cell* 118, 351–361.
- Pruyne D & Bretscher A (2000). Polarization of cell growth in yeast. *J Cell Sci* 113, 365–375.
- Pryciak PM & Huntress FA (1998). Membrane recruitment of the kinase cascade scaffold protein Ste5 by the G-complex underlies activation of the yeast pheromone response pathway. *Genes Dev* 12, 2684–2697.
- Qamra R & Hubbard SR (2013). Structural basis for the interaction of the adaptor protein grb14 with activated ras. *PloS one* 8, e72473.
- Qi M & Elion EA (2005). MAP kinase pathways. *J Cell Sci* 118(16), 3569-3572.
- Raaijmakers JH, Deneubourg L, Rehmann H, de Koning J, Zhang Z, Krugmann S, ... & Bos JL (2007). The PI3K effector Arap3 interacts with the PI (3, 4, 5) P3 phosphatase SHIP2 in a SAM domain-dependent manner. *Cell signal* 19(6), 1249-1257.
- Rad MR, Lutzenkirchen K, Xu G, Kleinhans U, Hollenberg CP (1991). The complete sequence of a 11953 bp fragment from CIG on chromosome III encompasses four new open reading frames. *Yeast* 7, 533-538.
- Rad MR, Xu G, Hollenberg CP (1992). STE50, a novel gene required for activation of conjugation at an early step in mating in *Saccharomyces cerevisiae*. *Mol Gen Genet* 236(1), 145-154.

- Rad MR, Jansen G, Bühring F, Hollenberg CP (1998). Ste50p is involved in regulating filamentous growth in the yeast *Saccharomyces cerevisiae* and associates with Ste11p. *Mol Gen Genet* 259(1), 29-38.
- Rad MR (2003). The role of adaptor protein Ste50-dependent regulation of the MAPKKK Ste11 in multiple signalling pathways of yeast. *Curr Genet* 43(3), 161-170.
- Raitt DC, Posas F, Saito H (2000). Yeast Cdc42 GTPase and Ste20 PAK-like kinase regulate Sho1-dependent activation of the Hog1 MAPK pathway. *EMBO J* 19, 4623–4631.
- Rapoport TA, Li L, Park E (2017). Structural and mechanistic insights into protein translocation. *Annu Rev Cell Dev Biol* 33, 369-390.
- Rassow J & Pfanner N (2000). The protein import machinery of the mitochondrial membranes. *Traffic* 1, 457-464.
- Ray LB & Sturgill TW (1988). Insulin-stimulated microtubule-associated protein kinase is phosphorylated on tyrosine and threonine in vivo. *Proc Nat Acad Sci* 85(11), 3753-3757.
- Reiser V, Salah SM, Ammerer G (2000). Polarized localization of yeast Pbs2 depends on osmostress, the membrane protein Sho1 and Cdc42. *Nat Cell Biol* 2, 620–627.
- Reiser V, Raitt DC, Saito H (2003). Yeast osmosensor Sln1 and plant cytokinin receptor Cre1 respond to changes in turgor pressure. *J Cell Biol* 161, 1035–1340.
- Remenyi A, Good MC, Lim WA (2006). Docking interactions in protein kinase and phosphatase networks. *Curr Opin Struct Biol* 16, 676–685.

- Renner F & Schmitz ML (2009). Autoregulatory feedback loops terminating the NF-kappaB response. *Trends Bio-chem Sci* 34, 128–135.
- Rine J (1991). Gene overexpression in studies of *Saccharomyces cerevisiae*. *Methods Enzymol* 194, 239–251.
- Roberts CJ, Nelson B, Marton MJ, Stoughton R, Meyer MR, Bennett HA, He YD, Dai H, Walker WL, Hughes TR, Tyers M, Boone C, Friend SH (2000). Signaling and circuitry of multiple MAPK pathways revealed by a matrix of global gene expression profiles. *Science* 287, 873–880.
- Roberts RL & Fink GR (1994). Elements of a single MAP kinase cascade in *Saccharomyces cerevisiae* mediate two developmental programs in the same cell type: mating and invasive growth. *Genes Dev* 8, 2974–2985.
- Rodriguezviciano P, Warne PH, Dhand R, Vanhaesebroeck B, Gout I, Fry MJ, Waterfield MD, Downward J (1994). Phosphatidylinositol-3-OH Kinase as a Direct Target of Ras. *Nature* 370, 527-532.
- Rothman JE & Wieland FT (1996). Protein sorting by transport vesicles. *Science* 272, 227-234.
- Rout MP, Aitchison JD, Suprapto A, Hjertaas K, Zhao Y, Chait BT (2000). The yeast nuclear pore complex: composition, architecture, and transport mechanism. *The Journal of cell biology* 148(4), 635-652.
- Ryan O, Shapiro RS, Kurat CF, Mayhew D, Baryshnikova A, Chin B, Lin ZY, Cox MJ, Vizeacoumar F, Cheung D, Bahr S, Tsui K, Tebbji F, Sellam A, Istel F, Schwarzmuller T, Reynolds TB, Kuchler K, Gifford DK, Whiteway M, Giaever G, Nislow C, Costanzo

- M, Gingras AC, Mitra RD, Andrews B, Fink GR, Cowen LE, Boone C (2012). Global gene deletion analysis exploring yeast filamentous growth. *Science* 337, 1353–1356.
- Saito H & Posas F (2012). Response to hyperosmotic stress. *Genet* 192(2), 289-318.
- Sakai N, Saito Y, Fujiwara Y, Shiraki T, Imanishi Y, Koshimizu TA, Shibata K (2015). Identification of protein arginine N-methyltransferase 5 (PRMT5) as a novel interacting protein with the tumor suppressor protein RASSF1A. *Biochem Biophys Res Commun* 467, 778-784.
- Santangelo GM (2006). Glucose signaling in *Saccharomyces cerevisiae*. *Microbiol Mol Biol Rev* 70, 253–282.
- Sarokin L & Carlson M (1986). Short repeated elements in the upstream regulatory region of the SUC2 gene of *Saccharomyces cerevisiae*. *Mol Cell Biol* 6, 2324–2333.
- Schiavone M, Vax A, Formosa C, Martin-Yken H, Dague E, Francois JM (2014). A combined chemical and enzymatic method to determine quantitatively the polysaccharide components in the cell wall of yeasts. *FEMS Yeast Res* 14, 933–947.
- Schultz J, Milpetz F, Bork P, Ponting CP (1998). SMART, a simple modular architecture research tool: identification of signaling domains. *Proc Natl Acad Sci USA* 95, 5857–5864.
- Schwartz MA & Madhani HD (2004). Principles of MAP kinase signaling specificity in *Saccharomyces cerevisiae*. *Annu Rev Genet*, 38, 725-748.
- Schwartz MA & Madhani HD (2006). Control of MAPK signaling specificity by a conserved residue in the MEK-binding domain of the yeast scaffold protein Ste5. *Curr Genet* 49(6), 351-363.

Schwartz R, Ting CS, King J (2001). Whole proteome pI values correlate with subcellular localizations of proteins for organisms within the three domains of life. *Gen Res* 11, 703-709.

Schwartz TU (2005). Modularity within the architecture of the nuclear pore complex. *Curr Opin Struct Biol* 15(2), 221-226.

Schwartz TU (2016). The structure inventory of the nuclear pore complex. *J Mol Biol* 428, 1986–2000.

Segall JE (1993). Polarization of yeast cells in spatial gradients of alpha mating factor. *Proc Nat Acad Sci* 90(18), 8332-8336.

Sharrocks AD, Yang SH, Galanis A (2000). Docking domains and substrate-specificity determination for MAP kinases. *Trends Biochem Sci* 25, 448–453.

Shen D, Yuan H, Hutagalung A, Verma A, Kümmel D, Wu X, Reinisch K, McNew JA, Novick P (2013). The synaptobrevin homologue Snc2p recruits the exocyst to secretory vesicles by binding to Sec6p. *J Cell Biol* 202, 509–526.

Shi Z, Resing KA, Ahn NG (2006). Networks for the allosteric control of protein kinases. *Curr Opin Struct Biol* 16, 686–692.

Shively CA, Kweo HK, Norman KL, Mellacheruvu D, Xu T, Sheidy DT, ... & Nesvizhskii A (2015). Large-scale analysis of kinase signaling in yeast pseudohyphal development identifies regulation of ribonucleoprotein granules. *PLoS Genet* 11(10), e1005564.

Sim AT & Scott JD (1999). Targeting of PKA, PKC and protein phosphatases to cellular

microdomains. *Cell Calcium* 26, 209–217.

Slaughter BD, Huff JM, Wiegraebe W, Schwartz JW, Li R (2008). SAM domain-based protein oligomerization observed by live-cell fluorescence fluctuation spectroscopy. *PLoS one* 3(4), e1931.

Smith FD & Scott JD (2002). Signaling complexes: junctions on the intracellular information super highway. *Curr Biol* 12, R32–R40.

Smith MG, Swamy SR, Pon LA (2001). The life cycle of actin patches in mating yeast. *J Cell Sci* 114(8), 1505-1513.

Smith SE, Rubinstein B, Pinto IM, Slaughter BD, Unruh JR, Rong Li (2013). Independence of symmetry breaking on Bem1-mediated autocatalytic activation of Cdc42. *J Cell Biol* 202.7, 1091-1106.

Songyang Z, Shoelson SE, Chaudhuri M, Gish G, Pawson T, Haser WG, King F, Roberts T, Ratnofsky S, Lechleider RJ, Neel BJ, Birge RB, Fajardo JE, Chou MM, Hanafusa H, Schaffhausen B, Cantley LC (1993): SH2 domains recognize specific phosphopeptide sequences. *Cell* 72, 767-778.

Stein EG, Ghirlando R, Hubbard SR (2003). Structural basis for dimerization of the Grb10 Src homology 2 domain implications for ligand specificity. *J Biol Chem*, 278(15), 13257-13264.

Ström AC & Weis K (2001). Importin-beta-like nuclear transport receptors. *Gen Biol* 2(6), reviews3008-1.

- Sturgill TW & Ray LB (1986). Muscle proteins related to microtubule associated protein-2 are substrates for an insulin-stimulatable kinase. *Biochem Biophys Res Comm* 134, 565–571.
- Sun Y, Hays NM, Periasamy A, Davidson MW, Day RN (2012). Monitoring protein interactions in living cells with fluorescence lifetime imaging microscopy. In *Methods in enzymology* (Vol. 504, pp. 371-391). Academic Press.
- Swift S, Throup JP, Williams P, Salmond GP, Stewart GS (1996). Quorum sensing: a population-density component in the determination of bacterial phenotype. *Trends in biochemical sciences*, 21(6), 214-219.
- Takahashi S & Pryciak PM (2007). Identification of novel membrane-binding domains in multiple yeast Cdc42 effectors. *Mol Biol Cell* 18, 4945–4956.
- Takayama T, Yamamoto K, Saito H, Tatebayashi K (2019). Interaction between the transmembrane domains of Sho1 and Opy2 enhances the signaling efficiency of the Hog1 MAP kinase cascade in *Saccharomyces cerevisiae*. *PloS One* 14(1), e0211380.
- Tamanoi F (2011). Ras signaling in yeast. *Gen Cancer* 2(3), 210-215.
- Tatebayashi K, Tanaka K, Yang HY, Yamamoto K, Matsushita Y, Tomida T, Imai M, Saito H (2007). Transmembrane mucins Hkr1 and Msb2 are putative osmosensors in the SHO1 branch of yeast HOG pathway. *EMBO J* 26, 3521–3533.
- Tatebayashi K, Yamamoto K, Nagoya M, Takayama T, Nishimura A, Sakurai M, Momma T, Satio H (2015). Osmosensing and scaffolding functions of the oligomeric four-transmembrane domain osmosensor Sho1. *Nat Commun* 6, 6975.

- Tedford K, Kim S, Sa D, Stevens K, Tyers M (1997). Regulation of the mating pheromone and invasive growth responses in yeast by two MAP kinase substrates. *Curr Biol* 7, 228–238.
- Thorner J (2003). Signal Transduction. In: Linder, P.; Shore, D.; Hall, MN., editors. *Landmark Papers in Yeast Biology*. Plainview (NJ): Cold Spring Harbor Laboratory Press.
- Thorsen M, Di Y, Tangemo C, Morillas M, Ahmadpour D, Van der Does C, Wagner A, Johansson E, Boman J, Posas F, Wysocki R (2006). The MAPK Hog1p Modulates Fps1p-dependent arsenite uptake and tolerance in yeast. *Mol Biol Cell* 17, 4400–4410.
- Timmons S, Coakley MF, Moloney AM, O'Neill C (2009). Akt signal transduction dysfunction in Parkinson's disease. *Neurosci Lett* 467(1), 30-35.
- Tong Y, Chugha P, Hota PK, Alviani RS, Li M, Tempel W, Shen L, Park HW, Buck M (2007). Binding of Rac1, Rnd1, and RhoD to a novel Rho GTPase interaction motif destabilizes dimerization of the plexin-B1 effector domain. *J Biol Chem* 282, 37215–37224.
- Tran EJ & Wente SR (2006). Dynamic nuclear pore complexes: life on the edge. *Cell* 125(6), 1041- 1053.
- Tripathi A & Varadarajan R (2014). Residue specific contributions to stability and activity inferred from saturation mutagenesis and deep sequencing. *Curr Opin Struct Biol*, 24, 63-71.
- Tripathi A, Gupta K, Khare S, Jain PC, Patel S, Kumar P, Pulianmackal AJ, Aghera N, Varadarajan R (2016). Molecular determinants of mutant phenotypes, inferred from saturation mutagenesis data. *Mol Biol Evol* 33, 2960-2975.

- Truckses DM, Bloomekatz JE, Thorner J (2006). The RA domain of Ste50 adaptor protein is required for delivery of Ste11 to the plasma membrane in the filamentous growth signaling pathway of the yeast *Saccharomyces cerevisiae*. *Mol Cell Biol* 26, 912–928.
- Ubersax JA & Ferrell Jr JE (2007). Mechanisms of specificity in protein phosphorylation. *Nat Rev Mol Cell Biol* 8(7), 530.
- Ullrich A & Schlessinger J (1990). Signal transduction by receptors with tyrosine kinase activity. *Cell* 61, 203–212.
- Utsugi T, Minemura M, Hirata A, Abe M, Watanabe D, Ohya Y (2002). Movement of yeast 1, 3- β -glucan synthase is essential for uniform cell wall synthesis. *Genes to Cells* 7(1), 1-9.
- Valdespino-Gómez VM, Valdespino-Castillo PM, Valdespino-Castillo VE (2015). Cell signalling pathways interaction in cellular proliferation: Potential target for therapeutic interventionism. *Cirugía y Cirujanos (English Edition)*, 83(2), 165-174.
- van Drogen F, O'Rourke SM, Stucke VM, Jaquenoud M, Neiman AM, Peter M (2000). Phosphorylation of the MEKK Ste11p by the PAK-like kinase Ste20p is required for MAP kinase signaling in vivo. *Curr Biol* 10, 630–639.
- Versele M, Lemaire K, Thevelein JM (2001). Sex and sugar in yeast: two distinct GPCR systems. *EMBO Reports* 2(7), 574-579.
- Vasen G & Lerner AC (2018). Intrinsic polarization cues interfere with pheromone gradient sensing in *S. cerevisiae*. *bioRxiv*, 502856.
- Von Heijne G (1990). Protein targeting signals. *Curr Opin Cell Biol* 2(4), 604-608.

- Waddle JA, Karpova TS, Waterston RH, Cooper JA (1996). Movement of cortical actin patches in yeast. *J Cell Biol* 132(5), 861-870.
- Wang ZY, Bai MY, Oh E, Zhu JY (2012). Brassinosteroid signaling network and regulation of photomorphogenesis. *Annual review of genetics*, 46, 701-724.
- Warner N, & Núñez G (2013). MyD88: a critical adaptor protein in innate immunity signal transduction. *J Immunol* 190(1), 3-4.
- Wassmann K, & Ammerer G (1997). Overexpression of the G1-cyclin gene *CLN2* represses the mating pathway in *Saccharomyces cerevisiae* at the level of the MEKK Ste11. *J Biol Chem* 272, 13180 – 13188.
- Weibull C (1960). *The Bacteria*, I. C. Gunsalus and R. Y. Stanier, Eds. (Academic Press, New York, 1960) vol. 1, p. 153.
- Westfall PJ, Patterson JC, Chen RE, Thorner J (2008). Stress resistance and signal fidelity independent of nuclear MAPK function. *Proc Nat Acad Sci* 105(34), 12212-12217.
- White MA & Anderson RG (2005). Signaling networks in living cells. *Annu Rev Pharmacol Toxicol* 45, 587–603.
- Whiteway MS, Wu C, Leeuw T, Clark K, Fourest-Lieuvin A, Thomas DY, Leberer E (1995). Association of the yeast pheromone response G protein beta gamma subunits with the MAP kinase scaffold Ste5p. *Science* 269(5230), 1572-1575.
- Whiteway M, Hougan L, Dignard D, Bell L, Saari G, Grant F, ... & Thomas DY (1988). Function of the STE4 and STE18 genes in mating pheromone signal transduction in

Saccharomyces cerevisiae. In Cold Spring Harbor symposia on quantitative biology (Vol. 53, pp. 585-590). Cold Spring Harbor Laboratory Press.

Whiteway M, Hougan L, Dignard D, Thomas DY, Bell L, Saari GC, ... & MacKay VL (1989). The STE4 and STE18 genes of yeast encode potential β and γ subunits of the mating factor receptor-coupled G protein. *Cell* 56(3), 467-477.

Whitmarsh AJ & Davis RJ (1998). Structural organization of MAP-kinase signaling modules by scaffold proteins in yeast and mammals. *Trends Biochem Sci* 23, 481-485.

Winters MJ, Lamson RE, Nakanishi H, Neiman AM, Pryciak PM (2005a). A membrane binding domain in the Ste5 scaffold synergizes with G-binding to control localization and signaling in pheromone response. *Mol Cell* 20, 21-32.

Winters MJ & Pryciak PM (2005b). Interaction with the SH3 domain protein Bem1 regulates signaling by the *Saccharomyces cerevisiae* p21-activated kinase Ste20. *Mol Cell Biol* 25, 2177-2190.

Wu C, Whiteway M, Thomas DY, Leberer E (1995). Molecular characterization of Ste20p, a potential mitogen-activated protein or extracellular signal-regulated kinase kinase (MEK) kinase kinase from *Saccharomyces cerevisiae*. *J Biol Chem*, 270(27), 15984-15992.

Wu C, Leberer E, Thomas DY, Whiteway M (1999). Functional characterization of the interaction of Ste50p with Ste11p MAPKKK in *Saccharomyces cerevisiae*. *Mol Biol Cell* 10(7), 2425-2440.

Wu C, Arcand M, Jansen G, Zhong M, Iouk T, Thomas DY, Meloche S, Whiteway M (2003). Phosphorylation of the MAPKKK regulator Ste50p in *Saccharomyces cerevisiae*: a

casein kinase I phosphorylation site is required for proper mating function. Eukaryot cell 2(5), 949-961.

Wu C, Jansen G, Zhang J, Thomas DY, Whiteway M (2006). Adaptor protein Ste50p links the Ste11p MEKK to the HOG pathway through plasma membrane association. Gen Dev 20(6), 734-746.

Xu G, Jansen G, Thomas DY, Hollenberg CP, Ramezani RM (1996). Ste50p sustains mating pheromone-induced signal transduction in the yeast *Saccharomyces cerevisiae*. Mol Microbiol 20, 773–783.

Yamamoto K, Tatebayashi K, Tanaka K, Saito H (2010). Dynamic control of yeast MAP kinase network by induced association and dissociation between the Ste50 scaffold and the Opy2 membrane anchor. Mol cell 40(1), 87-98.

Yamaoka S, Shimono Y, Shirakawa M, Fukao Y, Kawase T, Hatsugai N, Tamura K, Shimada T, Hara-Nishimura I (2013). Identification and dynamics of Arabidopsis adaptor protein-2 complex and its involvement in floral organ development. The Plant Cell 25(8), 2958-2969.

Yates CM & Sternberg MJ (2013). The effects of non-synonymous single nucleotide polymorphisms (nsSNPs) on protein–protein interactions. J Mol Biol 425, 3949-3963.

Ydenberg CA & Rose MD (2009). Antagonistic regulation of Fus2p nuclear localization by pheromone signaling and the cell cycle. JCB 184(3), 409-422.

Yerko V, Sulea T, Ekiel I, Harcus D, Baardsnes J, Cygler M, ... & Wu C (2013). Structurally unique interaction of RBD-like and PH domains is crucial for yeast pheromone signaling. Mol Biol Cell 24(3), 409-420.

Zaman S, Lippman SI, Zhao X, Broach JR (2008). How *Saccharomyces* responds to nutrients. *Annu Rev Genet*, 42: 27–81.

Zlobin A, Bloodworth JC, Osipo C (2019). Mitogen-Activated Protein Kinase (MAPK) Signaling, Predictive Biomarkers in Oncology, © Springer Nature Switzerland AG
213 S. Badve, G. L. Kumar (eds.).